THE UNIVERSITY OF QUEENSLAND

AUSTRALIA

Junctional Rho GTPase signalling: Molecules and Mechanisms

Rashmi Priya

Bachelor of Science (Honours) and Master of Science

A thesis submitted for the degree of Doctor of Philosophy at

The University of Queensland in 2014

Institute for Molecular Bioscience

Abstract

Epithelial tissues coat our body surfaces and act as a strong mechanical barrier against external stresses like pathogens and chemicals. They are robust tissues made up of polarised epithelial cells that are strongly adhered to one another. However, during development, these tissues behave like a 'fluid' and undergo extensive rearrangement. This mechanical robustness and fluidity is conferred to them by the specialized adhesive structures called zonula adherens (ZA). It is an E-cadherin based adhesion-complex, which acts like a *Velcro,* thus stitching epithelial cells together. Remarkably, ZA also regulates proper co-ordination of adhesion, cytoskeleton and mechanical tension in response to the developmental cues, thus ensuring the cohesive behaviour of epithelial tissues during morphogenetic events. To achieve this multi-step process of epithelial homeostasis, ZA acts as an anchorage site for the convergence of many signalling pathways; most important of them are being modulated by Rho GTPases. Rho GTPases are powerful molecular switches, whose spatio-temporal activity needs to be finely balanced by GEFs, GAPs and GDIs. Various studies have established an undisputed contribution of Rho GTPases in ZA biogenesis and functions, but the mechanistic details have been missing. Also, a great deal of knowledge is lacking about the upstream elements, which are required to produce an active Rho at the ZA. This study aims to identify the molecules and mechanisms underlying the regulation and functions of junctional Rho signalling.

I initiated the study by aiming for a deeper understanding of how Rho GTPase produces a functional ZA. I have proposed that ECT2, earlier believed to be cytokinetic Rho-GEF, mediates Rho functions at the ZA. ECT2 depletion led to gross disruption of ZA architecture, with significant loss of E-cadherin from junctions. Further, ECT2 KD did not affect steady-state junctional actin content but perturbed the junctional localization of myosin IIA, thus establishing myosin IIA as a downstream effector of Rho-ECT2 pathway. Indeed, the disrupted cadherin phenotype was restored in ECT2 KD cells by driving the expression of Myosin IIA. Also, using laser nanoscissors, I found that ECT2-Rho-Myosin II signalling pathway regulates junctional tension. Depletion of ECT2, Myosin IIA or pharmacological inhibition of Rho led to reduction in the cortical tension, thus suggesting that these molecules act in concert to maintain this functional property of the ZA. Next, to understand the impact of ECT2-Rho pathway on the dynamic properties of E-Cadherin, I performed FRAP on GFP-E-cadherin. Using this tool, I have demonstrated that ZA is composed of two dynamically distinct pools of E-cadherin. The apical pool posses a lesser mobile fraction and thus is more stabilized and restricted, while the sub-apical pool has a larger mobile fraction. This differential stabilization of the pools was abolished when the ECT2-Rho pathway was perturbed,

thus establishing an important role of ECT2-Rho signalling in stabilizing cadherin at the apical zone of the cells. Taken together, these findings identify ECT2 as a major upstream regulator of junctional Rho signalling, which is vital for ZA organization and functions. Also, using genetic ablation and reconstitution approaches, I have demonstrated that the interaction between cadherin and Rho GTPase is reciprocal and indeed E-cadherin is required for junctional Rho localization and activity by anchoring the upstream Rho activators; ECT2 and centralspindlin complex.

The other aspect of this study involved the unravelling of a novel signalling network that ensures to produce a robust and spatially restricted GTP-Rho zone at the ZA. Using a combination of pharmacological and genetic manipulations along with activity/location based Rho biosensors; I have uncovered that this signalling cascade involves an unexpected feedback loop from myosin IIA-ROCK to Rho. Myosin IIA is essential for Rho signalling at the ZA by specifically blocking the action of the GAP; p190B. Depletion or inhibition of myosin II led to the increased cortical localization of the p190B and decreased Rho activity accompanied by the broadening of the ZA Rho zone. Interestingly, this cross-talk between myosin IIA and p190B GAP is mediated by another small GTPase Rnd3, as depletion of Rnd3 compromised the junctional enrichment of p190B GAP. Further, I have illustrated a role for ROCK-1 in this pathway, as inhibiting ROCK-1 mediated phosphorylation of Rnd3 promotes its junctional association and a concomitant increase in p190B GAP localization, thus depleting junctional Rho. Also, I discovered that myosin IIA directly influences this whole cascade by acting as a scaffold for ROCK-1 via its rod-domain. Myosin IIA could support junctional ROCK-1 localization, independent of its actin-binding capacity and motor functions. Finally, using numerical simulations, we modeled this signaling architecture and observed that the junctional Rho signaling exhibits ‘bistability’ and toggles between Rho-ON to Rho-OFF states. Strikingly, addition of the myosin to ROCK loop turns the switch to ON, thus further corroborating with our experimental findings. In summary, our results identify a novel regulatory pathway, orchestrated by myosin IIA, which is essential for the sustenance of the spatially restricted GTP-Rho zone at the ZA.

Declaration by author

This thesis *is composed of my original work, and contains* no material previously published or written by another person except where due reference has been made in the text. I have clearly stated the contribution by others to jointly-authored works that I have included in my thesis.

I have clearly stated the contribution of others to my thesis as a whole, including statistical assistance, survey design, data analysis, significant technical procedures, professional editorial advice, and any other original research work used or reported in my thesis. The content of my thesis is the result of work I have carried out since the commencement of my research higher degree candidature and does not include a substantial part of work that has been submitted *to qualify for the award of any* other degree or diploma in any university or other tertiary institution. I have clearly stated which parts of my thesis, if any, have been submitted to qualify for another award.

I acknowledge that an electronic copy of my thesis must be lodged with the University Library and, subject to the General Award Rules of The University of Queensland, immediately made available for research and study in accordance with the *Copyright Act 1968*.

I acknowledge that copyright of all material contained in my thesis resides with the copyright holder(s) of that material. Where appropriate I have obtained copyright permission from the copyright holder to reproduce material in this thesis.

Publications during candidature

Peer-reviewed papers:

1. E-cadherin supports steady-state Rho signalling at the epithelial zonula adherens.
Rashmi Priya, Alpha S. Yap and Guillermo A. Gomez
Differentiation, 2013

2. Centralspindlin and α-catenin regulate Rho signaling at the epithelial zonula adherens.
Aparna Ratheesh, Guillermo A. Gomez, **Rashmi Priya,** Suzie Verma, Eva M. Kovacs, Kai Jiang, Nicholas H. Brown, Anna Akhmanova, Samantha J. Stehbens and Alpha S. Yap
Nature Cell Biology, 2012

3. Measurement of Junctional Protein Dynamics Using Fluorescence Recovery After Photobleaching (FRAP).
Rashmi Priya and Guillermo Gomez.
Bioprotocols, 2013
http://www.bio-protocol.org/e937

4. Coordinating Rho and Rac: the Regulation of Rho GTPase Signaling and Cadherin Junctions.
Aparna Ratheesh, **Rashmi Priya** and Alpha S. Yap
Prog Mol Biol Transl Sci. 2013

5. E-cadherin loss alters cytoskeletal organization and adhesion in non-malignant breast cells but is insufficient to induce an epithelial-mesenchymal transition
Augustine Chen, Henry Beetham, Michael A Black, **Rashmi Priya,** Bryony J Telford, Joanne Guest, George A R Wiggins, Tanis D Godwin, Alpha S Yap and Parry J Guilford.
BMC Cancer, 2014

6. Tension-sensitive actin assembly supports contractility at the epithelial zonula adherens.
Joanne M. Leerberg, Guillermo A. Gomez, Suzie Verma, Elliott J. Moussa, Selwin K. Wu, **Rashmi Priya**, Brenton D. Hoffman, Carsten Grashoff, Martin A. Schwartz and Alpha S. Yap.
Current Biology, 2014

7. Active Tension: The role of Cadherin adhesion and signaling in generating junctional contractility.
Rashmi Priya and Alpha S. Yap
Current Topics in Developmental Biology, *In press*

8. A PTPRA/SFK/Rap1 signaling module regulates Myosin IIB to support contractile tension at apical E-cadherin junctions.
Guillermo A. Gomez, Robert W. McLachlan, Selwin K. Wu, Benjamin J. Caldwell, Elliott Moussa, Suzie Verma, Michelle Bastiani, **Rashmi Priya,** Robert G. Parton, Katharina Gaus, Jan Sap and Alpha S. Yap
MBoC, January 2015

9. Myosin II anchors feedback regulation to confer robustness on Rho signaling at E-cadherin junctions.
Rashmi Priya, Guillermo A. Gomez, Hayley Cox, Suzie Verma, Nicholas A. Hamilton and Alpha S. Yap
Manuscript submitted to Nature Cell Biology, *Under Revision*

Conference Presentations:

Oral presentations:

1. Junctional Rho GTPase cycle: how to keep the wheel turning.
Rashmi Priya, Guillermo A. Gomez and Alpha S.Yap
Organizational principles for Membrane Signaling, 21-26th October 2013, Corsica, France

2. A myosin II scaffold anchors feedback regulation of Rho signaling at epithelial cadherin junctions.
Rashmi Priya, Guillermo A. Gomez and Alpha S.Yap
Brisbane Cell and Developmental Biology Meeting, 26th September 2014, Brisbane Australia

3. The Essentials of light microscopy and immunofluorescence
Rashmi Priya
IMB Microscopy Forum; 21st may, 2013 at Institute for Molecular Bioscience, The University of Queensland, Brisbane

Posters:

1. From Cell Division to Cell Adhesion: A novel function for ECT2
Rashmi Priya, Guillermo Gomez and Alpha S. Yap
Brisbane Cell and Developmental Biology Meeting - Oct 2012, held at QBI, UQ, Brisbane

2. A novel cell signaling apparatus that regulates Adherens Junctions
Rashmi Priya, Guillermo Gomez and Alpha S. Yap
3rd Brisbane ECR Poster Symposium, held at Institute for Molecular Bioscience, The University of Queensland, Brisbane in November, 2012

3.Non-muscle Myosin supports Rho signaling: emergent properties
Rashmi Priya, Guillermo Gomez and Alpha S. Yap
'Organizational principles for Membrane Signaling', 21-26th October 2013, Corsica, France

Publications included in this thesis

1.Centralspindlin and α-catenin regulate Rho signaling at the epithelial zonula adherens.
Aparna Ratheesh, Guillermo A. Gomez, **Rashmi Priya,** Suzie Verma, Eva M. Kovacs, Kai Jiang, Nicholas H. Brown, Anna Akhmanova, Samantha J. Stehbens and Alpha S. Yap
Nature Cell Biology, 2012
Results from chapter 2 published in this article, included in Appendix 1.

Contributor	Statement of contribution
Rashmi Priya (Candidate)	Designed and performed experiments (20%) Wrote the paper (10%) Responsible for figures 2f, 3a, 3b, 3c, 3d, 3e, 3f, 3g, 3i, 3j, 3k, s3a, s3b, s3c, s3d, s3e, s3f, s2e and s2g
Aparna Ratheesh	Designed and performed experiments (40%) Wrote the paper (30%)
Guillermo A. Gomez	Designed and performed experiments (40%) Wrote the paper (30%) Guidance to Rashmi Priya
Suzie Verma	Performed experiments
Eva M. Kovacs	Generated reagents
Kai Jiang	Generated reagents
Anna Akhmanova, Samantha Stehbens	Guidance and contribution to project discussion
Nicholas H. Brown	Performed experiments, Guidance and contribution to project discussion
Alpha S. Yap	Wrote the paper (30%) Edited the paper (100%) Guidance to Rashmi Priya Supervision of the study

2. E-cadherin supports steady-state Rho signalling at the epithelial zonula adherens.
Rashmi Priya, Alpha S. Yap and Guillermo A. Gomez
Differentiation, 2013
Incorporated as chapter 3, Section 3.2.1

Contributor	Statement of contribution
Rashmi Priya (Candidate)	Performed experiments (90%) Designed experiments (80%)

	Data analysis (80%) Wrote the paper (50%)
Guillermo A. Gomez	Designed experiments (20%) Performed experiments (10%) Data analysis (20%) Assisted in the overall preparation of the figures. Discussion and mentoring of confocal microscopy. Discussion and interpretation of the results Supervised the study and guidance to Rashmi Priya
Alpha S Yap	Edited the paper (100%) Wrote the paper (50%) Supervised the study and guidance to Rashmi Priya

3.Measurement of Junctional Protein Dynamics Using Fluorescence Recovery After Photobleaching (FRAP).
Rashmi Priya and Guillermo Gomez.
Article in Bioprotocols, 2013
Incorporated as chapter 3, Section 3.2.2

Contributor	Statement of contribution
Rashmi Priya (Candidate)	Standardized the protocol and wrote the paper (50%)
Guillermo Gomez	Standardized the protocol, wrote and edited the paper (50%) Supervised the study and guidance to Rashmi Priya

4. Myosin II anchors feedback regulation to confer robustness on Rho signaling at E-cadherin junctions.
Rashmi Priya, Guillermo A. Gomez, Hayley Cox, Suzie Verma, Nicholas A. Hamilton and Alpha S. Yap
Manuscript submitted to Nature Cell Biology
Incorporated as chapter 4, Section 4.1

Contributor	Statement of contribution
Rashmi Priya (Candidate)	Designed and performed experiments (70%) Wrote the paper (90%)
Guillermo A. Gomez	Designed and performed experiments (25%) Wrote and edited paper (10%)

	Assisted in the overall preparation of the figures. Discussion and mentoring of confocal microscopy Responsible for the mathematical modelling section
Suzie Verma	Performed experiments (4%)
Hayley Cox	Performed experiments (1%)
Nicholas A. Hamilton	Responsible for the mathematical modelling section
Alpha S. Yap	Edited and wrote the paper (100%) Assisted in discussion and interpretation of the results Supervised the study and guidance to Rashmi Priya

5. Active tension: the role of cadherin adhesion and signaling in generating junctional contractility.

Rashmi Priya and Alpha S. Yap

Current Topics in Developmental Biology, *In press*

Included in Appendix 2

Contributor	Statement of contribution
Rashmi Priya (Candidate)	Wrote the review article (70%)
Alpha S. Yap	Wrote and edited the review article (30%) Guidance to Rashmi Priya

Contributions by others to the thesis

Prof. Alpha Yap gave intellectual support and direction in developing the project throughout the tenure of PHD. He also proofread the thesis and provided valuable feedback.

Dr. Guillermo Gomez assisted in the microscopy techniques and helped in interpretation and analysis of FRAP, FRET and laser-ablation experiments. He also assisted in the general-discussion of the project and provided valuable suggestions.

Ms. Suzie Verma assisted in processing the samples obtained from immunoprecipitation experiments (chapter 4).

Statement of parts of the thesis submitted to qualify for the award of another degree

None

Acknowledgements

उद्यमेन हि सिद्धयान्ति कार्याणि न मनोरथैः
Udyamena hi siddhayānti kāryāṇi na manorathaiḥ
(A goal is achieved through labour, not by desire only)

This PHD has been a remarkable journey, with its fair share of ups and downs; but at the end of it I feel enriched. Obviously, this would not have been possible without all those people who have supported me throughout this tenure.

First and foremost, I would like to express my deepest gratitude to my advisor Prof. Alpha Yap for believing in my capabilities and giving me this wonderful opportunity to be a part of his team. I don't see myself achieving all this without his constant encouragement, intellectual guidance and insightful critique. Thanks Alpha, for all your support, patience and motivating-discussions that has helped me evolve during the course of this tenure.

My sincere thanks to my co-supervisor Dr. Guillermo Gomez. GG, it's been an absolute pleasure working with you. I am truly grateful to you for your unending patience and help in reaching my everyday goals. You are a source of inspiration for me and I look up to you. I have learnt a lot from you and hope to continue to do so.

I would also like to thank my thesis committee: Prof. Peter Thorn, Dr. Kelly Smith and Associate Prof. Carol Wicking for their pragmatic suggestions and encouragement. A massive thanks to the very efficient and active IMB postgraduate staff Dr. Amanda Carozzi and Cody Mudgway for always being helpful. Special mention to Amanda; we (IMB PhD students) are so fortunate to have you. Thanks so much for taking such good care of us! I would also like to extend my gratitude to the core IMB facilities like IT (especially Christian), the CSF staff and stores for keeping IMB on-move.

I would like to acknowledge the generous support from following funding sources: UQI (UQ International) scholarship, ANZ Trustees *PhD Scholarships* in *Medical* Research and Cancer Council Queensland for providing me with scholarships and travel-grants.

A big shout-out to the present and past members of Yap lab; you guys have been amazing and I have thoroughly enjoyed working with you all. Especially, Suzie; you are such a kind soul and I can't thank you enough for everything you have helped me with; Joanne for pushing me through the

milestones deadlines, encouraging words and delicious cakes; Aparna, Siew-ping, Selwin, Srikanth, Mag, Carol, Xuan and Bipul for fruitful discussions and help with the reagents, and the 'kids'; Ben, Joyce, Maedeh, Elliott and Magda for keeping the lab-life lively and for those refreshing lunch and coffee breaks. Massive thanks to the wonderful group of people I have met after coming to Australia; Paola, Gaby, Praveer, Amrita, Carlos, Praj, Yash, Kasturee, Soumya and Venky; for their support and the good-times we had. Also, thanks to cute little Aarna for brightening up my days!

To my early Science 'gurus' Dr. Ashraf Dar and Dr. Dhaneshwar Prushty; thanks for teaching me the basics of lab-work and good lab-practices and also motivating me to move ahead and do better in science.
Also, I would like to express my deepest gratitude to Dr. Sorab Dalal, whom I admire and respect a lot. Sorab, I am indebted to you for support, encouragement and mentorship in the early days of my career and also for making the transition from Mumbai to Brisbane very smooth.

I am very fortunate to have two people in my life: my best friends Sunita and Suman. You both have been a rock-solid support for me throughout my life and thanks for being there! Love you both!
I would also like to thank my family (especially my brother Annu, Papa, Bade mamu and Mausi) and my extended family (Ajay, Bhagwat, Papa ji and Mummy ji) for always being there and supporting me in everyway.

I could not have reached here without my husband Vikram being my side. Your positive attitude and calmness has helped me immensely during the rough phases. Your affection, love, unwavering care and unending cups of amazing tea have kept me going! Thanks a lot for sustaining me in everyway.

Lastly, I would like to dedicate this thesis to two very important people in my life.
My confidant and mentor Binay: Thanks for letting me be a part of your life. Your kindness and encouragement have shaped me what I am today.
My late mother: mom, I missed you in all these years. I hope you are happy with what I am today. Thanks for instilling resilience, punctuality and importance of hard work in me, that has helped me reach wherever I am today.

Keywords

rho gtpase, cadherin, myosin, ect2, rock, feedback signalling, p190b rho gap
epithelial morphogenesis, cancer, bistability

Australian and New Zealand Standard Research Classifications (ANZSRC)

ANZSRC code: 060111 Signal Transduction, 50%
ANZSRC code: 060106 Cellular Interactions (incl. Adhesion, Matrix, Cell Wall), 30%
ANZSRC code: 111201 Cancer Cell Biology, 20%

Fields of Research (FoR) Classification

FoR code: 0601 Biochemistry and Cell Biology, 80%
FoR code: 1112 Oncology And Carcinogenesis, 20%

Table of Contents

List of Figures

Chapter 4:

Chapter 5:

List of Abbreviations

3D	three-dimensional
Ab	Antibody
ADP	Adenosine diphosphate
ATP	Adenosine triphosphate
Arp2/3	Actin Related Protein 2/3
BSA	Bovine Serum Albumin
C3-T	C3-Transferase
CS	Centralspindlin
CaCO-2	Human colorectal adenocarcinoma cell-line
CFP	Cyan fluorescent protein
CO-IP	Co-immunoprecipitation
CRIB	Cdc42 and rac interactive binding
DAPI	4',6-diamidino-2-phenylindole
DTT	Dithiothreitol
DMEM	Dulbecco's Modified Eagle Medium
DH	Dbl-homologous
E-cadherin	Epithelial cadherin
ECT2	Epithelial cell transforming 2
EGFP	enhanced GFP
F-actin	Filamentous actin
FBS	Foetal bovine serum
FRAP	Fluorescence recovery after photobleaching
FRET	Fluorescence resonance energy transfer
GFP	Green fluorescent protein
GEF	Guanine Exchange Factors
GST	Glutathione S-transferase
GAP	GTPase activating protein
GDI	Guanosine nucleotide dissociation inhibitors
GST	Glutathione S-transferase
HBBS	Hank's Balanced Salt Solution
HRP	Horse Radish Peroxidase
IQGAP	IQ motif containing GTPase activating protein 1
IF	Immunofluorescence

KD	Knock-down
MCF-7	Mammary breast adenocarcinoma cell line
MDCK	Mardin-Darby Canine Kidney
mDia	Mammalian Diaphanous
MLCP	Myosin light chain Phosphatase
MLCK	Myosin light chain Kinase
MLC	Myosin light chain
MKLP-1	Mitotic kinesin-like protein
MT	Microtubules
NMII	Non-muscle Myosin II
NP	n-propyl-gallate
NP-40	nonyl phenoxylpolyethoxylethanol
PAGE	Polyacrylamide gel electrophoresis
PBS	Phosphate Buffered Saline
PH	Pleckstrin homology
PFA	Paraformaldehyde
RacGAP	Rac GTPase-activating protein 1
RPMI	Roswell Park Memorial Institute medium
ROI	region of interest
RT	room temperature
RLC	regulatory light chain
ROCK	Rho Kinase
SDS	Sodium dodecyl sulphate
siRNA	Small interfering Ribonucleic acid
TCA	Trichloroacetic acid
WCL	Whole cell lysate
WASP	WASP family verprolin homologous protein
WT	Wild type
ZA	Zonula adherens
ZO-1	Zonula occludens 1

Chapter 1: General Introduction and Literature Review

1.1 Cell-cell adhesion

Epithelial tissues line our body surfaces and protect the exteriors and interiors of our body (Fristrom, 1988; Schock and Perrimon, 2002). Epithelial cohesion requires them to be connected to each other via various macromolecular complexes, defined as intercellular junctions. There are mainly three kinds of intercellular junctions in vertebrates: tight junctions, adherens junctions and desmosomes. These intercellular adhesion complexes are crucial for the biogenesis, maintenance and function of epithelia (Schock and Perrimon, 2002).

Tight junctions are located in the most apical region and serve to prevent the diffusion of small molecules and ions through the space between cells (Matter and Balda, 2007). They also maintain cell polarity by acting as a fence, which bars the mixing of apical and baso-lateral membrane components (Hartsock and Nelson, 2008). Desmosomes are spot-like adhesions arranged on the lateral surface of cells. They tether intermediate filaments at membrane-associated plaques, thus forming a three-dimensional scaffold, which provides the tissue with mechanical rigidity and resistance (Delva et al., 2009).

Adherens junctions are cadherin-based adhesive structures, which perform an array of functions, including the initiation and stabilization of cell-cell adhesion, regulating actin cytoskeleton and intracellular signaling, to name a few (Niessen et al., 2011). Ultrastructurally, adherens junction can be identified as a plasma membrane structure composed of dense plaque on opposing membranes, which holds two membranes together (Meng and Takeichi, 2009). They are the first to get assembled at the initial sites of cell-cell contact and precede the formation of other junctional complexes (desmosomes and tight junctions). Stable adhesion mediated by adherens junctions brings the membranes of adjacent cells in close proximity, thus allowing the formation of other junctions. Also, it ensures proper targeting of junctional constituents on the membrane by providing spatial cues and triggers signaling events that are required for the assembly of desmosomes and tight junctions (Benjamin and Nelson, 2008; Braga, 2002).

The Zonula Adherens (ZA) is an important feature of epithelial morphology (Braga, 2000). It is the apical-most part of these cadherin-based adherens junctions characterized by the presence of a circumferential actomyosin belt and a ring of E-cadherin. It provides strong adhesive strength that

prevents tissues from dissociating into individual cells. However, it is also a dynamic entity that facilitates the organizational changes that take place during the various stages of morphogenesis, which give rise to the various shapes and appearances of different organs of the body (Gumbiner, 2005). It is therefore important to understand the underlying mechanisms behind regulation of this adhesive structure. Over the years, various studies have been done to address the issue of how the ZA modulates, and is modulated by, various signaling pathways. Although this question is not fully unravelled yet, it has built up a complex yet intriguing picture of signaling molecules that are active at the ZA; Rho GTPase is one of them. In this study, I aim to expand our basic understanding of the interplay between E-cadherin adhesion, the actomyosin apparatus and RhoA signaling.

1.2 Molecular architecture of Zonula Adherens

Cadherins and catenins constitute the major components of the Zonula Adherens (Fig 1.1) (Harris and Tepass, 2010). The classical cadherins belong to a large superfamily of cell-cell adhesion molecules, which show various expression patterns and support calcium-dependent adhesion (Niessen et al., 2011). They are transmembrane glycoproteins, classified based on the tissues in which they are expressed. For example, E-cadherin is expressed in epithelia and N-cadherin is widely expressed in the nervous system. E-cadherin is one of most studied of the classical cadherins (Overduin et al., 1995).

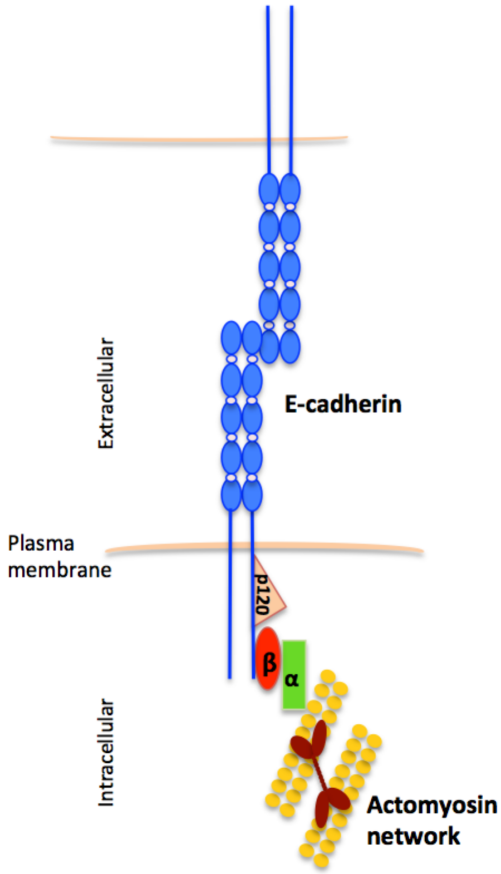

Figure 1.1 Schematic representing molecular architecture of the Zonula Adherens. Lateral dimer of E-cadherin traverses the membrane and engages in homophilic ligation with the opposing dimer. The cytoplasmic tail binds to α, β and p120-catenin and also associates with the actomyosin cytoskeleton.

Along the intercellular interface within epithelia, E-cadherin organizes itself into two distinct pools: apical; which is the concentrated zone of E-cadherin at the ZA and lateral; which consists of small clusters and puncta of E-cadherin throughout lateral axis of the cell-cell contact (Fig 1.2) (Kametani and Takeichi, 2007; Wu et al., 2014). These two pools of cadherin differ in terms of morphology, stability and also generate different levels of contractile tension (Priya et al., 2013; Wu et al., 2014).

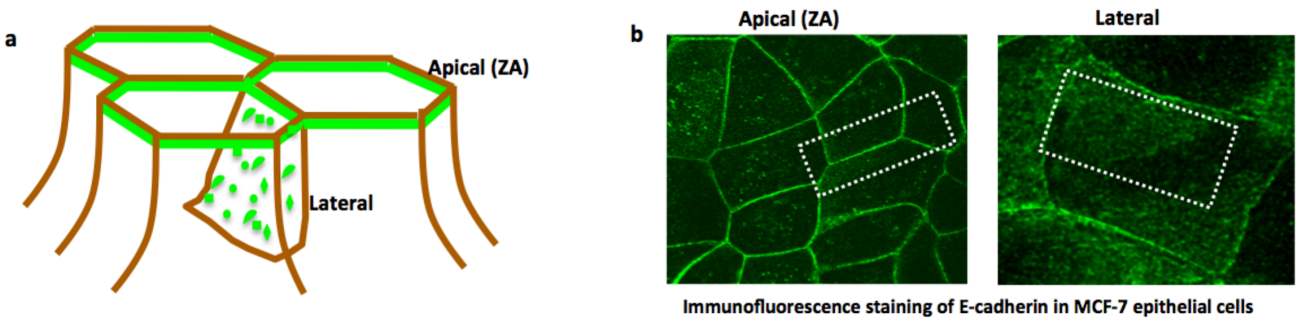

Figure 1.2 E-cadherin organization in MCF-7 epithelial cells. At the apical zone of the cell, E-cadherin forms a tight belt like structure, referred to as ZA. This appears like a linear peri-junctional staining in the fixed MCF-7 epithelial cells (a). The lateral surface of the cell is decorated by small clusters of E-cadherin, as evident in the *en face* contacts (b)

The extracellular domain of E-cadherin engages in homophilic binding with the extracellular domain of E-cadherin present on the opposing cell (Fig 1.1). It is a 'rod' like structure consisting of five cadherin repeats and calcium binding sites. The cytoplasmic domains are highly conserved among classical cadherins as they mediate binding with cytoplasmic molecules called catenins. Catenins are often considered as molecular sensors that integrate cell-cell junctions and cytoskeleton dynamics with various signaling pathways. The catenin family comprises p120-catenin, β-catenin and α-catenin (Fig 1.1). Some of the important functions mediated by these catenins include regulation of Rho GTPases by p120-catenin (Perez-Moreno and Fuchs, 2006), modulating actin dynamics by α-catenin (Drees et al., 2005), and stabilization of the unstructured cytoplasmic domain of E-cadherin by β-catenin (Huber et al., 2001; Benjamin and Nelson, 2008).

1.3 Zonula Adherens is an active site of Rho GTPase signaling

Cadherin-based junctions have significant impacts on various cellular processes like embryogenesis and tissue homeostasis. They are not merely passive adhesion molecules; instead they actively participate in dynamic morphogenetic events like tissue segregation, gastrulation and synaptogenesis (Halbleib and Nelson, 2006; Harris and Tepass, 2010; Schock and Perrimon, 2002). The fact that the ZA contributes to all these multi-faceted processes suggests that it can contribute beyond its canonical adhesive function. Indeed, it is increasingly becoming apparent that cadherins can initiate a number of cellular and molecular events by the productive ligation of two cadherin receptors on opposing cells and thus act as signaling receptors (McCormack et al., 2013; Niessen et al., 2011; Ratheesh et al., 2013; Wheelock and Johnson, 2003; Yap and Kovacs, 2003)

The field of cadherin-signaling biology has been dominated by the three best-characterized members of the Rho GTPase family: RhoA, Rac1 and Cdc42 (Braga and Yap, 2005; Fukata and

Kaibuchi, 2001; Ratheesh et al., 2013). The first insight into the functional relationship between cadherins and small GTPases came with the observation that small GTPases (mainly Rho and Rac) localize to cadherin-based junctions (Braga et al., 1997; Braga et al., 2000). These small GTPases are important for junctional integrity and support junctional biogenesis by regulating the assembly and dynamics of the cellular cytoskeleton and/or by initiating certain signaling events required to maintain the epithelial phenotype (Braga, 2002; Fukata and Kaibuchi, 2001; Kovacs et al., 2002a; Niessen et al., 2011; Ratheesh et al., 2012; Ratheesh et al., 2013; Terry et al., 2011). In turn, cadherins can modulate the activity and localization of these small GTPases at junctions (McCormack et al., 2013; Priya et al., 2013), thereby suggesting that functional co-operation between them is reciprocal.

Using a recombinant functional E-cadherin ligand consisting of the full ectodomain of E-cadherin fused to the Fc region of IgG, Kovacs et al reported that Rac gets recruited and activated at newly formed cadherin-adhesive sites (Kovacs et al., 2002a). This early activation of Rac was important for contact maturation via the actin cytoskeleton, because when Rac was inhibited this process was compromised (Kovacs et al., 2002a). E-cadherin facilitates contact formation by recruiting the Arp 2/3 complex (an actin nucleator which relies on Rac for its activation) to nascent adhesive sites during initiation of junction formation. So cadherin-mediated homophilic adhesion leads to recruitment of Rac and Arp 2/3 complex at nascent adhesive sites, which leads to actin assembly and contact-zone extension (Kovacs et al., 2002b). Further, binding to p120 catenin was essential for E-cadherin to activate Rac1 (Goodwin et al., 2003). Also, by manipulating extracellular calcium levels to initiate the formation of cell-cell contacts (often referred as “calcium-switch assay”), Braga and colleagues have reported that E-cadherin clustering activates Rac1 in keratinocytes (Betson et al., 2002).

Another small GTPase required for cadherin homeostasis is Rho; however the impact of cadherin signaling on Rho activity is still not very conclusive. Using the calcium switch assay, Noren *et al* showed that upon E-cadherin ligation Rac1 gets activated, but the activity of Rho is diminished (Noren et al., 2001). Further they demonstrated that this cadherin-mediated inhibition of Rho occurs by activation of a GAP called p190RhoGAP (Noren et al., 2003). It is also believed that Rac and Rho occupy different contact zones during junction formation (Yamada and Nelson, 2007). As cells first make contact, Rac takes the center stage along with Arp2/3 and is later replaced by Rho (Yamada and Nelson, 2007) The other interesting candidate thought to regulate Rho at junctions is p120-catenin. Overexpression studies in fibroblasts showed that p120-catenin could mimic the phenotype induced by Rho inhibition. It sequesters Rho in the cytoplasm in a GDP-bound state,

thus further inhibiting it (Anastasiadis et al., 2000). Interestingly, Rac can also induce translocation of p190 Rho GAP to adherens junction, where it gets coupled with p120 (Wildenberg et al., 2006). Here, p120 acts as a platform to bring the GAP and its substrate Rho together and thus inhibit Rho (Wildenberg et al., 2006).

In the light of the above observations, one can appreciate that cadherin based junctions act as an active site for Rho GTPase signaling. These small GTPases have far-ranging impacts on cellular morphogenetic processes like wound healing, epithelial-mesenchymal transition and maintaining epithelial polarity (Van Aelst and Symons, 2002). So, the understanding of their precise regulation and effects is important not only for the basic biology but also for the better understanding of diseases.

1.4 Rho GTPases

Rho GTPases belong to the Ras superfamily and are molecular switches that cycle between two conformational states: a GTP-bound state which is 'active' and a GDP-bound state which is 'inactive' (Etienne-Manneville and Hall, 2002). Regulation of Rho GTPase occurs through a GDP–GTP cycle that is controlled by the opposing activities of guanine nucleotide-exchange factors (GEFs), which catalyze the exchange of GDP for GTP, and GTPase-activating proteins (GAPs), which increase the rate of GTP hydrolysis to GDP.

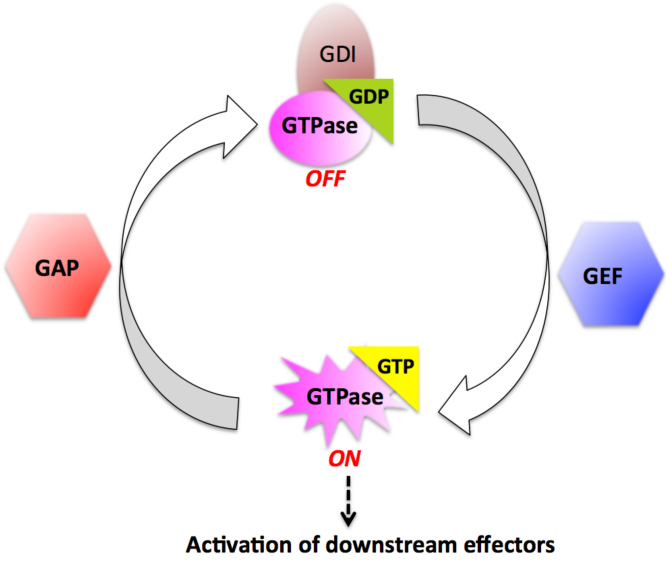

Fig 1.3 Regulation of the Rho GTPase cycle. The cycling between the ON and OFF state is facilitated by GEFs (promote the exchange of GDP to GTP), GAPs (catalyse GTP hydrolysis to GDP) and GDIs (sequester the GDP-bound Rho in cytoplasm).

Another layer of regulation is provided by Rho–GDP-dissociation inhibitors (RHOGDIs), which sequester Rho away from the GDP–GTP cycle (Fig 1.3).

Rho, Rac and Cdc42 are the prominent members of this family and are believed to be the crucial regulators behind many cellular processes like polarity, cell migration, microtubule dynamics and transcription (Etienne-Manneville and Hall, 2002).

The Rho sub-family of small GTPases includes three proteins: RhoA, RhoB and RhoC. They are very similar in sequence and when overexpressed lead to the formation of stress fibers and contribute to contractility (Wheeler and Ridley, 2004). All these three isoforms share a sequence homology of around 85%. The c-terminus is the most divergent domain and determines their intracellular localization (Wheeler and Ridley, 2004). All the three isoforms get post-translationally modified at their c-terminus with the addition of a prenyl group at a conserved cysteine residue. This prenyl group anchors Rho GTPase to the membrane and is important for its stabilization (Wheeler and Ridley, 2004). The length of the prenyl group differs in the three isoforms, which leads to their differential localization, with RhoB localizing mainly to endosomes and lysosomes while RhoA and RhoC localize to the plasma membrane and cytosol (Wheeler and Ridley, 2004). These three isoforms also show differences in their function. For example, RhoB mainly inhibits growth, as opposed to RhoA and RhoC, and they can also bind to different effectors and regulators (Burridge and Wennerberg, 2004).

Recently, there is a growing interest in the atypical members of the Rho family: Rnd1, Rnd2 and Rnd3 (Nobes et al., 1998; Riento et al., 2005b; Riou et al., 2013; Wennerberg et al., 2003). These are atypical in the sense that they don't undergo the canonical GTP-GDP cycle, being deficient in the amino-acid residues required for GTPase activity. Thus they are always GTP-loaded and potentially constitutively active (Chardin, 2006). Their regulatory mechanisms involve gene-expression, protein degradation, post-translation modification (e.g. phosphorylation) and sub-cellular localization (Chardin, 2006; Riento et al., 2005b). Like other members of Rho family, they are also post-translationally modified at their c-terminus by farnesylation, thus enabling their membrane association (Chardin, 2006). Rnd1 and Rnd3 show prominent plasma membrane localization while Rnd2 is usually found in early endosomes (Chardin, 2006). Also, Rnd1 and Rnd3 (but not Rnd2) can antagonize Rho activity primarily by promoting the GAP activity of p190-B RhoGAP (Oinuma et al., 2012; Riou et al., 2013; Wennerberg et al., 2003). Overexpression of these proteins leads to loss of focal adhesions, disrupts stress fibers and causes rounding of cells (Chardin, 2006)

1.5 Rho GTPase effectors at the ZA (ROCK and Myosin II)

The Rho GTPases regulate a variety of basic cellular processes like organization of acto-myosin cytoskeleton, gene transcription, trafficking and polarity. The ability of Rho to carry out these functions depends on its effectors (Bishop and Hall, 2000). A large number of Rho effectors have been identified to-date, including various kinases, phosphatases, scaffolding proteins and lipases. These effectors prefer GTP-bound Rho and show high specificity and selectivity for Rho family

members; i.e. a particular effector will only bind to a particular GTPase (Bustelo et al., 2007). Mutational analysis has revealed the presence of highly conserved GTPase binding domains (GBD) in these effectors, which provide the specificity (Bishop and Hall, 2000). Although these Rho-effectors are highly diverse structurally, their activation by the GTPase involves certain similar mechanisms. So, upon binding, a GTPase can translocate the effector to the signaling-zone, anchors it to the membrane and/or induces a conformational change that activates the effector (Bustelo et al., 2007). Interestingly, once activated, these effectors can also modulate Rho GTPase signaling by regulating GEFs, GAPs or GDIs, thus implying the presence of extensive feed-back loops in GTPase signaling pathways (Ivetic and Ridley, 2004; Kitzing et al., 2007).

1.5.1 ROCK

One of the earliest identified Rho effectors were the ROCKs (Rho-dependent kinases). They belong to the family of Ser/Thr protein kinases and two isoforms have been identified in mammalian cells: ROCK-1 and ROCK-2 (Amano et al., 2010; Julian and Olson, 2014; Riento and Ridley, 2003). Broadly, these kinases have an N-terminal kinase domain, followed by a coiled-coil domain and the c-terminus region. The kinase domain of both isoforms is highly conserved at the amino-acid level (92% identity), while overall they share 62% identity. The c-terminus comprises both a Rho-binding domain (RBD) and a PH domain. In the absence of GTP-Rho, ROCK exists in an autoinhibited conformation: binding between the C-terminal region and the N-terminal kinase domain inhibits ROCK activity. Binding of GTP-Rho to the RBD then releases this auto-inhibitory conformation to activate the kinase (Amano et al., 2010; Riento and Ridley, 2003; Schofield and Bernard, 2013) (Fig1.4).

Since the kinase domain is highly conserved between these two isoforms, it has often been thought that these isoforms phosphorylate common substrates. Nonetheless, they differ in their expression, subcellular localization, functions and interactions (Amano et al., 2010; Schofield and Bernard, 2013).

ROCK-1 is highly transcribed in kidney, liver, spleen and lung, while ROCK-2 shows higher expression in brain and heart (Schofield and Bernard, 2013). The C-terminal PH domain mediates the subcellular localization of these kinases. ROCK-2 has been shown to localize in cytoplasm, at the plasma membrane and at cleavage furrow during cytokinesis (Schofield and Bernard, 2013). ROCK-1 localization is not well studied, however recent studies have shown that ROCK-1 can specifically concentrate at the apical junctions of the cells by associating with junctional protein shroom-3 (Nishimura and Takeichi, 2008) or p120-catenin (Smith et al., 2012).

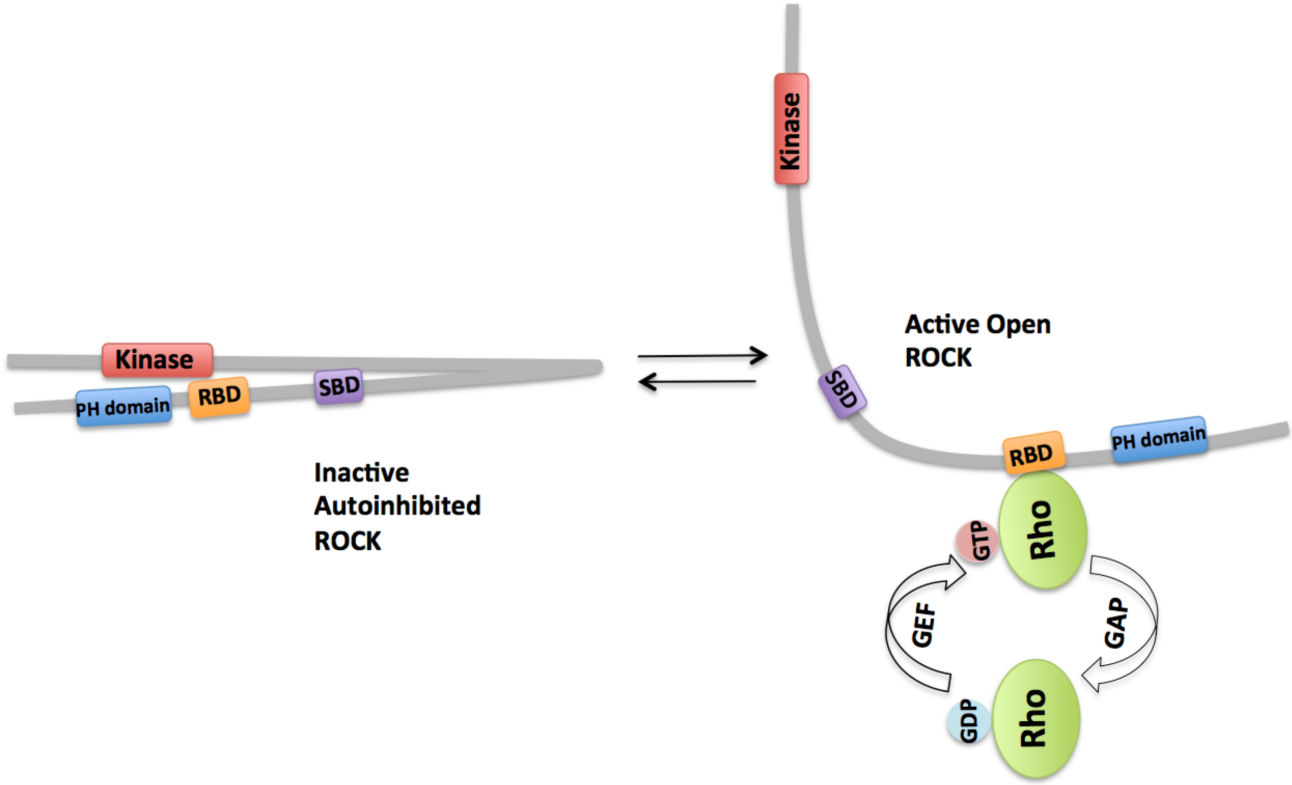

Fig 1.4 Activation of ROCK via GTP-Rho. The pleckstrin homology (PH) domain and the Rho-binding domain (RBD) associate with the amino-terminal region of the protein and form an auto inhibitory loop. Binding of GTP-Rho to the RBD domain opens up the conformation, leading to activation of ROCK.

ROCK-1, but not ROCK-2, has been proven to bind RhoE/Rnd3 (Riento et al., 2005a) and p120-catenin (Smith et al., 2012), while MYPT1 (myosin phosphatase target subunit 1) interacts with ROCK-2 only (Wang et al., 2009). Further, genetic ablation studies have revealed that these two kinases have different functions, with ROCK-2 regulating cell-contraction and phagocytosis while ROCK-1 is essential for stress-fiber formation (Schofield and Bernard, 2013).

ROCK proteins can phosphorylate a number of substrates, which are capable of modifying/organizing the actomyosin cytoskeleton inside the cells. Both of these isoforms modulate a plethora of signaling events by phosphorylating substrates such as RLC (regulatory light chain of myosin), MLCP (myosin light-chain phosphatase), LIM kinase 1 and 2 and profilin, to name but a few (Riento and Ridley, 2003).

Non-muscle myosin (NMII) is one of the principal substrates of ROCK at the ZA (Shewan et al., 2005) (discussed in detail further). Downstream of Rho, ROCK promotes the activation of NMII, which further supports cadherin clustering and stabilization, thus acting as a principal effector of the Rho-ROCK pathway at cadherin junctions (Fig 1.5) (Shewan et al., 2005). Phosphorylation of the regulatory light chain (RLC) of myosin stimulates its ATPase activity and this relies on the subtle balance between kinases (ROCK, MLCK) and phosphatases (MLCP; myosin light chain

phosphatase) (Julian and Olson, 2014; Schofield and Bernard, 2013). MLCK is a calcium dependent enzyme, known to phosphorylate Ser 19 of RLC; however in vitro studies have reported that ROCK can also phosphorylate the same site independent of calcium (Amano et al., 1996; Totsukawa et al., 2000). In contrast to MLKC, ROCK can also phosphorylate the Myosin binding subunit (MBS) of MLCP at various Ser/Thr sites, which limits its activity and thus keeps NMII activated by increasing net RLC phosphorylation (Kawano et al., 1999; Kimura et al., 1996). Indeed MLCP inhibition may the dominant pathway via which ROCK can activate Myosin.

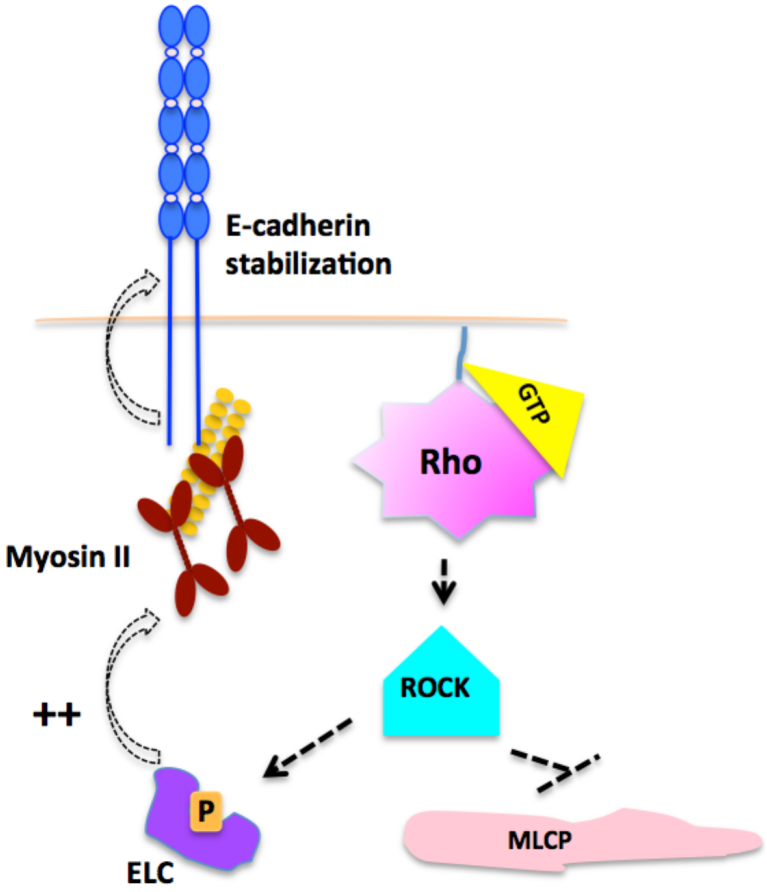

Fig 1.5 Rho effectors at the ZA: Myosin II and ROCK. Upon activation by Rho, ROCK activates Myosin by two means: phosphorylation of the regulatory myosin light chain (MLC) and MLC phosphatases (MLCP). The active myosin then further mediates cadherin clustering and stabilization.

1.5.2 Non-muscle Myosin II

Non-muscle Myosin II (NMII) belongs to a superfamily of motor proteins and is responsible for generation of contractile forces and tension by catalysing ATP hydrolysis and translocation of actin filaments (Conti and Adelstein, 2008; Heissler and Manstein, 2013). There are three mammalian paralogs of Myosin II, which are encoded by separate genes: these are Myosin IIA, Myosin IIB and Myosin IIC. These paralogs are 64-78% identical at the amino-acid level. NMII is a large hexamer, consisting of a homodimer of heavy chains, which non-covalently associates with two pairs of light chains (Fig 1.6). The first ~ 800 amino acids of the heavy chain forms the catalytic head or motor domain. This domain harbors the actin-binding ATPase site and is the most conserved domain of heavy chain between different myosins. The next ~60 amino acids constitute the neck region, which contains binding sites for the ELC (Essential light chain) and the RLC (Regulatory light chain). This is followed by a ~1100 amino-acid rod domain, which is much-less well conserved between different isoforms (Conti and Adelstein, 2008; Heissler and Manstein, 2013; Vicente-Manzanares et al., 2009) (Fig 1.6).

Although all the three NMII paralogs are known to perform mainly two similar functions that is ATP-dependent contraction of actin filaments and filament assembly; there is enough evidence suggesting these isoforms are not simply redundant. Indeed they exhibit distinct motor activity, cellular and tissue distribution, molecular interactions, upstream signaling regulators and functions (Betapudi, 2010; Sandquist and Means, 2008; Smutny et al., 2010; Wang et al., 2009). Using gene-knockout technology in mice, it has been shown that NMIIA and NMIIB null mice have strikingly different developmental defects. While NMIA null mice embryos die early in development because

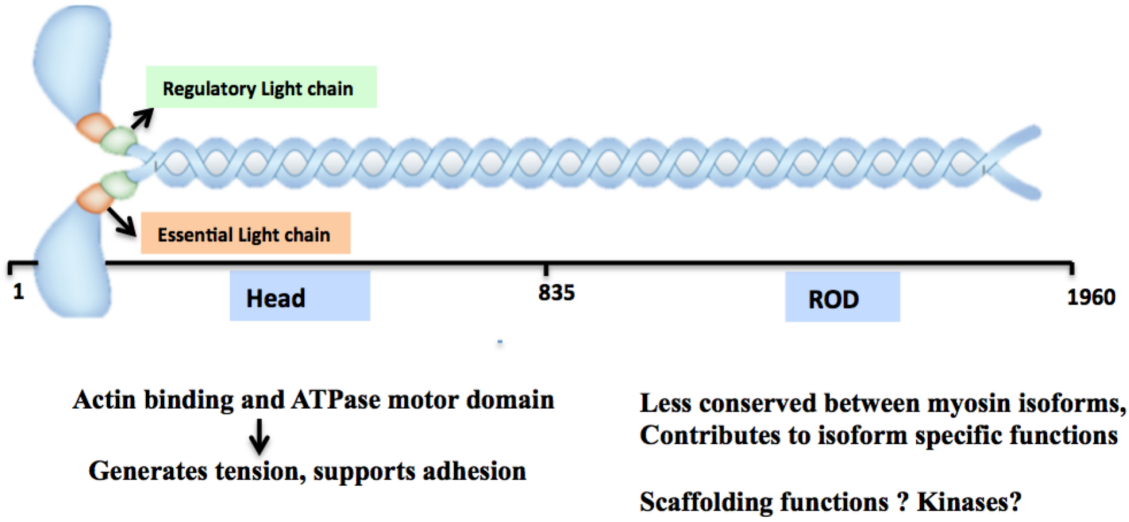

Fig 1.6 Myosin IIA domain structure and functions: The head domain binds to actin and is responsible for its motor activity and contractile functions. The Rod domain mediates filament-assembly and is speculated to have regulatory roles by acting as a scaffold *(Reproduced and Modified from Kopp et al, Kidney International, 2010)*

of gross perturbation of cadherin-dependent junctions and tissue organization (Conti et al., 2004), the NMIIB null mice die just after the birth due to major developmental defects in heart and neurons (Conti and Adelstein, 2008). In cell-biological studies, these two isoforms have been shown to perform unique functions in cell motility, adhesion and wound healing (Betapudi, 2010; Sandquist and Means, 2008; Smutny et al., 2010). Interestingly, the C-terminal rod domain of NMII has been speculated to contribute towards these differences, which is not surprising considering that the rod domains of these isoforms are highly divergent (Sandquist and Means, 2008). Using chimeric NMII constructs, Sandquist *et al* have shown that the rod domain of NMII overcomes its motor functions and is the prime determinant of its subcellular distribution (Sandquist and Means, 2008). The C-terminal rod fragment of NMII has been established to harbor isoform-specific regulatory elements; for example both isoforms are known to get phosphorylated within the rod domain via different kinases at distinct sites (Dulyaninova et al., 2007; Rosenberg and Ravid, 2006). Also, the coiled-coil region in the rod domain of NMIIA shows a specific interaction with S100A4, which is a small calcium-binding protein known to influence filament assembly and cell

motility (Li and Bresnick, 2006). Strikingly, during cell division, it has been shown that the rod domain of NMIIA alone is sufficient to localize to the furrow, thus raising the possibility that myosin can participate in cellular functions by mechanisms that are independent of its motor-activity or actin binding (Beach and Egelhoff, 2009). Indeed, the fact that the rod domain can localize to the cortex suggest that the NMII has yet to be identified binding partners and functions.

Although myosins are best known for their capacity to generate contractile force, recent studies have indicated that Myosin can also act as a scaffolding protein for various signaling elements like kinases, GEFs or GAPs (Conti and Adelstein, 2008). Lee *et a*l established that Dbl family of GEFs can bind to NMII via their highly conserved PH domain. This interaction was found to depend on NMII activity and is required to suppress the activity of these GEFs (Lee et al., 2010). Similarly, another GEF; MyoGEF has been proven to regulate cytokinesis by directly binding Myosin II and co-localizing with it during cleavage furrow (Wu et al., 2006). These observations hint towards a relatively unexplored signaling function of NMII, which is an exciting question for future studies.

1.6 Rho GTPases supports cadherin mediated adhesion

Cell-cell adhesions undergo constant rearrangement during a diverse range of physiological processes such as cell scattering, wound healing and also tumour metastasis (Fukata and Kaibuchi, 2001). Rho GTPases are important for this process as they regulate both junctional biogenesis (from nascent contact formation to maturation) and junctional dynamics (Braga et al., 2000).

Braga and colleagues first reported that treating cells with a Rho inhibitor or injecting them with a dominant negative Rac inhibited the accumulation of cadherin at sites of cell-cell contact (Braga et al., 1997). The importance of Rac in maintaining cadherin-dependent adhesion was further supported by Takaishi and colleagues, showing that overexpression of constitutive active Rac mutants led to accumulation of E-cadherin and actin filaments at sites of cell-cell contact (Takaishi et al., 1997). Rac GTPases can support adhesion by modulating the actin cytoskeleton through activation of various actin nucleators like Arp2/3 and WAVE (Niessen et al., 2011).The other RAC effector that has been reported at the ZA is IQGAP1 (Fukata and Kaibuchi, 2001). IQGAP1 localized to the ZA and negatively regulated adhesion by interacting with β-catenin, which caused α-catenin to dissociate from the cadherin-catenin complex. Rac inhibits the interaction between IQGAP1 and β-catenin, and thus positively regulates cadherin-based adhesion (Fukata and Kaibuchi, 2001).
Cdc42 has been shown to positively regulate cadherin based junctions (Fukata and Kaibuchi, 2001) but compared to Rho and Rac, its contribution is less well studied (Braga et al., 2000).

Rho GTPases (mostly RhoA) are essential for maintaining the stability of cadherin-based junctions. It has been established that when Rho signaling is compromised via various means, it leads to the perturbation of cadherin-based junctions (Braga, 2000; Braga et al., 1997; Priya et al., 2013; Ratheesh et al., 2012; Ratheesh and Yap, 2012; Shewan et al., 2005; Smith et al., 2012; Takaishi et al., 1997). Rho signaling can contribute to adherens junction integrity by stabilizing cadherin receptors, cytoskeleton organization, generation of tension and possibly by facilitating E-cadherin clustering (Braga et al., 2000; Priya et al., 2013; Ratheesh et al., 2012; Ratheesh et al., 2013; Shewan et al., 2005; Smutny et al., 2010; Smutny et al., 2011) .

Myosin II acts downstream of Rho to positively promote cadherin function. When treated with drugs (ML-7 and blebbistatin) that can inhibit Myosin II activity, cells could not concentrate E-cadherin at apical junctions (Shewan et al., 2005). The recruitment and activity of Myosin II at junctions responded to the Rho pathway as inhibition of Rho kinase signaling not only led to the loss of Myosin II from junctions but also abolished its activity as suggested by the loss of MLC phosphorylation and decreased junctional staining of ppMLC (Shewan et al., 2005). Moreover, the phenotype observed after Rho kinase inhibition was very similar to that of Myosin inhibition, namely, inability to concentrate E-cadherin in junctions and reduced adhesion to cadherin-coated substrata. These observations placed Myosin II as a potent downstream effector that allows Rho to modulate the ZA (Shewan et al., 2005).

Further, Smutny *et al* proposed that the two isoforms of Myosin II, IIA and IIB make distinct contributions to adherens junction function and assembly (Smutny et al., 2010). Both isoforms localized to junctions, but they responded to different upstream regulators. While junctional localization of Myosin IIA was dependent on the Rho/ROCK pathway, Myosin IIB was recruited to junctions in response to Rap1 (Smutny et al., 2010). Using a knockdown approach they showed that Myosin IIA supports cadherin clustering, cadherin concentration and proper adhesion at junctions, while Myosin IIB is responsible for maintaining a continuous distribution of E-cadherin along the junctions and also regulates normal levels of ZA-associated F-actin (Smutny et al., 2010).

The above observations support a Rho-Myosin IIA-E-cadherin pathway required for the integrity of the ZA. However, to perform its biological functions, Rho must undergo a regulated activation/inactivation cycle facilitated by GEFs and GAPs. The spatio-temporal activity of these regulatory molecules decides the site and timing of Rho signaling.

1.7 Regulators of Rho GTPases; GEFs, GAPs and GDIs

The nucleotide status of Rho is controlled by three sets of regulatory proteins: GEFs (guanine nucleotide exchange factors), which promote the exchange of GDP to GTP; GDIs (guanine nucleotide dissociation inhibitors), which sequester Rho in its GDP-bound state and GAPs (GTPase activating proteins), which accelerate the process of GTP hydrolysis. The activity and localization of these proteins ensure specificity of Rho signaling inside a cell (Etienne-Manneville and Hall, 2002).

GEFs are multidomain proteins that facilitate the release of GDP from Rho and promote the binding of GTP, thus activating Rho. In biological processes, activation of the small GTPases occurs within minutes or even less than that. GEFs can accelerate this process of nucleotide exchange activity by several folds (Bos et al., 2007). Inside cells, the concentration of GTP is usually ten times higher then GDP. GEF favors the binding of GTP to GTPase by modifying the nucleotide-binding site of GTPase, such that GDP is released and replaced by GTP (Bos et al., 2007).

Rho GDIs belong to a group of regulatory proteins that are capable of binding GDP bound inactive Rho and blocking nucleotide dissociation. In this capacity, they act as negative regulators of Rho by blocking GEF mediated exchange activity and maintaining it in a GDP-bound inactive form. They also act to extract inactive Rho from the membrane and sequester it in the cytoplasm (Kaibuchi et al., 1999)

GAPs, like GEFs, are multidomain proteins, and many of these domains are lipid or protein interaction domains, suggesting their role as localization signals or scaffolding complexes (Bos et al., 2007) Although the GTPases have their own intrinsic GTP hydrolysis activity, this is usually very slow and requires an interaction with GAPs. These GAPs accelerate the hydrolysis step by several orders of magnitude and thus inactivate GTPases precisely and rapidly (Bos et al., 2007). GAPs are regulated by protein-protein interactions or post-translational modifications. These modifications induce a change in localization to a compartment where the GTPase is located, release from autoinhibition, or change in catalytic activity (Bos et al., 2007).

These three sets of regulatory molecules orchestrate Rho signaling in a restricted manner, which is essential for junctional dynamics and integrity.

1.8 The Rho GEF: ECT2

ECT2 belongs to Dbl family of GEFs for Rho GTPases and was first identified as a proto-oncogene (Miki et al., 1993). ECT2 is highly conserved across evolution, as human ECT2 shares a significant degree of similarity in its coding region with murine ECT2, *Let-21* (ECT2 ortholog in *Caenorhabditis elegans*) and *XECT2* (*Xenopus* ECT2) (Fields and Justilien, 2010). ECT2 is composed of various structural domains, each with a distinct role (Fig 1.7). The N-terminal half contains many domains which are common to cell-cycle regulators, while the C-terminal half is

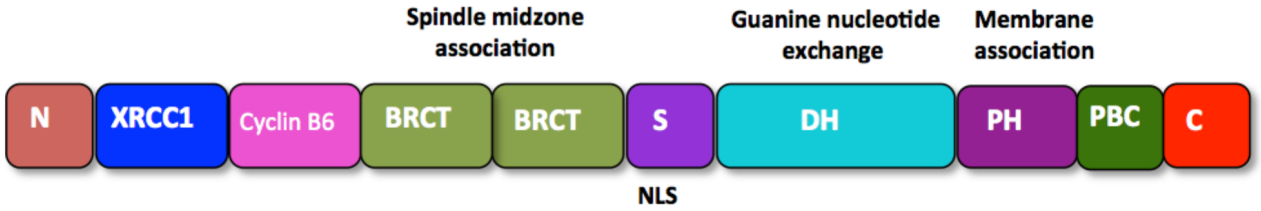

Fig 1.7 Schematic diagram of the domain structure of the ECT2 protein. N, Amino-terminal region; XRCC1, X-ray repair complementing defective repair in Chinese hamster cells 1 domain; Cyclin B6, cyclin B6-like domain; BRCT, BRAC1 C-terminal domain;S, small central region; NLS, nuclear localization sequence; DH, Dbl-homology domain; PH, pleckstrin-homology domain; C, Carboxyl-terminal region.

mainly responsible for the Rho GEF catalytic activity (Tatsumoto et al., 1999). At the extreme N-terminus lies a XRCC1 domain, which shows sequence homology to human XRCC1, a protein involved in DNA repair. The major structural motif in the N-terminal half is a tandem array of BRCT repeats, which are highly conserved in proteins involved in DNA repair and cell cycle checkpoint responses (Fields and Justilien, 2010). This BRCT motif can bind phosphorylated peptides (Manke et al., 2003) and it is suggested that it can also bind to the C-terminal half of ECT2, leading to autoinhibition (discussed in detail later). The C-terminal half is the catalytic core of the protein and contains a tandem array of Dbl-homology (DH) and pleckstrin-homology (PH) domains (Tatsumoto et al., 1999). The extreme c-terminus region of ECT2 does not exhibit significant homology to any known protein domains or motifs (Fields and Justilien, 2010). The N- and C- terminal domains of ECT2 are separated by a small central S domain, which harbors two nuclear localization sequences that regulate the intra-cellular localization of ECT2 (Fields and Justilien, 2010).

1.8.1 Biological functions of ECT2

In Cytokinesis

The best-characterized function of ECT2 is its contribution in cytokinesis (Glotzer, 2005; Piekny et al., 2005; Wolfe and Glotzer, 2009; Wolfe et al., 2009; Yuce et al., 2005). RhoA plays the role of chief modulator in cytokinesis by initiating the formation of the contractile ring (Werner and Glotzer, 2008). This involves the Rho-mediated activation of the actin assembly factor, formin, and phosphorylation of the regulatory light chain of myosin II. ECT2 acts as a primary GEF for Rho during cytokinesis. It ensures the correct localization and activation of Rho during cell division and is a crucial regulator for cytokinesis in all the eukaryotes analyzed to date (Werner and Glotzer, 2008; Yuce et al., 2005).

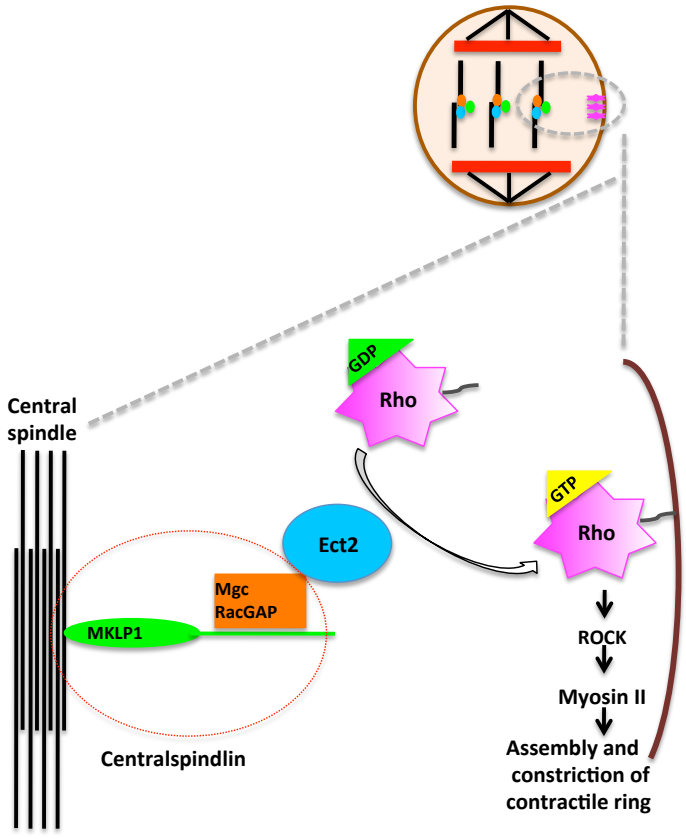

Fig 1.8 Action of ECT2 at the cytokinetic furrow: During anaphase, centralspindlin (MgcRacGAP and MKLP1) recruits ECT2 at the central spindle and activates it. ECT2 further activates Rho, which leads to the assembly and constriction of contractile ring via Myosin II (adapted from Kamijo et al, 2006)

To facilitate Rho activity during cytokinesis, ECT2 collaborates with a protein complex called centralspindlin (Fig 1.8). Centralspindlin is an evolutionarily conserved protein complex, which is necessary for assembly of the central spindle: a microtubule-based structure formed during cytokinesis (Mishima et al., 2002). It is a tetrameric complex that consists of a dimer of a kinesin protein called MKLP-1/ZEN-4 which is attached to a dimer of the Rho family GTPase activating protein (GAP) called CYK-4/MgcRacGAP (Glotzer, 2009). This complex stays at the centre of the central spindle during cytokinesis where it bundles microtubules, regulates RhoA and also recruits regulators of abscission (Glotzer, 2009) (Fig 1.8).

ECT2 recruitment to the central spindle is regulated in a cell-cycle dependent manner through its association with MgcRacGAP (Wolfe and Glotzer, 2009). ECT2 interaction with MgcRacGAP is

dependent on phosphorylation. The tandem BRCT repeats at the N-terminus of ECT2 mediate its interaction with MgcRacGAP (Yuce et al., 2005). Polo-like kinase 1 (Plk1) phosphorylates MgcRacGAP, thus creating a phosphoepitope recognized by the BRCT domain of ECT2 (Wolfe et al., 2009). This direct interaction of ECT2 with MgcRacGAP activates ECT2 by relieving its autoinhibition. Thus the GEF domain becomes free to catalyze its enzymatic reaction (Yuce et al., 2005). Recently, it has been reported that the extreme c-terminus of ECT2 directs it to the cortex during cell-division and ECT2 is actually present at the plasma membrane during anaphase to locally activate Rho. This targeting of ECT2 to the plasma membrane is controlled strictly in a spatio-temporal manner by centralspindlin and CDK1 (Su et al., 2011).

Since ECT2 is essential for successful cell-division, it is required at a very early stage during development in mice (Cook et al., 2013). Genetic ablation of ECT2 results in embryonic lethality and there were gross defects in the pre-implantation stage (Cook et al., 2013). Interestingly, MgcRacGAP, which acts to activate ECT2 during cytokinesis, also shows a similar embryonic lethality (Cook et al., 2013).

Regulation of the cell cycle

Using the Xenopus egg cell-free system it has been demonstrated that ECT2 acts as a potential regulator of spindle assembly (Tatsumoto et al., 2003). ECT2 depletion leads to disruption in attachment of microtubules to kinetochores and also causes prometaphase delay and abnormal chromosome segregation (Oceguera-Yanez et al., 2005). Although most of the studies to date have related to the M phase, increasing evidence suggest that it does play role in G1-S progression. Using inducible knockdown cell-lines, it has been shown that depletion of ECT2 can trigger cell-cycle arrest in G1 phase (Scoumanne and Chen, 2006).

As a polarity determinant

Cell polarization is very important for various biological processes like cell division, cell migration and establishment of apico-basal polarity. An evolutionarily conserved multi protein complex called Par3/Par6/aPKC functions to establish polarity in various organisms such as C.elegans, *Drosophila* and also in mammalian epithelial cell lines (Liu et al., 2004). The Rho family of proteins also plays a key role in the regulation of cell polarity. Recently, two research articles from Toru Miki's group have suggested that ECT2 is important for polarity. Using highly polarized MDCK cell lines and the yeast two-hybrid system, they have shown that ECT2 interacts with the polarity component Par6 and also associates with Par3 and PKCzeta (Liu et al., 2004). One of the mechanisms by which

ECT2 is thought to affect epithelial cell polarity is by recruiting Par3/Par6/aPKC polarity complex to the tight junctions (Liu et al., 2006)

1.8.2 Regulation of ECT2 function

ECT2 is subjected to several layers of regulation by intra-cellular localization, phosphorylation and inter- and intra-molecular interactions.

Phosphorylation of ECT2

Phosphorylation of ECT2 is a very dynamic and cell-cycle dependent process. The first studies on ECT2 phosphorylation were done by Toru Miki's group. They found that at G2/M phase, there is a mobility shift in the ECT2 band, and, when treated with phosphatase, this band reverts to normal size (Tatsumoto et al., 1999), thus suggesting that ECT2 gets phosphorylated at G2/M phase. The same group has suggested that the kinases, CDK1 and Plk1, phosphorylate ECT2 *in vitro* (Niiya et al., 2006). At G2/M phase, CDK1 phosphorylates ECT2 at Thr 412; which serves as a priming event to create a phosphospecific-binding site for Plk1 PBD and thus these two kinases act in concert to activate ECT2. Another report suggests that ECT2 gets phosphorylated at Thr 341 during G2/M phase by CDK1 (Hara et al., 2006). This mutation leads to a conformational change in ECT2, possibly leading to the open conformation, thus making it more accessible to other signaling molecules and further activating it (Hara et al., 2006).

The other phosphorylation site on ECT2 that regulate its spatio-temporal localization is Thr 815. CDK1 is believed to phosphorylate ECT2 at Thr 815 at G2/M phase (Hara et al., 2006; Niiya et al., 2006) and it has been shown recently that this modification prevents ECT2 from associating with the membrane before anaphase (Su et al., 2011). At the onset of anaphase CDK1 gets degraded and the subsequent dephosphorylation of this site leads to the translocation of ECT2 to the cortex thereby allowing it to activate Rho locally.

Intracellular localization

Tatsumoto *et al* studied localization of ECT2 in Hela cells. They reported that in interphase cells, ECT2 is predominantly nuclear, however as mitosis progresses and the nuclear envelope breaks down, ECT2 gets localized to the cytoplasm. This leads to its phosphorylation and activation (Tatsumoto et al., 1999). In metaphase, ECT2 accumulates in the region of the mitotic spindle. In late anaphase and telophase, ECT2 is at the midzone, the origin of the cleavage furrow. During

cytokinesis, ECT2 accumulates at the midbody, which joins the two daughter cells (Tatsumoto et al., 1999). Recently Su *et al* demonstrated that during cytokinesis both the PH domain and the PBC domain target ECT2 to the plasma membrane to perform its cortical activity (Su et al., 2011).

Localization of ECT2 affects its function. As opposed to nuclear ECT2, cytoplasmic ECT2 is believed to be a potent transforming factor, being capable of activating RhoA. Mutants of ECT2 in which the nuclear localization sequence (NLS) is truncated or disrupted get localized to cytoplasm throughout the cell cycle and show a transformed phenotype (Saito et al., 2004).

Interestingly, recent studies have established that ECT2 shows junctional localization. In MDCK cells, Liu *et al* observed that ECT2 is junctional and interacts with junctional proteins like Par3 (Liu et al., 2006).

Inter- and intra-molecular interactions

ECT2 remains in an inactive or partially active state through inter- or intra- molecular interactions. The tandem BRCT domains of ECT2 play an important role in regulating the biochemical and biological functions of ECT2 (Kim et al., 2005). The N-terminus of ECT2 associates very strongly with the catalytic c-terminus thus regulating its activity by autoinhibition. When this interaction is lost, the ECT2 structure opens up, the autoinhibition is released and this leads to activation of RhoA. Consistent with this model, deletion of the BRCT domain generates a mutant that is constitutively capable of binding to RhoA and has greater basal GEF activity than the full length form. However, this BRCT domain is also required for ECT2 function in cytokinesis, as absence of functional BRCT domain leads to a multinucleated phenotype, indicating a failure of cytokinesis (Kim et al., 2005).

ECT2 also interacts with other proteins to perform an array of diverse functions. One of the most intensively studied is its interaction with the centralspindlin complex in cytokinesis. The N-terminus of ECT2 also associates with MgcRacGAP and this interaction is important for its activity and also for its recruitment to the cortex (Yuce et al., 2005).

Another newly found interacting partner for ECT2 is KLEIP, which stands for Kelch-like ECT2 interacting protein (Hara et al., 2004). Identified by the yeast two-hybrid system with ECT2 as a bait, KLEIP showed significant interaction with F-actin in vitro and is localized to cell-cell junctions (Hara et al., 2004). The impact of ECT2 on the junctional function of KLEIP was not

analyzed, but the interaction with KELIP hints at a role for ECT2 in junctional/cytoskeleton regulation.

1.9 The Rho GAP: p190B Rho GAP

The p190RhoGAP family comprises two members: p190-A and p190-B, which are widely, expressed in human, rat, fly and mouse (Chakravarty et al., 2000; Settleman et al., 1992). Both of these members are encoded by separate genes and share 50% sequence homology (Ponik et al., 2013). Both are composed of three major motifs: a N-terminal GTP binding domain (GBD), a large middle domain responsible for various protein-protein interactions, and a C-terminal GAP domain (Tcherkezian and Lamarche-Vane, 2007). They show GAP activity towards RhoA, Rac 1 and Cdc42, with highest specificity for RhoA (Settleman et al., 1992). For the sake of this study, we will focus on p190-B Rho GAP.

1.9.1 Regulation of p190-B function

p190-B has been shown to mediate the cross talk between Rac and Rho GTPase (Bustos et al., 2008). Rac1 showed direct binding to p190-B but not to p190-A in a GTP-dependent manner (Bustos et al., 2008). This binding targets p190-B to the plasma membrane where it leads to loss of GTP-Rho from membranes (Bustos et al., 2008). Rac has also been shown to localize p190-B to junctions when MT dynamics were perturbed in MCF-7 epithelial cells (Ratheesh et al., 2012). Dominant-negative Rac or the Rac inhibitor NSC 23766 abolished junctional localization of p190-B induced by nocodazole. Also, a p190-B mutant that could not bind Rac was unable to localize at junctions, thus suggesting that p190-B recruitment to junctions responds to Rac signaling (Ratheesh et al., 2012).

Also, IGF-1 can phosphorylate p190-B at tyrosine-306; this does not alter its GAP activity but translocates it to plasma membrane domains enriched in lipid-rafts. These domains are known to concentrate GTP-Rho and thus redistribution of p190-B to the same subcellular compartment promotes its ability to inactivate Rho (Sordella et al., 2003). It is possible that other phosphorylation events take place on p190-B, but it has not been explored yet.

The Rnd GTPase protein (primarily Rnd3) has also been established to regulate p190-B localization and activity (Oinuma et al., 2012; Riou et al., 2013; Wennerberg et al., 2003). Using yeast two-hybrid assay and immunoprecipitation experiments, it has been shown that the middle domain of p190-B binds to Rnd proteins (Wennerberg et al., 2003). Further, the ‘rounding’ phenotype elicited

by Rnd1/Rnd3 overexpression in cells was not observed in the background of p190-B depletion, suggesting that this function is mediated by p190-B. Rnd1/3 were shown to increase the GAP activity of p190-B towards RhoA by two-fold (Wennerberg et al., 2003). Apart from influencing its activity, Rnd1 and Rnd3 also control p190-B localization by targeting it to lipid rafts of plasma membrane via their N-terminus KERRA sequence. This targeting enhances their interaction with p190-B and also promotes its GAP activity (Oinuma et al., 2012).

Rho-kinase or ROCK can also modulate the activity of p190-B. ROCK can phosphorylate both p190-A and p190-B. This phosphorylation inhibits the binding of p190-A to Rnd1, another Rnd family protein which can stimulate the GAP activity of p190-A. Thus, ROCK-mediated phosphorylation inhibits p190-A GAP activity and leads to 'sustained' Rho-signaling (Mori et al., 2009). Also, ROCK-mediated phosphorylation can critically inhibit the association of Rnd3 with p190-B (Riento et al., 2005b; Riou et al., 2013). Phosphorylation of Rnd3 at its c-terminus by ROCK1 leads to its translocation from the plasma membrane to the cytoplasm. In the cytoplasm, 14-3-3 binds to phosphorylated Rnd3 and sequesters it. This prevents Rnd3 from localizing to the membrane and activating p190-B and thus leads to active Rho signaling (Riou et al., 2013).

1.9.2 p190-B Rho GAP in cell-adhesion and morphogenesis

In morphogenesis

p190-B is ubiquitously expressed in various human tissues like brain, heart, kidney, liver and mammary glands (Burbelo et al., 1998; Chakravarty et al., 2003; Chakravarty et al., 2000). Independent reports suggest that p190-B is essential for ductal morphogenesis in mice (Chakravarty et al., 2000; Ponik et al., 2013). In breast epithelial cells, p190B is required to spatially modulate RhoA activity at cell-cell contacts in response to tensional homeostasis (Ponik et al., 2013). p190-B showed high expression in terminal end buds and its deficiency in mice led to abnormal ductal morphogenesis, and aberrant insulin signaling (Chakravarty et al., 2003). Conversely, overexpression of p190B in mice under the control of a tetracycline-inducible promoter caused complete disruption of mammary gland architecture (Vargo-Gogola et al., 2006). Further, p190-B is essential for normal size development in mice via modulation of CREB activity as mice lacking p190-B were 30% smaller in size than their normal counterparts (Sordella et al., 2002). In mouse brain, p190-B exhibits abundant expression and is required for its proper development (Matheson et al., 2006). Specifically, proper axonal tract development and neuronal differentiation requires p190-B function and thus its depletion leads to gross neurodevelopmental defects (Matheson et al., 2006).

In cell adhesion

Members of p190RhoGAP family have been shown to modulate cadherin-based junctions (Noren et al., 2003; Wildenberg et al., 2006). Earlier studies showed that cadherin engagement facilitates phosphorylation of p190RhoGAP by Src kinase (though these studies did not assess which p190 Rho GAP isoform was involved). This phosphorylation activates and targets p190 to adherens junctions and thus leads to GTP hydrolysis of Rho (Noren et al., 2003). According to a different study, Rac signaling can induce tyrosine phosphorylation and translocation of p190-A to membranes. Here p190-A interacts with p120 catenin, which directs its activity to adherens junctions and leads to local inactivation of the Rho-ROCK pathway. This transient reduction in contractility is required for the formation of nascent adherens junction formation and is initiated by Rac activation (Wildenberg et al., 2006).

At mature epithelial junctions, p190B GAP localization is inhibited by centralspindlin complex to ensure active Rho-signaling, which is crucial for cadherin stability and junctional tension (Ratheesh et al., 2012). Microtubules support the recruitment of centralspindlin complex at junctions and hence treating cells with nocodazole, or depleting centralspindlin by RNAi led to the enrichment of p190-B at junctions. Also, p190-B was responsible for reducing junctional Rho signaling upon nocodazole treatment: depleting p190-B restored junctional Rho-GTP levels in nocodazole treated cells to the levels similar to control cells (Ratheesh et al., 2012). Interestingly, p190-B localization responded to Rac signaling as treatment with a Rac inhibitor or expressing dominant-negative Rac abolished junctional p190-B, even when treated with nocodazole (Ratheesh et al., 2012). The model implies that at steady state, the centralspindlin component MgcRacGAP, being a GAP for Rac, inhibits its activity at junctions and thus disables Rac-mediated localization of p190-B. When MgcRacGAP is depleted or its transport to junctions is compromised by blocking microtubules, Rac gets activated, and thus recruits p190-B, which further inactivates Rho (Ratheesh et al., 2012).

1.10 RhoA during morphogenesis

Morphogenesis involves coordinated self-assembly of cells into multi-layer tissues that undergo deformations like bending, folding, tube formation and pitting to generate specialized 3-D structures (Guillot and Lecuit, 2013; Mammoto et al., 2013). To achieve this plasticity, the contractile cytoskeleton of the cell (composed of F-actin and myosin II filaments) generates mechanical forces, which are transmitted across ECM and cell-junctions. In epithelial cells, cadherin-based junctions sense these forces and this leads to an active multicellular process called junctional remodeling (Gomez et al., 2011; Halbleib and Nelson, 2006; Niessen et al., 2011). Since Rho sits at the

interface of adherens junction and cytoskeleton, it plays a significant role in this co-ordination between cytoskeleton and adhesion and thus is essential in all the aspects of tissue morphogenesis in mammals.

Rho acts as the prime regulator of actomyosin dependent changes in epithelial cells like neural-tube closure, gastrulation and tissue invagination (Mammoto et al., 2013). DRhoGEF2 (a Rho GEF) has been shown to be important for cell-shape changes required for gastrulation during early stages of Drosophila embryogenesis. Deletion of DRhoGEF2 or expression of dominant-negative Rho led to failure of gastrulation in Drosophila embryos (Barrett et al., 1997). Also, the transcription factor Twist induces the expression of T48 in Drosophila; this facilitates the concentration of RhoGEF2 at cell-junctions, thereby initiating mesoderm invagination by promoting Rho signaling (Kolsch et al., 2007). Rho-ROCK activity is crucial for apical constriction during fly gastrulation and is facilitated by the transcription factor Snail, along with Fog (Mammoto et al., 2013). The process of Drosophila germ-band extension involves epithelial remodelling by cell intercalation, which is regulated by Rho-signaling (Guillot and Lecuit, 2013; Mammoto et al., 2013). Here Rho-mediated activation of ROCK leads to polarized localization of Myosin filaments at the junctional interface undergoing shrinkage and at the same time regulates the preferential localization and stability of adherens junction components at the growing interface (Bertet et al., 2004). The Rho effector Drok in Drosophila acts downstream of Frizzled (Fz) and Dishevelled (Dsh) to modulate epithelial polarization events like orientation of wing hairs (Winter et al., 2001). In chick embryos, spatiotemporal co-ordination between Rho localization, Myosin activation and neural plate formation has been observed. Rho, along with its downstream effector Myosin, gets concentrated at the apical surface of neural plate cells, and inactivating this cascade by pharmacological inhibitors led to gross disruptions in neural plate morphogenesis (Kinoshita et al., 2008). ROCK has been shown to regulate neural tube closure in chick embryos (Nishimura and Takeichi, 2008; Wei et al., 2001). In the conditions when ROCK1 signal was diminished at the apical surface of neural plates, neural plates did not bend normally and did not close (Nishimura and Takeichi, 2008).

RhoA null knockout mice are embryonic lethal (Thumkeo et al., 2013), but using strategies like conditional knockouts and gene-targeting, it has been established that Rho activity is necessary for cell-cell adhesion and contractility in epithelial tissues during development in mice (Thumkeo et al., 2013).The Rho effector ROCK is necessary for eye-lid formation. ROCK mediated phosphorylation of MLC is required for eye-lid closure as gross defects in actin-filament organization and loss of pMLC were observed in the eyelid epithelia of ROCK-1 knockout mice (Shimizu et al., 2005). Similarly, using conditional knockout in lens epithelium, Chauhan *et al* reported that mutual

antagonism of Rho and Rac modulates apical constriction and the changes in cell-width required for epithelial invagination. RhoA, via ROCK, generates active Myosin and contractile actin, which is needed for apical constriction. Thus, when RhoA was deleted, lens pits were open in shape (Chauhan et al., 2011). In the central nervous system of mice, ablation of RhoA leads to disruption of adherens junctions, apical-basal cell polarity, aberrant proliferation of neuronal progenitors and defects in organization of ventricular region (Herzog et al., 2011; Katayama et al., 2011); thus RhoA is crucial for the integrity of neuroepithelium. In the lymphoid system, inhibition of RhoA activity by expressing C3-transferase leads to developmental block of T-cells because of defects in integrin dependent cell-matrix adhesion (Thumkeo et al., 2013). Another Rho effector, mDia is critical for the maintenance of adherens junctions and the apical actin belt in the neuroepithelium cells of mice. Loss of mDia led to disruption of adherens junction, the associated actin-belt and the apical-basal polarity in neuroepithelium cells during embryonic brain development in mice (Thumkeo et al., 2011). Modulation of cytoskeleton tension by Rho-ROCK signaling is essential for branching morphogenesis in embryonic mouse-lung (Moore et al., 2005). Also, depletion of RhoA in mice leads to abnormal platelet formation and blood coagulation (Pedersen and Brakebusch, 2012).

1.11 Perspective

Epithelial morphogenesis is a multistep process, which requires precise co-ordination between cell-cell adhesion and cytoskeleton (Mammoto et al., 2013). Adherens junctions constitute one of the major adhesion complexes in epithelia and give epithelia their characteristic cohesiveness. Despite acting as a static anchor for cells, adherens junctions undergo extensive reorganization to facilitate diverse morphogenetic processes like cell-shape change, intercalation, elongation or migration (Nishimura and Takeichi, 2009; Schock and Perrimon, 2002). Cadherin, one of the major component of adherens junctions, dictates the basic principles of morphogenesis right from embryonic development to adult tissue formation (Gumbiner, 2005). Cadherins, in association with catenins, respond to various developmental cues and enforce physiological changes like assembly and disassembly of junctions, cytoskeletal remodelling and cell sorting to name a few (Niessen et al., 2011). Given the variety of cellular processes that they are involved in, it is not surprising that these cadherin-based junctions collaborate with multiple signaling pathways, the best understood of them are Rho GTPases.

Rho GTPases are master regulators of various cellular processes, ranging from cell division to epithelial-mesenchymal transition (Etienne-Manneville and Hall, 2002). There is ample evidence from cell-based experiments suggesting that cadherins regulate the activity and localization of these

GTPases, and, in turn, these GTPases are required for the maintenance of these adhesive structures (McCormack et al., 2013). Once activated, these GTPases initiate a signaling cascade via their effectors (like ROCK), which ultimately translates into junctional remodelling. This enables epithelia to adopt various shapes and forms with 'ease' during development (Mammoto et al., 2013). However, its is important to emphasize here that most of the cellular and biochemical studies of Rho GTPases relied on cells in culture and one has to be cautious while discussing the relevance of these results in various developmental and physiological regulation occurring inside a organism. Nevertheless, the use of conditional knockouts and gene-targeting in mice have revealed that apart from few exception, most of the *in vivo* physiological roles of Rho align with its previously reported *in vitro* functions (Thumkeo et al., 2013).

Rho GTPases are molecular switches, with their spatio-temporal activity tightly controlled by GEFs, GAPs and GDIs (Etienne-Manneville and Hall, 2002). Various morphogenetic processes require these Rho GTPases to undergo rapid activations and inactivation cycle. This is facilitated by these regulatory molecules as they can specifically increase the levels of active GTPase at a distinct sub-cellular site during junctional remodelling (Guillot and Lecuit, 2013). Since most of these GEFs and GAPs harbor additional domains (kinase domain, protein-protein interactions domain), this further enables them to control their localization and activity in a very precise manner (Bos et al., 2007; Rossman et al., 2005); thus ensuring a strict regulation of Rho signaling. These GEFs and GAPs (Rho GDIs are not well-understood) act as the key mediators of Rho signaling and thus it is not surprising that the aberrant expression/activity/localization of these molecules lead to various physiological defects (Cook et al., 2013). Increasing evidence suggest that these GEFs and GAPs contribute to almost all the aspects of junctional biogenesis (McCormack et al., 2013) and are essential for the maintenance of junctional properties like tension and adhesiveness (Ratheesh et al., 2012; Terry et al., 2011). Conversely, in many cases the localization and activity of these molecules are itself modulated by these junctional components (Ratheesh et al., 2012; Terry et al., 2011). However, there are a number of outstanding questions like how these GEFs and GAPs specifically signal to Rho at a particular site, what are the molecular mechanisms controlling their localization, how do they achieve substrate-specificity *in vivo* and how do they mediate the cross-talk between various small GTPases.

Remodelling of adherens junction by Rho GTPases is a key feature of tissue morphogenesis and its dysregulation leads to various pathological conditions including cancer, neurodegenrative diseases and inflammatory diseases to name a few. So, to better understand the cross-talk between cadherins

and Rho GTPases and how this is linked to regulate cell-adhesion in development and disease, it is inevitable to study the molecules and mechanisms involved in Rho GTPase regulation.

1.12 Research Aims

Cadherins; one of the core constituents of zonula adherens mediates several aspects of morphogenesis and are being dynamically regulated in response to developmental or physiological signaling cues (Gumbiner, 2005). Cadherin act in concert with Rho GTPase signaling to acquire this plasticity during morphogenesis while holding the two cells together (Guillot and Lecuit, 2013; McCormack et al., 2013; Niessen et al., 2011). The contribution of Rho towards maintaining a functional zonula adherens in steady state and its dynamic reorganization during tissue-formation is undisputed but a great deal of knowledge is lacking about how Rho acts at junctions and what are the molecules that orchestrate this multi-faceted signalling event to generate a relevant biological response.

In my PHD, I have tried to address the above questions by dissecting the mechanistic and functional details of junctional Rho signalling. Following are the broad aims that will form the basis of each research chapter:

1. Understanding the significance of Rho-GEF ECT2 and Rho signaling for a functional zonula adherens.
2. Addressing the interplay between E-cadherin and Rho-GTPase signalling
3. Dissection of a novel feedback-loop co-ordinated by Myosin IIA, which sustains ZA Rho zone.

Note: ***This chapter has been extended in the form a of review article, which has been accepted for publication in "Current Topics in Developmental Biology". The accepted manuscript is attached in the Appendix 2.***

1.13 References

Amano, M., M. Ito, K. Kimura, Y. Fukata, K. Chihara, T. Nakano, Y. Matsuura, and K. Kaibuchi. 1996. Phosphorylation and activation of myosin by Rho-associated kinase (Rho-kinase). *J Biol Chem*. 271:20246-20249.

Amano, M., M. Nakayama, and K. Kaibuchi. 2010. Rho-kinase/ROCK: A key regulator of the cytoskeleton and cell polarity. *Cytoskeleton*. 67:545-554.

Anastasiadis, P.Z., S.Y. Moon, M.A. Thoreson, D.J. Mariner, H.C. Crawford, Y. Zheng, and A.B. Reynolds. 2000. Inhibition of RhoA by p120 catenin. *Nat Cell Biol*. 2:637-644.

Barrett, K., M. Leptin, and J. Settleman. 1997. The rho GTPase and a putative RhoGEF mediate a signaling pathway for the cell shape changes in Drosophila gastrulation. *Cell*. 91:905-915.

Beach, J.R., and T.T. Egelhoff. 2009. Myosin II recruitment during cytokinesis independent of centralspindlin-mediated phosphorylation. *J Biol Chem*. 284:27377-27383.

Benjamin, J.M., and W.J. Nelson. 2008. Bench to bedside and back again: molecular mechanisms of alpha-catenin function and roles in tumorigenesis. *Semin Cancer Biol*. 18:53-64.

Bertet, C., L. Sulak, and T. Lecuit. 2004. Myosin-dependent junction remodelling controls planar cell intercalation and axis elongation. *Nature*. 429:667-671.

Betapudi, V. 2010. Myosin II motor proteins with different functions determine the fate of lamellipodia extension during cell spreading. *PLoS One*. 5:e8560.

Betson, M., E. Lozano, J. Zhang, and V.M. Braga. 2002. Rac activation upon cell-cell contact formation is dependent on signaling from the epidermal growth factor receptor. *J Biol Chem*. 277:36962-36969.

Bishop, A.L., and A. Hall. 2000. Rho GTPases and their effector proteins. *Biochemical Journal*. 348:241-255.

Bos, J.L., H. Rehmann, and A. Wittinghofer. 2007. GEFs and GAPs: critical elements in the control of small G proteins. *Cell*. 129:865-877.

Braga, V. 2000. Epithelial cell shape: cadherins and small GTPases. *Exp Cell Res*. 261:83-90.

Braga, V.M. 2002. Cell-cell adhesion and signalling. *Curr Opin Cell Biol*. 14:546-556.

Braga, V.M., M. Betson, X. Li, and N. Lamarche-Vane. 2000. Activation of the small GTPase Rac is sufficient to disrupt cadherin-dependent cell-cell adhesion in normal human keratinocytes. *Mol Biol Cell*. 11:3703-3721.

Braga, V.M., L.M. Machesky, A. Hall, and N.A. Hotchin. 1997. The small GTPases Rho and Rac are required for the establishment of cadherin-dependent cell-cell contacts. *J Cell Biol*. 137:1421-1431.

Braga, V.M., and A.S. Yap. 2005. The challenges of abundance: epithelial junctions and small GTPase signalling. *Curr Opin Cell Biol*. 17:466-474.

Burbelo, P.D., A.A. Finegold, C.A. Kozak, Y. Yamada, and H. Takami. 1998. Cloning, genomic organization and chromosomal assignment of the mouse p190-B gene. *Bba-Gene Struct Expr*. 1443:203-210.

Burridge, K., and K. Wennerberg. 2004. Rho and Rac take center stage. *Cell*. 116:167-179.

Bustelo, X.R., V. Sauzeau, and I.M. Berenjeno. 2007. GTP-binding proteins of the Rho/Rac family: regulation, effectors and functions in vivo. *BioEssays*. 29:356-370.

Bustos, R.I., M.A. Forget, J.E. Settleman, and S.H. Hansen. 2008. Coordination of Rho and Rac GTPase Function via p190B RhoGAP. *Curr Biol*. 18:1606-1611.

Chakravarty, G., D. Hadsell, W. Buitrago, J. Settleman, and J.M. Rosen. 2003. p190-B RhoGAP regulates mammary ductal morphogenesis. *Molecular endocrinology*. 17:1054-1065.

Chakravarty, G., D. Roy, M. Gonzales, J. Gay, A. Contreras, and J.M. Rosen. 2000. p190-B, a Rho-GTPase-activating protein, is differentially expressed in terminal end buds and breast cancer. *Cell Growth Differ*. 11:343-354.

Chardin, P. 2006. Function and regulation of Rnd proteins. *Nat Rev Mol Cell Biol*. 7:54-62.

Chauhan, B.K., M. Lou, Y. Zheng, and R.A. Lang. 2011. Balanced Rac1 and RhoA activities regulate cell shape and drive invagination morphogenesis in epithelia. *Proceedings of the National Academy of Sciences of the United States of America*. 108:18289-18294.

Conti, M.A., and R.S. Adelstein. 2008. Nonmuscle myosin II moves in new directions. *J Cell Sci*. 121:11-18.

Conti, M.A., S. Even-Ram, C. Liu, K.M. Yamada, and R.S. Adelstein. 2004. Defects in cell adhesion and the visceral endoderm following ablation of nonmuscle myosin heavy chain II-A in mice. *J Biol Chem*. 279:41263-41266.

Cook, D.R., K.L. Rossman, and C.J. Der. 2013. Rho guanine nucleotide exchange factors: regulators of Rho GTPase activity in development and disease. *Oncogene*. 33(31):4021-35

Delva, E., D.K. Tucker, and A.P. Kowalczyk. 2009. The desmosome. *Cold Spring Harb Perspect Biol*. 1:a002543.

Drees, F., S. Pokutta, S. Yamada, W.J. Nelson, and W.I. Weis. 2005. Alpha-catenin is a molecular switch that binds E-cadherin-beta-catenin and regulates actin-filament assembly. *Cell*. 123:903-915.

Dulyaninova, N.G., R.P. House, V. Betapudi, and A.R. Bresnick. 2007. Myosin-IIA heavy-chain phosphorylation regulates the motility of MDA-MB-231 carcinoma cells. *Mol Biol Cell*. 18:3144-3155.

Etienne-Manneville, S., and A. Hall. 2002. Rho GTPases in cell biology. *Nature*. 420:629-635.

Fields, A.P., and V. Justilien. 2010. The guanine nucleotide exchange factor (GEF) Ect2 is an oncogene in human cancer. *Adv Enzyme Regul*. 50:190-200.

Fristrom, D. 1988. The cellular basis of epithelial morphogenesis. A review. *Tissue Cell*. 20:645-690.

Fukata, M., and K. Kaibuchi. 2001. Rho-family GTPases in cadherin-mediated cell-cell adhesion. *Nat Rev Mol Cell Biol*. 2:887-897.

Glotzer, M. 2005. The molecular requirements for cytokinesis. *Science*. 307:1735-1739.

Glotzer, M. 2009. The 3Ms of central spindle assembly: microtubules, motors and MAPs. *Nat Rev Mol Cell Biol*. 10:9-20.

Gomez, G.A., R.W. McLachlan, and A.S. Yap. 2011. Productive tension: force-sensing and homeostasis of cell-cell junctions. *Trends Cell Biol*. 21:499-505.

Goodwin, M., E.M. Kovacs, M.A. Thoreson, A.B. Reynolds, and A.S. Yap. 2003. Minimal mutation of the cytoplasmic tail inhibits the ability of E-cadherin to activate Rac but not phosphatidylinositol 3-kinase - Direct evidence of a role for cadherin-activated Rac signaling in adhesion and contact formation. *J Biol Chem*. 278:20533-20539.

Guillot, C., and T. Lecuit. 2013. Mechanics of epithelial tissue homeostasis and morphogenesis. *Science*. 340:1185-1189.

Gumbiner, B.M. 2005. Regulation of cadherin-mediated adhesion in morphogenesis. *Nat Rev Mol Cell Bio*. 6:622-634.

Halbleib, J.M., and W.J. Nelson. 2006. Cadherins in development: cell adhesion, sorting, and tissue morphogenesis. *Genes Dev*. 20:3199-3214.

Hara, T., M. Abe, H. Inoue, L.R. Yu, T.D. Veenstra, Y.H. Kang, K.S. Lee, and T. Miki. 2006. Cytokinesis regulator ECT2 changes its conformation through phosphorylation at Thr-341 in G2/M phase. *Oncogene*. 25:566-578.

Hara, T., H. Ishida, R. Raziuddin, S. Dorkhom, K. Kamijo, and T. Miki. 2004. Novel kelch-like protein, KLEIP, is involved in actin assembly at cell-cell contact sites of Madin-Darby canine kidney cells. *Molecular biology of the cell*. 15:1172-1184.

Harris, T.J.C., and U. Tepass. 2010. Adherens junctions: from molecules to morphogenesis. *Nat Rev Mol Cell Bio*. 11:502-514.
Hartsock, A., and W.J. Nelson. 2008. Adherens and tight junctions: structure, function and connections to the actin cytoskeleton. *Biochim Biophys Acta*. 1778:660-669.
Heissler, S.M., and D.J. Manstein. 2013. Nonmuscle myosin-2: mix and match. *Cell Mol Life Sci*. 70:1-21.
Herzog, D., P. Loetscher, J. van Hengel, S. Knusel, C. Brakebusch, V. Taylor, U. Suter, and J.B. Relvas. 2011. The Small GTPase RhoA Is Required to Maintain Spinal Cord Neuroepithelium Organization and the Neural Stem Cell Pool. *J Neurosci*. 31:5120-5130.
Huber, A.H., D.B. Stewart, D.V. Laurents, W.J. Nelson, and W.I. Weis. 2001. The cadherin cytoplasmic domain is unstructured in the absence of beta-catenin. A possible mechanism for regulating cadherin turnover. *J Biol Chem*. 276:12301-12309.
Ivetic, A., and A.J. Ridley. 2004. Ezrin/radixin/moesin proteins and Rho GTPase signalling in leucocytes. *Immunology*. 112:165-176.
Julian, L., and M.F. Olson. 2014. Rho-associated coiled-coil containing kinases (ROCK): Structure, regulation, and functions. *Small GTPases*. 5.
Kaibuchi, K., S. Kuroda, M. Fukata, and M. Nakagawa. 1999. Regulation of cadherin-mediated cell-cell adhesion by the Rho family GTPases. *Curr Opin Cell Biol*. 11:591-596.
Kametani, Y., and M. Takeichi. 2007. Basal-to-apical cadherin flow at cell junctions. *Nat Cell Biol*. 9:92-U118.
Kamijo, K., Ohara, N., Abe, M., Uchimura, T., Hosoya, H., Lee, J.S. and Miki, T. 2006. Dissecting the role of Rho-mediated signaling in contractile ring formation. *Mol.Biol.Cell*. 17, 43-55
Katayama, K.I., J. Melendez, J.M. Baumann, J.R. Leslie, B.K. Chauhan, N. Nemkul, R.A. Lang, C.Y. Kuan, Y. Zheng, and Y. Yoshida. 2011. Loss of RhoA in neural progenitor cells causes the disruption of adherens junctions and hyperproliferation. *P Natl Acad Sci USA*. 108:7607-7612.
Kawano, Y., Y. Fukata, N. Oshiro, M. Amano, T. Nakamura, M. Ito, F. Matsumura, M. Inagaki, and K. Kaibuchi. 1999. Phosphorylation of myosin-binding subunit (MBS) of myosin phosphatase by Rho-kinase in vivo. *J Cell Biol*. 147:1023-1038.
Kim, J.E., D.D. Billadeau, and J. Chen. 2005. The tandem BRCT domains of Ect2 are required for both negative and positive regulation of Ect2 in cytokinesis. *J Biol Chem*. 280:5733-5739.
Kimura, K., M. Ito, M. Amano, K. Chihara, Y. Fukata, M. Nakafuku, B. Yamamori, J. Feng, T. Nakano, K. Okawa, A. Iwamatsu, and K. Kaibuchi. 1996. Regulation of myosin phosphatase by Rho and Rho-associated kinase (Rho-kinase). *Science*. 273:245-248.
Kinoshita, N., N. Sasai, K. Misaki, and S. Yonemura. 2008. Apical accumulation of rho in the neural plate is important for neural plate cell shape change and neural tube formation. *Mol Biol Cell*. 19:2289-2299.
Kitzing, T.M., A.S. Sahadevan, D.T. Brandt, H. Knieling, S. Hannemann, O.T. Fackler, J. Grosshans, and R. Grosse. 2007. Positive feedback between Dia1, LARG, and RhoA regulates cell morphology and invasion. *Genes Dev*. 21:1478-1483.
Kolsch, V., T. Seher, G.J. Fernandez-Ballester, L. Serrano, and M. Leptin. 2007. Control of Drosophila gastrulation by apical localization of adherens junctions and RhoGEF2. *Science*. 315:384-386.
Kopp, J.B. 2010. Glomerular pathology in autosomal dominant MYH9 spectrum disorders: what are the clues telling us about disease mechanism?. *Kidney International.*78:130-133
Kovacs, E.M., R.G. Ali, A.J. McCormack, and A.S. Yap. 2002a. E-cadherin homophilic ligation directly signals through Rac and phosphatidylinositol 3-kinase to regulate adhesive contacts. *J Biol Chem*. 277:6708-6718.

Kovacs, E.M., M. Goodwin, R.G. Ali, A.D. Paterson, and A.S. Yap. 2002b. Cadherin-directed actin assembly: E-cadherin physically associates with the Arp2/3 complex to direct actin assembly in nascent adhesive contacts. *Current biology*.12:379-382.

Lee, C.S., C.K. Choi, E.Y. Shin, M.A. Schwartz, and E.G. Kim. 2010. Myosin II directly binds and inhibits Dbl family guanine nucleotide exchange factors: a possible link to Rho family GTPases. *J Cell Biol*. 190:663-674.

Li, Z.H., and A.R. Bresnick. 2006. The S100A4 metastasis factor regulates cellular motility via a direct interaction with myosin-IIA. *Cancer Res*. 66:5173-5180.

Liu, X.F., H. Ishida, R. Raziuddin, and T. Miki. 2004. Nucleotide exchange factor ECT2 interacts with the polarity protein complex Par6/Par3/protein kinase Czeta (PKCzeta) and regulates PKCzeta activity. *Mol Cell Biol*. 24:6665-6675.

Liu, X.F., S. Ohno, and T. Miki. 2006. Nucleotide exchange factor ECT2 regulates epithelial cell polarity. *Cellular signalling*. 18:1604-1615.

Mammoto, T., A. Mammoto, and D.E. Ingber. 2013. Mechanobiology and Developmental Control. *Annu Rev Cell Dev Bi*. 29:27-61.

Manke, I.A., D.M. Lowery, A. Nguyen, and M.B. Yaffe. 2003. BRCT repeats as phosphopeptide-binding modules involved in protein targeting. *Science*. 302:636-639.

Matheson, S.F., K.Q. Hu, M.R. Brouns, R. Sordella, J.D. VanderHeide, and J. Settleman. 2006. Distinct but overlapping functions for the closely related p190 RhoGAPs in neural development. *Dev Neurosci-Basel*. 28:538-550.

Matter, K., and M.S. Balda. 2007. Epithelial tight junctions, gene expression and nucleo-junctional interplay. *J Cell Sci*. 120:1505-1511.

McCormack, J., N.J. Welsh, and V.M. Braga. 2013. Cycling around cell-cell adhesion with Rho GTPase regulators. *J Cell Sci*. 126:379-391.

Meng, W.X., and M. Takeichi. 2009. Adherens Junction: Molecular Architecture and Regulation. *Csh Perspect Biol*. 1.

Miki, T., C.L. Smith, J.E. Long, A. Eva, and T.P. Fleming. 1993. Oncogene ect2 is related to regulators of small GTP-binding proteins. *Nature*. 362:462-465.

Mishima, M., S. Kaitna, and M. Glotzer. 2002. Central spindle assembly and cytokinesis require a kinesin-like protein/RhoGAP complex with microtubule bundling activity. *Dev Cell*. 2:41-54.

Moore, K.A., T. Polte, S. Huang, B. Shi, E. Alsberg, M.E. Sunday, and D.E. Ingber. 2005. Control of basement membrane remodeling and epithelial branching morphogenesis in embryonic lung by Rho and cytoskeletal tension. *Dev Dynam*. 232:268-281.

Mori, K., M. Amano, M. Takefuji, K. Kato, Y. Morita, T. Nishioka, Y. Matsuura, T. Murohara, and K. Kaibuchi. 2009. Rho-kinase Contributes to Sustained RhoA Activation through Phosphorylation of p190A RhoGAP. *J Biol Chem*. 284:5067-5076.

Niessen, C.M., D. Leckband, and A.S. Yap. 2011. Tissue organization by cadherin adhesion molecules: dynamic molecular and cellular mechanisms of morphogenetic regulation. *Physiol Rev*. 91:691-731.

Niiya, F., T. Tatsumoto, K.S. Lee, and T. Miki. 2006. Phosphorylation of the cytokinesis regulator ECT2 at G2/M phase stimulates association of the mitotic kinase Plk1 and accumulation of GTP-bound RhoA. *Oncogene*. 25:827-837.

Nishimura, T., and M. Takeichi. 2008. Shroom3-mediated recruitment of Rho kinases to the apical cell junctions regulates epithelial and neuroepithelial planar remodeling. *Development*. 135:1493-1502.

Nishimura, T., and M. Takeichi. 2009. Remodeling of the adherens junctions during morphogenesis. *Current topics in developmental biology*. 89:33-54.

Nobes, C.D., I. Lauritzen, M.G. Mattei, S. Paris, A. Hall, and P. Chardin. 1998. A new member of the Rho family, Rnd1, promotes disassembly of actin filament structures and loss of cell adhesion. *J Cell Biol*. 141:187-197.

Noren, N.K., W.T. Arthur, and K. Burridge. 2003. Cadherin engagement inhibits RhoA via p190RhoGAP. *J Biol Chem*. 278:13615-13618.
Noren, N.K., C.M. Niessen, B.M. Gumbiner, and K. Burridge. 2001. Cadherin engagement regulates Rho family GTPases. *J Biol Chem*. 276:33305-33308.
Oceguera-Yanez, F., K. Kimura, S. Yasuda, C. Higashida, T. Kitamura, Y. Hiraoka, T. Haraguchi, and S. Narumiya. 2005. Ect2 and MgcRacGAP regulate the activation and function of Cdc42 in mitosis. *J Cell Biol*. 168:221-232.
Oinuma, I., K. Kawada, K. Tsukagoshi, and M. Negishi. 2012. Rnd1 and Rnd3 targeting to lipid raft is required for p190 RhoGAP activation. *Mol Biol Cell*. 23:1593-1604.
Overduin, M., T.S. Harvey, S. Bagby, K.I. Tong, P. Yau, M. Takeichi, and M. Ikura. 1995. Solution Structure of the Epithelial Cadherin Domain Responsible for Selective Cell-Adhesion. *Science*. 267:386-389.
Pedersen, E., and C. Brakebusch. 2012. Rho GTPase function in development: How in vivo models change our view. *Exp Cell Res*. 318:1779-1787.
Perez-Moreno, M., and E. Fuchs. 2006. Catenins: keeping cells from getting their signals crossed. *Dev Cell*. 11:601-612.
Piekny, A., M. Werner, and M. Glotzer. 2005. Cytokinesis: welcome to the Rho zone. *Trends Cell Biol*. 15:651-658.
Ponik, S.M., S.M. Trier, M.A. Wozniak, K.W. Eliceiri, and P.J. Keely. 2013. RhoA is down-regulated at cell-cell contacts via p190RhoGAP-B in response to tensional homeostasis. *Mol Biol Cell*. 24:1688-1699.
Priya, R., A.S. Yap, and G.A. Gomez. 2013. E-cadherin supports steady-state Rho signaling at the epithelial zonula adherens. *Differentiation*; 86:133-140.
Ratheesh, A., G.A. Gomez, R. Priya, S. Verma, E.M. Kovacs, K. Jiang, N.H. Brown, A. Akhmanova, S.J. Stehbens, and A.S. Yap. 2012. Centralspindlin and alpha-catenin regulate Rho signalling at the epithelial zonula adherens. *Nat Cell Biol*. 14:818-828.
Ratheesh, A., R. Priya, and A.S. Yap. 2013. Coordinating Rho and Rac: the regulation of Rho GTPase signaling and cadherin junctions. *Progress in molecular biology and translational science*. 116:49-68.
Ratheesh, A., and A.S. Yap. 2012. A bigger picture: classical cadherins and the dynamic actin cytoskeleton. *Nat Rev Mol Cell Bio*. 13:673-679.
Riento, K., and A.J. Ridley. 2003. Rocks: multifunctional kinases in cell behaviour. *Nat Rev Mol Cell Biol*. 4:446-456.
Riento, K., N. Totty, P. Villalonga, R. Garg, R. Guasch, and A.J. Ridley. 2005a. RhoE function is regulated by ROCK I-mediated phosphorylation. *Embo Journal*. 24:1170-1180.
Riento, K., P. Villalonga, R. Garg, and A. Ridley. 2005b. Function and regulation of RhoE. *Biochem Soc T*. 33:649-651.
Riou, P., S. Kjaer, R. Garg, A. Purkiss, R. George, R.J. Cain, G. Bineva, N. Reymond, B. McColl, A.J. Thompson, N. O'Reilly, N.Q. McDonald, P.J. Parker, and A.J. Ridley. 2013. 14-3-3 proteins interact with a hybrid prenyl-phosphorylation motif to inhibit G proteins. *Cell*. 153:640-653.
Rosenberg, M., and S. Ravid. 2006. Protein kinase Cgamma regulates myosin IIB phosphorylation, cellular localization, and filament assembly. *Mol Biol Cell*. 17:1364-1374.
Rossman, K.L., C.J. Der, and J. Sondek. 2005. GEF means go: turning on RHO GTPases with guanine nucleotide-exchange factors. *Nat Rev Mol Cell Biol*. 6:167-180.
Saito, S., X.F. Liu, K. Kamijo, R. Raziuddin, T. Tatsumoto, I. Okamoto, X. Chen, C.C. Lee, M.V. Lorenzi, N. Ohara, and T. Miki. 2004. Deregulation and mislocalization of the cytokinesis regulator ECT2 activate the Rho signaling pathways leading to malignant transformation. *J Biol Chem*. 279:7169-7179.

Sandquist, J.C., and A.R. Means. 2008. The C-terminal tail region of nonmuscle myosin II directs isoform-specific distribution in migrating cells. *Mol Biol Cell*. 19:5156-5167.
Schock, F., and N. Perrimon. 2002. Molecular mechanisms of epithelial morphogenesis. *Annu Rev Cell Dev Biol*. 18:463-493.
Schofield, A.V., and O. Bernard. 2013. Rho-associated coiled-coil kinase (ROCK) signaling and disease. *Critical reviews in biochemistry and molecular biology*. 48:301-316.
Scoumanne, A., and X. Chen. 2006. The epithelial cell transforming sequence 2, a guanine nucleotide exchange factor for Rho GTPases, is repressed by p53 via protein methyltransferases and is required for G1-S transition. *Cancer Res*. 66:6271-6279.
Settleman, J., V. Narasimhan, L.C. Foster, and R.A. Weinberg. 1992. Molecular cloning of cDNAs encoding the GAP-associated protein p190: implications for a signaling pathway from ras to the nucleus. *Cell*. 69:539-549.
Shewan, A.M., M. Maddugoda, A. Kraemer, S.J. Stehbens, S. Verma, E.M. Kovacs, and A.S. Yap. 2005. Myosin 2 is a key Rho kinase target necessary for the local concentration of E-cadherin at cell-cell contacts. *Mol Biol Cell*. 16:4531-4542.
Shimizu, Y., D. Thumkeo, J. Keel, T. Ishizaki, H. Oshima, M. Oshima, Y. Noda, F. Matsumura, M.M. Taketo, and S. Narumiya. 2005. ROCK-I regulates closure of the eyelids and ventral body wall by inducing assembly of actomyosin bundles. *J Cell Biol*. 168:941-953.
Smith, A.L., M.R. Dohn, M.V. Brown, and A.B. Reynolds. 2012. Association of Rho-associated protein kinase 1 with E-cadherin complexes is mediated by p120-catenin. *Mol Biol Cell*. 23:99-110.
Smutny, M., H.L. Cox, J.M. Leerberg, E.M. Kovacs, M.A. Conti, C. Ferguson, N.A. Hamilton, R.G. Parton, R.S. Adelstein, and A.S. Yap. 2010. Myosin II isoforms identify distinct functional modules that support integrity of the epithelial zonula adherens. *Nat Cell Biol*. 12:696-702.
Smutny, M., S.K. Wu, G.A. Gomez, S. Mangold, A.S. Yap, and N.A. Hamilton. 2011. Multicomponent analysis of junctional movements regulated by myosin II isoforms at the epithelial zonula adherens. *PLoS One*. 6:e22458.
Sordella, R., M. Classon, K.Q. Hu, S.F. Matheson, M.R. Brouns, B. Fine, L. Zhang, H. Takami, Y. Yamada, and J. Settleman. 2002. Modulation of CREB activity by the Rho GTPase regulates cell and organism size during mouse embryonic development. *Dev Cell*. 2:553-565.
Sordella, R., W. Jiang, G.C. Chen, M. Curto, and J. Settleman. 2003. Modulation of Rho GTPase signaling regulates a switch between adipogenesis and myogenesis (vol 113, pg 147, 2003). *Cell*. 113:547-547.
Su, K.C., T. Takaki, and M. Petronczki. 2011. Targeting of the RhoGEF Ect2 to the Equatorial Membrane Controls Cleavage Furrow Formation during Cytokinesis. *Dev Cell*. 21:1104-1115.
Takaishi, K., T. Sasaki, H. Kotani, H. Nishioka, and Y. Takai. 1997. Regulation of cell-cell adhesion by rac and rho small G proteins in MDCK cells. *J Cell Biol*. 139:1047-1059.
Tatsumoto, T., H. Sakata, M. Dasso, and T. Miki. 2003. Potential roles of the nucleotide exchange factor ECT2 and Cdc42 GTPase in spindle assembly in Xenopus egg cell-free extracts. *J Cell Biochem*. 90:892-900.
Tatsumoto, T., X.Z. Xie, R. Blumenthal, I. Okamoto, and T. Miki. 1999. Human ECT2 is an exchange factor for Rho GTPases, phosphorylated in G2/M phases, and involved in cytokinesis. *J Cell Biol*. 147:921-927.
Tcherkezian, J., and N. Lamarche-Vane. 2007. Current knowledge of the large RhoGAP family of proteins. *Biology of the cell / under the auspices of the European Cell Biology Organization*. 99:67-86.

Terry, S.J., C. Zihni, A. Elbediwy, E. Vitiello, I.V.L.C. San, M.S. Balda, and K. Matter. 2011. Spatially restricted activation of RhoA signalling at epithelial junctions by p114RhoGEF drives junction formation and morphogenesis. *Nat Cell Biol*. 13:159-U120.

Thumkeo, D., R. Shinohara, K. Watanabe, H. Takebayashi, Y. Toyoda, K. Tohyama, T. Ishizaki, T. Furuyashiki, and S. Narumiya. 2011. Deficiency of mDia, an actin nucleator, disrupts integrity of neuroepithelium and causes periventricular dysplasia. *PLoS One*. 6:e25465.

Thumkeo, D., S. Watanabe, and S. Narumiya. 2013. Physiological roles of Rho and Rho effectors in mammals. *European journal of cell biology*. 92:303-315.

Totsukawa, G., Y. Yamakita, S. Yamashiro, D.J. Hartshorne, Y. Sasaki, and F. Matsumura. 2000. Distinct roles of ROCK (Rho-kinase) and MLCK in spatial regulation of MLC phosphorylation for assembly of stress fibers and focal adhesions in 3T3 fibroblasts. *J Cell Biol*. 150:797-806.

Van Aelst, L., and M. Symons. 2002. Role of Rho family GTPases in epithelial morphogenesis. *Genes Dev*. 16:1032-1054.

Vargo-Gogola, T., B.M. Heckman, E.J. Gunther, L.A. Chodosh, and J.M. Rosen. 2006. P190-B Rho GTPase-activating protein overexpression disrupts ductal morphogenesis and induces hyperplastic lesions in the developing mammary gland. *Molecular endocrinology*. 20:1391-1405.

Vicente-Manzanares, M., X. Ma, R.S. Adelstein, and A.R. Horwitz. 2009. Non-muscle myosin II takes centre stage in cell adhesion and migration. *Nat Rev Mol Cell Biol*. 10:778-790.

Wang, Y., X.R. Zheng, N. Riddick, M. Bryden, W. Baur, X. Zhang, and H.K. Surks. 2009. ROCK isoform regulation of myosin phosphatase and contractility in vascular smooth muscle cells. *Circulation research*. 104:531-540.

Wei, L., W. Roberts, L. Wang, M. Yamada, S.X. Zhang, Z.Y. Zhao, S.A. Rivkees, R.J. Schwartz, and K. Imanaka-Yoshida. 2001. Rho kinases play an obligatory role in vertebrate embryonic organogenesis. *Development*. 128:2953-2962.

Wennerberg, K., M.A. Forget, S.M. Ellerbroek, W.T. Arthur, K. Burridge, J. Settleman, C.J. Der, and S.H. Hansen. 2003. Rnd proteins function as RhoA antagonists by activating p190 RhoGAP. *Curr Biol*. 13:1106-1115.

Werner, M., and M. Glotzer. 2008. Control of cortical contractility during cytokinesis. *Biochem Soc Trans*. 36:371-377.

Wheeler, A.P., and A.J. Ridley. 2004. Why three Rho proteins? RhoA, RhoB, RhoC, and cell motility. *Exp Cell Res*. 301:43-49.

Wheelock, M.J., and K.R. Johnson. 2003. Cadherin-mediated cellular signaling. *Curr Opin Cell Biol*. 15:509-514.

Wildenberg, G.A., M.R. Dohn, R.H. Carnahan, M.A. Davis, N.A. Lobdell, J. Settleman, and A.B. Reynolds. 2006. p120-catenin and p190RhoGAP regulate cell-cell adhesion by coordinating antagonism between Rac and Rho. *Cell*. 127:1027-1039.

Winter, C.G., B. Wang, A. Ballew, A. Royou, R. Karess, J.D. Axelrod, and L.Q. Luo. 2001. Drosophila Rho-associated kinase (Drok) links frizzled-mediated planar cell polarity signaling to the actin cytoskeleton. *Cell*. 105:81-91.

Wolfe, B.A., and M. Glotzer. 2009. Single cells (put a ring on it). *Genes Dev*. 23:896-901.

Wolfe, B.A., T. Takaki, M. Petronczki, and M. Glotzer. 2009. Polo-like kinase 1 directs assembly of the HsCyk-4 RhoGAP/Ect2 RhoGEF complex to initiate cleavage furrow formation. *PLoS Biol*. 7:e1000110.

Wu, D., M. Asiedu, R.S. Adelstein, and Q.Z. Wei. 2006. A novel guanine nucleotide exchange factor MyoGEF is required for cytokinesis. *Cell Cycle*. 5:1234-1239.

Wu, S.K., G.A. Gomez, M. Michael, S. Verma, H.L. Cox, J.G. Lefevre, R.G. Parton, N.A. Hamilton, Z. Neufeld, and A.S. Yap. 2014. Cortical F-actin stabilization generates apical-lateral patterns of junctional contractility that integrate cells into epithelia. *Nat Cell Biol*. 16:167-178.

Yamada, S., and W.J. Nelson. 2007. Localized zones of Rho and Rac activities drive initiation and expansion of epithelial cell-cell adhesion. *J Cell Biol*. 178:517-527.
Yap, A.S., and E.M. Kovacs. 2003. Direct cadherin-activated cell signaling: a view from the plasma membrane. *J Cell Biol*. 160:11-16.
Yuce, O., A. Piekny, and M. Glotzer. 2005. An ECT2-centralspindlin complex regulates the localization and function of RhoA. *J Cell Biol*. 170:571-582.

Chapter 2: An ECT2-Rho pathway supports the zonula adherens

2.1 Introduction

The Zonula adherens (ZA) mediates cell-cell interaction between epithelial cells and a functional ZA is indispensible for the maintenance and morphology of the epithelial sheets that line our body (Niessen et al., 2011; Guillot and Lecuit, 2013; Gumbiner, 2005; Harris and Tepass, 2010; Munjal and Lecuit, 2014). Recent studies reveal that the ZA is not a static site of adhesion but modulates and, in turn, is modulated by a host of signaling molecules; Rho GTPases are among one of them (Braga, 2000; Braga, 2002; Braga and Yap, 2005; McCormack et al., 2013). Rho acts as the principal regulator in variety of cellular processes like epithelial remodelling, polarity, migration and trafficking (Jaffe and Hall, 2005; Ratheesh et al., 2013; Thumkeo et al., 2013). To understand the cell biology of Rho, it is essential to identify the molecular mechanisms that control its activity and localization. Being a potent molecular switch, Rho is subjected to a very tight spatio-temporal regulation by GEFs and GAPs (Cherfils and Zeghouf, 2013). These regulatory molecules have profound implications for many cellular events and their deviation from the normal functioning can have deleterious effects like cancer (Bos et al., 2007; Etienne-Manneville and Hall, 2002).

ECT2 is a well-established Rho GEF, and is central to the process of cytokinesis (Yuce et al., 2005). It was initially identified as an oncogene, important for cell cycle and the transformed phenotype (Fields and Justilien, 2010; Yuce et al., 2005). However there is emerging evidence indicating that it performs extra-cytokinetic functions such as regulation of polarity via conserved Par proteins (Liu et al., 2004) or modulation of the actin cytoskeleton by interacting with the junctional protein KLEIP (Hara et al., 2004).

The zonula adherens is the major site for Rho signalling where Rho functions to confer junctional integrity and stability. But the precise mechanistic details of the Rho functions at ZA remain a largely unexplored area. In this research chapter, I will give an overview of how Rho modulates various core components of the ZA to maintain its organization via its GEF ECT2.

The major part of the results presented in this chapter has been published in Nature Cell Biology, 2012 Aug; 14(8): 818-28 of which I am second author. The paper is attached in Appendix 1.

2.2 Material and Methods

Cell culture, transfection and Plasmids

MCF-7 and Caco-2 cells were cultured in DMEM and RPMI complete growth medium respectively and grown at 37ºC in 5% CO_2 atmosphere. Cells were transfected using Lipofectamine 2000 (Invitrogen) for expression constructs according to manufacturer's instructions and analysed 24-48 hours after transfection.

EGFP Myosin IIA (GFP-Myo IIA) and E-cadherin GFP constructs have been described previously (Smutny et al., 2010; Smutny et al., 2011). EGFP-ECT2 was a kind gift from Robert Saint (Australian National University).

A lentivirus-based shRNA system was used to deplete ECT2 in MCF-7 cells. The lentivirus expression vector pLL5.0 (backbone pLL3.7) and the third-generation packaging constructs pMDLg/pRRE, RSV-Rev and pMD.G were gifts from Jim Bear (UNC Chapel Hill, North Carolina, USA). Algorithms from Dharmacon were used to predict sequences that would lead to silencing of human ECT2 (NM_018098). Predicted sequences were used to design shRNAs containing a stem loop sequence based on previous studies, and these were cloned into the lentivirus expression vector LentiLox pLL5.0 yielding pLL5.0 Cherry-sh-ECT2. In brief, shRNA was cloned downstream of the U6 promoter (*Hpa*I and *Xho*I) into a modified version of lentivirus expression vector pLL5.0 carrying a soluble cherry as reporter gene (pLL5.0 Cherry-shECT2).

The generation and titer of lentivirus stocks has been described previously (Smutny et al., 2011). MCF-7 cells were infected with lentiviral particles at a multiplicity of infection of 10 per cell as described previously (Smutny et al., 2011) and used within the first week after infection.

Antibodies and Inhibitors

Primary antibodies used in this study were: (1) mouse monoclonal antibody (mAb) against the cytoplasmic domain of E-cadherin (transduction labs, cat #610182) 1:2500; (2) mouse mAb HECD-1 against the ectodomain of E-cadherin 1:50 (a gift from Peggy Wheelock, University of Nebraska, Omaha, NE; with the permission of M. Takeichi); (3) rabbit polyclonal antibody (pAb) for non-muscle myosin IIA heavy chain (Covance, cat #PRB-440P),1:1000); (4) rabbit pAb for non-muscle myosin IIB heavy chain (Covance, cat #PRB-445P),1:1000); (5) rabbit pAb (cat #A-6455)(1:2000) or mouse mAb (cat #A-1120)(1:200) against GFP (Molecular Probes/Invitrogen); (6) rabbit pAb (Invitrogen, cat #61-7300)(1:300) and (7) mouse mAb (Invitrogen cat #33-9100) against human ZO-1(1:300); (8) mouse monoclonal antibody against α catenin (Transduction Laboratories cat #610194),1:500); (9) rabbit polyclonal antibody against α-catenin (Zymed Laboratories cat #711200),1:500); (10) rabbit polyclonal antibody against α-catenin (a gift from Dr. Barry

Gumbiner, University of Virginia School of Medicine, USA; 1:100); mouse mAbs against (11) RhoA (SantaCruz Biotechnology Inc,, cat #sc418, 1:100), (12) MKLP1(SantaCruz Biotechnology Inc, cat #sc-136473,1:300), (13) RacGAP1(SantaCruz Biotechnology Inc, cat #sc-166477, 1:300); and rabbit polyclonal antibodies against (14) ECT2 (SantaCruz Biotechnology Inc, cat #sc:1005, 1:100) and Millipore (cat #07-1364), 1:50), (15) MKLP1(cat #sc: 22793, 1:50) and (16) RacGAP1(cat #sc:98617, 1:50) (SantaCruz Biotechnology Inc); mouse mABs against (17) p190 (cat #610150, 1:50) and (18) p190B (cat #611612, 1:50) (BD Biosciences); (19) mouse mAB against β tubulin (cat #T4026) and (20) FLAG (cat #F4042) (Sigma, 1:500) ; (21) rat monoclonal anti-EB1/EB3 and (23) rat-anti-EB1 and rat anti-EB3 , 1:50, (cat # 010815H11, Absea, China).

F-actin was stained with AlexaFluor 488-phalloidin or 594-phalloidin (1:1,000 dilution; Invitrogen). Secondary antibodies were species-specific antibodies conjugated with AlexaFluor 488, 594 or 647 (Invitrogen) (1:500) for immunofluorescence, or with horseradish peroxidase (Bio-Rad Laboratories) (1:5000) for immunoblotting.

Immunofluorescence microscopy

Cells were fixed with 10% TCA on ice for 15 minutes for RhoA staining. For visualizing F-actin, cells were fixed with 4% paraformaldehyde in PBS at 22°C for 20 min. For both of the above, cells were subsequently permeabilized with 0.25% Triton-X-100 in PBS for 5 min at room temperature. Otherwise, cells were fixed with ice-cold methanol for 5 minutes on ice.

Wide-field images were acquired with either an IX81 Olympus epi-illumination microscope (60X and 100X, 1.4 numerical aperture objectives) and a Hamamatsu Orca-1 ER camera driven by Metamorph imaging software (version 7; Universal Imaging) or a Personal Deltavision deconvolution microscope (Applied Precision, 60 X, 1.4 numerical aperture objectives) and a Roper Coolsnap HQ2 monochrome camera. Confocal images were captured with a Zeiss 510 or a Zeiss 710 Meta laser-scanning confocal microscope, and *z*-stacks were processed with ImageJ (National Institutes of Health) software. Background correction, contrast adjustment and Z-projections of raw data images were performed with ImageJ, Imaris (Bitplane) or Photoshop (Adobe).

Fluorescence intensity at contacts was quantitated using the line scan function in ImageJ as described earlier (Smutny et al., 2011).

FRAP Analysis

Cells

To address the issue of E-cadherin turnover, E-cadherin GFP was expressed in an endogenous E-cadherin knockdown background by infecting MCF-7 cells with GFP tagged E-cadherin, which

simultaneously expresses a shRNA against E-cadherin. ECT2 and myosin IIA KD was performed by coinfecting the above cells with either lentivirus encoding shRNA designed against the 3'UTR region of ECT2 or lentivirus encoding shRNA against Myosin IIA (MYH9, (Smutny et al., 2010). 48 hs after infection cells were split into glass bottom dishes (N 1.5, MatTek corporation, MA) and grown to full confluency. For image acquisition, cell were washed and incubated in the presence of imaging media (Hank's balanced salt solution supplemented with 10 mM HEPES pH 7.4 and 5 mM $CaCl_2$). For these experiments, only cells co-expressing E-cadherin GFP and cherry were chosen to ensure the presence of knockdown phenotype. For inhibition of Rho signaling, cells were treated with 500 ng/µl of cell permeable C3 Transferase (Rho inhibitor I, Cytoskeleton) in imaging media for 1 hour, washed off and incubated in the same. Cells with *en face* contacts were chosen which allowed us to precisely identify and photobleach the zonula adherens.

Image acquisition and analysis

FRAP experiments were performed on a LSM 510 Meta Zeiss confocal microscope with a heated stage maintained at 37°C. Images (416x416 pixels, 0.086 um/pixel) were acquired using 60x objective, 1.4 NA oil Plan Apochromat immersion lens at 4X digital magnification with 0.7 um optical section. Time-lapse images were acquired before and after photo bleaching with an interval of approx. 5 seconds per frame for the total time of 280 seconds. A constant ROI, 2.8 x 1.7 um with the longer axis parallel to the cell-cell contact, was marked for each experiment and the E-cadherin-GFP was bleached with 50 iterations of 488 nm laser with 100% transmission resulting in maximum bleach of approx. 70%.

Image analysis was performed using Image J. Noise on images was reduced by applying a median filter of 2 pixels radii. Focal drifts were eliminated using Turbo-reg plug-in of Image J. To calculate FRAP profiles, a ROI at the bleached GFP-E-cadherin area was marked and the plug-in FRAP profiler (McMaster University, Canada) was applied to obtain fluorescence intensity profiles. Fluorescence intensities were normalized to pre-bleach values and imported into Prism software for statistics. Data from 11 replicates (3 independent experiments) were pooled and fitted to the equation:

$$\frac{F(t)}{F(0)} = Mf \cdot (1 - e^{-\frac{\ln 2 \cdot t}{t_{1/2}}})$$

where F is the average fluorescence of the ROI, Mf is the mobile fraction, t ½ is the half time of recovery and t is time in seconds. Data shown is the average ± SEM and statistical significance assessed by t-test.

Trypsin protection Assay

The surface expression of E-cadherin was measured by sensitivity to surface trypsinization (as described previously (Verma et al., 2004). In brief, cells were incubated with crystalline trypsin (0.05% wt/vol) in HBSS in the presence of either 2 mM CaCl2 or 5 mM EDTA for 20 min at 37°C. Cells were collected and lysed directly into Laemmli sample buffer. Equal volumes of the cellular extracts were separated by SDS-PAGE followed by Western analysis with antibodies specific for the ectodomain of E-cadherin (HECD-1) and β-tubulin (as a loading control).

Laser Ablation

The cells and culture conditions used in ablation experiments were similar to those used for the FRAP experiments**.**

Ablation experiments were performed on a LSM 510 Meta Zeiss confocal microscope equipped with a heating stage set to 37 ^{o}C for the duration of the experiment. Images (300x300 pixels, 0.19 um/pixel) were acquired using 63x objective, 1.4 NA oil Plan Apochromat immersion lens at 1.5X digital magnification and pinhole adjusted to 3 Airy units to obtain optical sections 2 um thick. Time-lapse images were acquired before (3 frames) and after (4 frames) ablation with an interval of 15 seconds per frame. For ablation, a tuneable Ti:Sapphire laser (Chameleon Ultra, Coherent Scientific, US) tuned to 790 nm was used to ablate cell contacts labeled with *E-cadherin-GFP*. A constant ROI, 3.8 x 0.6 um with the longer axis orthogonal to the cell-cell contact, was marked for each experiment and ablated with 30 iterations of 790 nm laser with 50 % transmission. GFP fluorescence was determined before and after the induced ablation using a 488 nm laser for excitation and 500-550 nm emission filter.

Image analysis was performed using Image J. The distance (d) between vertices that define the ablated contact was measured as a function of time (t). Then obtained values d(t) were subtracted from the average distance before the ablation step d(0). After plotting the resulting values were fitted to the following equation:

$$d(t) - d(0) = plateau \cdot (1 - e^{-ktt})$$

Then the instantaneous recoil (rate of recoil at t=0 s) was determined as:

$$\text{Instantaneous recoil} = plateau \cdot k$$

Average instantaneous recoil was determined for 10 to 15 contacts in three independent experiments and then normalized to the value observed in control conditions.

3-D Cyst culture

Caco-2 cells were transduced with lentivirus encoding ECT2 shRNA. Two days after infection cells were trypsinized, counted and diluted to 1.5 X 10^4 cells/ml in RPMI medium. This cell suspenion

was mixed with matrigel (BD cat# 356230) at a final concentration of 2%. Eight well chamber-slides (#Nun155411) were coated thinly with 100% matrigel and let to settle at 37 ° for 15 minutes. The cell suspenion was plated in these wells and placed in the 37 ° degree incubator with media changes (RPMI with 2% matrigel) every fourth day. Cysts were ready in 10-12 days.

For immunofluorescence, cysts were removed from the incubator, washed twice with ice-cold PBS and fixed with 4% PFA in PBS for 30 minutes at room temperature. This was followed by two washes with ice-cold PBS, permeabilization with 0.5% Triton-X-100 in PBS for 15 minutes and blocking with 3% BSA (1 hour) at room temperature. Cysts were incubated with primary antibody over night at 4° and with secondary antibody for 1-2 hour at room temperature. After two PBS washes, cysts were incubated with the nuclear dye DAPI (1:500 in PBS) for 30 minutes which was again followed by two quick PBS washes. The cysts were stored in PBS and imaged within 24-36 hours.

2.3 Results and Discussion

2.3.1: ECT2 localizes to zonula adherens and regulates its integrity

I started with an aim to understand the molecular and mechanistic detail of Rho functions at ZA in a detailed fashion. Since Rho is activated by the enzymatic action of GEFs, a pilot experiment was done in the Yap laboratory where many Rho GEFs were screened for their junctional localization. Among them Rho GEF ECT2 was found to be present prominently at junctions (Ratheesh et al., 2012). When the cells were depleted of ECT2, there was significant loss of junctional Rho staining and Rho activity as measured by activity-based Rho FRET biosensor, thus identifying ECT2 as a Rho regulator at junctions (Ratheesh et al., 2012).

I began by characterizing the cellular localization of ECT2 in MCF-7 monolayers by immunofluorescence. ECT2 was found to be concentrated at the ZA along with E-cadherin (Fig 2.1a) To further confirm the junctional localization of ECT2, a GFP-tagged transgene was expressed in MCF-7 cells and junctional ECT2 was observed in live cells along with a prominent nuclear fraction (Fig 2.1b).

ECT2 is a well-established Rho GEF, known for its role in cytokinesis during cleavage furrow formation (Piekny et al., 2005). The prevalent notion in existing literature is that ECT2 displays exclusive nuclear localization in interphase cells (Fields and Justilien, 2010). However, the majority

of those experiments were performed on isolated cells (Mikawa et al., 2008; Su et al., 2011; Yuce et al., 2005), which do not make contact with each other, and thus this might have limited the junctional visualization of ECT2 in their system. Indeed a strong accumulation of ECT2 was visualized in our cells, thus enforcing that ECT2 is relevant for cell-cell junctions.

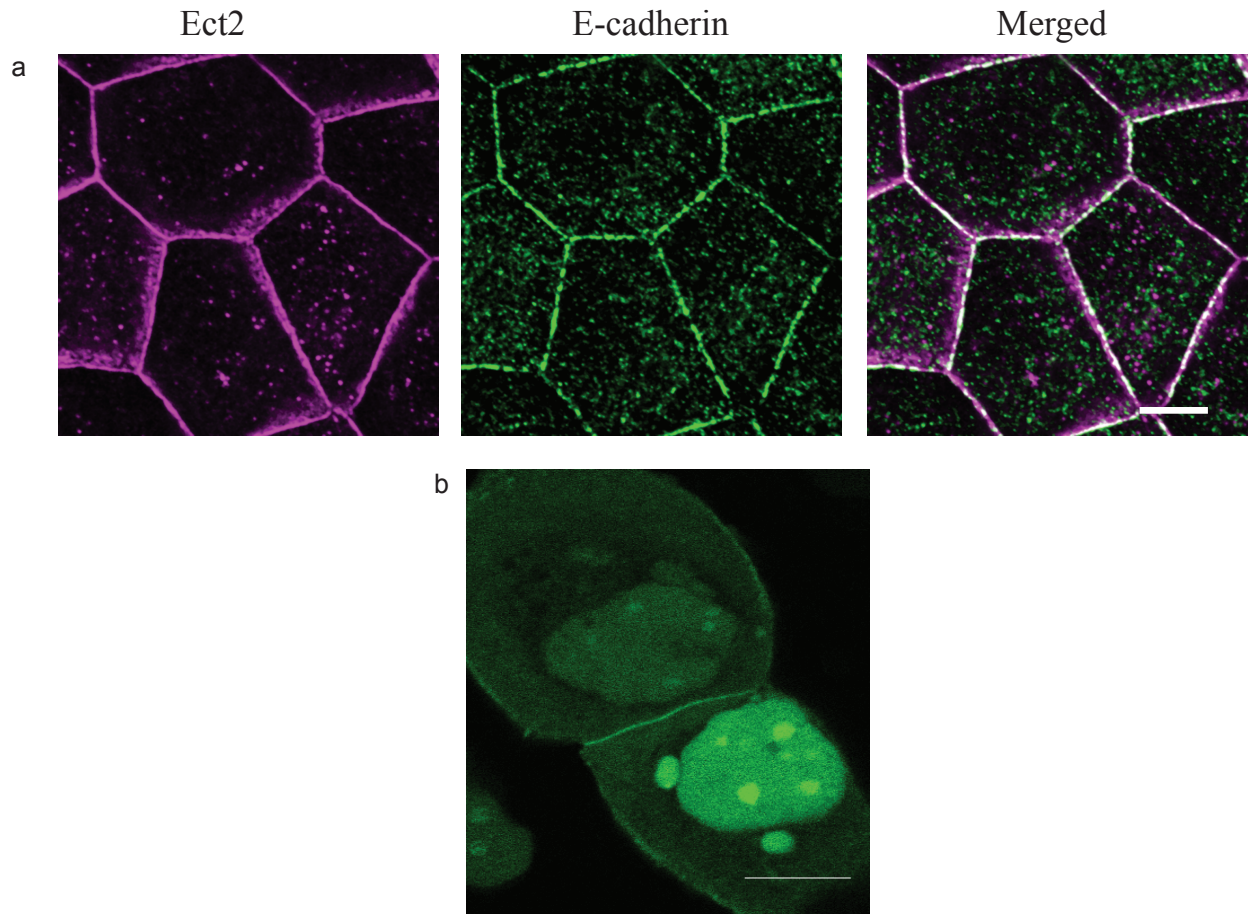

Fig 2.1 Ect2 localization in MCF-7 monolayers.

(a) MCF-7 cells monolayers were fixed in ice-cold methanol and stained for indicated proteins. Representative confocal images acquired at the apical junctions are shown. (b) GFP-Ect2 was transfected in MCF-7 cells and live cells were imaged 48 hours post-transfection. Represented is a still (sum of all the z-sections) from the movie. (scale bars=10 µm)

To address the functional significance of junctional ECT2, shRNA-mediated knockdown of ECT2 was performed. Lentivirus encoding shRNA directed against ECT2 was prepared and MCF-7 cells were infected. The cells were harvested 48-hours post-infection and ECT2 knockdown was confirmed with western blotting (Fig 2.2c). Also, a loss of junctional ECT2 by ~70% was observed in the MCF-7 cells infected with lentiviral shRNA, further confirming the specificity of ECT2 immunostaining at junctions (Fig 2.2 a,b).

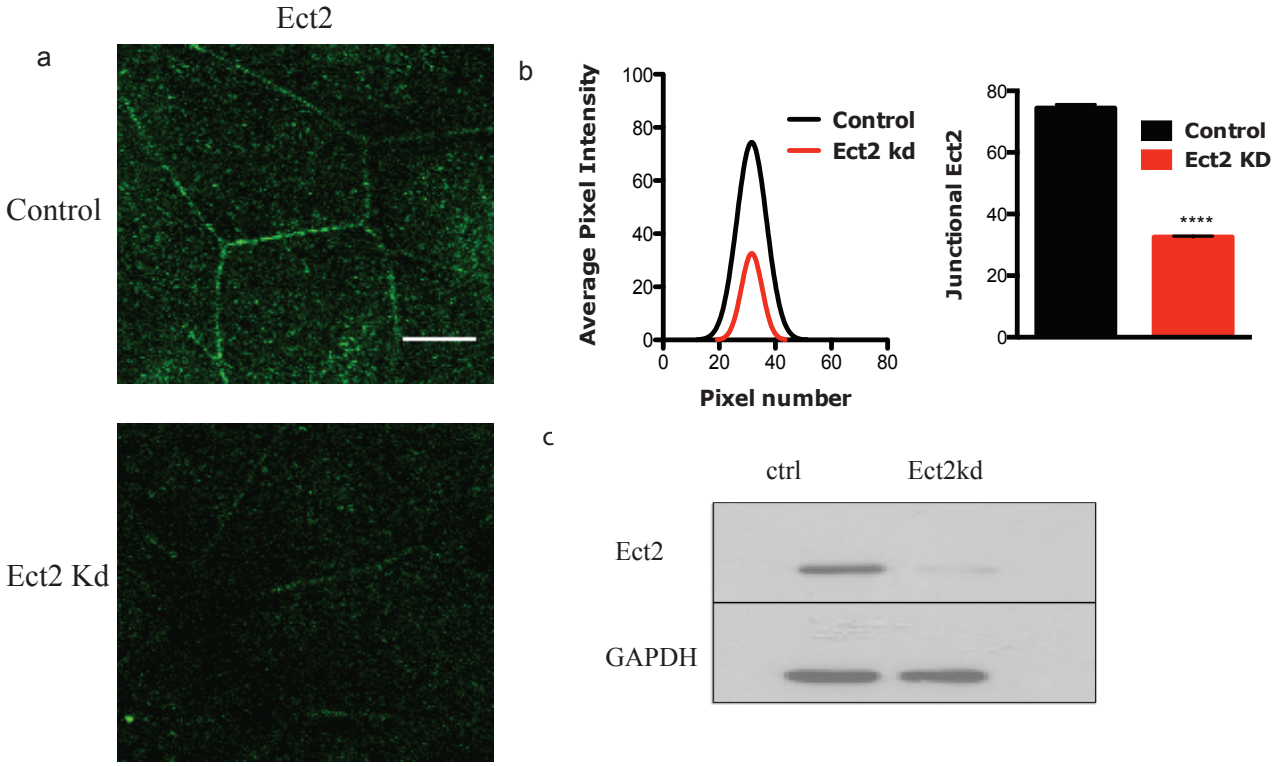

Fig 2.2 Lentivirus mediated knockdown of ECT2.

(a) Ect2 immunostaining in Control and Ect2 knockdown (Ect2 Kd) cells imaged by confocal microscopy (b) Represented are Gaussian fit curves of contact profiles in control (black) and Ect2 Kd cells (red) and peak fluorescence intensity at cell-cell contacts. Data represents mean ± S.E.M of data pooled from three independent experiments (n=30; ***P<0.0001,Student's t-test) (c) Lysates from MCF-7 cells infected with lentivirus bearing an empty vector control (Ctrl) or an shRNA-directed against Ect2 (Ect2 kd) were immunoblotted for Ect2 and GAPDH (loading control) scale bars=10 µm

To understand the impact of ECT2 depletion on the ZA, ECT2 knockdown cells were stained for junctional proteins. MCF-7 cells infected with lentivirus encoding ECT2 shRNA were grown to confluence till they formed a monolayer and E-cadherin immunostaining was performed in these cells. In control cells, a well-defined apical ring of E-cadherin, representing the ZA was observed along with punctate staining of E-cadherin at lateral clusters. In contrast, in ECT2 knockdown (ECT2 KD) cells, the apical ring pattern of the ZA was lost and E-cadherin was not able to concentrate in its well-defined apical zone of cells (Fig 2.3). The crisp, linear staining of E-cadherin was lost in ECT2 KD cells. A linescan analysis was performed in these cells, where a line is drawn across the contact and fluorescence intensity is measured along that line. In ECT2 KD cells, the cadherin fluorescence peak intensity was decreased by 50% (Fig 2.3 b, c); further strengthening the observation that ECT2 KD perturbs ZA integrity.

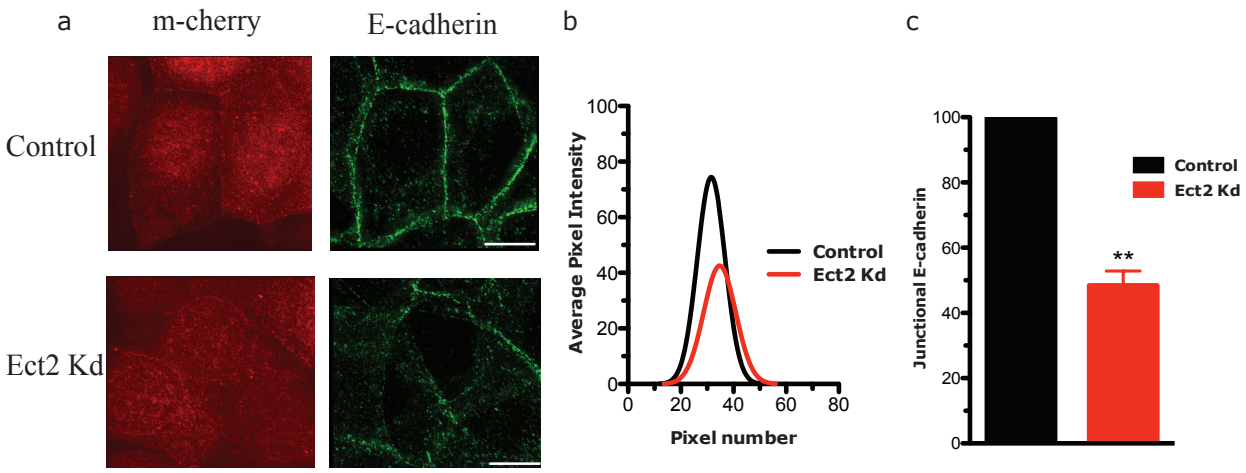

Figure 2.3 ECT2 KD perturbs E-cadherin organization

(a) E-cadherin immunostaining in control and Ect2 knockdown (Ect2 kd) cells imaged by wide- field deconvolution microscopy (b) Represented are Gaussian fit curves of contact profiles in control (black) and Ect2 Kd cells (red) and peak fluorescence intensity at cell-cell contacts (c) Data represents mean ± S.E.M of three independent experiments (n=3, in each experiment, 25 contacts were analyzed; ** p=0.005; Student's t-test) Scale bars = 10 µm

A trypsin protection assay was performed to measure the surface levels of E-cadherin. It was observed that neither total nor surface level of E-cadherin (which is susceptible to trypsinisation in the presence of calcium) was changed in ECT2 KD cells, suggesting that the loss of apical E-cadherin observed was because of the inability of the ECT2kd cells to locally concentrate E-cadherin in the apical ring (Fig 2. 4), and not because of defects in transcription or trafficking.

To further delineate whether ECT2 functions specifically at the ZA, the tight junctions component ZO-1 was studied in the ECT2 knockdown cells. The ZO-1 staining was comparable in both control and ECT2 KD cells (supported by linescan analysis and bar graphs), thus indicating that ECT2 specifically acts on the ZA to maintain its integrity (Fig 2.5).

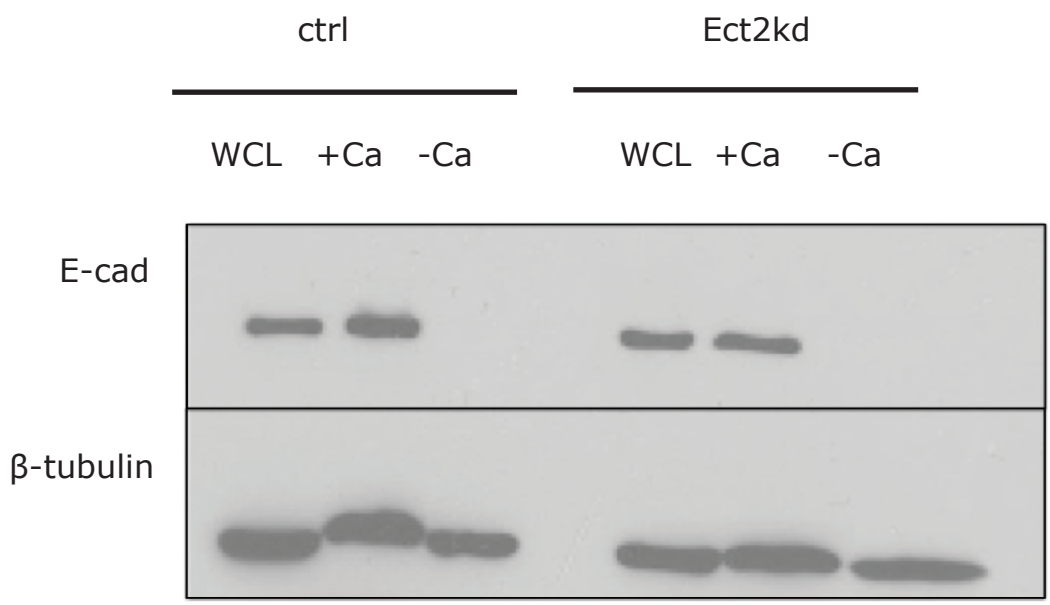

Fig 2.4 Trypsin protection assay

Surface expression of E-cadherin was measured using surface trypsin protection assays in control (Ctrl) and Ect2 knockdown (Ect2kd) cells. Cells were lysed immediately (WCL) or after trypsinisation in the presence (+Ca) or absence (–Ca) of extracellular Ca2+ . Lysates were immunoblotted for E-Cadherin (E-Cad) and β-tubulin (β-tub

2.3.2 Identification of ECT2 effectors at junctions

The Zonula adherens is a cellular structure composed of E-cadherin that is extensively regulated and supported by the actomyosin network. This actomyosin network comprises of the cytoskeleton component actin and motor protein Myosin. The Yap laboratory has previously identified that Myosin IIA supports E-cadherin clustering at junctions, and thus maintains ZA integrity (Smutny et al., 2011; Shewan et al., 2005; Smutny et al., 2010).

So, to identify the molecules that ECT2 might utilize to preserve ZA architecture, I focussed on this actomyosin cytoskeleton. MCF-7 ECT2 KD cells were stained for F-actin and no change was observed in steady state junctional actin content in ECT2 KD cells compared to control (Fig 2.6). This suggests that ECT2 does not regulate the ZA by modulating junctional actin.

The cadherin phenotype observed in ECT2 KD cells was similar to that of observed in Myosin IIA KD cells (Smutny et al., 2010), i.e. failure of E-cadherin to concentrate on the apical ring of the cells. So, Myosin IIA appeared to be a strong candidate for mediating ECT2 functions at the ZA.

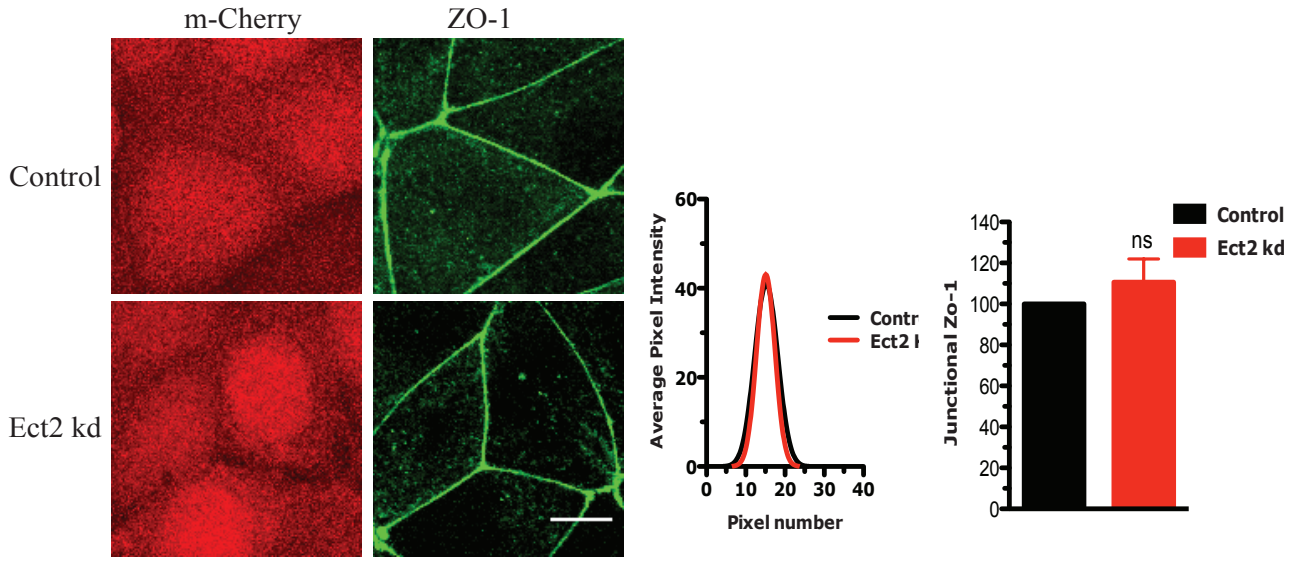

Fig 2.5 ECT2 KD does not perturb tight junctions.

(a) ZO-1 immunostaining in Control and Ect2 knockdown (Ect2 Kd) cells imaged by confocal microscopy (b) Represented are Gaussian fit curves of contact profiles in control (black) and Ect2 Kd cells (red) and peak fluorescence intensity at cell-cell contacts (c) Data represents mean ± S.E.M of three independent experiments (n=3, in each experiment 20 contacts were analysed; Student's t-test) Scale bars = 10 µm

Accordingly, the Myosin isoforms, Myosin IIA and Myosin IIB were analysed for their junctional localization in ECT2 KD cells. A distinct loss of Myosin IIA (~50%) from junctions was observed in ECT2 KD cells, that was confirmed by line scan analysis (Fig 2.7). But interestingly there was no change in Myosin IIB staining at junctions in ECT2 KD cells (Fig 2.8), thus suggesting that Myosin IIA is the downstream effector of Rho-ECT2 pathway at ZA. This supports the previous observations from this laboratory (Smutny et al., 2010), suggesting that Myosin IIA and IIB respond to different upstream regulators, with Rho regulating IIA exclusively.

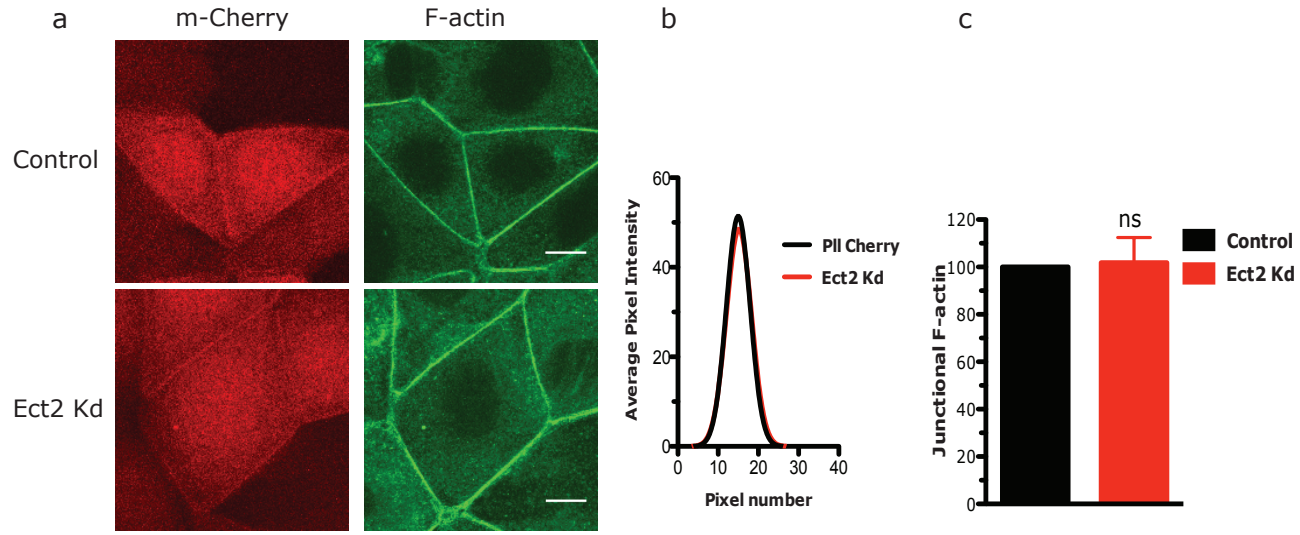

Fig 2.6 ECT2 KD does not perturb F-actin content.

F-actin immunostaining in Control and Ect2 knockdown (Ect2 Kd) cells imaged by confocal microscopy (b) Represented are Gaussian fit curves of contact profiles in control (black) and Ect2 Kd cells (red) and peak fluorescence intensity at cell-cell contacts (c) Data represents mean ± S.E.M of three independent experiments (n=3, in each experiment 20 contacts were analyzed; Student's t-test)
Scale Bar=10µm

The hypothesis that Myosin IIA is a downstream effector of ECT2 predicted further that the ECT2 KD phenotype might be reverted if amount of junctional Myosin IIA is enhanced. To test this, Myosin IIA was overexpressed in ECT2 KD cells. ECT2 KD cells were transiently transfected with GFP-tagged Myosin IIA constructs and then studied for cadherin phenotype (Fig 2.9).

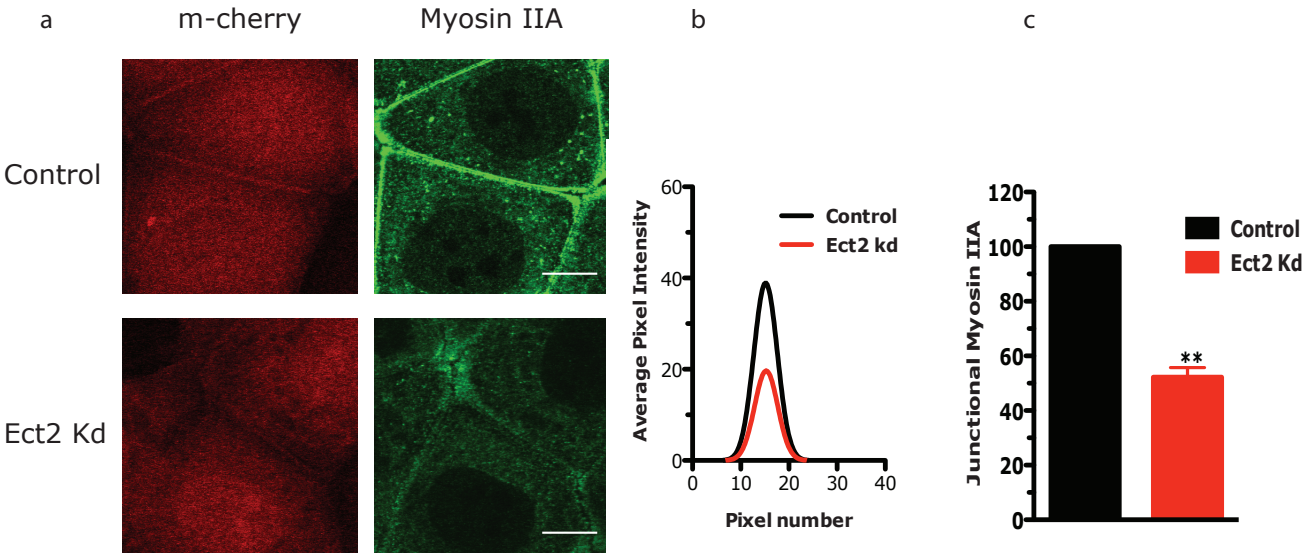

Fig 2.7 ECT2 KD perturbs Myosin IIA junctional localization

(a) Myosin IIA immunostaining in Control and Ect2 knockdown (Ect2 Kd) cells imaged by confocal microscopy (b) Represented are Gaussian fit curves of contact profiles in control (black) and Ect2 Kd cells (red) and peak fluorescence intensity at cell-cell contacts (c) Data represents mean ± S.E.M of three independent experiments (n=3), in each experiment 25 contacts were analysed; ** p=0.005 Student's t-test)
Scale bar = 10 µm

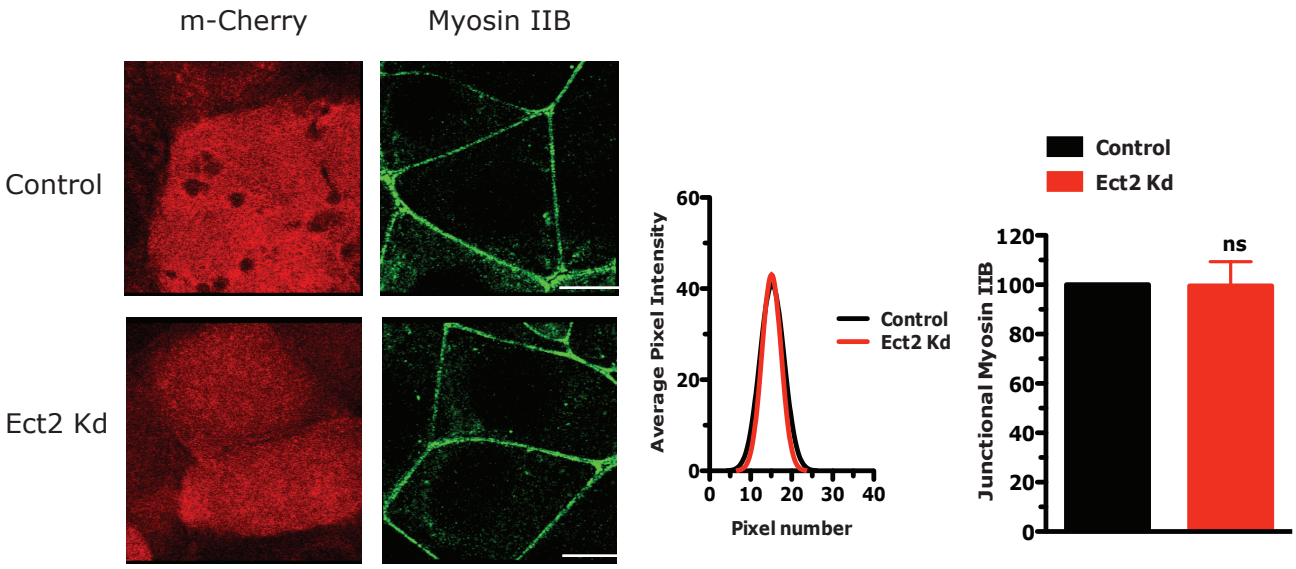

Fig 2.8 ECT2 KD does not affect Myosin IIB.
(a) Myosin IIB immunostaining in Control and Ect2 knockdown (Ect2 Kd) cells imaged by confocal microscopy (b) Represented are Gaussian fit curves of contact profiles in control (black) and Ect2 Kd cells(red) and peak fluorescence intensity at cell-cell contacts (c) Data represents mean ± S.E.M of three independent experiments (n=3, in each experiment 20 contacts were analyzed; Student's t-test) Scale bar = 10 µm

Indeed, Myosin IIA expression led to the restoration of the 'dispersed cadherin phenotype' and well-defined linear staining for apical E-cadherin was observed in the cells expressing GFP-tagged Myosin IIA. Moreover, this observation was specific for Myosin IIA as the ECT2 KD cells transiently transfected with GFP alone looked similar to ECT2 KD cells (Fig 2.9). Overall, these results suggest that ECT2 acts specifically via Myosin IIA pathway to support E-cadherin organization and zonula adherens biology.

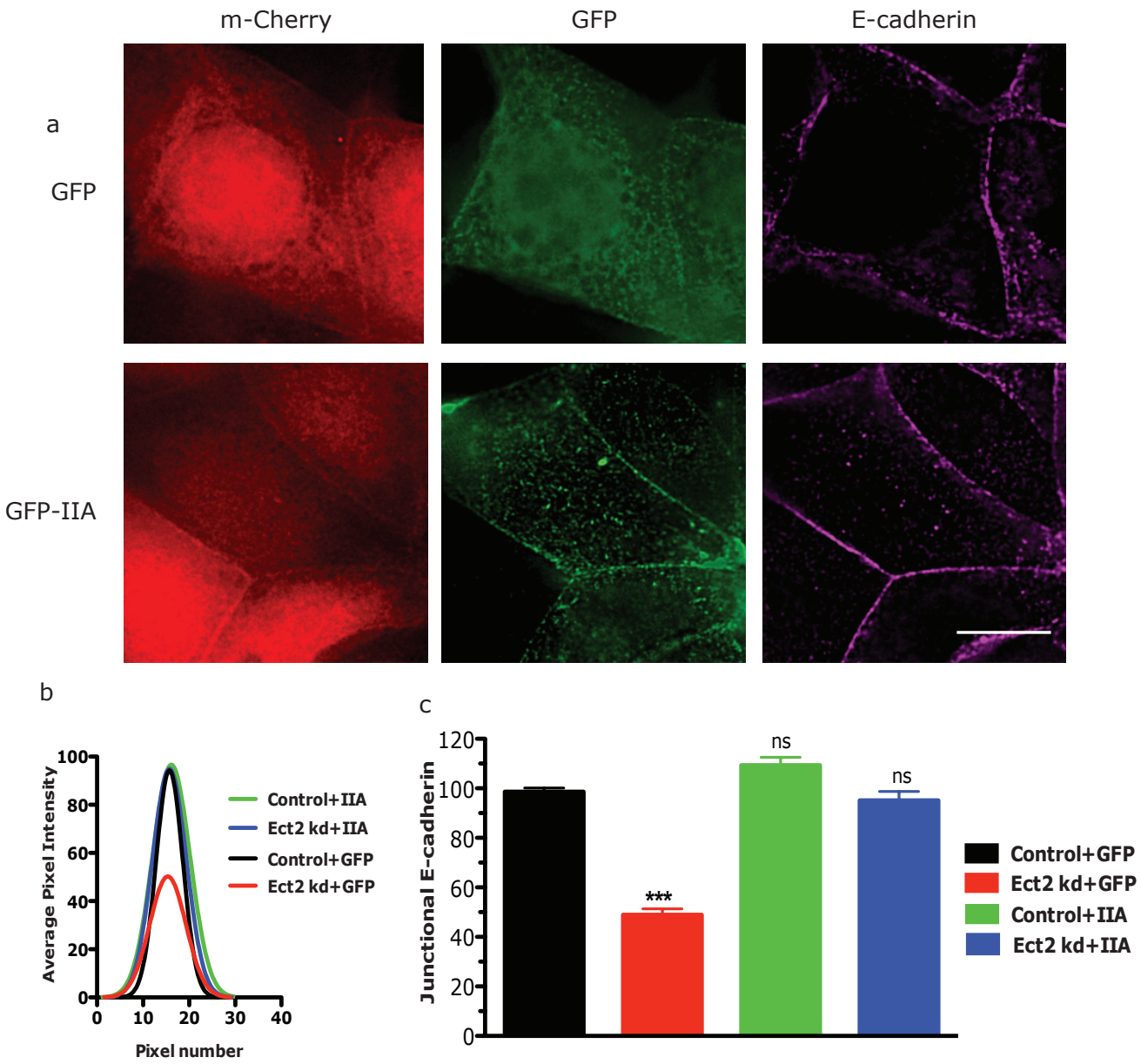

Fig 2.9 Myosin IIA can rescue ECT2 KD phenotype

Control and Ect2 knockdown (Ect2 kd) cells were transfected with p-EGFPC1 (GFP) or EGFP-Myosin IIA (GFP-IIA) and were fixed and stained for E-cadherin (magenta) and GFP (green). (a) Representative epi-illumination images were taken from the apical junctions of Ect2 kd cells. (b) Changes in junctional E-cadherin was analyzed by line-scan analysis. Gaussian fit curves of contact profiles are shown.(c) Fluorescence intenisty at cell contacts were quantified and data represents mean ± S.E.M of three independent experiments (n=3, in each experiment, 25 contacts were analyzed; ***P<0.0001;
One way Annova, Dunnett's post hoc test.)Scale bars = 10 µm

2.3.3 ECT2-Rho signaling stabilizes E-cadherin at the apical junctions

I then sought to understand the impact of ECT2-Rho signaling on zonula adherens in a more detailed fashion. Since ECT2 depletion led to the loss of cadherin-belt at ZA (a phenotype similar to Myosin IIA depletion), I postulated that the apical pool of cadherin is getting destabilized when Rho signalling is compromised. To test this, GFP-tagged E-cadherin was expressed in control and ECT2 KD cells and FRAP (Fluorescence recovery after photobleaching) was performed on the apical cadherin pool. The recovery was monitored over a period of time and FRAP profiles were obtained using Image J and Prism softwares (see material and methods for details).

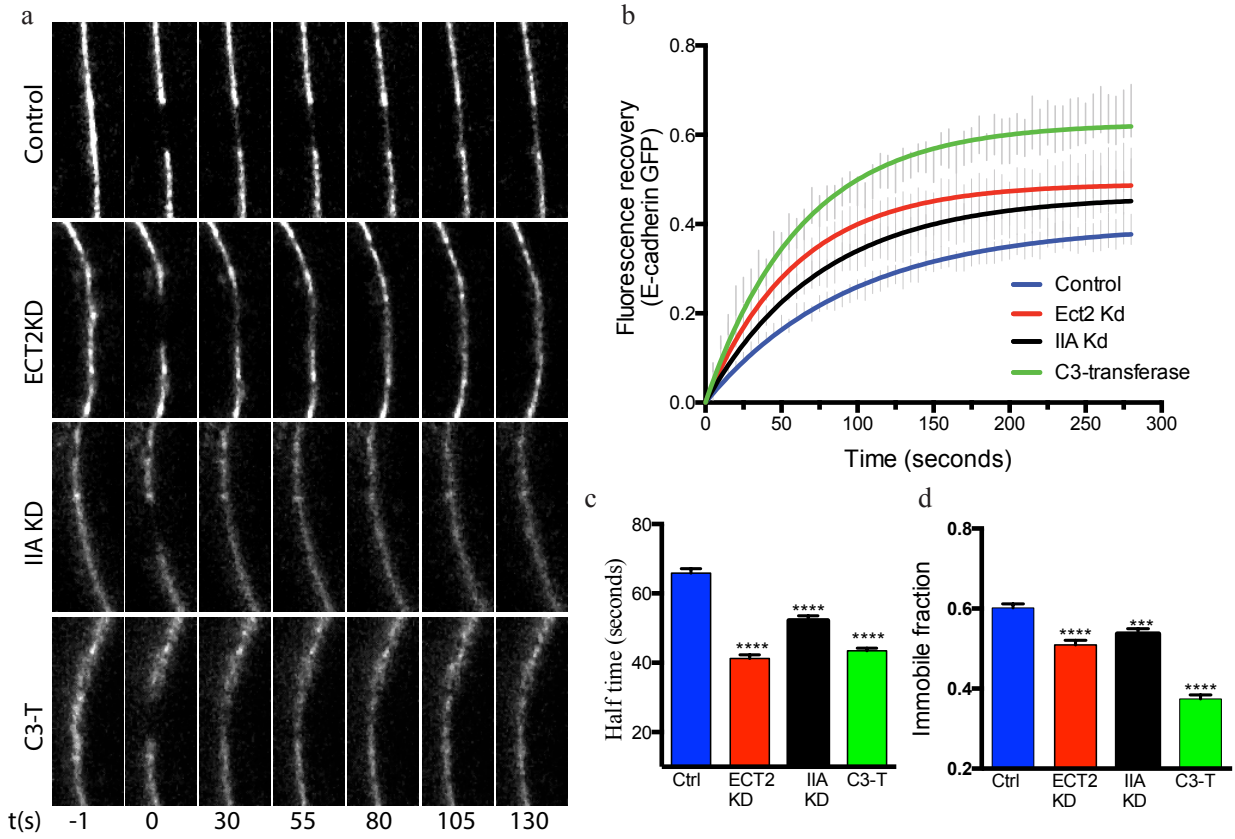

Fig 2.10 ECT2-Rho signaling stabilizes E-cadherin at the apical junctions

(a-b) E-cadherin GFP was expressed in MCF-7 cells (ctrl, Ect2 KD, IIA KD and c-3transferase treated) and the desired area of it was photobleached and observed for recovery over a period of time. Representative frames after photobleaching in the apical zones of an individual contact in the indicated conditions and the one-phase association curves corresponding to it. (d) Immobile fraction and (c) Half time of E-cadherin were extracted from the one-phase association curves. (n=11); ***p<0.001, **** p<0.0001 compared with controls (Student's T-test).

Strikingly, compared to control, the turnover of apical cadherin pool was significantly higher in ECT2 KD cells as exemplified by a significant decrease in the immobile fraction and half time (Fig

2.10). Also, direct inhibition of Rho by the pharmacological inhibitor C3-T and depletion of its downstream effector Myosin IIA led to a similar phenotype, as there was marked increase in GFP-E-cad mobility (Fig 2.10). This strongly supports the theory that ECT2-mediated activation of Rho leads to the stabilization of apical cadherin pool by the Myosin IIA pathway. Rho activates Myosin IIA by phosphorylating its regulatory light chain via ROCK. This puts Myosin IIA in a pathway in which ECT2, a GEF, activates Rho, which drives Myosin activity. Myosin IIA in turns helps in clustering of E-cadherin and thus maintains ZA integrity.

2.3.4 ECT2 is important for junctional tension

Tension imparted by Myosin motors on actin filaments generates contractile forces inside the cells. This actomyosin-generated tension is necessary for morphogenesis and regulates cell-cell adhesion (Gomez et al., 2011; Liu et al., 2010). Myosin II appears to be important for the generation of this tension as when inhibited or depleted, it leads to a decrease in forces and also cadherin adhesion is compromised (Ladoux et al., 2010). Also, adherens junctions act to transmit this mechanical tension across neighbouring cells as integration of these forces is important for producing tissue level changes during morphogenesis (Maitre et al., 2012; Parsons et al., 2010; Kasza and Zallen, 2011).

As ECT2 knockdown cells showed decreased Myosin IIA localization, I sought to test the hypothesis that junctional tension is compromised in these cells. For this a multi-mode tuneable Chameleon laser was used to ablate cell-cell contacts labelled with E-cadherin GFP (see Material and Methods for details). Instantaneous recoil of the contacts at its vertices was measured as an index of junctional tension(Fernandez-Gonzalez et al., 2009).

Inside the cells, the actomyosin network ring beneath the contact imparts its tension and thus when ablated, this ring is disrupted and the tension is released which leads to the expansion of contact. This degree of expansion is correlated to the tension inherent to that contact. As evident, control cells showed a visible expansion in contact length after the ablation, but depletion of ECT2, Myosin IIA and inhibition of Rho signalling led to no change in contact length after ablation (Fig 2.11).

This contact expansion was measured by determining the difference between the position of two vertices before and after ablation and the resulting values (vertex separation) were fitted in a one-phase association curve (Fig 2.12). The value of initial recoil (parameter of junctional tension) was obtained from these curves and as shown, there was a decrease in junctional tension in ECT2 KD,

Myosin II KD and C3-transferase treated cells thus suggesting that ECT2 supports junctional tension via the Myosin IIA pathway (Fig 2.12).

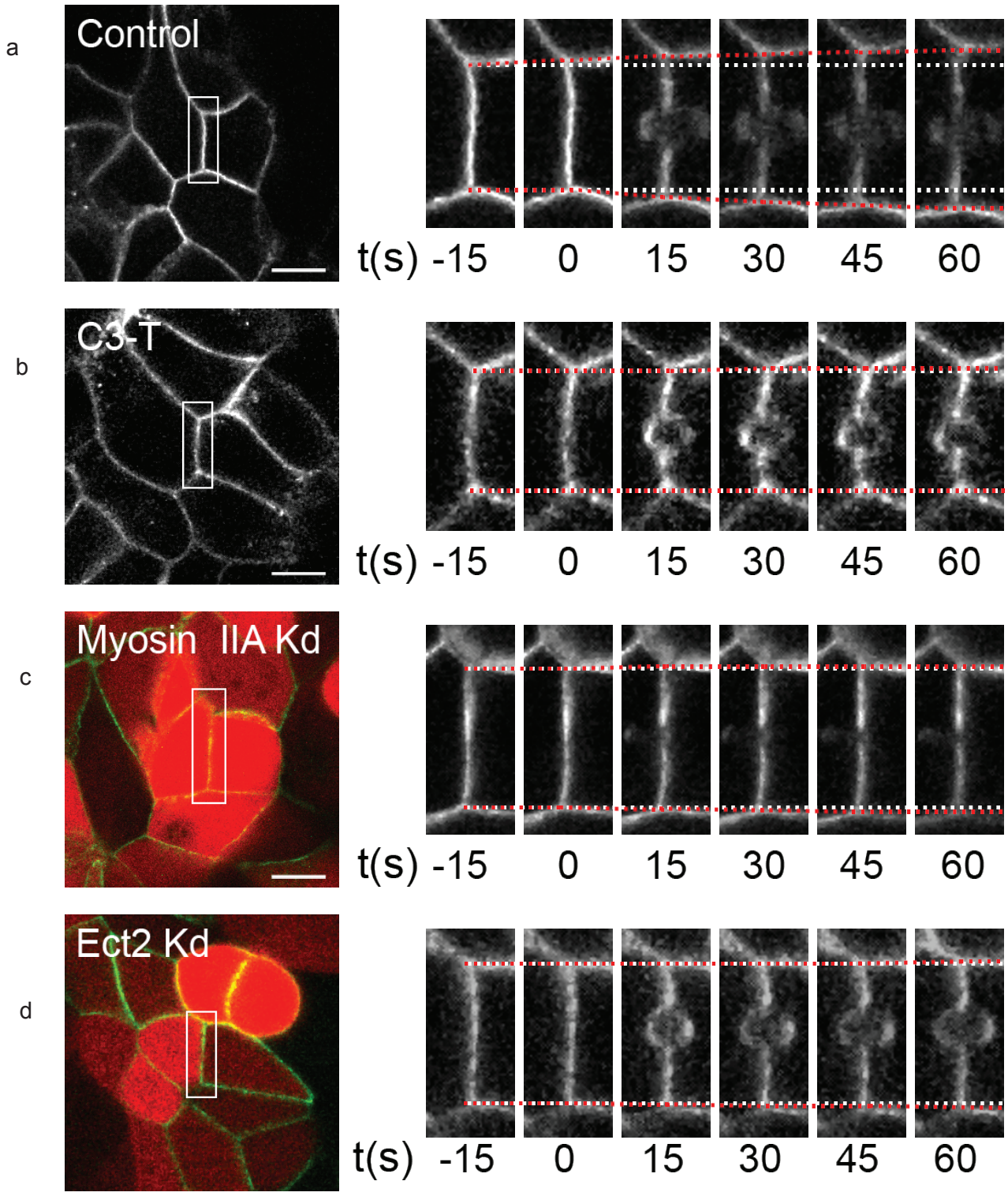

Fig 2.11 Contact expansion after laser-ablation in the indicated conditions

MCF-7 cells expressing (a) E-cadherin GFP (control) were infected with virus encoding (c) Myosin IIA KD shRNA, (d) Ect2 KD shRNA and were treated with (b) c3-trasnferase (500 ng/µl for 1 hour). A constant ROI was marked for each experiment and contacts marked with GFP-cadherin were ablated with 3 iterations of 790 nm laser with 100 % transmission. Represented are the still from the movie at indicated time frames.

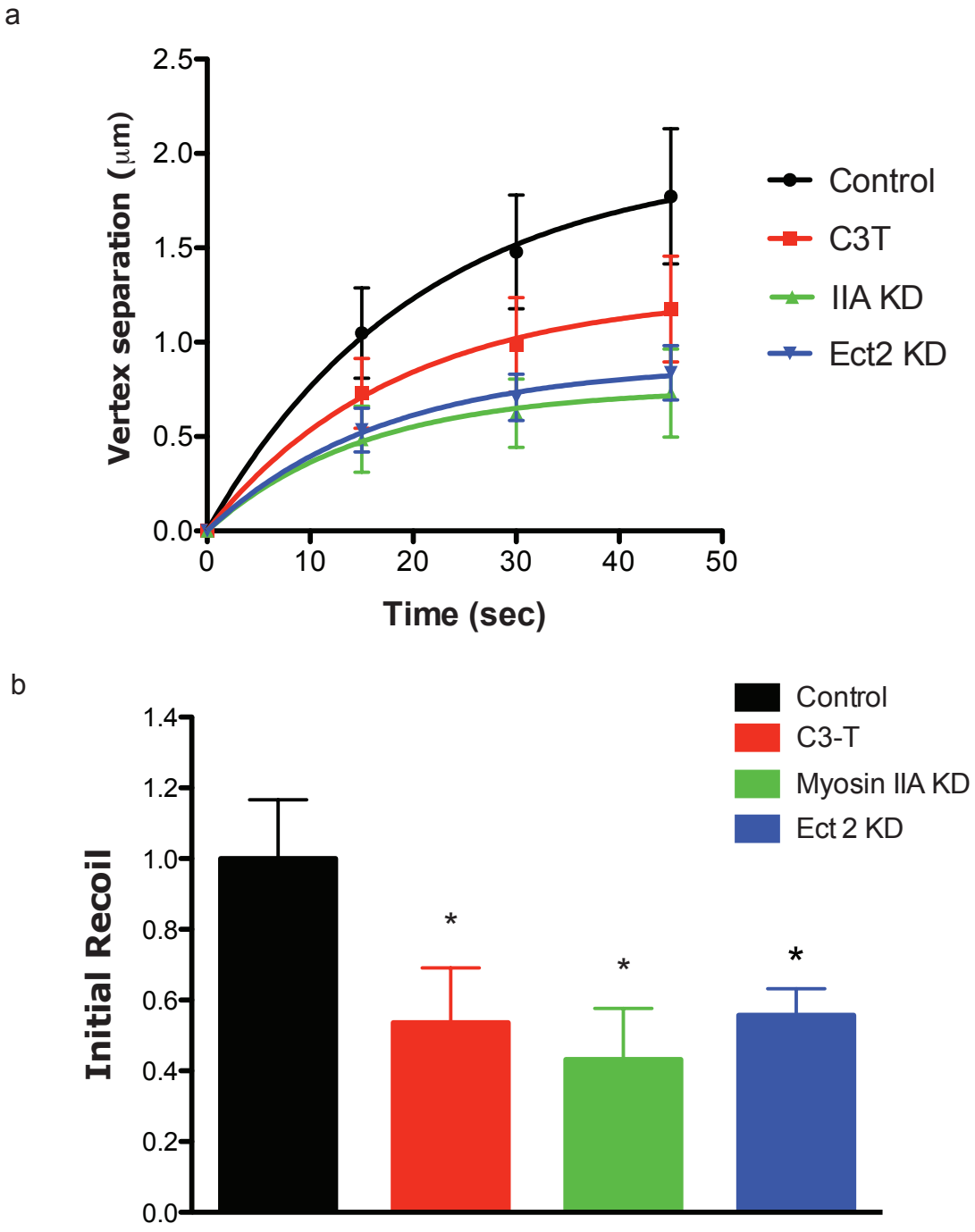

Fig 2.12 ECT2-Rho signaling is essential for junctional tension

(a) The distance (d) between vertices that define the ablated contact was measured as a function of time (t). Then obtained values d(t) were subtracted from the average distance before the ablation step d(0) and the resulted values were fitted in an one-phase association curve.(b) Average Instantaneous recoil for 10-15 contacts was determined from the curve and then normalized to value according to control conditions (n=10-15) , where * p< 0.03, Student's t-test)

2.3.5 Functional implications of ECT2 knockdown on morphogenesis using cyst culture

Cadherins mediate many aspects of morphogenesis and are dynamically regulated in response to developmental or physiological signaling pathways (Gumbiner, 2005). The above results suggest that ECT2 is important for E-cadherin organization at the ZA (Ratheesh et al., 2012). To further pursue this, I aimed to assess the functional relevance of this phenotype in a physiological relevant setting. So, to identify the importance of ECT2 for epithelial morphogenesis I used 3-D cyst culture of ECT2 knockdown cells. A lentivirus-mediated knockdown of ECT2 was performed in human colon carcinoma cell lines Caco-2. Caco-2 cells were chosen because, although derived from tumor cells, they polarize to form cysts in 3-D culture (Jaffe et al., 2008). Briefly, Caco-2 cells were trypsinized to form a single cell suspension and 2 X 10^4 cells were mixed in a solution containing RPMI and matrigel (reduced growth factor, Becton Dickinson) to a final concentration of 2%. Then 200 µl of above solution was added to each well of a chambered cover glass and placed in 37° C incubator. The cysts were ready in 10 days and then were stained for the relevant proteins.

Recently two research articles from Toru Miki's group have suggested that ECT2 is important for polarity. Using highly polarized MDCK cell lines and the yeast two-hybrid system, they have shown that ECT2 interacts with the polarity component Par6, also associates with Par3 and PKCzeta, and is required for the Par3/Par6/aPKC polarity complex to be recruited to tight junctions (Liu et al., 2004; Liu et al., 2006). Surprisingly, in the Caco-2 cyst cultures depleted of ECT2, loss of polarity was not observed, as assessed by the apical localization of aPKC, ZO-1, actin and lateral distribution of E-cadherin (Fig 2.13 a,b,c,d). However, ECT2 knockdown leads to certain defects in cysts formation. There were fewer cysts formed from ECT2 KD cells, and the ones formed were strikingly smaller in size and were generally devoid of lumens (Fig 2,13 e). Also, we observed less E-cadherin concentration at the intercellular contacts (Fig 2.13 f); in most of the cases the E-cadherin organization was grossly disrupted or altogether reduced levels of E-cadherin was observed. E-cadherin has been shown to be essential for proper lumen formation in 3-D cysts cultures (Marciano et al., 2011; Jia et al., 2011).

So, above results suggest an alternative role of ECT2 in morphogenesis by regulating the size of cysts and lumen formation and this may be via regulating the organization of E-cadherin. However, further experiments are needed to support and build up on this observation. Due to the time-constraints of my PHD tenure, I was not able to pursue this further, but it remains an exciting possibility to be explored.

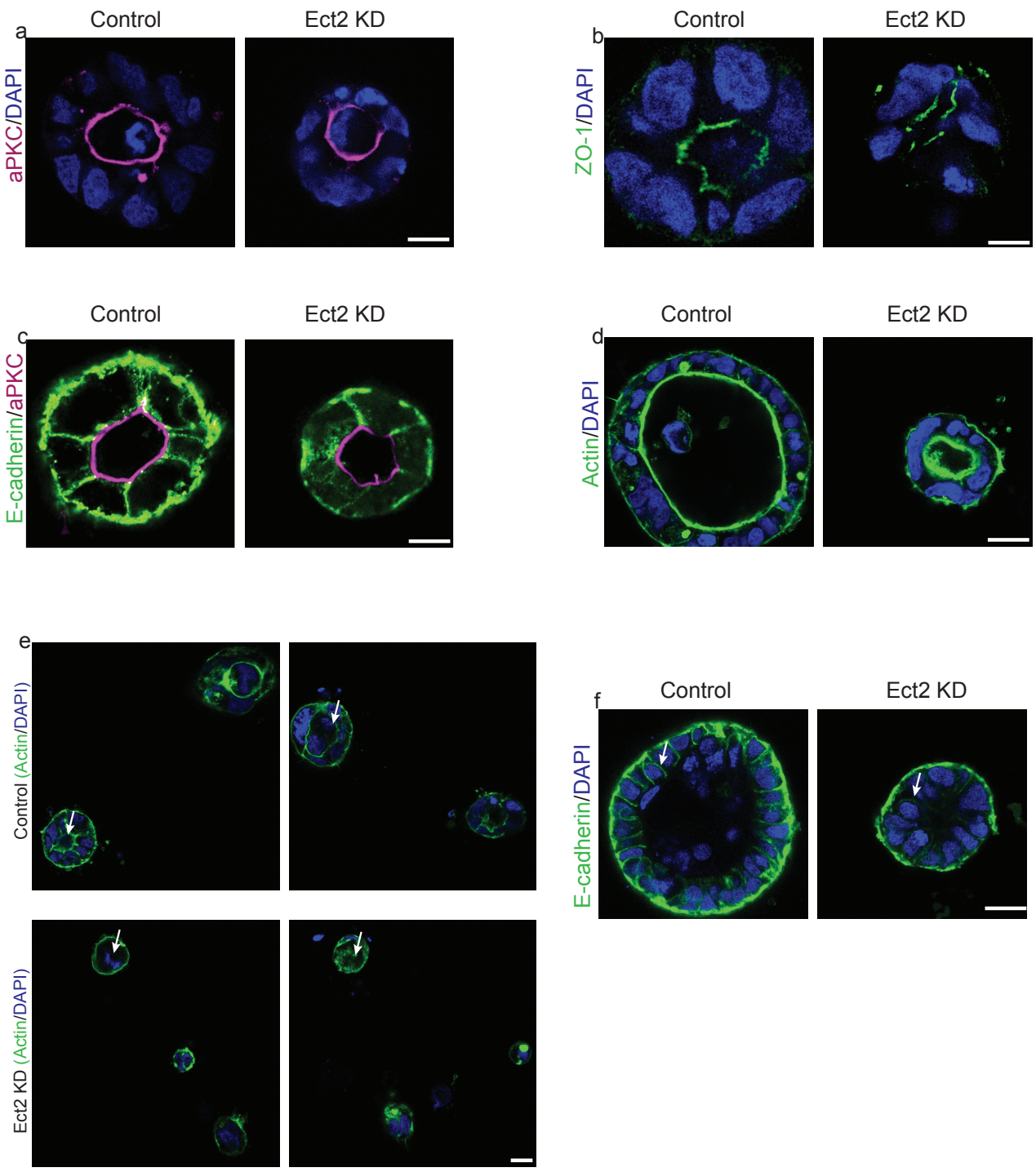

Fig 2.13 ECT2KD does not affect polarity but perturbs E-cadherin distribution

Ect2 KD does not affect polarity (a,b,d) but leads to smaller cyst size (e), absence of lumen (e) and disruption of E-cadherin (c,f). Caco-2 cysts were transduced with lentivirus encoding ECT2 shRNA or control shRNA, grown for 10-12 days, fixed with 4% PFA and stained for indicated proteins as shown.
Scale Bar = 20 µm

2.4 Significance and outcomes

Rho GTPases are the key regulators of epithelial cell junctions (Amano et al., 2010). They act in concert with various downstream effectors to dynamically organize various cellular structures like acto-myosin network, cell-adhesion proteins and microtubules (Bishop and Hall, 2000; Etienne-Manneville and Hall, 2002). At a given time and space, the activity of Rho is very finely tuned to generate a proper biological response via its upstream regulators: GEFs, GAPs and GDIs (Etienne-Manneville and Hall, 2002; Rossman et al., 2005). However, we still don't understand the exact molecular pathway and relevant components required to generate a functional Rho circuit.

The results presented in this study strengthen the notion that junctional Rho signaling is required to maintain a functional zonula adherens and detail the mechanism behind it. Also, it identifies ECT2 as the prominent 'functional' Rho-GEF at ZA and implies its role in supporting ZA organization and junctional tension via the Myosin IIA pathway. These findings suggest a novel extra-mitotic role for ECT2 in supporting junctional biology. This is significant, as the general consensus is that ECT2 is mostly nuclear in interphase cells and functions mainly during cytokinesis (Fields and Justilien, 2010). However all these studies were done in single cells which cannot form intercellular junctions. Apart from the Yap laboratory, other groups have also confirmed that ECT2 can localize to junctions in epithelial cells and can perform junction specific functions like regulating cell polarity and interacting with junctional complexes (Liu et al., 2006)

The work presented here establishes that ECT2 supports ZA architecture by stabilizing cadherin at the apical zone of the cells via Myosin IIA. ECT2 depletion led to loss of cadherin ring at the apical zone of cells and this could be restored back by the expression of Myosin IIA. Also, using FRAP analysis of GFP-E-cadherin, it was found that this Rho-ECT2 pathway is essential to constrain E-cadherin mobility at the ZA, mostly by supporting Myosin IIA accumulation (as ECT2 depletion specifically perturbs Mysoin IIA, but not IIB). Strikingly, these functions of Rho-GEF ECT2 are specific for ZA, as ECT2 knockdown did not affect tight junctions marked by ZO-1. Interestingly, p115 Rho GEF has been demonstrated to specifically support tight junctions but not ZA, thus further re-enforcing the idea that spatio-temporal activity of Rho GTPase is tightly regulated by their regulators depending on the cellular context. Further, using a two-photon laser to cut junctions and by measuring the instant recoil as a measure of tension, I have shown that ECT2 acts in concert with myosin IIA to maintain the junctional tension, which is critical for epithelial remodeling during tissue organization.

Overall, these results uncover a novel role of Rho GEF ECT2; that is to promote ZA organization and cortical tension in interphase epithelial cells.

2.5 References

Amano, M., M. Nakayama, and K. Kaibuchi. 2010. Rho-kinase/ROCK: A key regulator of the cytoskeleton and cell polarity. *Cytoskeleton*. 67:545-554.

Bishop, A.L., and A. Hall. 2000. Rho GTPases and their effector proteins. *Biochemical Journal*. 348:241-255.

Bos, J.L., H. Rehmann, and A. Wittinghofer. 2007. GEFs and GAPs: critical elements in the control of small G proteins. *Cell*. 129:865-877.

Braga, V. 2000. Epithelial cell shape: cadherins and small GTPases. *Exp Cell Res*. 261:83-90.

Braga, V.M. 2002. Cell-cell adhesion and signalling. *Curr Opin Cell Biol*. 14:546-556.

Braga, V.M., and A.S. Yap. 2005. The challenges of abundance: epithelial junctions and small GTPase signalling. *Curr Opin Cell Biol*. 17:466-474.

Cherfils, J., and M. Zeghouf. 2013. Regulation of Small Gtpases by Gefs, Gaps, and Gdis. *Physiol Rev*. 93:269-309.

Etienne-Manneville, S., and A. Hall. 2002. Rho GTPases in cell biology. *Nature*. 420:629-635.

Fernandez-Gonzalez, R., M. Simoes Sde, J.C. Roper, S. Eaton, and J.A. Zallen. 2009. Myosin II dynamics are regulated by tension in intercalating cells. *Dev Cell*. 17:736-743.

Fields, A.P., and V. Justilien. 2010. The guanine nucleotide exchange factor (GEF) Ect2 is an oncogene in human cancer. *Adv Enzyme Regul*. 50:190-200.

Gomez, G.A., R.W. McLachlan, and A.S. Yap. 2011. Productive tension: force-sensing and homeostasis of cell-cell junctions. *Trends Cell Biol*. 21:499-505.

Guillot, C., and T. Lecuit. 2013. Mechanics of epithelial tissue homeostasis and morphogenesis. *Science*. 340:1185-1189.

Gumbiner, B.M. 2005. Regulation of cadherin-mediated adhesion in morphogenesis. *Nat Rev Mol Cell Bio*. 6:622-634.

Hara, T., H. Ishida, R. Raziuddin, S. Dorkhom, K. Kamijo, and T. Miki. 2004. Novel kelch-like protein, KLEIP, is involved in actin assembly at cell-cell contact sites of Madin-Darby canine kidney cells. *Mol Biol Cell*. 15:1172-1184.

Harris, T.J.C., and U. Tepass. 2010. Adherens junctions: from molecules to morphogenesis. *Nat Rev Mol Cell Bio*. 11:502-514.

Jaffe, A.B., and A. Hall. 2005. Rho GTPases: biochemistry and biology. *Annu Rev Cell Dev Biol*. 21:247-269.

Jaffe, A.B., N. Kaji, J. Durgan, and A. Hall. 2008. Cdc42 controls spindle orientation to position the apical surface during epithelial morphogenesis. *J Cell Biol*. 183:625-633.

Jia, L., F. Liu, S.H. Hansen, M.B. Ter Beest, and M.M. Zegers. 2011. Distinct roles of cadherin-6 and E-cadherin in tubulogenesis and lumen formation. *Mol Biol Cell*. 22:2031-2041.

Kasza, K.E., and J.A. Zallen. 2011. Dynamics and regulation of contractile actin-myosin networks in morphogenesis. *Current opinion in cell biology*. 23:30-38.

Ladoux, B., E. Anon, M. Lambert, A. Rabodzey, P. Hersen, A. Buguin, P. Silberzan, and R.M. Mege. 2010. Strength dependence of cadherin-mediated adhesions. *Biophys J*. 98:534-542.

Liu, X.F., H. Ishida, R. Raziuddin, and T. Miki. 2004. Nucleotide exchange factor ECT2 interacts with the polarity protein complex Par6/Par3/protein kinase Czeta (PKCzeta) and regulates PKCzeta activity. *Mol Cell Biol*. 24:6665-6675.

Liu, X.F., S. Ohno, and T. Miki. 2006. Nucleotide exchange factor ECT2 regulates epithelial cell polarity. *Cellular signalling*. 18:1604-1615.

Liu, Z., J.L. Tan, D.M. Cohen, M.T. Yang, N.J. Sniadecki, S.A. Ruiz, C.M. Nelson, and C.S. Chen. 2010. Mechanical tugging force regulates the size of cell-cell junctions. *Proc Natl Acad Sci U S A*. 107:9944-9949.

Maitre, J.L., H. Berthoumieux, S.F. Krens, G. Salbreux, F. Julicher, E. Paluch, and C.P. Heisenberg. 2012. Adhesion functions in cell sorting by mechanically coupling the cortices of adhering cells. *Science*. 338:253-256.

Marciano, D.K., P.R. Brakeman, C.Z. Lee, N. Spivak, D.J. Eastburn, D.M. Bryant, G.M. Beaudoin, I. Hofmann, K.E. Mostov, and L.F. Reichardt. 2011. p120 catenin is required for normal renal tubulogenesis and glomerulogenesis (vol 138, pg 2099, 2011). *Development*. 138:2632-2632.

McCormack, J., N.J. Welsh, and V.M. Braga. 2013. Cycling around cell-cell adhesion with Rho GTPase regulators. *J Cell Sci*. 126:379-391.

Mikawa, M., L. Su, and S.J. Parsons. 2008. Opposing roles of p190RhoGAP and Ect2 RhoGEF in regulating cytokinesis. *Cell Cycle*. 7:2003-2012.

Munjal, A., and T. Lecuit. 2014. Actomyosin networks and tissue morphogenesis. *Development*. 141:1789-1793.

Niessen, C.M., D. Leckband, and A.S. Yap. 2011. Tissue organization by cadherin adhesion molecules: dynamic molecular and cellular mechanisms of morphogenetic regulation. *Physiol Rev*. 91:691-731.

Parsons, J.T., A.R. Horwitz, and M.A. Schwartz. 2010. Cell adhesion: integrating cytoskeletal dynamics and cellular tension. *Nat Rev Mol Cell Biol*. 11:633-643.

Piekny, A., M. Werner, and M. Glotzer. 2005. Cytokinesis: welcome to the Rho zone. *Trends Cell Biol*. 15:651-658.

Ratheesh, A., G.A. Gomez, R. Priya, S. Verma, E.M. Kovacs, K. Jiang, N.H. Brown, A. Akhmanova, S.J. Stehbens, and A.S. Yap. 2012. Centralspindlin and alpha-catenin regulate Rho signalling at the epithelial zonula adherens. *Nat Cell Biol*. 14:818-828.

Ratheesh, A., R. Priya, and A.S. Yap. 2013. Coordinating Rho and Rac: the regulation of Rho GTPase signaling and cadherin junctions. *Progress in molecular biology and translational science*. 116:49-68.

Rossman, K.L., C.J. Der, and J. Sondek. 2005. GEF means go: turning on RHO GTPases with guanine nucleotide-exchange factors. *Nat Rev Mol Cell Biol*. 6:167-180.

Shewan, A.M., M. Maddugoda, A. Kraemer, S.J. Stehbens, S. Verma, E.M. Kovacs, and A.S. Yap. 2005. Myosin 2 is a key Rho kinase target necessary for the local concentration of E-cadherin at cell-cell contacts. *Mol Biol Cell*. 16:4531-4542.

Smutny, M., H.L. Cox, J.M. Leerberg, E.M. Kovacs, M.A. Conti, C. Ferguson, N.A. Hamilton, R.G. Parton, R.S. Adelstein, and A.S. Yap. 2010. Myosin II isoforms identify distinct functional modules that support integrity of the epithelial zonula adherens. *Nat Cell Biol*. 12:696-702.

Smutny, M., S.K. Wu, G.A. Gomez, S. Mangold, A.S. Yap, and N.A. Hamilton. 2011. Multicomponent analysis of junctional movements regulated by myosin II isoforms at the epithelial zonula adherens. *PLoS One*. 6:e22458.

Su, K.C., T. Takaki, and M. Petronczki. 2011. Targeting of the RhoGEF Ect2 to the Equatorial Membrane Controls Cleavage Furrow Formation during Cytokinesis. *Dev Cell*. 21:1104-1115.

Thumkeo, D., S. Watanabe, and S. Narumiya. 2013. Physiological roles of Rho and Rho effectors in mammals. *European journal of cell biology*. 92:303-315.

Verma, S., A.M. Shewan, J.A. Scott, F.M. Helwani, N.R. den Elzen, H. Miki, T. Takenawa, and A.S. Yap. 2004. Arp2/3 activity is necessary for efficient formation of E-cadherin adhesive contacts. *The Journal of biological chemistry*. 279:34062-34070.

Yuce, O., A. Piekny, and M. Glotzer. 2005. An ECT2-centralspindlin complex regulates the localization and function of RhoA. *J Cell Biol*. 170:571-582.

Chapter 3: E-cadherin supports steady-state Rho signaling at the epithelial zonula adherens

3.1 Introduction

The Zonula Adherens (ZA) is a cadherin based cell-cell adhesive structure found in epithelia. E-cadherin forms the core component of ZA and maintains epithelial cell shape and morphology. The extracellular domain of E-cadherin mediates calcium-dependent adhesion while the cytoplasmic domain associates with actomyosin cytoskeleton (reviewed in (Niessen et al., 2011). This actomyosin cytoskeleton is mainly regulated by Rho family GTPases. These small GTPases (mainly Rho and Rac) localize to cadherin-based junctions and together with the actomyosin cytoskeleton, they ensure proper organization and functionality of these adhesive structures (Braga, 2000). In turn, the localization and activity of these small GTPases is regulated in a cadherin-dependent manner (Braga and Yap, 2005; Kovacs et al., 2002; Wheelock and Johnson, 2003). This hints that junctions and Rho GTPases act in a co-operative manner to achieve significant biological outcome but the exact nature of this interaction is not well-understood.

One of the open questions in the field is how cadherin signaling regulates Rho GTPases. By plating CHO cells expressing C-cadherin on the immobilized extracellular domain of C-cadherin, Noren *et al* showed that upon cadherin ligation, Rac1 gets activated but activity of Rho is diminished (Noren et al., 2001). They further proposed that cadherin engagement leads to activation of a Rho GAP, p190RhoGAP, that dampens Rho signaling (Noren et al., 2003). Rho and Rac are believed to occupy two distinct zones during nascent junction formation. As cells make contact with each other, Rac takes the centre stage along with its effectors and later on is replaced by Rho (Yamada and Nelson, 2007). However, these reports of Rho inhibition by cadherin adhesion are studied in a context that is different from steady-state homeostasis that we investigate.

Recently we discovered a pathway that regulates Rho signaling at ZA. We have shown that ZA is a Rho zone and harbors a conserved molecular ensemble known to control Rho at the cytokinetic furrow (Ratheesh et al., 2012). This ensemble is comprised of ECT2, a GEF for Rho, and the centralspindlin (CS) complex (composed of MgcRACGAP and MKLP1). The CS complex supports junctional Rho signaling by concentrating ECT2 at ZA and also by interfering with the junctional localization of p190RhoGAP, a GAP for Rho (Ratheesh et al., 2012). Together, this pathway facilitates the downstream activation of Myosin IIA, which promotes E-cadherin concentration and

junctional tension. Interestingly, in our hands α-catenin was necessary for junctional Rho signaling as it supports CS and ECT2 retention at junctions (Ratheesh et al., 2012).

In this chapter, I have taken a step further and aimed to study the direct impact of E-cadherin on steady-state Rho signaling and extended my previous observation that Rho signaling stabilizes cadherin at the apical junctions.

3.2 Result

This research chapter has been divided into sections:

3.2.1 The results related to this chapter have been published as a research article in Differentiation, 86 (2013) 133–140, May 2013, of which I am the first author. The article is attached here.

Erratum: **The images corresponding to MgcRacGAP for Control and E-cad GFP (Fig 3a) got swapped during the preparation of manuscript. This is an unwanted technical error and has no consequences on the meaning of the figure and/or the rest of the manuscript**.

3.2.2 An article published in www.bio-protocol.org, expanding on the FRAP experiments I performed in the research chapter 1 and 2.

http://www.bio-protocol.org/e937

The article is attached here.

Differentiation 86 (2013) 133–140

Contents lists available at ScienceDirect

Differentiation

journal homepage: www.elsevier.com/locate/diff

E-cadherin supports steady-state Rho signaling at the epithelial zonula adherens

Rashmi Priya, Alpha S. Yap *, Guillermo A. Gomez

Division of Molecular Cell Biology, Institute for Molecular Bioscience, The University of Queensland, St. Lucia, Brisbane, Queensland 4072, Australia

ARTICLE INFO

Available online 2 May 2013

Keywords:
E-cadherin
Zonula adherens
Rho
ECT2
Centralspindlin
Myosin II

ABSTRACT

In simple polarized epithelial cells, the Rho GTPase commonly localizes to E-cadherin-based cell–cell junctions, such as the zonula adherens (ZA), where it regulates the actomyosin cytoskeleton to support junctional integrity and tension. An important question is how E-cadherin contributes to Rho signaling, notably whether junctional Rho may depend on cadherin adhesion. We sought to investigate this by assessing Rho localization and activity in epithelial monolayers depleted of E-cadherin by RNAi. We report that E-cadherin depletion reduced both Rho and Rho-GTP at the ZA, an effect that was rescued by expressing a RNAi-resistant full-length E-cadherin transgene. This impact on Rho signaling was accompanied by reduced junctional localization of the Rho GEF ECT2 and the centralspindlin complex that recruits ECT2. Further, the Rho signaling pathway contributes to the selective stabilization of E-cadherin molecules in the apical zone of the cells compared with E-cadherin at the lateral surface, thereby creating a more defined and restricted pool of E-cadherin that forms the ZA. Thus, E-cadherin and Rho signaling cooperate to ensure proper ZA architecture and function.

1. Introduction

Classical cadherin adhesion receptors control morphogenesis and tissue organization through close cooperation with the acto-myosin cytoskeleton (Mason and Martin, 2011; Roh-Johnson et al., 2012). Cadherin extracellular domains mediate adhesive binding, while their cytoplasmic tails can functionally interact with the cytoskeleton through physical binding to actin filaments as well as regulation of filament dynamics and organization (Ratheesh and Yap, 2012). This apparatus integrates cell–cell adhesion and the cytoskeleton. Indeed, cadherins may play a significant morphogenetic role by mechanically coupling the tension-generating apparatuses of cortical cytoskeletons in neighboring cells (Maitre et al., 2012). In simple epithelia, this integration is exemplified by the zonula adherens (ZA) (Meng et al., 2008; Otani et al., 2006), a specialized adhesive junction where Myosin II is locally recruited to concentrate E-cadherin and generate junctional tension (Ratheesh et al., 2012; Smutny et al., 2010).

Rho family GTPases play important roles in supporting cadherin–actin cooperation at junctions such as the ZA (Braga, 2000). The canonical members of this family (Rho, Rac, and Cdc42) have been identified at cadherin junctions. In particular, Rho and Rac may play pivotal roles by regulating myosin II recruitment (Ratheesh et al., 2012; Shewan et al., 2005; Smutny et al., 2010) and actin assembly (Insall and Machesky, 2009; Kraemer et al., 2007; Yamazaki et al., 2007), respectively. Further, disruption of Rho and/or Rac signaling can perturb junctional integrity; therefore expression of these signals may be important for junctional homeostasis. Rho GTPases are molecular switches that shuttle between a GTP-bound active state and a GDP-bound inactive state. The nucleotide status of GTPases is, in turn, controlled by three sets of regulatory proteins: guanine nucleotide exchange factors (GEFs) that activate GTPases by the exchange of GDP for GTP; GTPase-activating proteins (GAPS) that inhibit GTPases by accelerating the hydrolysis of GTP to GDP; and GDP dissociation inhibitors (GDIs) that extract GTPases from membranes and sequester them in the cytosol (Etienne-Manneville and Hall, 2002). Potentially the interplay between these three sets of regulators, or subsets of them, may determine the stringent expression of GTPase signaling (Miller and Bement, 2009).

Indeed, we recently identified a regulatory apparatus that coordinates the balance between GEF and GAP activity to influence Rho signaling at the epithelial ZA (Ratheesh et al., 2012). This apparatus involved the centralspindlin (CS) complex, composed of MgcRacGAP and MKLP1, which is best-understood to control Rho at the cytokinetic furrow of dividing cells. However, we found that CS also localizes to the ZA of interphase epithelial cells. There it supported Rho signaling by localizing a GEF, ECT2, to activate Rho, and also by preventing the junctional localization of p190B RhoGAP, a GAP for Rho (Ratheesh et al., 2012). Together,

Abbreviations: CS, centralspindlin; E-cad, E-cadherin; ZA, zonula adherens; IIA, myosin IIA; KD, knockdown

* Corresponding author. Tel.: +61 7 3346 2013; fax: +61 7 3346 2101.
E-mail address: a.yap@uq.edu.au (A.S. Yap).

0301-4681/$ - see front matter © 2013 International Society of Differentiation. Published by Elsevier B.V. All rights reserved.
Join the International Society for Differentiation (www.isdifferentiation.org)
http://dx.doi.org/10.1016/j.diff.2013.01.002

this pathway facilitates the downstream activation of Myosin IIA, which promotes E-cadherin concentration and junctional tension.

An important cognate question is the role that the E-cadherin adhesion system plays in the control of junctional GTPase signaling. Ligation of E-cadherin can activate Rac (Kovacs et al., 2002; Kraemer et al., 2007; Nakagawa et al., 2001; Yamada and Nelson, 2007)) and Cdc42 (Kim et al., 2000; Kraemer et al., 2007), suggesting that these may be directly downstream of E-cadherin. Further, we found that the centralspindlin complex was localized to the ZA through an interaction with the *N*-terminus of α-catenin (Ratheesh et al., 2012), implying a supportive influence of E-cadherin on junctional Rho signaling at established junctions. In contrast, ligation of Xenopus C-cadherin caused an acute reduction in Rho-GTP levels (Noren et al., 2001), apparently due to the activation of p190 RhoGAP (Noren et al., 2003). This suggested that cadherin adhesion might inhibit Rho signaling. Accordingly, in this paper we sought to test the impact of E-cadherin on Rho signaling at mature zonulae adherente.

2. Materials and methods

2.1. Cell culture, antibodies, plasmids and shRNA reagents

MCF-7 cells were cultured in a Dulbecco's modified Eagle's medium supplemented with 10% FBS, 2 mM glutamine, non-essential amino acids, 100 units/ml penicillin, 100 μg/ml streptavidin and 0.01 mg/ml bovine insulin. Lipofectamine RNAi-MAX (Invitrogen) was used for transfection of RNAi oligonucleotides according to the manufacturer's instructions and cells were analyzed 48 h after transfection.

A lentivirus-based shRNA system was used to deplete endogenous E-cadherin, ECT2 and Myosin IIA (Rubinson et al., 2003); it was also used to simultaneously deplete endogenous E-cadherin and express mouse E-cadherin fused to GFP (Smutny et al., 2011). The lentivirus expression vector LentiLox pLL5.0 (backbone pLL3.7) and the third-generation packaging constructs pMDLg/pRRE, RSV-Rev and pMD.G were gifted from James Bear (UNC Chapel Hill, USA) (Vitriol et al., 2007). E-cadherin, ECT2 and Myosin IIA shRNA sequences and virus production and infection methods have been described earlier (Ratheesh et al., 2012; Smutny et al., 2010). pTriEx-RhoA Biosensor WT used for RhoA FRET experiments was obtained from Addgene and has been described previously (Pertz et al., 2006).

Primary antibodies used in this study were as follows: (1) mouse monoclonal antibody (mAb) directed against the ectodomain of human E-cadherin (HECD-1) (a gift from Peggy Wheelock, University of Nebraska, Omaha, NE; with the permission of M. Takeichi); (2) E-cad mouse IgG2a mAb against cytoplasmic tail, BD Transduction Laboratories (cat #610182); (3) rabbit polyclonal Ab (pAB) against human E-cadherin (generated in-house) (Helwani et al., 2004); (4) E-cadherin rat mAb (ECCD-2, Invitrogen, cat #13-1900); (5) ECT2 rabbit pAb (Millipore, cat #07-1364); (6) human ZO-1, rabbit pAb (Invitrogen, cat #61-7300); (7) MKLP1, rabbit pAb (Santa Cruz, cat #22793); (8) MgcRacGAP, rabbit pAb (Santa Cruz, cat #sc98617); (9) RhoA, mouse mAb (Santa Cruz, cat #sc418); and (10) GAPDH, rabbit pAb (R&D systems). Secondary antibodies were species-specific antibodies conjugated with Alexa-Fluor 488, 594 or 647 (Invitrogen) for immunofluorescence, or with horseradish peroxidase (Bio-Rad Laboratories) for immunoblotting. Western Blots were performed as described previously (Mangold et al., 2011).

2.2. Immunofluorescence, confocal microscopy, image acquisition and processing

MCF-7 cells were fixed with 10% TCA on ice for 15 min for Rho staining or with ice-cold methanol for 5 min on ice for ECT2/MgcRacGAP/MKLP1 staining. To stain for cytoplasmic GFP, cells were fixed with 4% Paraformaldehyde in PBS on ice for 20 min and then permeabilized with 0.25% Triton-X100 in PBS for 5 min at room temperature.

For immunofluorescence, confocal images were acquired with a Zeiss 710 Meta laser scanning confocal microscope, with a 60× objective, 1.4 NA oil Plan Apochromat immersion lens with 0.6–1.0 μm optical sections. Contrast adjustment, background corrections and z-projections of raw images were done by using ImageJ software (National Institutes of Health), Imaris (Bitplane) and Illustrator (Adobe). For quantitation of fluorescence intensity at contacts of immunofluorescence images, the line scan function of ImageJ was used as described in detail previously (Smutny et al., 2010). For each experiment, up to 25 contacts were analyzed. Data were processed using Prism.

The Z-stack profile of fluorescence intensity at cell–cell junctions was determined as follows: Z-stacks of the entire lateral region of cells stained for RhoA, E-cadherin and ZO1 were acquired by confocal microscopy with 0.3 μm interval steps and 0.6 μm optical sections. Junctional average and background intensities for each protein at different *z*-positions were determined in small regions located at the junctions and next to these. After background subtraction and normalization along the *Z*-axis, z-profiles of normalized fluorescence for multiple contacts ($n=15$) were aligned using the position of the maximum normalized intensity of ZO1 as a reference (0 μm), where positive values correspond to lower z-sections.

2.3. Fluorescence recovery after photobleaching (FRAP)

To address the issue of E-cadherin dynamics, E-cadherin GFP was expressed in an endogenous E-cadherin knockdown background using lentivrus infection (Smutny et al., 2011). ECT2 and Myosin IIA KD was performed by coinfecting the above cells with either lentivirus encoding shRNA designed against the 3′UTR

Fig. 1. Rho signaling at the zonula adherens requires E-cadherin. (a) RhoA (green), E-cadherin (red) and ZO-1 (magenta) immunostaining in confluent MCF-7 cells. *Left*; Representative confocal sections of a 3D Z-stack showing E-cadherin (middle panel) and RhoA (top panel) distribution at the zonula adherens ($Z=1.2$ μm) and ZO-1 (bottom panel) distribution at tight junctions ($Z=0$ μm). The position of the tight junctions was used as reference. Right, Merge of E-cadherin and RhoA at the zonula adherens and *X–Z* projection (taken at the horizontal line) showing the distribution of E-cadherin, RhoA and ZO-1. (b) Z-stack profile of fluorescence intensity for RhoA, E-cadherin and ZO-1 at cell–cell junctions, data represent means ± SEM. (c and d) MCF-7 cells were infected with lentivirus encoding GFP (Control) or lentivirus encoding an shRNA for human E-cadherin (E-cad KD) and GFP, or virus encoding both an shRNA for human E-cad and a mouse E-cad GFP transgene (E-cadKD+rescue). (c) Immunoblots were probed for endogenous human E-cadherin and mouse E-cad GFP using the same antibody directed against the cytoplasmic domain of E-cadherin and GAPDH. (d) Infected cells were examined for GFP fluorescence, endogenous E-cadherin and ZO-1 by immunostaining. (e–g) Control, E-cad KD or E-cad KD+rescue (E-cad GFP) MCF-7 cells co-stained for RhoA and E-cad. Representative confocal images acquired at apical junctions are shown and fluorescence intensity at cell junctions was quantitated by linescan analysis (f). Represented are mean values ± SEM of contact profiles in control (blue), E-cad KD (red) and E-cad GFP (green) cells and peak fluorescence intensity at cell–cell contacts (g). Data represent means ± SD of data pooled from three individual experiments ($n=25$), $P<0.001$; One-way Anova, Dunnett's post hoc test. (h–j) E-cadherin depletion reduces junctional Rho-GTP. MCF-7 cells transfected with E-cad siRNA or scrambled siRNA and a RhoA biosensor were immunoblotted for E-cadherin and GAPDH (h). (i) Cells were imaged live using confocal microscopy and representative images (YFP and ratio of FRET/CFP) are shown. (j) Average emission ratios (FRET/CFP) were determined at the apical junctions. Data represent means ± SEM pooled from three individual experiments ($n=35$), $P<0.0001$; Student's *t*-test. Scale bars: (a) 5 μm and (d, e and i) 10 μm. (For interpretation of the references to color in this figure legend, the reader is referred to the web version of this article.)

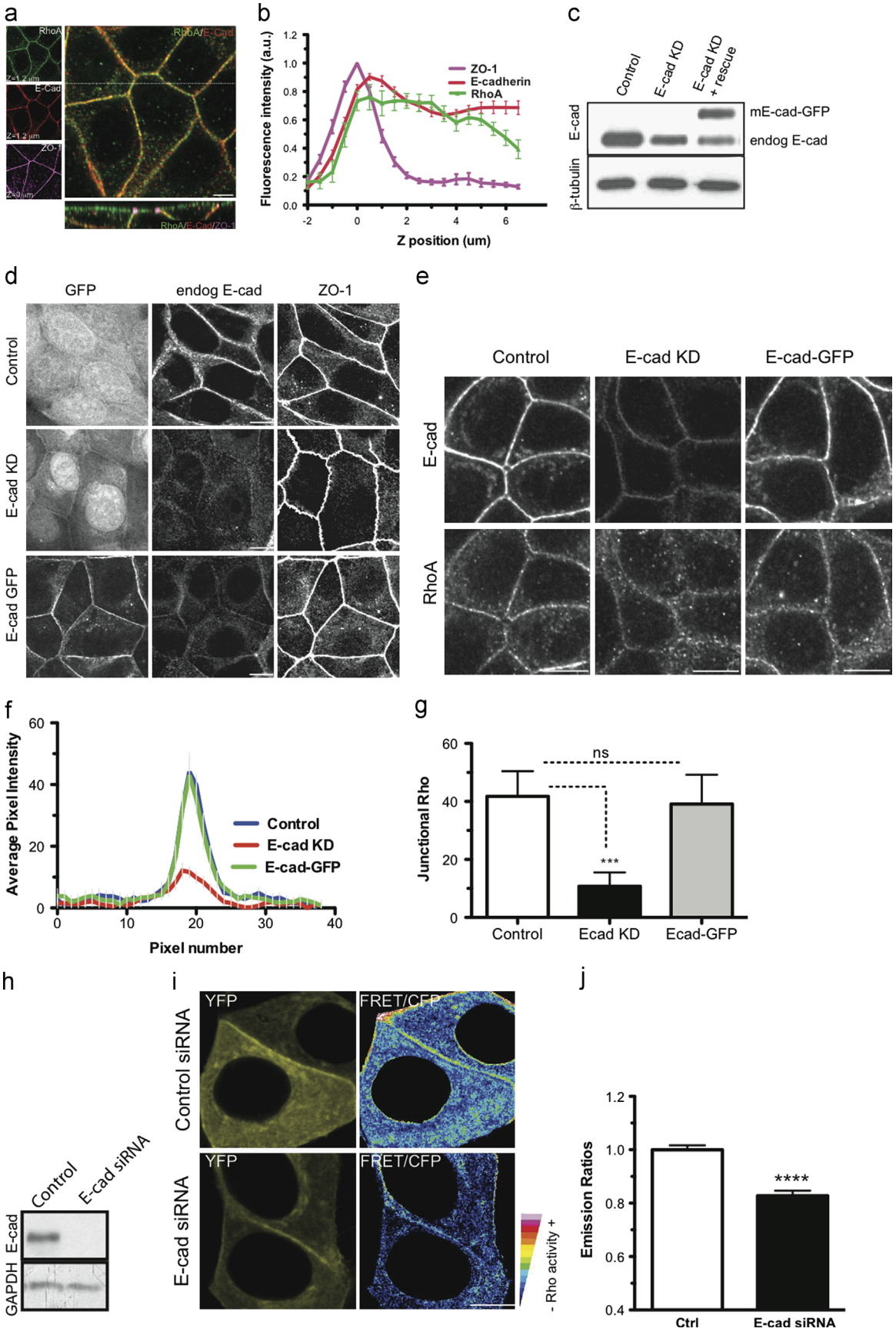
a
RhoA
RhoA/E-Cad
E-Cad
ZO-1
RhoA/E-Cad/ZO-1
b
Fluorescence intensity (a.u.)
ZO-1
E-cadherin
RhoA
Z position (um)
c
Control
E-cad KD
E-cad KD + rescue
E-cad
β-tubulin
mE-cad-GFP
endog E-cad
d
GFP
endog E-cad
ZO-1
Control
E-cad KD
E-cad GFP
e
Control
E-cad KD
E-cad-GFP
E-cad
RhoA
f
Average Pixel Intensity
Control
E-cad KD
E-cad-GFP
Pixel number
g
Junctional Rho
ns
***
Control
Ecad KD
Ecad-GFP
h
Control
E-cad siRNA
E-cad
GAPDH
i
Control siRNA
E-cad siRNA
YFP
FRET/CFP
- Rho activity +
j
Emission Ratios
****
Ctrl
E-cad siRNA

region of ECT2 or lentivirus encoding shRNA against Myosin IIA (MYH9) (Ratheesh et al., 2012; Smutny et al., 2010). Cells were split into glass bottom dishes (N 1.5, MatTek corporation, MA) 48 h after infection and grown to full confluency. For image acquisition, cells were washed and incubated in the presence of imaging media (Hank's balanced salt solution supplemented with 10 mM HEPES pH 7.4 and 5 mM $CaCl_2$). For these experiments, only cells co-expressing E-cadherin GFP and cherry were chosen to ensure the presence of the knockdown phenotype. To inhibit Rho signaling, cells were treated with 500 ng/μl of cell-permeant C3 Transferase (Rho inhibitor I, Cytoskeleton, CO) in imaging media for 1 h, washed and incubated in the same. Cells with en face contacts were chosen, which allowed us to precisely identify and photobleach the zonula adherens and the lateral contacts.

Image acquisition and analysis for FRAP experiments have been described previously (Ratheesh et al., 2012). Briefly, time-lapse images were acquired before and after photo bleaching with an interval of 5 s per frame (total 280 s). Image analysis was performed using ImageJ. Fluorescence intensities values $F(t)$ in the bleached area were normalized to prebleach values and fitted to the equation:

$$\text{Fluorescence recovery} = \frac{F(t)-F(0)}{F(-t)} = Mf(1-e^{\ln 2t/t_{1/2}})$$

where $F(t)$ is the average fluorescence of the bleached area during the time series, Mf is the mobile fraction, $t_{1/2}$ is the half time of recovery and t is time in seconds.

2.4. Fluorescence resonance energy transfer (FRET) microscopy

MCF-7 cells were transiently transfected with the RhoA biosensor and E-cadherin Dharmacon SMARTpool siRNA (50 nM) directed against human CDH1 (NM_004360). Non-targeting siRNA pools were used as controls (Dharmacon). FRET measurements were performed 48 h after transfection as described previously (Ratheesh et al., 2012). Briefly, cells were imaged live at 37 °C by confocal microscopy and images acquired on a LSM710 Zeiss confocal microscope equipped with a 63× oil Immersion objective (Plan Apochromat 63 × 1.4NA, Zeiss, Jena, GER). Donor (D) and FRET (F) channels were recorded by scanning using a 458 nm laser line and collecting the emission in the donor emission range (BP 470–490 nm) and acceptor emission range (BP 530–590 nm), respectively. In addition, the acceptor (A) channel was acquired using the 514 nm laser line for excitation and collecting the emission in the acceptor emission range. Images were acquired by sequential line acquisition.

[FRET/Donor] emission ratios calculated for pixels located at the cell–cell junctions in every image were normalized to the value corresponding to the average FRET emission ratio value observed in control conditions. Data presented are mean FRET emission ratios calculated across the different images and their standard errors.

3. Results

3.1. E-cadherin is necessary for junctional Rho signaling

To investigate the impact of E-cadherin on RhoA signaling, we first used immunofluorescence and confocal microscopy to characterize the distribution of RhoA and E-cadherin at cell–cell interfaces in confluent MCF-7 cells monolayers. We found that RhoA concentrates with E-cadherin at the apical region of cells, but below the tight junction marker ZO1 (Fig. 1a, and b), thus reinforcing the idea that cadherin junctions, such as the ZA, are sites that accumulate Rho (Ratheesh et al., 2012). In addition, our detailed analysis of junctional RhoA distribution showed that it is also present, though less prominent, with E-cadherin at the lateral surface (Fig. 1a, and b).

To analyze if E-cadherin supports junctional RhoA, MCF-7 cells were infected with a lentivirus encoding E-cadherin shRNA. A significant reduction in E-cadherin expression was detected by both immunofluorescence (~80%, Fig. 1d) and western blot analysis (50%, Fig. 1c) where the difference observed is mainly due to the heterogeneity of lentiviral infection. In control cells, RhoA staining was evident at the ZA (along with cytoplasmic staining) and this junctional staining was diminished upon E-cadherin depletion (E-cad KD), becoming more diffused and punctated (Fig. 1e). This was not a consequence of the loss of cell junctions as tight junctions, identified by ZO-1 staining, remained intact in E-cad KD cells (Fig. 1d). We quantified the reduction in RhoA junctional intensity in E-cadherin KD cells using line scan analysis and confirmed the significant reduction when compared to control cells (Fig. 1f, and g). Also, by expressing a RNAi resistant mouse-E-cad-GFP transgene (Fig. 1c), we were able to restore junctional RhoA, indicating that the changes in RhoA localization were attributable to the reduction in E-cadherin (Fig. 1e–g).

These results, together with our previous observations that its active state was closely related to the junctional concentration of RhoA (Ratheesh et al., 2012), suggested that E-cadherin is required to maintain an active pool of Rho at the ZA. To confirm if this was indeed the case, we used a RhoA-FRET biosensor to analyze the impact of E-cadherin on RhoA activation at the ZA in live cells (Pertz et al., 2006; Ratheesh et al., 2012). For these experiments the RhoA biosensor was co-transfected with a Dharmacon smartpool siRNA targeted against E-cadherin (Fig. 1h) as the E-cadherin shRNA lentiviral system also expresses GFP as an infection marker, which interferes with the detection of CFP and YFP fluorescence. FRET measurements were performed 48 h after transfection (Ratheesh et al., 2012). Indeed, E-cad KD reduced junctional Rho-GTP significantly compared to control cells (Fig. 1i and j). Overall, these results imply that E-cadherin is required to sustain Rho signaling at the ZA.

3.2. Junctional localization of Rho-GEF ECT2 and centralspindlin requires E-cadherin

The spatial expression of RhoA activity can reflect tight regulation by GEFs and GAPs. We recently demonstrated that ECT2, a member of the Dbl family of Rho GEFs, supports Rho signaling at the ZA in MCF-7 cells (Ratheesh et al., 2012). ECT2 localized to the ZA, in turn, through the action of the CS complex, which binds to α-catenin. Accordingly, we hypothesized that Rho signaling in E-cadherin KD cells might arise from loss of one or both of these elements from junctions.

To test this notion, we first examined the effect of E-cad KD on junctional ECT2. MCF-7 cells infected with lentivirus encoding E-cad shRNA were methanol fixed and stained for ECT2 and E-cad. In control cells, ECT2 accumulated at the cell–cell junctions, preferentially at the ZA (not shown) (Ratheesh et al., 2012). However, depletion of E-cadherin expression by shRNA caused a significant reduction in the junctional ECT2 as shown in Fig. 2a and further confirmed by line scan analysis (Fig. 2b and c). As with junctional RhoA, the loss of junctional ECT2 in E-cad KD cells was restored by expression of RNAi-resistant E-cad-GFP (Fig. 2b and c). Then we tested the impact of E-cadherin depletion on junctional CS, by co-staining E-cadherin either with MgcRacGAP (Fig. 3a–c) or MKLP1 (Fig. 3d–f), the components of the CS complex. Whereas MgcRacGAP and MKLP1 localized at the ZA in confluent control MCF7 cells, their junctional levels were substantially reduced by E-cadherin shRNA, and this was restored by expression of RNAi-resistant E-cad GFP (Fig. 3). Overall, these

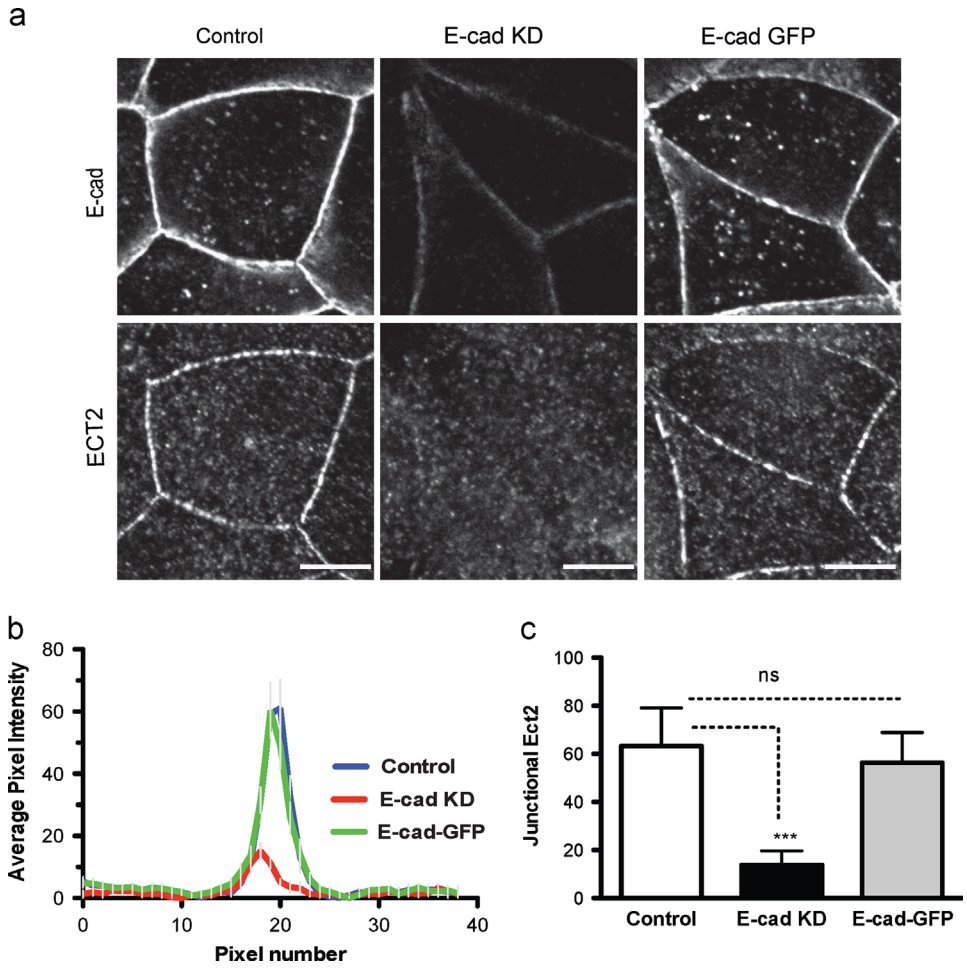

Fig. 2. E-cadherin is necessary for the junctional localization of Rho-GEF ECT2. (a) Control, E-cadherin KD or E-cad KD+rescue (E-cad GFP) MCF-7 cells co-stained for ECT2 and E-cadherin. Representative confocal images acquired at apical junctions are shown and fluorescence intensity at cell junctions was quantitated by linescan analysis. Represented are mean values ± SEM of contact profiles in control (blue), E-cad KD (red) and E-cad GFP (green) cells (b) and peak fluorescence intensity at cell-cell contacts (c). Data represent means ± SD of data pooled from three individual experiments ($n=20$), $P<0.001$; One way Anova, Dunnett's post hoc test. Scale bars: (a) 10 μm. (For interpretation of the references to color in this figure legend, the reader is referred to the web version of this article.)

findings suggest that E-cadherin may support Rho signaling at ZA by maintaining ECT2 and CS at these junctions.

3.3. *The ECT2-Rho signaling pathway specifically stabilizes apical, rather than lateral, E-cadherin*

A major target for Rho signaling at the ZA is non-muscle myosin II, especially the myosin IIA isoform (Smutny et al., 2010), which promotes junctional integrity by stabilizing mobility of E-cadherin at the ZA (Ratheesh et al., 2012). Further, elements of the CS-Rho signaling pathway also limit cadherin mobility, indicating that this whole pathway serves to stabilize E-cadherin at the ZA (Ratheesh et al., 2012).

However, E-cadherin can also be found elsewhere at cell–cell junctions. Notably, it often forms dispersed clusters and strands at the lateral junctions, below the ring-like structure of the apical ZA (Kametani and Takeichi, 2007; Klingelhofer et al., 2002; Meng and Takeichi, 2009). We therefore asked whether molecular mobility might differ between the apical (ZA) and lateral pools of cadherin. E-cadherin-GFP was expressed in MCF-7 cells depleted of endogenous E-cadherin by shRNA (Fig. 1c, Ratheesh et al., 2012; Smutny et al., 2011) and fluorescence recovery after photobleaching (FRAP) was monitored in small foci at the ZA and lateral regions of the same junctions. We found that the apical and lateral E-cadherin in control cells showed strikingly different patterns of fluorescence recovery (Fig. 4a and b). The lateral cadherin displayed a significantly shorter $t_{1/2}$ and greater mobile fraction than did the apical cadherin pool (Table 1). Thus, even within individual contacts, E-cadherin in the apical pool is relatively more stable and less mobile than that in the lateral pool.

We then asked whether E-cadherin stabilization in the ZA pool might reflect the action of the CS-ECT2-Rho signaling pathway and its effectors (Fig. 4c and e). We compared apical and lateral E-cadherin turnover in cells where ECT2 or Rho was perturbed by RNAi or C3-transferase, respectively. In both cases, the regional difference in E-cadherin turnover seen in control cells was abolished, and the FRAP curves largely coincided. In particular, the mobile fractions were indistinguishable in the apical and lateral zones from both ECT2-KD and C3-transferase-treated cells, although regional differences in $t_{1/2}$ persisted (Table 1). Further, the difference between apical and lateral turnover was also lost in Myosin IIA shRNA cells (Fig. 4d). Overall, these findings support the notion that local activation of myosin IIA by the ECT2-RhoA pathway creates a pool of E-cadherin at the ZA whose mobility is more restricted than that in the lateral pool.

4. Discussion

E-cadherin-based cell–cell junctions and Rho family GTPase signaling pathways interact cooperatively. Not only can GTPases

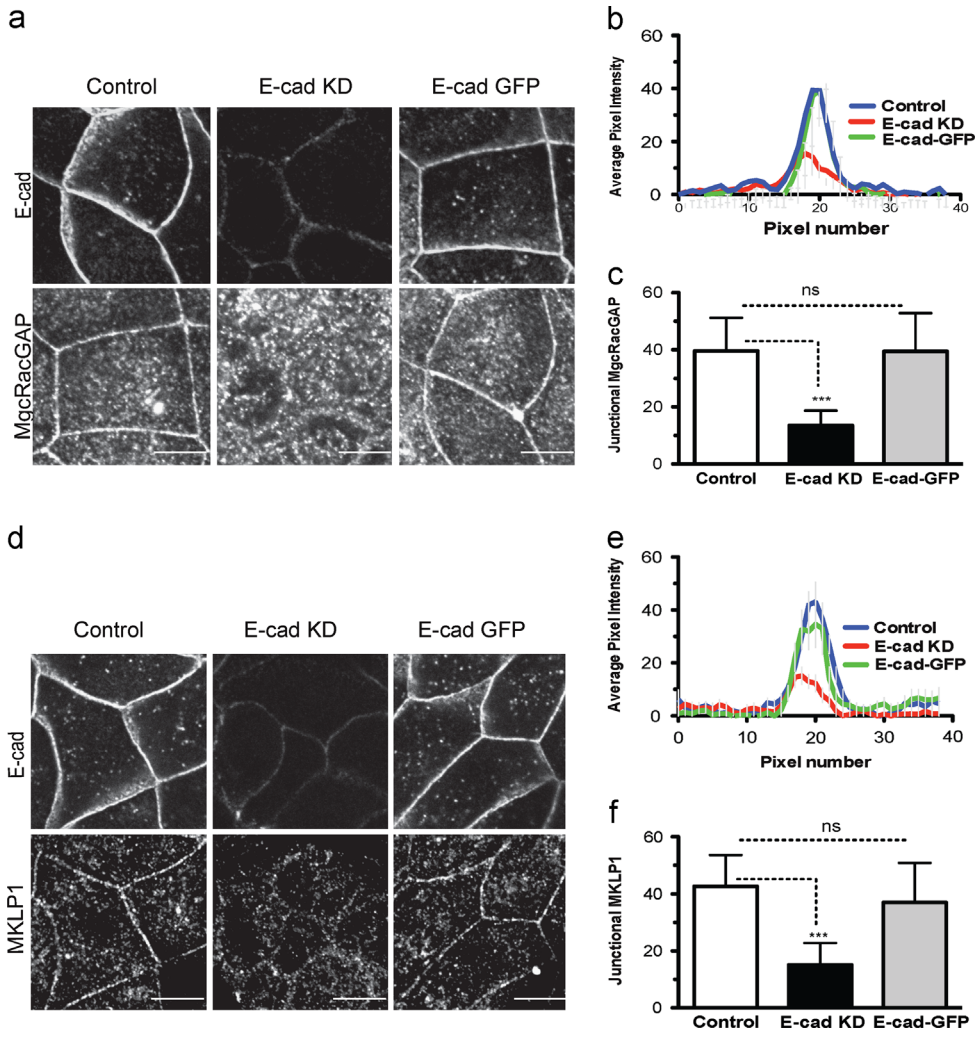

Fig. 3. E-cadherin supports junctional localization of the Centralspindlin complex. Control E-cadherin KD or E-cad KD+rescue (E-cad GFP) MCF-7 cells co-stained for E-cadherin and either MgcRacGAP (a–c) or MKLP1 (d–f). Representative confocal images acquired at apical junctions are shown (a, d) and fluorescence intensity at cell junctions was quantitated by linescan analysis (b, c, e, and f). (b and e) Represented are mean values ± SEM of contact profiles for MgcRacGAP (b) or MKLP1 (e) in control (blue), E-cad KD (red) and E-cad GFP (green) cells. (c and f) peak fluorescence intensity at cell–cell contacts for MgcRacGAP (c) or MKLP1 (f) pooled from three individual experiments ($n=20$). Data are means ± SD, $P<0.001$; One-way Anova, Dunnett's post hoc test. Scale bars: (a and d) 10 μm. (For interpretation of the references to color in this figure legend, the reader is referred to the web version of this article.)

and their downstream effectors influence junctional integrity and dynamics (commonly described as "inside-out" signaling) (Fukata and Kaibuchi, 2001; Wheelock and Johnson, 2003) but cadherin adhesion can itself regulate the localization and function of these GTPases ("outside-in signaling") (Braga, 2000; Wheelock and Johnson, 2003; Yap and Kovacs, 2003). In this report we sought to investigate both aspects of this signaling nexus.

Our analysis indicated that although Rho localizes throughout lateral cell–cell contacts, it preferentially concentrates at the zonula adherens with E-cadherin. Our results also suggest that E-cadherin is required to maintain active Rho signaling at established cell–cell junctions, especially at the specialized zonula adherens that we studied. Thus, both RhoA protein and RhoA-GTP signals at the junctions were significantly reduced in E-cadherin RNAi cells, although some degree of cell–cell contact was preserved (as indicated by the persistence of ZO-1 staining). This implied that the presence of E-cadherin, rather than simply cell–cell contact, was necessary for steady-state Rho signaling at the ZA. Further, Rho signaling at the ZA is regulated by the centralspindlin complex, which localizes by directly or indirectly binding to α-catenin (Ratheesh et al., 2012). This suggested that cadherin might ultimately influence Rho signaling through CS. Indeed, we now find that E-cadherin depletion displaced both CS and its effector, ECT2, from junctions. Together, these findings support the notion that E-cadherin supports RhoA signaling at the ZA by controlling the junctional localization of CS and, thereby, the RhoA activator, ECT2.

The apparently preferential localization of CS and ECT2 to the ZA implies that this pathway regulates Rho signaling in this spatially restricted region of the apical junction. Such spatial selectivity might, in turn, locally regulate downstream effectors and their potential impact on E-cadherin. One such effector is myosin IIA, which is necessary for ZA integrity (Ratheesh et al., 2012; Smutny et al., 2010) and selectively stabilizes E-cadherin in the apical (ZA) pool. Thus, our FRAP analysis indicates that E-cadherin at the ZA has a significantly restricted mobility compared with that found at the lateral surface of cell–cell contacts below the ZA. However, this difference was largely abolished in myosin IIA RNAi cells. Further, the spatial difference in mobility patterns was also abolished when elements of the upstream regulatory pathway, Rho and its apically confined activator ECT2, were perturbed. Overall, this suggests that the spatially confined localization of upstream Rho regulators, such as

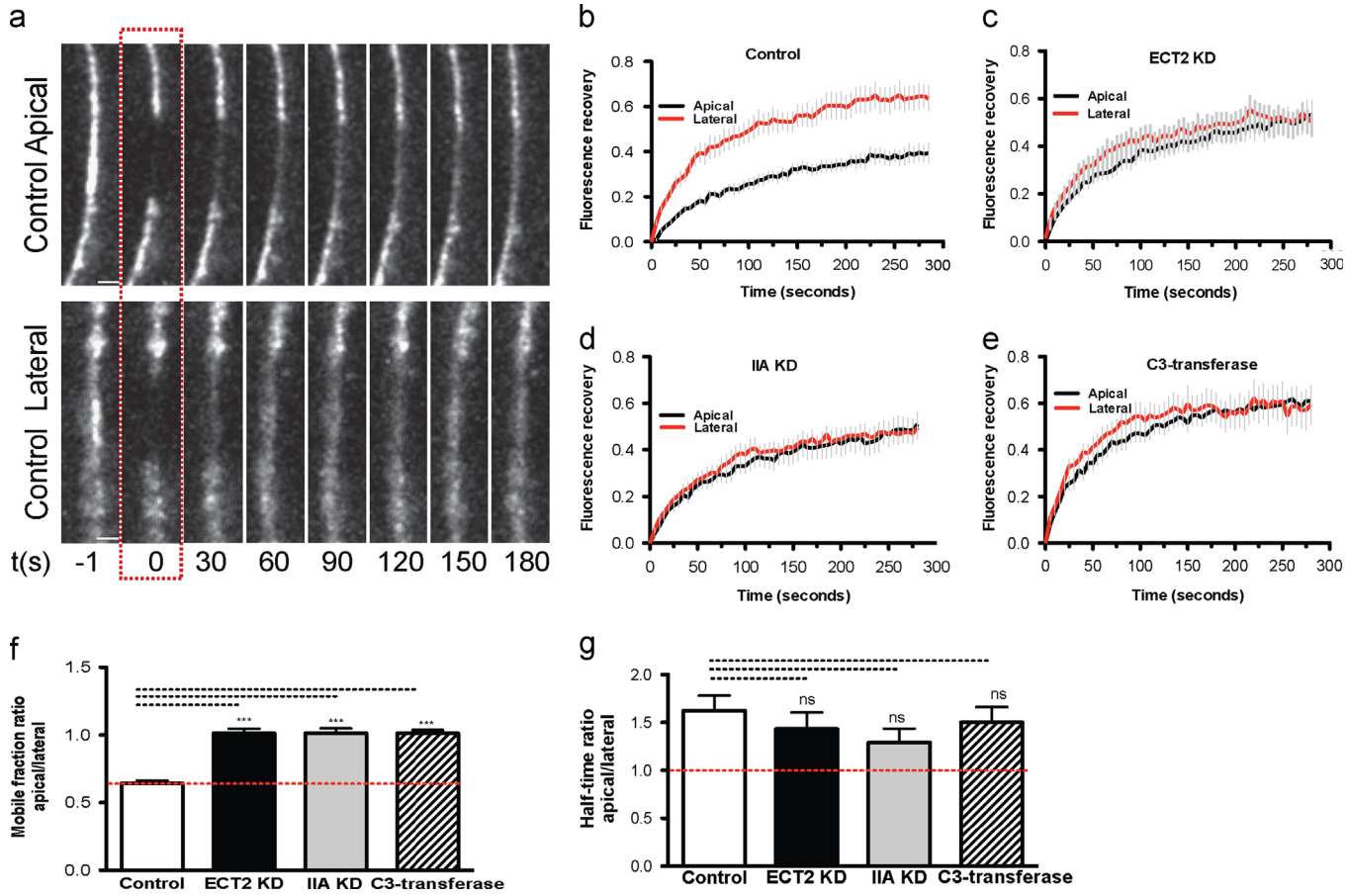

Fig. 4. Rho signaling differentially stabilizes two E-cadherin pools. Fluorescence recovery after photobleaching (FRAP) was performed with mouse E-cadherin-GFP expressed in MCF-7 cells depleted of endogenous E-cad by shRNA. (a) Representative frames after photobleaching in the apical and lateral zones of an individual contact. (b–e) FRAP profiles of apical (black) and lateral (red) E-cad-GFP in control MCF-7 cells (control, b) and cells treated with ECT2 RNAi (ECT2KD) (c), Myosin IIA RNAi (IIA KD) (d) or with C3-*T* (C3-transferase and (e) solid lines represent means ± SEM. Mobile fraction and half time values obtained from the best-fit single exponential curves of FRAP profiles and expressed as ratios of apical vs lateral values (f and g). Data represent means ± SEM of data pooled from three individual experiments ($n=10$), $P<0.001$; One way Anova, Dunnett's post hoc test. Scale bars: (a) 1 μm. (For interpretation of the references to color in this figure legend, the reader is referred to the web version of this article.)

Table 1
Half life and mobile fraction values obtained from non-linear regression analysis of FRAP profiles of E-cadherin GFP in control, Ect2KD, IIA KD and C-3 trasnferase treated cells. Data are presented as mean ± SEM ($n=10$). Statistical significance of the difference between apical vs lateral FRAP parameters for each condition was assessed by Student's *t*-test and is indicated in the brackets.

Conditions	Half life (s)	Mobile fraction
Control apical E-cadherin	65.62 ± 4.476	0.4038 ± 0.01046
Control lateral E-cadherin	40.400 ± 2.71***	0.6284 ± 0.01135****
ECT2 KD apical E-cadherin	49.98 ± 3.77	0.5018 ± 0.012
ECT2 KD lateral E-cadherin	34.91 ± 2.71**	0.4953 ± 0.00148 (ns)
IIA KD apical E-cadherin	53.36 ± 4.736	0.476 ± 0.01401
IIA KD lateral E-cadherin	41.31 ± 2.81*	0.4694 ± 0.00883 (ns)
C3-transferase apical E-cadherin	38.31 ± 2.71	0.5884 ± 0.0087
C3-transferase lateral E-cadherin	25.5 ± 2.33***	0.5811 ± 0.010 (ns)

* $p<0.05$.
** $p<0.01$.
*** $p<0.001$.
**** $p<0.0001$.

ECT2 ultimately affects local E-cadherin mobility through myosin IIA. One potential mechanism for this to happen might be via myosin IIA-induced clustering of E-cadherin (Smutny et al., 2010).

It should be noted that our current findings contrast with earlier work, which demonstrated that homophilic ligation of Xenopus C-cadherin acutely inhibited Rho signaling (Noren et al., 2001). The experimental systems used are not readily comparable. One important difference is the distinction between long-term contributions of cadherin, as studied in our experiments, compared with the acute stimulation used by earlier (Noren et al., 2001). As well, E-cadherin may act with other forms of junctional signaling when studied at native cell–cell contacts (Yap and Kovacs, 2003), whereas ligation with recombinant ligands isolates the influence of homophilic cadherin adhesion. More generally, these discrepancies may highlight the complex network of signals that determine the expression of Rho GTPase signaling at junctions. For example, whereas the inhibition of Rho by acute C-cadherin ligation involved cross-talk mediated by p190 RhoGAP (Noren et al., 2003) that can be downstream of Rac (Wildenberg et al., 2006), CS at the established ZA inhibited Rac signaling (Ratheesh et al., 2012). Such cross-talk between Rac and Rho signaling pathways implies that the functional outcome may be very sensitive to cellular context.

Finally, our current and recent findings (Ratheesh et al., 2012) suggest that Rho signaling at the ZA arises from the input of multiple cellular factors. In addition to E-cadherin, these include dynamic microtubules, which can be recruited to cadherin adhesions (Mary et al., 2002; Stehbens et al., 2006), which in turn control the junctional localization of CS (Ratheesh et al., 2012). Thus, rather than being the product of a linear signaling pathway, junctional Rho signaling may be better conceived as the product

of coincidence detection (Carlton and Cullen, 2005) where multiple factors must be spatially and temporally coordinated for productive signaling to occur. From this perspective, it might be useful to consider that, at the ZA, the E-cadherin molecular complex serves as a cortical platform to coordinate the multiple upstream elements that regulate Rho, thereby facilitating coincidence detection.

Acknowledgments

This work was supported by Grant (631377) and research fellowship to AY (631383) from the National Health and Medical Research Council; Australian Research Council (DP120104667) and the Oncology Children's Foundation. RP is supported by UQI (UQ International) Ph.D. Scholarship and ANZ Trustees Ph.D. Scholarship in Medical Research. Confocal microscopy was performed at the ACRF/IMB Cancer Biology Imaging Centre established with the generous support of the Australian Cancer Research Foundation.

References

Braga, V., 2000. Epithelial cell shape: cadherins and small GTPases. Experimental Cell Research 261, 83–90.
Carlton, J.G., Cullen, P.J., 2005. Coincidence detection in phosphoinositide signaling. Trends in Cell Biology 15, 540–547.
Etienne-Manneville, S., Hall, A., 2002. Rho GTPases in cell biology. Nature 420, 629–635.
Fukata, M., Kaibuchi, K., 2001. Rho-family GTPases in cadherin-mediated cell–cell adhesion. Nature Reviews Molecular Cell Biology 2, 887–897.
Helwani, F.M., Kovacs, E.M., Paterson, A.D., Verma, S., Ali, R.G., Fanning, A.S., Weed, S.A., Yap, A.S., 2004. Cortactin is necessary for E-cadherin-mediated contact formation and actin reorganization. Journal of Cell Biology 164, 899–910.
Insall, R.H., Machesky, L.M., 2009. Actin dynamics at the leading edge: from simple machinery to complex networks. Developmental Cell 17, 310–322.
Kametani, Y., Takeichi, M., 2007. Basal-to-apical cadherin flow at cell junctions. Nature Cell Biology 9, 92. (U118).
Kim, S.H., Li, Z.G., Sacks, D.B., 2000. E-cadherin-mediated cell–cell attachment activates Cdc42. Journal of Biological Chemistry 275, 36999–37005.
Klingelhofer, J., Laur, O.Y., Troyanovsky, R.B., Troyanovsky, S.M., 2002. Dynamic interplay between adhesive and lateral E-cadherin dimers. Molecular Cell Biology 22, 7449–7458.
Kovacs, E.M., Ali, R.G., McCormack, A.J., Yap, A.S., 2002. E-cadherin homophilic ligation directly signals through Rac and phosphatidylinositol 3-kinase to regulate adhesive contacts. Journal of Biological Chemistry 277, 6708–6718.
Kraemer, A., Goodwin, M., Verma, S., Yap, A.S., Ali, R.G., 2007. Rac is a dominant regulator of cadherin-directed actin assembly that is activated by adhesive ligation independently of Tiam1. American Journal of Physiology—Cell Physiology 292, C1061–C1069.
Maitre, J.L., Berthoumieux, H., Krens, S.F.G., Salbreux, G., Julicher, F., Paluch, E., Heisenberg, C.P., 2012. Adhesion functions in cell sorting by mechanically coupling the cortices of adhering cells. Science 338, 253–256.
Mangold, S., Wu, S.K., Norwood, S.J., Collins, B.M., Hamilton, N.A., Thorn, P., Yap, A.S., 2011. Hepatocyte growth factor acutely perturbs actin filament anchorage at the epithelial zonula adherens. Current Biology 21, 503–507.
Mary, S., Charrasse, S., Meriane, M., Comunale, F., Travo, P., Blangy, A., Gauthier-Rouviere, C., 2002. Biogenesis of N-cadherin-dependent cell–cell contacts in living fibroblasts is a microtubule-dependent kinesin-driven mechanism. Molecular Biology of the Cell 13, 285–301.
Mason, F.M., Martin, A.C., 2011. Tuning cell shape change with contractile ratchets. Current Opinion in Genetics and Development 21, 671–679.
Meng, W., Mushika, Y., Ichii, T., Takeichi, M., 2008. Anchorage of microtubule minus ends to adherens junctions regulates epithelial cell–cell contacts. Cell 135, 948–959.
Meng, W.X., Takeichi, M., 2009. Adherens junction: molecular architecture and regulation. Cold Spring Harbor Perspectives in Biology, 1.
Miller, A.L., Bement, W.M., 2009. Cell division: the need for speed. Current Biology 19, R1071–R1073.
Nakagawa, M., Fukata, M., Yamaga, M., Itoh, N., Kaibuchi, K., 2001. Recruitment and activation of Rac1 by the formation of E-cadherin-mediated cell–cell adhesion sites. Journal of Cell Science 114, 1829–1838.
Noren, N.K., Arthur, W.T., Burridge, K., 2003. Cadherin engagement inhibits RhoA via p190RhoGAP. Journal of Biological Chemistry 278, 13615–13618.
Noren, N.K., Niessen, C.M., Gumbiner, B.M., Burridge, K., 2001. Cadherin engagement regulates Rho family GTPases. Journal of Biological Chemistry 276, 33305–33308.
Otani, T., Ichii, T., Aono, S., Takeichi, M., 2006. Cdc42 GEF Tuba regulates the junctional configuration of simple epithelial cells. Journal of Cell Biology 175, 135–146.
Pertz, O., Hodgson, L., Klemke, R.L., Hahn, K.M., 2006. Spatiotemporal dynamics of RhoA activity in migrating cells. Nature 440, 1069–1072.
Ratheesh, A., Gomez, G.A., Priya, R., Verma, S., Kovacs, E.M., Jiang, K., Brown, N.H., Akhmanova, A., Stehbens, S.J., Yap, A.S., 2012. Centralspindlin and alpha-catenin regulate Rho signaling at the epithelial zonula adherens. Nature Cell Biology 14, 818–828.
Ratheesh, A., Yap, A.S., 2012. A bigger picture: classical cadherins and the dynamic actin cytoskeleton. Nature Reviews Molecular Cell Biology 13, 673–679.
Roh-Johnson, M., Shemer, G., Higgins, C.D., McClellan, J.H., Werts, A.D., Tulu, U.S., Gao, L., Betzig, E., Kiehart, D.P., Goldstein, B., 2012. Triggering a cell shape change by exploiting preexisting actomyosin contractions. Science 335, 1232–1235.
Rubinson, D.A., Dillon, C.P., Kwiatkowski, A.V., Sievers, C., Yang, L., Kopinja, J., Rooney, D.L., Zhang, M., Ihrig, M.M., McManus, M.T., Gertler, F.B., Scott, M.L., Van Parijs, L., 2003. A lentivirus-based system to functionally silence genes in primary mammalian cells, stem cells and transgenic mice by RNA interference. Nature Genetics 33, 401–406.
Shewan, A.M., Maddugoda, M., Kraemer, A., Stehbens, S.J., Verma, S., Kovacs, E.M., Yap, A.S., 2005. Myosin 2 is a key Rho kinase target necessary for the local concentration of E-cadherin at cell–cell contacts. Molecular Biology of the Cell 16, 4531–4542.
Smutny, M., Cox, H.L., Leerberg, J.M., Kovacs, E.M., Conti, M.A., Ferguson, C., Hamilton, N.A., Parton, R.G., Adelstein, R.S., Yap, A.S., 2010. Myosin II isoforms identify distinct functional modules that support integrity of the epithelial zonula adherens. Nature Cell Biology 12, 696. (U147).
Smutny, M., Wu, S.K., Gomez, G.A., Mangold, S., Yap, A.S., Hamilton, N.A., 2011. Multicomponent analysis of junctional movements regulated by myosin II isoforms at the epithelial zonula adherens. PLOS ONE, 6.
Stehbens, S.J., Paterson, A.D., Crampton, M.S., Shewan, A.M., Ferguson, C., Akhmanova, A., Parton, R.G., Yap, A.S., 2006. Dynamic microtubules regulate the local concentration of E-cadherin at cell–cell contacts. Journal of Cell Science 119, 1801–1811.
Vitriol, E.A., Uetrecht, A.C., Shen, F.M., Jacobson, K., Bear, J.E., 2007. Enhanced EGFP-chromophore-assisted laser inactivation using deficient cells rescued with functional EGFP-fusion proteins. Proceedings of the National Academy of Sciences of the United States of America 104, 6702–6707.
Wheelock, M.J., Johnson, K.R., 2003. Cadherin-mediated cellular signaling. Current Opinion in Cell Biology 15, 509–514.
Wildenberg, G.A., Dohn, M.R., Carnahan, R.H., Davis, M.A., Lobdell, N.A., Settleman, J., Reynolds, A.B., 2006. p120-Catenin and p190RhoGAP regulate cell–cell adhesion by coordinating antagonism between Rac and Rho. Cell 127, 1027–1039.
Yamada, S., Nelson, W.J., 2007. Localized zones of Rho and Rac activities drive initiation and expansion of epithelial cell–cell adhesion. Journal of Cell Biology 178, 517–527.
Yamazaki, D., Oikawa, T., Takenawa, T., 2007. Rac-WAVE-mediated actin reorganization is required for organization and maintenance of cell-cell adhesion. Journal of Cell Science 120, 86–100.
Yap, A.S., Kovacs, E.M., 2003. Direct cadherin-activated cell signaling: a view from the plasma membrane. Journal of Cell Biology 160, 11–16.

3.2.2 Results presented as accepted manuscript

Measurement of Junctional Protein Dynamics Using Fluorescence Recovery After Photobleaching (FRAP)

Rashmi Priya & Guillermo A. Gomez*

Division of Molecular Cell Biology, Institute for Molecular Bioscience, The University of Queensland, St. Lucia, Brisbane, Queensland, Australia 4072

* Corresponding author: Guillermo A. Gomez, E-mail: g.gomez@uq.edu.au

[Abstract] Fluorescence Recovery After Photobleaching (FRAP) (Lippincott-Schwartz *et al*., 2003; Reits and Neefjes, 2001) was employed to determine dynamic properties of proteins localized at the ephitelial zonula adherens (ZA) (Kovacs *et al*., 2011; Otani *et al*., 2006). The proteins of interest were expressed in cells using a knockdown and reconstitution approach in which endogenous proteins were depleted by RNA interference (RNAi) and replaced by expression of an RNAi-resistant gene fused to GFP (Priya *et al*., 2013; Smutny *et al*., 2010; Smutny *et al.,* 2011; Vitriol *et al*., 2007). By choosing expression levels of GFP-tagged proteins that were comparable to endogenous levels, we minimized transient overexpression artifacts due to overcoming regulatory mechanisms that directly affect protein dynamics (Goodson *et al*., 2010). Using this approach, junctional E-cadherin-GFP or GFP-Ect2 were subjected to FRAP analysis in small areas corresponding to the ZA using confocal microscopy (Priya *et al*., 2013; Ratheesh *et al.,* 2012; Gomez *et al*., 2005; Trenchi *et al*., 2009). Although in principle this approach is similar in every case, bleaching conditions, acquisition parameters and analysis details might differ depending on the time scale of the recovery process (Lippincott-Schwartz *et al*., 2003). In this protocol we will describe the experimental procedure to perform FRAP experiments and how to optimize bleaching and acquisition conditions for optimal measurements of protein dynamics at cell-cell junctions.

Materials and Reagents

1. MCF-7 cells, mammary carcinoma epithelial cells derived from metastatic site (ATCC® HTB22™)
2. HEK293T cells
3. Plasmids.
   - pLL5.0 lentiviral vector (Fig1) and packaging plasmids pMDLg/pRRE, pMD2.G (VSV G) and pRSV-Rev. pLL5.0 is a modified version of pLL3.7 and it was generously provided by Jim Bear, Department of Cell and Developmental Biology, University of North Carolina, Chapel Hill, NC 27599 (Vitriol *et al*., 2007; Rubinson *et al.,* 2003*)*.
   - pLL5.0 containing both a shRNA against the ORF of human CDH1 (NM_004360) (5′-GGGTTAAGCACAACAGCAA -3′) cloned downstream of the U6 promoter (HpaI and XhoI) (Fig1) and a mouse E-Cadherin(NM_009864)-GFP fusion construct cloned at SacII and SbfI sites. The E-cadherin-EGFP fusion protein expression was driven by a 5'LTR promoter to facilitate lower expression levels of GFP fusion proteins for imaging (Smutny *et al., 2011*).

- pLL5.0 containing both a shRNA against the 3'UTR of human ECT2 (NM_001258315) (5'-GCTGTTTCAAAGTGTGATA-3') and cloned downstream of the U6 promoter (HpaI and XhoI) (Fig1) in a modified version of pLL5.0. In this modified pLL5.0 the GFP reporter was replaced by the sequence that encompasses both the coding region for GFP and the multiple cloning site of pEGFP-C1 (Clontech) using EcoRI and SbfI sites. These restriction sites were not preserved after this cloning step. Then the human ECT2 coding sequence (NM_001258315) was cloned into the vector using EcoR1 and BamH1 sites

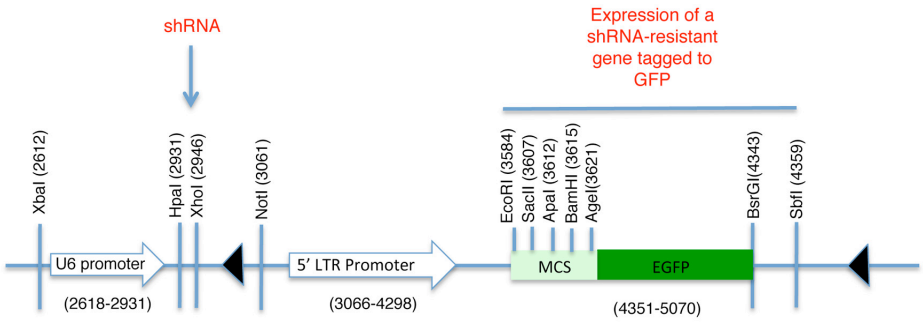

Figure 1. Schematic of pLL5.0 vector. Sites HpaI and XhoI are used for the subcloning of shRNA sequences desired to knockdown endogenous levels of the protein of interest. The U6 promoter drives the expression of this shRNA sequence. Contrarily, a shRNA resistant version of the same protein can be subcloned downstream of the 5'LTR promoter and fused to GFP. Thus, it is possible to achieve endogenous levels of expression for a fluorescent-tagged protein and preventing effects associated to its overexpression. MCS=Multiple cloning site

(pLL5.0 GFP–shRNA resistant ECT2).

4. Dulbecco's Modified Eagle's Medium High glucose with stable L-glutamine (DMEM) (Gibco/Life Technologies, catalog number: 11995-073)
5. Foetal Bovine Serum (FBS) (Gibco/Life Technologies, catalog number: 26140079)
6. PBS without Ca^{2+} and Mg^{2+} (Astral Scientific, catalog number: 09-8912-100)
7. 16% Paraformaldehyde (formaldehyde) aqueous solution (ProScitech, catalog number: C004)
8. Hank's balanced salt solution (HBSS) (Sigma, catalog number: H8264)
9. In-Fusion cloning kit (Clontech, CA, catalog number: 638909)
10. Sodium butyrate (Sigma, catalogue number: B5887). A 1M stock solution of Sodium butyrate is prepared in water, filter sterilized and stored at 4°C previous to use.
11. Hexadimethine bromide (polybrene), (Sigma, catalog number: H9268). A stock solution of polybrene is made by diluting it into water to a final stock concentration of 8 mg/mL and sterilizing by filtering trough a 0.2 µm filter).
12. Hank's Balanced Salt Solution (Sigma, catalogue number: H8264)
13. Imaging media (see Recipes)
14. 4% Paraformaldheyde in PBS (see Recipes)
15. 175 cm^2 and 25 cm^2 Nunclon Delta Flasks (Nunc, ThermoScientific, cat# 159910 (175cm^2 flask) and cat#156367 (25 cm^2 flasks).
16. Trypsin, 2.5% (10X) Liquid (Life Technologies, cat#15090046). NOTE: this solution is diluted to 0.25% final concentration with PBS.

17. Poly(vinylidene difluoride) spin columns (Amicon Ultra Centrifugal filters. UltraCel-100K, Millipore Catalogue number: UFC910024)

Equipment

1. Laser scanning confocal microscope equipped with acousto-optic tunable filters (AOTF) for bleaching of selected areas and heated chamber (37 °C) for live cell imaging. The microscope must also be equipped with dichroic and emission filter for the use of the 405 and 488 nm laser lines and detection of GFP fluorescence. The experiments shown were performed on LSM510 Meta or LSM710 inverted confocal microscopes (Zeiss, Jena, Germany)
2. 30 mW Argon (458, 488 and 514 nm laser lines) and 25 mW (405 nm) diode lasers (Lasos, Lasertechnik, GMbH)
3. Plug-in FRAP profiler (McMaster University, Canada)
4. Glass bottom dishes (#1.5 MatTek Corp, catalog number: P35G-1.5-20-C or Shengyou Biotechnology Co. Ltd, catalog number: D29-10-1.5-N)

Software

1. Image J software.
2. Prism, GraphPad.
3. Matlab, MathWorks.

Procedure

I Cell preparation

1. Expression of GFP-tagged proteins in a knockdown background

   We have used this approach in our recent article published in *Nature Cell Biology* (Ratheesh *et al.,* 2012) to characterize the dynamic properties of the adhesion molecule E-cadherin and the RhoA GEF, Ect2. For the expression of these proteins at endogenous levels, we used the pLL5.0 lentiviral vector (Vitriol *et al*., 2007; Rubinson *et al.,* 2003*)*. This vector contains two promoters, a U6 promoter that drives the expression of shRNA and a 5'LTR promoter that drives the expression of a shRNA-resistant gene (Fig.1).

2. Lentivirus preparation and viral transduction
   a. HEK293T cells were cultured in 20 mL DMEM supplemented with 10% FBS at 37°C and maintained under these condition during the following steps.
   b. Constructs made in the pLL5.0 vector were simultaneously transfected with packaging vectors into HEK-293T cells by $CaCl_2$ precipitation.
   c. 48 h after transfection, cells were treated with sodium butyrate (10 mM final concentration) to increase gene induction.
   d. Virus-like particles (VLPs) were harvested 48–72 h after transfection and concentrated on poly(vinylidene difluoride) spin column as follows:

- Collect media of cells and spin down in 50 mL conical tube.
- Filter the supernatant into new tubes using 0.2 μm syringe filters.
- Add 10 mL filtrate to the poly(vinylidene difluoride) spin column and centrifuge at 3200 rpm on a bench top centrifuge for 20 min at room temperature. This will reduce the volume of the suspension of VLPs to ~800 μL per tube).
- Discard the flow trough and add the remaining supernatant (~10mL) to the the poly(vinylidene difluoride) spin column and repeat the above step.
- Aliquots of virus were subsequently used for titration or stored at −80 °C. Titers were determined as described before (Smutny *et al*., 2010).

3. Preparation of the cells for image acquisition
   a. For FRAP experiments, MCF-7 cells were cultured in DMEM supplemented with 10% FBS and infected with lentiviral particles at a multiplicity of infection of 10 per cell on 25 cm^2 flasks.
   b. Cells were incubated at 37 °C with the lentivirus in DMEM + FBS and Polybrene (8 μg ml^{-1}) and harvested by trypsinization three days after infection.
   c. Single-cell suspensions were seeded on glass bottom dishes at 80% confluence and allowed to grow for 48 h (or until they reach full confluence) for FRAP experiments.
   d. Prior to image acquisition, cells were washed with imaging media and incubated with 1.5 mL of it for the duration of the experiment.

II Image Acquisition

1. FRAP experiments were performed on a LSM 510 Meta or LSM 710 Zeiss confocal microscope for E-cadherin-GFP or GFP-Ect2, respectively. Microscopes were equipped with a heated stage maintained at 37 °C and a 30 mW Argon laser (458, 488 and 514 nm laser lines). The LSM 710 Zeiss confocal microscope was also equipped with a 405 nm (25 mW) diode laser. Images (pre and post-bleach, Figure 1) were acquired using 60x objective, 1.4 NA oil Plan Apochromat immersion lens at 4x digital magnification with 0.7 μm optical section. A 488 nm laser line of an argon laser (30 mW) was used for fluorescence excitation at 1-3% transmission.
2. For E-cadherin-GFP dynamics, time-lapse images (416 x 416 pixels, 0.086 μm/pixel) were acquired before and after photobleaching with an interval of 5 seconds per frame for the total time of 280 seconds (Figure 1A). A constant region of interest (ROI) of 2.8 x 1.7 μm with the longer axis parallel to the cell-cell contact was marked for each experiment and E-cadherin-GFP was bleached with 50 iterations of the 488 nm laser with 100% transmission. This resulted in maximum bleach of approximately 70%.
3. Ect2 dynamics was assessed using GFP-Ect2 co-expressed with Ect2 shRNA by lentiviral infection. A constant circular ROI (1.4 μm diameter) in approximately the center of the cell-cell contact was bleached to ~ 70% with both the 488 and the 405 nm lasers turned on simultaneously at 100% transmission. Time-lapse images of the same region were acquired before (20 frames, 5 seconds) and after (210 frames, 50 seconds) photobleaching with an interval of ~ 250 m per frame (Figure 1B).
4. For these experiments, cells with slanted contacts were chosen which allowed us to precisely identify and photobleach the ZA.

Special considerations

a. For any experimental setup, it is important to consider that the bleaching process and the frequency of acquisition has to match the dynamics of the protein of interest (Lippincott-Schwartz *et al*., 2003; Weiss 2004). The above technical details should be first be tested to achieve the optimal conditions for FRAP experiments of specific proteins or for different subcellular compartments. Bleaching and acquisition conditions can be optimized by doing FRAP in fixed cells. We routinely grow cells on glass bottom dishes and fix using 4% paraformaldehyde (PFA) in phosphate buffered buffer saline (PBS) for 15 min at room temperature. After fixation, PFA solution is replaced by imaging media and the FRAP protocols tested on this set of cells. Following this approach, optimization can be achieved in conditions that match the real experimental setup.

   The major aims of these optimization experiments are to:

   i. Determine the best conditions suitable for a fast and efficient photobleaching of molecules in a region of interest that would be used in the real experiments.
   ii. Optimize the time-lapse settings for acquisition during pre- and, more importantly, post- bleaching regimes. The main aim is to acquire images without causing photobleaching (< ~5%) of the sample at a given frequency that does not compromise FRAP analysis.

b. Following the optimization steps, a FRAP test is performed in living cells. There are two important points that that needs to be considered that are related to the half time of the observed recovery process (Weiss, 2004). Firstly, if the half time is comparable to the bleaching step, then there is a high chance that recovery is underestimated as bleached molecules can diffuse away from the bleached area during the bleaching step (Weiss, 2004). If so, it is necessary to optimize the bleaching protocol to make this step faster (~< 3 times the half time of recovery). This can be achieved for example, by reducing the area of the region that is wanted to be bleached or, by increasing the laser power and reducing the number of iterations during the bleaching step or, by increasing the number of laser lines activated during the bleaching step or, by reducing the scan speed of the bleaching step at the same time the number of iterations it is also reduced. The conditions mentioned for the bleaching step of E-cadherin and Ect2 are good standard initial conditions to perform FRAP experiments on proteins that exhibits very distinctive dynamics. Secondly, slow post acquisition frames can compromise recovery measurements. As the half time of a FRAP curve is calculated with the information acquired during the first 1.5 half times of the recovery process, confident estimation of FRAP parameters requires that acquisition be fast enough to accurately sample this early period. To satisfy this requirement, increasing scan speed or reducing the area of sampling during pre and postbleaching acquisition can increase the speed of acquisition. This second option was chosen in order to capture the fast dynamics of Ect2 mobility.

c. After these conditions are set, it is essential to consider that the optimized protocol does not compromise the viability of cells. Normally, UV irradiation causes toxicity, which is evident by changes in the morphology of the cell and membrane blebbing (Frigault *et al*., 2009). Acquisition of phase contrast or Differential interference contrast (DIC) images before and after FRAP acquisition is a complementary test to assess cell viability. Of note, UV irradiation can cause membrane damage that often results in an unexpectedly high immobile fraction. For this, it has been suggested to perform 2 consecutive FRAP experiments on the same cells and on the same region, in order to determine that recovery occurs even after two consecutive rounds of photobleaching (Lippincott-Schwartz *et al*., 2003).

III Image analysis

1. E-cadherin Turnover

Image analysis was performed using Image J software. Noise on images was reduced by applying a median filter of 2 pixels radii. As E-cadherin dynamics at the ZA is relatively slow (in our experience, a FRAP experiment takes ~10 min to plateau), it is inevitable that some cell movements and/or drift occur during image acquisition. If these movements really compromise the measurements, then the experiment is discarded. However, those experiments with slight cell movements can be corrected and/or eliminated by aligning consecutive frames using Turbo-reg (http://bigwww.epfl.ch/thevenaz/turboreg/) plug-in of Image J. After that, FRAP profiles were calculated using a ROI marked at the bleached area and use the plug-in FRAP profiler to obtain fluorescence intensity profiles. Fluorescence intensities in the ROI immediately after bleaching ($F(0)$) were subtracted from fluorescence intensities at all times ($F(t)$) and results were then normalized to pre-bleaching values (Eq.1, Figure 2A). Results were then imported into Prism software for statistics analysis. Data from 11 replicates (3 independent experiments) were pooled and fluorescence intensity at time points after the bleaching step were fitted to the equation:

$$\text{Fluorescence Recovery} = \frac{F(t)-F(0)}{F(-t)-F(0)} = Mf \cdot (1 - e^{\frac{\ln 2 \cdot t}{t_{1/2}}}) \qquad \text{(Eq.1)}$$

where $F(t)$, $F(-t)$ and $F(0)$ are the average fluorescence of the ROI at any time, before bleaching and, immediately after bleaching, respectively. Mf is the mobile fraction, t½ is the half time of recovery and t is time in seconds. In Prism, this fitting is achieved by using non-linear regression and the exponential one-phase association model using Y_0=0 and where Mf corresponds to the plateau value. Data then are presented as the average ± SEM and the statistical significance assessed by t-test.

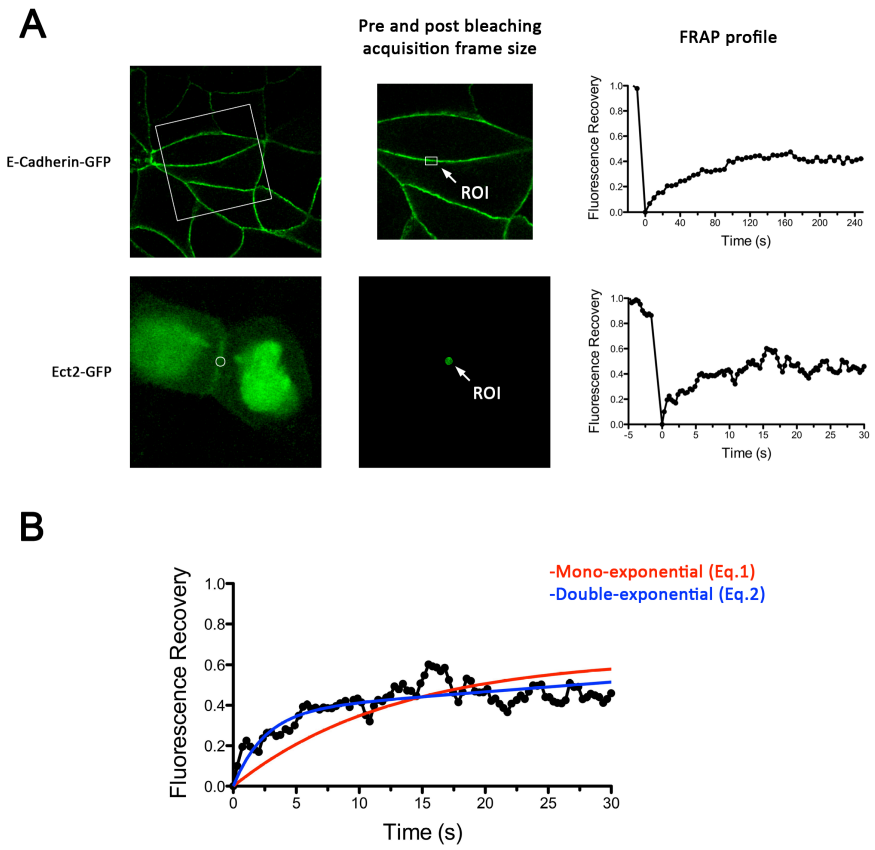

Figure 2. Examples of E-cadherin-GFP and GFP-Ect2 FRAP experiments. A. *Left*, Representative images using MCF-7 cells of the subcellular distribution of E-cadherin-GFP and GFP-Ect2 expressed in E-cadherin and Ect2 knockdown backgrounds, respectively. *Center*, details of acquisition frames during pre (shown) and post bleaching (not shown) stages during a FRAP experiment. *Right,* Fluorescence recovery plots for E-cadherin-GFP (top graph) and GFP-Ect-2 (bottom graph). Note the difference in time scales. **B.** Details of non-linear regression of GFP-Ect2 recovery plot using either mono-exponential (Eq.1) or double exponential (Eq.2) functions. This shows that a mono exponential function does not adjust properly to the experimental curve.

2. Ect2 Turnover

Image analysis was also performed using Image J software. It is worth to mentioning that an Ect2 FRAP experiment takes ~1 min, therefore no significant drifts or cell movements were observed. To calculate FRAP profiles, a ROI at the bleached GFP-Ect2 area was marked and its average fluorescence determined at every time point using the measure stack plugin in Image J software. Fluorescence intensities were treated as described above for E-cadherin-GFP to obtain recovery plots and data fitted to the double exponential equation (Figure 2B):

$$\text{Fluorescence Recovery} = \frac{F(t)-F(0)}{F(-t)-F(0)} = Mf \cdot \left[f_{fast} \cdot \left(1 - e^{\frac{\ln 2 \cdot t}{t_{1/2}^{fast}}}\right)\right] + Mf \cdot \left[f_{slow} \cdot \left(1 - e^{\frac{\ln 2 \cdot t}{t_{1/2}^{slow}}}\right)\right] \quad \text{(Eq.2)}$$

F(t) is the average fluorescence of the ROI, Mf is the mobile fraction, f_{fast} and f_{slow} are weighting factors for fast and slow mobile components, $t_{1/2}^{fast}$ and $t_{1/2}^{slow}$ their respective half times and t is time in seconds. In

Prism, this fitting is achieved by using non-linear regression and the exponential two-phase association model using Y_0=0 and where the plateau value corresponds to Mf .

For this case, a numerical solution to obtain the t value at which Fluorescence Recovery= 0.5 was applied to obtain the global half time for Ect2 recovery. This was performed in Matlab (MathWorks, Australia) as follows. Values from fitting can be introduced as:

>> Parameters=[M_f f_{fast} $t_{1/2}^{fast}$ f_{slow} $t_{1/2}^{slow}$] (In the brackets real values are introduced)

And then calculate the global $t_{1/2}$ using the FRAPtwo function (see below) and the following sentence:

>> $t_{1/2}$ = fzero(@(t) FRAPtwo(Parameters,t),7);

Data are then presented as the average ± SEM and the statistical significance assessed by t-test.

The following is the description of the Matlab function used for calculation of $t_{1/2}$.

```
function [ y ] = FRAPtwo(X,t);

 plateau=X(1);
 fractionfast=X(2);
 Kfast=ln(2)/X(3);
 fractionslow=X(4);
 Kslow=ln(2)/X(5);
 y=plateau*fractionfast*(1-exp(-Kfast*t))+plateau*fractionslow*(1-exp(-Kslow*t))-(plateau/2);

end
```

Recipes

1. Imaging media
   Hank's balanced salt solution supplemented with 10 mM HEPES pH 7.4 and 5 mM $CaCl_2$
2. 4% Paraformaldehyde in PBS
   Prepare by dilution of the stock solution (16% formaldehyde). Adjust pH to 7 with HCl or NaOH if necessary using pH indicator papers. Aliquot dilutions and store at -20 °C.

References

1. Lippincott-Schwartz, J., Altan-Bonnet, N. and Patterson, G. H. (2003). Photobleaching and photoactivation: following protein dynamics in living cells. *Nat Cell Biol* Suppl: S7-14.
2. Reits, E. A. and Neefjes, J. J. (2001). From fixed to FRAP: measuring protein mobility and activity in living cells. *Nat Cell Biol* 3(6): E145-147.

3. Kovacs, E. M., Verma, S., Ali, R. G., Ratheesh, A., Hamilton, N. A., Akhmanova, A. and Yap, A. S. (2011). N-WASP regulates the epithelial junctional actin cytoskeleton through a non-canonical post-nucleation pathway. *Nat Cell Biol* 13(8): 934-943.
4. Otani, T., Ichii, T., Aono, S. and Takeichi, M. (2006). Cdc42 GEF Tuba regulates the junctional configuration of simple epithelial cells. *J Cell Biol* 175(1): 135-146.
5. Priya, R., Yap, A. S. and Gomez, G. A. (2013). E-cadherin supports steady-state Rho signaling at the epithelial zonula adherens. *Differentiation*.
6. Smutny, M., Cox, H. L., Leerberg, J. M., Kovacs, E. M., Conti, M. A., Ferguson, C., Hamilton, N. A., Parton, R. G., Adelstein, R. S. and Yap, A. S. (2010). Myosin II isoforms identify distinct functional modules that support integrity of the epithelial zonula adherens. *Nat Cell Biol* 12(7): 696-702.
7. Smutny, M., Wu, S. K., Gomez, G. A., Mangold, S., Yap, A. S. and Hamilton, N. A. (2011). Multicomponent analysis of junctional movements regulated by myosin II isoforms at the epithelial zonula adherens. *PLoS One* 6(7): e22458.
8. Vitriol, E. A., Uetrecht, A. C., Shen, F., Jacobson, K. and Bear, J. E. (2007). Enhanced EGFP-chromophore-assisted laser inactivation using deficient cells rescued with functional EGFP-fusion proteins. *Proc Natl Acad Sci U S A* 104(16): 6702-6707.
9. Goodson, H. V., Dzurisin, J. S. and Wadsworth, P. (2010). Methods for expressing and analyzing GFP-tubulin and GFP-microtubule-associated proteins. *Cold Spring Harb Protoc* 2010(9): pdb top85.
10. * Ratheesh, A., Gomez, G. A., Priya, R., Verma, S., Kovacs, E. M., Jiang, K., Brown, N. H., Akhmanova, A., Stehbens, S. J. and Yap, A. S. (2012). Centralspindlin and alpha-catenin regulate Rho signalling at the epithelial zonula adherens. *Nat Cell Biol* 14(8): 818-828.
11. Gomez, G. A. and Daniotti, J. L. (2005). H-Ras dynamically interacts with recycling endosomes in CHO-K1 cells: involvement of Rab5 and Rab11 in the trafficking of H-Ras to this pericentriolar endocytic compartment. *J Biol Chem* 280(41): 34997-35010.
12. Trenchi, A., Gomez, G. A. and Daniotti, J. L. (2009). Dual acylation is required for trafficking of growth-associated protein-43 (GAP-43) to endosomal recycling compartment via an Arf6-associated endocytic vesicular pathway. *Biochem J* 421(3): 357-369.
13. Rubinson, D. A., Dillon, C. P., Kwiatkowski, A. V., Sievers, C., Yang, L., Kopinja, J., Rooney, D. L., Zhang, M., Ihrig, M. M., McManus, M. T., Gertler, F. B., Scott, M. L. and Van Parijs, L. (2003). A lentivirus-based system to functionally silence genes in primary mammalian cells, stem cells and transgenic mice by RNA interference. *Nat Genet* 33(3): 401-406.
14. Weiss, M. (2004). Challenges and artifacts in quantitative photobleaching experiments. *Traffic* 5(9): 662-671.
15. Frigault, M. M., Lacoste, J., Swift, J. L. and Brown, C. M. (2009). Live-cell microscopy - tips and tools. *J Cell Sci* 122(Pt 6): 753-767.

*How to cite this protocol: please cite References 10.

Acknowledgments: Confocal microscopy was performed at the IMB/ACRF Cancer Biology Imaging Facility, established with the generous support of the Australian Cancer Research Foundation.

3.3 Additional References

Braga, V. 2000. Epithelial cell shape: cadherins and small GTPases. *Exp Cell Res*. 261:83-90.

Braga, V.M., and A.S. Yap. 2005. The challenges of abundance: epithelial junctions and small GTPase signalling. *Curr Opin Cell Biol*. 17:466-474.

Kovacs, E.M., M. Goodwin, R.G. Ali, A.D. Paterson, and A.S. Yap. 2002. Cadherin-directed actin assembly: E-cadherin physically associates with the Arp2/3 complex to direct actin assembly in nascent adhesive contacts. *Current biology*. 12:379-382.

Niessen, C.M., D. Leckband, and A.S. Yap. 2011. Tissue organization by cadherin adhesion molecules: dynamic molecular and cellular mechanisms of morphogenetic regulation. *Physiol Rev*. 91:691-731.

Noren, N.K., W.T. Arthur, and K. Burridge. 2003. Cadherin engagement inhibits RhoA via p190RhoGAP. *The Journal of biological chemistry*. 278:13615-13618.

Noren, N.K., C.M. Niessen, B.M. Gumbiner, and K. Burridge. 2001. Cadherin engagement regulates Rho family GTPases. *The Journal of biological chemistry*. 276:33305-33308.

Ratheesh, A., G.A. Gomez, R. Priya, S. Verma, E.M. Kovacs, K. Jiang, N.H. Brown, A. Akhmanova, S.J. Stehbens, and A.S. Yap. 2012. Centralspindlin and alpha-catenin regulate Rho signalling at the epithelial zonula adherens. *Nat Cell Biol*. 14:818-828.

Wheelock, M.J., and K.R. Johnson. 2003. Cadherin-mediated cellular signaling. *Curr Opin Cell Biol*. 15:509-514.

Yamada, S., and W.J. Nelson. 2007. Localized zones of Rho and Rac activities drive initiation and expansion of epithelial cell-cell adhesion. *The Journal of cell biology*. 178:517-527.

Chapter 4: Myosin II anchors a novel feedback loop to sustain junctional Rho zone

In this chapter, I have illustrated a novel feedback loop mediated by Myosin II that is necessary to maintain junctional Rho zone. This chapter has been divided into two sections:

4.1 Here I am presenting the results as a manuscript, which has been submitted to the journal Nature Cell Biology and is under revision.

Please refer to the Author Contributions section of the manuscript, where each author has been acknowledged.

4.2 Here I have expanded the findings from section 4.1 and sought to understand the contribution of Rho pathway in a physiologically relevant system of oncogenic extrusion.

December 3, 2014

Myosin II anchors feedback regulation to confer robustness on Rho signaling at E-cadherin junctions.

Rashmi Priya, Guillermo A. Gomez#, Hayley Cox, Suzie Verma, Nicholas A. Hamilton and Alpha S. Yap#

Division of Cell Biology and Molecular Medicine, Institute for Molecular Bioscience, The University of Queensland, St. Lucia, Brisbane, Queensland, Australia 4072

#Correspondence should be addressed to: a.yap@uq.edu.au or g.gomez@uq.edu.au

Keywords: Myosin II, Rho, p190B RhoGAP, zonula adherens, bistability

Abstract

Actomyosin contractility at the epithelial zonula adherens (ZA) generates junctional tension for tissue integrity and morphogenesis. This requires the Rho GTPase, which establishes a strikingly stable active zone at the ZA. Mechanisms must then exist to confer robustness on junctional Rho signaling, buffering it against noise to preserve its stability. We now identify a feedback network that allows a stable mesoscopic Rho zone to be generated out of dynamic elements. The key is scaffolding of ROCK-1 to the ZA by Myosin II. Junctional ROCK-1 then phosphorylates Rnd3 to antagonize the Rho suppressor, p190B RhoGAP. This ultimately sustains junctional Rho and contractile tension. Combining predictive modelling and experimentation, we show that this network constitutes a bistable dynamical system that is realized at the population level of the ZA. Thus, stability of the Rho zone is an emergent consequence of the network of interactions that allow Myosin II to feedback to Rho.

Introduction

Apical actomyosin networks are characteristic features of simple epithelia, often found as medial-apical networks or as circumferential apical bundles juxtaposed to cell-cell junctions [1-4]. When coupled to E-cadherin adhesion they generate contractile tension at the junctions to drive epithelial morphogenesis and support homeostatic tissue integrity [1, 5, 6]. Commonly, apical actomyosin couples to a distinct cadherin junction, the zonula adherens (ZA), which typically appears as an apical ring where E-cadherin is stabilized relative to cadherin found in the lateral junctions below the ZA [2, 7, 8]. The ZA is the dominant site for junctional tension, which is substantially greater there than in the lateral junctions [8]. This is teleologically attractive, as it would allow adhesion to be reinforced precisely where it has to bear the greatest contractile stresses.

However, the biogenesis of contractility at the ZA does not simply reflect physical association of the cadherin molecular complex with the actin filaments of the actomyosin apparatus. Instead, multiple mechanisms interact to generate the contractile ZA. For example, non-muscle myosin II (NMII), which is necessary for contractile tension, also stabilizes E-cadherin to form the ZA [2, 7]. Similarly, actin regulators are necessary for ZA integrity, biogenesis of actomyosin, and for contractile tension [9]. Many of these regulatory molecules are recruited to the apical junctional cortex by E-cadherin [7, 9-11], suggesting that adhesion plays an active role in establishing junctional contractility. Thus, the specialized junction that is the ZA can be regarded as the emergent product of a complex, dynamical system that integrates adhesion, signaling and actomyosin. The challenge is to understand how salient features of this system are organized to establish effective apical contractility in coherent epithelia.

One key element is signaling by the Rho GTPase. Rho stabilizes E-cadherin to generate the ZA [2, 5, 7]; recruits NMII to the ZA, notably its myosin IIA (NMIIA) paralog [2]; and can influence actin modulators, such as mDia1 [12]. Active Rho is found at the apical ring of the ZA [5, 13], forming a zone of signaling akin to that of the cytokinetic furrow. Indeed, the activation of Rho at the ZA during interphase is mediated by the centralspindlin-ECT2 complex [5], which also supports Rho signaling during cell division [14]. This spatial concentration of Rho is plausibly located to coordinate adhesion and contractility at the ZA. Consistent with this, inhibiting the Rho pathway, including its upstream regulation by centralspindlin/ECT2, disrupts actomyosin and reduces junctional tension at the ZA [5].

Therefore, the mechanisms responsible for the Rho zone at the ZA likely play an important role in sustaining junctional tension for morphogenesis and tissue homeostasis. However, Rho can be influenced by many upstream inputs [15-17]. To establish a stable Rho zone at the ZA implies that mechanisms must exist that confer robustness on Rho signaling, i.e. which would buffer Rho at the ZA against small stochastic changes from other inputs that can impinge on the Rho pathway. Robustness in dynamical control systems often involves feedback loops [18-21], but whether this is so at the ZA is not yet understood. We now identify a bistable feedback system, anchored by Myosin II, that confers robustness to generate a stable Rho signaling zone at the ZA.

Results

Myosin II supports a stable Rho zone at the ZA. We used two approaches to evaluate endogenous Rho signaling at the ZA. First, we immunostained for Rho protein in TCA-fixed cells, as its steady-state localization at junctions requires that Rho be active [5]. Junctional localization thus serves as a useful proxy for the integration of stimulatory and inhibitory signals that impinge upon Rho at the ZA. As observed earlier [5, 7], Rho stained prominently at the ZA of confluent MCF-7 cells (Supplementary Fig 1a), a pattern that is rapidly reduced by C3-transferase [5].

We complemented this by using a location biosensor derived from the C-terminal fragment of anillin (GFP-AHPH) to characterize the spatiotemporal distribution of endogenous GTP-Rho [22, 23]. Confocal stacks revealed that GFP-AHPH concentrated in a narrow zone at the ZA, constituting the most prominent site for GTP-Rho in the cells (Fig. 1a, Supplementary video 1), and in puncta in the perijunctional regions (Supplementary video 2). Junctional concentration of GFP-AHPH was effectively blocked with C3-T, confirming that the reporter was sensitive to the location of GTP-Rho (Supplementary Fig 1b). Further, the tight ring-like pattern detected by GFP-AHPH persisted for the 30+ min duration of our movies (Supplementary video 2). Kymographs revealed that the Rho zone remains sharply defined (Fig 1b) and its intensity stable throughout the movies, despite minor cyclic fluctuations (Fig 1b,c). Therefore, mechanisms must exist that concentrate and sustain GTP-Rho at the ZA, to thereby establish a stable junctional Rho zone.

One possible factor was E-cadherin adhesion itself, as junctional Rho is reduced when E-cadherin is depleted [7]. To investigate this possibility, we expressed GFP-AHPH in E-cadherin RNAi cells (Supplementary Fig 1d). E-cadherin depletion abolished the ZA, but allowed cells to remain in contact with one another and

assemble tight junctions (Supplementary Fig 1c). Despite this, GFP-AHPH failed to concentrate in a focused peak at apical junctions in E-cadherin knock-down (KD) cells (Fig 1d), as confirmed by measurement of fluorescence intensity (Fig 1e). Instead, GFP-AHPH appeared to redistribute into the apical puncta (Fig 1d). Total cellular GTP-Rho levels, detected by pull-down with the Rho-binding domain of rhotekin, were not altered by E-cadherin KD (Supplementary Fig 1e). Thus, E-cadherin constitutes a major factor that maintains the apical junctional region as a site of concentrated Rho signaling.

In considering candidates that might mediate this impact of E-cadherin, we focused on NMII, which is recruited by E-cadherin adhesion to co-accumulate with GTP-Rho at the ZA [2, 5] and can interact with Rho GEFs [24-26]. First, we inhibited Myosin II activity with blebbistatin (100 μ M, 2 hr), which reduced NMIIA staining at cell-cell junctions (Supplementary Fig 1f) [2]. In contrast to control cells, junctional Rho was reduced by >70% in MCF-7 cells treated with blebbistatin (Fig 1 f,g). Similar effects were observed in Caco-2 and MDCK monolayers (Supplementary Fig 1g). As both NMIIA and Myosin IIB (NMIIB) accumulate at the ZA in MCF7 cells, we then used lentiviral shRNA to selectively deplete each of these proteins by ~ 90% (Supplementary Fig 1 h,i). Junctional Rho was substantially reduced in NMIIA KD cells, consistent with the effect of blebbistatin, but not significantly decreased in cells depleted of NMIIB (Fig 1 f,h).

The loss of steady state Rho protein was paralleled by degradation of the stable GTP-Rho zone at the junctions. As we had seen with E-cadherin KD, GFP-AHPH failed to concentrate in a focused region at contacts between cells treated with blebbistatin or NMIIA RNAi (Fig 1 i, j). None of these manoeuvres altered the total levels of Rho or GTP-Rho (Supplementary Fig 1 e), implying that NMII principally affected the stable subcellular distribution of active Rho. To test whether the apical redistribution of GTP-Rho might reflect an altered localization of residual NMII itself, we co-expressed mCherry-MRLC with GFP-AHPH and treated the cells with blebbistatin. However, mCherry-MRLC did not redistribute apically with GFP-AHPH (Supplementary Fig 1j). Altogether, these findings led us to conclude that NMIIA was necessary to generate a stable Rho zone at the ZA.

p190B RhoGAP degrades the junctional Rho zone when NMII is inactivated.
Formally, junctional Rho signaling might be compromised either through loss of the GEF activity that is responsible for its activation and/or by the action of a GAP that promotes GTP hydrolysis. Rho signaling at the ZA of MCF7 cells is activated by the

ECT2 GEF and inhibited by p190B RhoGAP (p190B) [5]. However, junctional staining for ECT2 was not affected by blebbistatin or NMIIA shRNA, examined under the exact conditions when Rho was reduced (Supplementary Fig 2a). Nor did we detect changes in hSyk-4/MgcRacGAP (Supplementary Fig 2 b), a component of the centralspindlin complex, which recruits ECT2 to the ZA [5, 14]. Therefore, loss of ECT2 did not readily explain how the Rho zone was compromised when NMII was inhibited.

We then examined whether inhibiting myosin affected the junctional accumulation of the RhoGAP, p190B. Scant staining for p190B was detected at the junctions and apical poles of control cells, but apical junctional staining was increased ~5-fold by blebbistatin (Fig 2 a,b). p190B also increased at the apical junctions in NMIIA KD cells but not NMIIB KD cells (Fig 2 a,c), exactly the conditions which compromised the junctional Rho zone. None of these conditions affected cellular p190B expression (Supplementary Fig 2 f,g), indicating that inactivating NMII allowed p190B to become recruited to the ZA. In contrast, p190A RhoGAP did not localize to junctions under control or NMII-inhibited conditions (Supplementary Fig 2 c-e).

p190B was thus a potential candidate to disrupt Rho signaling at the ZA when myosin II was blocked. To test this, we asked how myosin inhibition affected the integrity of the junctional Rho zone when p190B was depleted by RNAi (~ 90% reduction, Fig 2d,e). Whereas blebbistatin substantially decreased junctional Rho in wild-type (WT) cells, it had no detectable impact on Rho in p190B KD cells (Fig 2 d,f). Similarly, stable concentration of GFP-AHPH at the apical junctions was preserved (Fig 2 g,h) when blebbistatin was added to p190B KD cells. Therefore, p190B was responsible for degrading the Rho zone at the ZA when myosin II was perturbed.

Rnd3 recruits p190B to the ZA. These findings implied that NMII might support Rho signaling by antagonizing the junctional accumulation of p190B. To understand how this could be achieved, we then turned to identify the mechanism that recruited p190B to junctions when myosin was inhibited. One potential candidate was Rac, which can be activated when myosin is disabled [25, 27] and can also induce the cortical recruitment of p190B [5, 28]. However, inhibiting NMII did not alter either Rac (Supplementary Fig 3 a-c) or GTP-Rac levels at the ZA (Supplementary Fig 3g). Nor was the ability of p190B to accumulate at junctions in blebbistatin-treated cells affected by inactivating Rac (Supplementary Fig 3 d-f) or blocking Src [29] (Supplementary Fig 3h).

Alternatively, the Rnd3 GTPase can also directly bind p190B to activate and recruit it to the cell cortex [30, 31]. We found that GFP-Rnd3 localized clearly with E-

cadherin at the ZA (Fig 3a) and this was increased by treatment with blebbistatin (Fig 3 b,c), without any change in total expression levels (Supplementary Fig 4 d). Thus, Rnd3 showed a suitably responsive pattern of localization to mediate the junctional recruitment of p190B. Nor did p190B recruit Rnd3, as Rnd3 T55V, which cannot bind p190B [30, 31], also translocated to junctions when myosin was blocked (Fig 3 b,c).

However, p190B failed to recruit to junctions in blebbistatin-treated cells when Rnd3 was depleted by siRNA (Fig 3 d,e, Supplementary Fig. 3 i-k). Junctional p190B was restored by expression of RNAi-resistant Rnd3 (Fig 3 d,e, Supplementary Fig. 3l), confirming the specificity of the effect, but depletion of the related Rnd1 had no effect (Supplementary Fig. 3 j,k). As well, blebbistatin did not inhibit junctional Rho in Rnd3 KD cells; but its effect was restored by reconstitution of WT Rnd3 (Fig 3 f, Supplementary Fig. 3m). This implied that Rnd3 was necessary to recruit p190B to junctions when myosin was inhibited. Confirming this, Rnd3 T55V failed to restore either p190B recruitment or Rho inhibition at junctions when Rnd3 KD cells were treated with blebbistatin (Fig 3 d-f, Supplementary Fig. 3m). Thus, Rnd3 and p190B constituted the functional module responsible for inhibiting junctional Rho when myosin was inactivated.

Protein phosphorylation regulates Rnd3 recruitment to the ZA. Serine/Threonine phosphorylation plays a critical role in regulating the cortical localization of Rnd3 [31]. When phosphorylated, Rnd3 binds to 14-3-3 ζ , which sequesters it in the cytosol. Effectively, phosphorylation antagonizes Rnd3 signaling by blocking its association with the plasma membrane. We therefore asked if this might influence whether Rnd3 localizes at the ZA.

To test this, we reconstituted Rnd3 KD cells with transgenes lacking key phosphorylation sites that affect its cortical recruitment (Supplementary Fig. 3 l): Rnd3 AllA, which lacks all the known phosphorylation sites, and Rnd3 S240A, which cannot bind 14-3-3 ζ [31]. Strikingly, we found that even under basal conditions Rnd3 AllA showed strong junctional staining, comparable to that seen in myosin-inhibited control cells (Fig 3b,c). Moreover, this was not further increased by blebbistatin, suggesting that Rnd3 became constitutively localized to the ZA when it could no longer be phosphorylated (Fig 3b,c). Similarly, Rnd3 S240A showed strong baseline localization that was not enhanced by blebbistatin (Fig 3b,c). Consistent with what we had already found, the apparently constitutive localization of both these phosphodeficient mutants increased the basal levels of p190B (Fig 3d,e), and decreased Rho levels (Fig 3f, Supplementary Fig. 3m) at junctions; nor were these

further altered by blebbistatin. Thus phosphorylation of Rnd3 is a key determinant of Rho signaling at the ZA.

Rnd3 negatively regulates ZA tension. These findings provided the opportunity to test whether Rnd3 could ultimately influence contractility at E-cadherin junctions. The constitutively-localized phosphodeficient Rnd3 mutants allowed us to assess contractility without the need to inhibit myosin, which was otherwise necessary to recruit Rnd3/p190B to junctions. Using laser nanoablation assays, we found that apical junctional tension was conspicuously reduced in Rnd3 KD cells reconstituted with either Rnd3 AllA or Rnd3 S240A compared with those expressing WT Rnd3 (Fig 3 g,h), exactly the conditions where junctional Rho was decreased. Altogether, then, the Rnd3/p190B module constitutes a potent suppressor of junctional contractility.

ROCK phosphorylates Rnd3 to support junctional Rho signaling. These findings suggested that NMII at the ZA might ultimately act through a protein kinase to antagonize Rnd3. Here, ROCK-1 presented an interesting candidate as it is a Rnd3 kinase that can localize to cell-cell junctions [32-34]. Indeed, we found that ROCK-1 (Fig 4a), but not ROCK2 (Supplementary Fig. 4a), concentrated at the ZA of MCF7 cells. Immunoprecipitation analysis confirmed Rnd3 as a ROCK target in these cells, as its Ser-phosphorylation was reduced by the ROCK inhibitor, Y-27632 (Fig 4b). ROCK-1 therefore had the potential to antagonize junctional Rnd3 in epithelial cells.

Consistent with this hypothesis, Y-27632 increased the amount of GFP-Rnd3 found at junctions without affecting its overall expression (Fig 4c, Supplementary Fig. 4b and 4d). Turnover studies suggested that this was due to stabilization of GFP-Rnd3 at the ZA (Fig 4d). Protein phosphorylation of Rnd3 was necessary for ROCK to antagonize its junctional accumulation, as Y-27632 did not enhance the already elevated baseline levels of either GFP-Rnd3 AllA or GFP-Rnd3 S240A (Fig 4c, Supplementary Fig. 4b). The recruitment of Rnd3 to junctions in ROCK-inhibited cells was accompanied by increased junctional p190B (Fig 4e, Supplementary video 3) and suppressed junctional Rho (Fig 4f). Y-27632 also decreased the ability of Rho to be activated, as measured with a FRET activity biosensor (Supplementary Fig 4c) and degraded the ability of cells to concentrate GFP-AHPH in the apical junction region (Fig 4g, h), exactly as we had observed when either E-cadherin or NMII were directly disrupted.

Given its junctional localization (Fig 4a), we then tested how Rho signaling was affected when we depleted ROCK-1 by siRNA (Supplementary Fig 4e). Under baseline conditions ROCK-1 KD cells displayed elevated junctional p190B (Fig 4i,

Supplementary Fig. 4f) with concomitantly depressed junctional Rho (Fig 4j, Supplementary Fig. 4f), consistent with a dominant effect on the junctional recruitment of p190B. Moreover, neither of these parameters were further affected by blebbistatin (Fig 4 i,j, Supplementary Fig. 4f), suggesting that the impact of inhibiting NMII on Rho regulation was principally mediated through ROCK-1. Together, these findings identified ROCK-1 as responsible for antagonizing Rnd3-p190B to support Rho signaling at the ZA.

Myosin II scaffolds ROCK-1 at the epithelial ZA. We then entertained the possibility that Myosin II might serve to localize ROCK-1 at the ZA. Consistent with this, the conspicuous junctional ROCK-1 staining was substantially reduced by blebbistatin (Fig 5 a,b) or NMII RNAi (Fig 5c, Supplementary Fig. 5 a and b). Interestingly, junctional ROCK-1 was reduced by NMIIA KD to a greater extent than by NMIIB depletion (Fig 5c, Supplementary Fig. 5 a and b), paralleling the impact of their selective depletion on junctional Rho.

We then performed co-immunoprecipitation analyses to further characterize how NMII localized ROCK-1 to the ZA. GFP-ROCK-1 expressed in HEK 293 cells associated with endogenous NMIIA, but not with NMIIB, and this was not affected by blocking motor activity with blebbistatin (Fig 5d). Conversely, GFP-NMIIA immunoprecipitated endogenous ROCK-1 (Fig 5e). This implied that Myosin IIA can interact, directly or indirectly, with ROCK-1. The rod domain of NMIIA was sufficient to associate with ROCK-1 and this was independent of kinase activity, being unaffected by Y-27632 (Fig 5e).

NMIIA mutants were then reconstituted in NMIIA KD MCF7 cells in order to assess what properties of this molecule were required to localize ROCK-1 at the ZA (Fig 5 f,g). Expression of WT NMIIA restored junctional ROCK-1, confirming the specificity of this effect. Interestingly, ROCK-1 was restored as effectively by reconstitution with NMIIA N93K, a mutant which localizes to the ZA [2] and retains the ability to bind F-actin, but is an ineffective filament slider [35]. The Rod domain also localized to junctions, as it does to the contractile furrow in dividing cells [36], and this was sufficient to restore junctional ROCK-1 (Fig 5 f,g). Together, these data suggested that the ability to generate contractile force, and hence junctional tension, might be dispensible for Myosin IIA to recruit ROCK-1 to junctions. Consistent with this, depleting either Cdc42 or N-WASP (Supplementary Fig 5 d,e), manoeuvres that decrease apical junctional tension [8, 37] (M.Michael, not shown), did not affect junctional ROCK-1, Rho or p190B (Supplementary Fig 5 f-h). Altogether, these

findings suggested that Myosin II acted as a cortical scaffold to localize ROCK-1 to the ZA.

Myosin-Rho feedback represents a bistable control system. We then developed a numerical model to explore the potential dynamical properties of the regulatory network that we had identified. This network can be represented by a minimal architecture that consists of two interlocked feedback loops that intersect at ROCK-1 (Fig 6a; discussed in detail in the Computational modelling section of the Supplementary Information). In the first loop, activated ROCK-1 supports Rho by antagonizing Rnd3/p190B. In the second loop Myosin II is activated by ROCK-1 and feeds back to concentrate ROCK-1 at the ZA. We used first-order differential equations to model the kinetics of each step and analysed the variable space of activation coefficients to identify regions distinguished by different levels of active Rho. We focused especially on how Myosin might be necessary to generate a stable Rho zone at the ZA.

The behaviour of the model is illustrated in Fig 6b, where all constituents began with equal initial concentrations and feedback from NMIIA to ROCK-1 was present. We found that the system initially showed dynamic behaviour but then evolved to a stable state with high concentrations of active Rho/ROCK and concomitantly low levels of Rnd3/p190B (consistent with a “Rho-ON” state). Strikingly, however, if the feedback from NMIIA to ROCK-1 was disabled without any other parameter change, then the system reversed to a “Rho-Off” state distinguished by low levels of Rho/ROCK, but high concentrations of p190B and Rnd3. This implied that the presence or absence of feedback from myosin to ROCK could profoundly affect the signaling output of the system.

We pursued this by investigating the dynamical implications of systematically varying the strength of feedback from NMIIA to ROCK-1; in the model this corresponds to the association constant between NMIA and ROCK1 ($1/K_{NMIIA}^{ROCK1}$), reflecting the affinity of association between these two proteins. We found that at low values of feedback, i.e. low affinity interactions, the system persisted in a Rho-OFF state that was insensitive to the specific concentrations of the components at the start of the simulation (Fig 6c, Supplementary Fig. 6a). Conversely, for high affinities of association between NMIIA and ROCK-1, the system stably locked in a Rho-ON state. Interestingly, for intermediate affinities, the system could achieve either a Rho-OFF state or an Rho-ON state, depending on the initial concentrations of the components. However, even within this intermediate zone, for any specific association constant between NMIIA and ROCK-1, the system evolved to establish

only one level of Rho-ON activity; it did not establish other levels of stable activity. Thus, our numerical analysis showed that the architecture of the system that we studied has the capacity to generate bistability, a property that might confer robustness on the system [18-20].

Then we sought to test the predictions of this model. We reasoned that, while individual Rho molecules can only be active or inactive, there was no *a priori* reason why, at the population level, different junctions might not have different concentrations of active Rho molecules. If bistability were to manifest at the population level, we predicted that junctions would fall into either of two categories: those with some level of Rho signaling – which would trend towards a single level of activity - and those where Rho signaling was inactive. Further, our model predicted that myosin was essential for the active state to be achieved. To test this, we measured Rho intensity in a large cohort of junctions (Fig 6d), as the level in each junction would reflect the steady-state integration of Rho activation and inactivation over populations of Rho molecules. Control junctions showed a non-Gaussian profile with two apparent inflections (Fig 6e, e'). This profile could be well-fit to two separate Gaussians, one centred on zero intensity, consistent with an inactive state (as Rho delocalizes from junctions when it is inhibited [5]), and a positive signal corresponding to an active state. Furthermore, only a single population centred on zero intensity was seen in blebbistatin-treated cells (Fig 6e, e'), exactly in agreement with the prediction of the model. This suggested that the bistability predicted by dynamical analysis of the regulatory network that we have identified is manifest at the population level of junctional Rho signaling.

Finally, we extended the model to test how this feedback system can influence the spatial expression of Rho signaling. As a test of principle, the model was expressed in 3-dimensions as a sphere where the GEF was globally distributed and therefore unable to confer spatial information (Fig 6f). We found that when NMII was unstable throughout the cortex, the system evolved to establish a stable state where GTP-Rho was uniformly low and p190B uniformly high (Fig 6f). In contrast, if we stabilized NMII at the equator, the system generated a stable zone of high Rho activity at the equator, with a complementary pattern of p190B distribution elsewhere (Fig 6f). Thus, even without spatial localization of the Rho activator, the minimal feedback architecture that we had identified has the capacity to support spatial organization of Rho signaling that is directly analogous to the Rho zone that we had characterized.

Discussion

Rho signaling is necessary for junctional contractility to support adhesion and morphogenesis [2, 38]. Consistent with this, in mammalian epithelial cells GTP-Rho concentrates prominently at the ZA itself [5], which is a major site where adhesion and actomyosin cooperate to generate junctional tension [1, 8]. Our live-cell imaging now reveals that this zone displays a striking stability: GTP-Rho is confined to a narrow zone with an average intensity that is constant for tens of minutes. This stability contrasts with many other signaling pathways, which are intrinsically transient or lead to state changes that ultimately limit the signal itself. For example, the Rho zone of the cytokinetic furrow, which shares many molecular similarities with the ZA [5, 39], is terminated by cell division [14, 40]. Teleologically, the stability of the Rho zone at the ZA may allow junctional tension to be sustained during epithelial homeostasis. Indeed, we found that constitutive localization of Rnd3 to inhibit Rho at the ZA profoundly reduced junctional tension. Therefore, cells must have a strategy to sustain Rho signaling in the spatially defined region of the ZA and buffer it against stochastic noise in the many pathways that can converge upon Rho.

We propose that robust stability is conferred by feedback that couples a canonical Rho effector, NMII, to Rho itself (Supplementary Fig. 6c). The key to the network that we have identified lies in the localization of ROCK-1 at the ZA through its interaction with NMIIA. This allows ROCK-1 to antagonize p190B by opposing the cortical association of Rnd3. One predicted consequence is to increase the lifetime of GTP-loaded Rho, potentially from ~ 0.5 sec to ~ 30 min [41], a time scale consistent with that which we observed for the stable Rho zone. We cannot exclude the possibility that other GAPs influence Rho signaling at junctions. Nonetheless, p190B appears to be a dominant influence, since it was necessary for the junctional Rho zone to be compromised when NMII was inhibited. While individual Rho molecules will eventually inactivate, stochastic activation by GEFs such as ECT2 [5] may be sufficient to sustain signaling at the population level of the junction. Antagonism of p190B would then allow the intrinsically slow GTPase activity of Rho to confer temporal stability on the Rho signal at the ZA.

Our analysis further revealed that this feedback system can confer bistability on Rho signaling outcomes. Bistability represents a dynamical feature that can support robustness by buffering the system against noise [18-20]. Computationally, we found that the system was resistant to changes in the values of inputs for individual parameters, as might be represented by noise impinging on Rho. This translated to the population level of signaling at junctions, as we found that the Rho content of the junctions fell into either of only two populations, consistent with a “Rho-off” state and

a single “On” state. Note that we deliberately used the coarse-grained metameter of junctional Rho content for two reasons. It allowed us to assess endogenous Rho, providing a proxy for the integration of the many inputs that may affect it at junctions. It also allowed us to survey Rho at the population level, which was the scale at which stability of the Rho zone was evident.

A key feature in any bistable signaling network is the presence of positive feedback in the system. Our analysis identified the loop between ROCK-1 and NMII as a central factor. Ablating feedback from NMII to ROCK-1, either computationally or experimentally, caused the system to be incapable of sustaining stable Rho signaling at the ZA. How, then, might NMII support positive feedback to ROCK-1? ROCK signaling promotes the accumulation of NMIIA at the ZA [2, 42], where we now find that it serves to also localize ROCK. Such localization would allow NMIIA to recruit inactive ROCK to the apical junctions, where it could be activated by GTP-Rho. Further, scaffolding to NMII might also serve to retain ROCK at the ZA so that it can be reactivated by Rho. Of note, the biochemical interaction between ROCK-1 and NMIIA did not appear to require either the motor activity of NMII or kinase activity of ROCK1, as it was resistant to both blebbistatin and Y-27632. Effectively, localization of ROCK in proximity to GTP-Rho at the ZA would allow NMIIA to close a loop that promotes ROCK activity.

Local feedback can also contribute to spatially defining the Rho zone of the ZA. Spatial patterning can be generated by the combination of short-range positive feedback combined with long-range inhibition [43, 44]. Here we envisage that scaffolding of ROCK-1 by NMII at the ZA represents the local activatory feedback element, whereas Rnd3/p190B may constitute a long-range inhibitory component. Indeed, p190B was extensively distributed at the cortices of cells (not shown), likely reflecting the ability of Rnd3 to localize at the plasma membrane through its C-terminal farnasyl group [31, 32]. At the ZA, however, myosin-localized ROCK-1 would antagonize the cortical association of Rnd3, yielding complementary patterns for ROCK and Rnd3/p190B. Therefore, in this model localization of the NMII-ROCK-1 network would not only define the site of positive feedback, but also influence the patterning of a potential antagonist. Consistent with this, extension of our numerical model to a spatial form revealed that local stabilization of NMII was sufficient to generate a stable Rho zone and a complementary distribution of p190B, even when the activatory GEF was uniformly distributed. Interestingly, for a stable Rho zone to be established it was also necessary for the cortical dynamics of NMII to be significantly slower than those of Rho (see also Supplementary Experimental Procedures). Indeed, the scale of this predicted difference was comparable to that which we have

measured by FRAP for junctional Rho (T1/2 ~ 0.5 sec) and NMIIA (T1/2 ~ 5 sec at the ZA, unpublished). This implies that the spatial stability of the Rho zone at the ZA would reflect the effective local time scale of NMII dynamics.

Our findings add to the increasing appreciation that NMIIA can exert biological functions through an ability to scaffold signaling molecules (Lee, 2010; Wu, 2006; Kuo, 2011; Shin, 2014) that can be separated from its ability to exert contractile force. Thus, we found that ROCK-1 could be restored at the ZA when NMIIA KD cells were reconstituted with mutants (N93K, Rod) which are themselves unable to generate high levels of contractility [45]. Although blebbistatin inhibits NMII-dependent contractility, it also causes NMIIA to be lost from junctions [2]. Similarly, ROCK-1 localization was resistant to alternative manoeuvres that inhibited tension. However, these findings are consistent with our earlier observation that NMIIA N93K could restore the integrity of the ZA to NMIIA-depleted cells [2].

Overall, we propose that NMIIA establishes a cortical landmark for a feedback network that confers the stability and robustness necessary to sustain contractility at the ZA. It is attractive to postulate that the junctional recruitment of GEFs, such as ECT2 [5], defines where Rho is activated, while the NMII-ROCK network that we have identified serves to sustain the activated Rho and confine it to the region of the ZA. However, it should be noted that NMIIA is found in many other parts of the cell [46], including the lateral junctions located below the ZA [8]. Despite this, NMIIA principally localized ROCK-1 to the ZA. Therefore, factors other than the presence of NMIIA alone must also contribute to scaffolding ROCK at these junctions. One possibility is that proteins, such as Shroom [38, 47], contribute to localizing ROCK. Nevertheless, they did not appear to be sufficient to compensate for loss of NMII in our experiments. Alternatively, the apparently privileged location of ROCK-1 at the ZA may reflect local differences in the cortical dynamics of NMII (not shown) that can result in advective flows of NMII at the cell cortex towards the sites of more stable myosin [48]. This may ultimately cause the distribution of ROCK-1 to be influenced by active cortical mechanics [48-50], in addition to passive reaction-diffusion patterning. Exploring the dynamical properties of these possibilities, both at the theoretical and experimental level, may then provide a fruitful approach to understanding the systems cell biology that controls contractile tension at cell-cell junctions.

Acknowledgements.
We thank our laboratory colleagues for their unstinting support and advice during the course of this project, and our colleagues elsewhere for their kind gifts of reagents.

We also thank Marino Zerial and Lisa Tucker-Kellogg for thought-provoking discussions and Elliott Moussa for his help in nano-ablation analysis. This work was supported by the National Health and Medical Research Council of Australia (1044041, 1037320, 1067405), The Kids Cancer Project of the Oncology Research Foundation, the EMPathy National Collaborative Research Program (CG-10-04) of the National Breast Cancer Foundation (Australia), a University of Queensland Early Career Research Grant to GAG (2012003354) and an ANZ Trustees PhD Scholarship in Medical Research to RP.

Author contributions

R.P, G.A.G and A.S.Y conceived the project and designed the experiments. R.P. performed most of the experiments in-collaboration with G.A.G for nano-ablation, FRAP and Rho biosensor experiments, with technical assistance from S.V for western blotting. G.A.G and N.H performed the mathematical modelling. S.V. and H.C. performed experiments. R.P. and G.A.G analyzed the data. R.P., G.A.G and A.S.Y wrote the paper.

Competing financial interests.

The authors declare no competing financial interests.

References

1. Fernandez-Gonzalez, R., Simoes Sde, M., Roper, J.C., Eaton, S. & Zallen, J.A. Myosin II dynamics are regulated by tension in intercalating cells. *Dev Cell* **17**, 736-743 (2009).
2. Smutny, M. *et al.* Myosin II isoforms identify distinct functional modules that support integrity of the epithelial zonula adherens. *Nature cell biology* **12**, 696-702 (2010).
3. Martin, A.C., Kaschube, M. & Wieschaus, E.F. Pulsed contractions of an actin-myosin network drive apical constriction. *Nature* **457**, 495-499 (2009).
4. Rauzi, M., Lenne, P.F. & Lecuit, T. Planar polarized actomyosin contractile flows control epithelial junction remodelling. *Nature* **468**, 1110-1114 (2010).
5. Ratheesh, A. *et al.* Centralspindlin and alpha-catenin regulate Rho signalling at the epithelial zonula adherens. *Nature cell biology* **14**, 818-828 (2012).

6. Martin, A.C., Gelbart, M., Fernandez-Gonzalez, R., Kaschube, M. & Wieschaus, E. Integration of contractile forces during tissue invagination. *J. Cell Biol.* **188**, 735-749 (2010).
7. Priya, R., Yap, A.S. & Gomez, G.A. E-cadherin supports steady-state Rho signaling at the epithelial zonula adherens. *Differentiation* **86**, 133-140 (2013).
8. Wu, S.K. *et al.* Cortical F-actin stabilization generates apical-lateral patterns of junctional contractility that integrate cells into epithelia. *Nature cell biology* **16**, 167-178 (2014).
9. Verma, S. *et al.* A WAVE2-Arp2/3 actin nucleator apparatus supports junctional tension at the epithelial zonula adherens. *Mol Biol Cell* **23**, 4601-4610 (2012).
10. Kovacs, E.M., Goodwin, M., Ali, R.G., Paterson, A.D. & Yap, A.S. Cadherin-directed actin assembly: E-cadherin physically associates with the Arp2/3 complex to direct actin assembly in nascent adhesive contacts. *Current biology : CB* **12**, 379-382 (2002).
11. Kovacs, E.M. *et al.* N-WASP regulates the epithelial junctional actin cytoskeleton through a non-canonical post-nucleation pathway. *Nature cell biology* **13**, 934-943 (2011).
12. Carramusa, L., Ballestrem, C., Zilberman, Y. & Bershadsky, A.D. Mammalian diaphanous-related formin Dia1 controls the organization of E-cadherin-mediated cell-cell junctions. *J Cell Sci* **120**, 3870-3882 (2007).
13. Yamada, S. & Nelson, W.J. Localized zones of Rho and Rac activities drive initiation and expansion of epithelial cell-cell adhesion. *The Journal of cell biology* **178**, 517-527 (2007).
14. Yuce, O., Piekny, A. & Glotzer, M. An ECT2-centralspindlin complex regulates the localization and function of RhoA. *The Journal of cell biology* **170**, 571-582 (2005).
15. Bos, J.L., Rehmann, H. & Wittinghofer, A. GEFs and GAPs: critical elements in the control of small G proteins. *Cell* **129**, 865-877 (2007).
16. Bement, W.M., Miller, A.L. & von Dassow, G. Rho GTPase activity zones and transient contractile arrays. *Bioessays* **28**, 983-993 (2006).
17. Jaffe, A.B. & Hall, A. Rho GTPases: biochemistry and biology. *Annu Rev Cell Dev Biol* **21**, 247-269 (2005).
18. Ferrell, J.E. & Machleder, E.M. The biochemical basis of an all-or-none cell fate switch in *Xenopus* oocytes. *Science* **280**, 895-898 (1998).
19. Huang, C.-Y.F. & Ferrell, J.E. Ultrasensitivity in the mitogen-activated protein kinase cascade. *Proc. Natl. Acad. Sci. USA* **93**, 10078-10083 (1996).
20. Angeli, D., Ferrell, J.E., Jr. & Sontag, E.D. Detection of multistability, bifurcations, and hysteresis in a large class of biological positive-feedback systems. *Proc Natl Acad Sci U S A* **101**, 1822-1827 (2004).
21. Del Conte-Zerial, P. *et al.* Membrane identity and GTPase cascades regulated by toggle and cut-out switches. *Mol Syst Biol* **4**, 206 (2008).
22. Piekny, A.J. & Glotzer, M. Anillin is a scaffold protein that links RhoA, actin, and myosin during cytokinesis. *Current biology : CB* **18**, 30-36 (2008).
23. Tse, Y.C. *et al.* RhoA activation during polarization and cytokinesis of the early Caenorhabditis elegans embryo is differentially dependent on NOP-1 and CYK-4. *Mol Biol Cell* **23**, 4020-4031 (2012).

24. Lee, C.S., Choi, C.K., Shin, E.Y., Schwartz, M.A. & Kim, E.G. Myosin II directly binds and inhibits Dbl family guanine nucleotide exchange factors: a possible link to Rho family GTPases. *The Journal of cell biology* **190**, 663-674 (2010).
25. Kuo, J.C., Han, X., Hsiao, C.T., Yates, J.R., 3rd & Waterman, C.M. Analysis of the myosin-II-responsive focal adhesion proteome reveals a role for beta-Pix in negative regulation of focal adhesion maturation. *Nature cell biology* **13**, 383-393 (2011).
26. Wu, D., Asiedu, M. & Wei, Q. Myosin-interacting guanine exchange factor (MyoGEF) regulates the invasion activity of MDA-MB-231 breast cancer cells through activation of RhoA and RhoC. *Oncogene* (2009).
27. Even-Ram, S. *et al.* Myosin IIA regulates cell motility and actomyosin-microtubule crosstalk. *Nature cell biology* **9**, 299-309 (2007).
28. Bustos, R.I., Forget, M.A., Settleman, J.E. & Hansen, S.H. Coordination of Rho and Rac GTPase function via p190B RhoGAP. *Current biology : CB* **18**, 1606-1611 (2008).
29. Wu, M.H. *et al.* MCT-1 expression and PTEN deficiency synergistically promote neoplastic multinucleation through the Src/p190B signaling activation. *Oncogene* **33**, 5109-5120 (2014).
30. Wennerberg, K. *et al.* Rnd proteins function as RhoA antagonists by activating p190 RhoGAP. *Current biology : CB* **13**, 1106-1115 (2003).
31. Riou, P. *et al.* 14-3-3 proteins interact with a hybrid prenyl-phosphorylation motif to inhibit G proteins. *Cell* **153**, 640-653 (2013).
32. Riento, K. *et al.* RhoE function is regulated by ROCK I-mediated phosphorylation. *The EMBO journal* **24**, 1170-1180 (2005).
33. Riento, K., Villalonga, P., Garg, R. & Ridley, A. Function and regulation of RhoE. *Biochem Soc Trans* **33**, 649-651 (2005).
34. Smith, A.L., Dohn, M.R., Brown, M.V. & Reynolds, A.B. Association of Rho-associated protein kinase 1 with E-cadherin complexes is mediated by p120-catenin. *Molecular Biology of the Cell* **23**, 99-110 (2012).
35. Hu, A., Wang, F. & Sellers, J.R. Mutations in human nonmuscle myosin IIA found in patients with May-Hegglin anomaly and Fechtner syndrome result in impaired enzymatic function. *The Journal of biological chemistry* **277**, 46512-46517 (2002).
36. Beach, J.R. & Egelhoff, T.T. Myosin II recruitment during cytokinesis independent of centralspindlin-mediated phosphorylation. *The Journal of biological chemistry* **284**, 27377-27383 (2009).
37. Otani, T., Ichii, T., Aono, S. & Takeichi, M. Cdc42 GEF Tuba regulates the junctional configuration of simple epithelial cells. *The Journal of cell biology* **175**, 135-146 (2006).
38. Simoes Sde, M., Mainieri, A. & Zallen, J.A. Rho GTPase and Shroom direct planar polarized actomyosin contractility during convergent extension. *The Journal of cell biology* **204**, 575-589 (2014).
39. Reyes, C.C. *et al.* Anillin regulates cell-cell junction integrity by organizing junctional accumulation of Rho-GTP and actomyosin. *Current biology : CB* **24**, 1263-1270 (2014).
40. Miller, A.L. & Bement, W.M. Regulation of cytokinesis by Rho GTPase flux. *Nature cell biology* **11**, 71-77 (2009).

41. Zhang, B. & Zheng, Y. Regulation of RhoA GTP hydrolysis by the GTPase-activating proteins p190, p50RhoGAP, Bcr, and 3BP-1. *Biochemistry* **37**, 5249-5257 (1998).
42. Shewan, A.M. *et al.* Myosin 2 Is a Key Rho Kinase Target Necessary for the Local Concentration of E-Cadherin at Cell-Cell Contacts. *Mol Biol Cell* **16**, 4531-4532 (2005).
43. Gierer, A. & Meinhardt, H. A theory of biological pattern formation. *Kybernetik* **12**, 30-39 (1972).
44. Kondo, S. & Miura, T. Reaction-diffusion model as a framework for understanding biological pattern formation. *Science* **329**, 1616-1620 (2010).
45. Heissler, S.M. & Manstein, D.J. Nonmuscle myosin-2: mix and match. *Cellular and molecular life sciences : CMLS* **70**, 1-21 (2013).
46. Vicente-Manzanares, M., Ma, X., Adelstein, R.S. & Horwitz, A.R. Non-muscle myosin II takes centre stage in cell adhesion and migration. *Nature reviews. Molecular cell biology* **10**, 778-790 (2009).
47. Nishimura, T. & Takeichi, M. Shroom3-mediated recruitment of Rho kinases to the apical cell junctions regulates epithelial and neuroepithelial planar remodeling. *Development* **135**, 1493-1502 (2008).
48. Moore, T. *et al.* Self-organizing actomyosin patterns on the cell cortex at epithelial cell-cell junctions. *Biophysical J.* **107**, In press. (2014).
49. Bois, J.S., Julicher, F. & Grill, S.W. Pattern formation in active fluids. *Physical review letters* **106**, 028103 (2011).
50. Goehring, N.W. *et al.* Polarization of PAR proteins by advective triggering of a pattern-forming system. *Science* **334**, 1137-1141 (2011).

Figure Legends

Figure 1: Myosin II supports a stable Rho zone at the ZA.

(a) GFP-AHPH and cortical F-actin (RFP-UtrCH) localization in live MCF-7 cells monolayers at the apical (z=0 μ m) vs. sub-apical (z= -3 μ m) junctions imaged by spinning disc confocal microscopy.

(b-c) Kymograph (b) and fluorescence intensity (FI) (c) of GTP-Rho (GFP-AHPH) at the ZA, (30 min, Supplementary video 1) imaged by spinning disc confocal microscopy).

(d, e) MCF-7 cells were transfected with control siRNA (Ctrl) or E-cadherin siRNA (E-cad KD) along with GFP-AHPH and imaged for GTP-Rho distribution by spinning disc confocal microscopy. Representative images acquired at the apical junctions of the cells (d) and junctional/cytoplasmic fluorescence intensity ratio of GTP-Rho (e).

(f-h) RhoA immunostaining in TCA-fixed MCF-7 cells transduced with lentivirus encoding control shRNA (Ctrl), NMIIA (IIAKD), NMIIB (IIB KD) shRNA or treated with blebbistatin (BLB) (100 μ M, 2 hours). Representative confocal images were acquired at the apical junctions (f) and fluorescence intensity at cell junctions was quantitated by linescan analysis (g, h).

(i, j) Junctional/cytoplasmic fluorescence intensity ratio of GTP-Rho measured in MCF-7 cells treated with blebbistatin (BLB) (100 μ M, 2 hours) (i) or transduced with lentivirus encoding non-targeting control shRNA (Ctrl), NMIIA (IIAKD) or NMIIB (IIB KD) shRNA (j).

Data represent mean $\pm$ S.E.M. of three individual experiments (n=3), **P<0.01, ****P<0.0001; Student's t-test (e,g, i); **P<0.01, ***P<0.001 one-way ANOVA, Dunnett's multiple comparisons test (h,j).

Scale bars: 10 μ m

Figure 2: p190B RhoGAP degrades the junctional Rho zone when NMII is inactivated.

(a-c) Junctional p190B Rho GAP (p190B) in MCF-7 cells transduced with lentivirus encoding non-targeting control shRNA (Ctrl); NMIIA (IIAKD) and NMIIB (IIB KD) shRNA or treated with blebbistatin (BLB) (100 μ M, 2 hours). Representative confocal images were acquired at the apical junctions (a) and fluorescence intensity at cell junctions was quantitated by linescan analysis (b, c).

(d-f) RhoA localization in TCA-fixed MCF-7 cells transfected with non-targeting control siRNA (Ctrl) or siRNA against p190B Rho GAP (p190B KD), then treated with

blebbistatin (100 μ M, 2 hours). Representative confocal images were acquired at the apical junctions (d) and fluorescence intensity at cell junctions was quantitated by linescan analysis (f).(e) Lysates from MCF-7 cells transfected with non-targeting control siRNA (Ctrl) or siRNA against p190B Rho GAP (p190B KD were immunoblotted for p190B RhoGAP and β -tubulin (loading control) (e).
(g,h) GFP-AHPH distribution imaged by spinning disc confocal microscopy (g) in MCF-7 cells transfected with non-targeting control siRNA (Ctrl) or siRNA against p190B Rho GAP (p190B KD) along with GFP-AHPH and treated with blebbistatin (BLB) (100 μ M, 2 hours). Junctional/cytoplasmic fluorescence intensity ratio of GTP-Rho was calculated using line-scan function of ImageJ.
Data represent mean $\pm$ S.E.M. of three individual experiments (n=3), **P<0.01 Student's t-test (b) and **P<0.01 (c,h), ****P<0.0001 (f) one-way ANOVA, Dunnett's multiple comparisons test.
Scale bars: 10 μ m

Figure 3: Rnd3 recruits p190B to the ZA.
(a) MCF-7 cells transfected with GFP-Rnd3 and E-cadherin-tdTomato were imaged by spinning disc confocal microscopy. Merged image shows co-localisation of GFP-Rnd3 with E-cadherin-tdTomato at the apical junctions.
(b,c) MCF-7 cells transfected with Rnd3 siRNA and reconstituted with mCherry tagged WT Rnd3 (WT), AIIA Rnd3 (AIIA), S240A Rnd3 (S240A) and T55V Rnd3 (T55V) were treated with either DMSO (Ctrl) or blebbistatin (100 μ M, 2 hours) and the transgenes imaged by confocal microscopy. The ratio of mean fluorescence intensity from junctions and cytoplasm were obtained using ImageJ (c).
(d,e) p190B Rho GAP immunolocalization in MCF-7 cells transfected with non-targeting siRNA (Ctrl) or Rnd3 siRNA and GFP, WT Rnd3 (WT), AIIA Rnd3 (AIIA), S240A Rnd3 (S240A), T55V Rnd3 (T55V) were treated with either DMSO (Ctrl) or blebbistatin (BLB) (100 μ M, 2 hours). Representative confocal images were acquired at the apical junctions (d) and fluorescence intensity at cell-junctions was quantitated by linescan analysis (e). Asterisks mark the transfected cells.
(f) Fluorescence intensity of RhoA at cell junctions (corresponding to representative images shown in Supplementary Fig. 3m) measured in MCF-7 cells transfected with non-targeting siRNA (Ctrl) or Rnd3 siRNA and GFP, WT Rnd3 (WT), AIIA Rnd3 (AIIA), S240A Rnd3 (S240A), T55V Rnd3 (T55V) treated with either DMSO (Ctrl) or blebbistatin (BLB) (100 μ M, 2 hours).

(g,h) Junctional tension at the ZA of MCF-7 cells expressing E-cadherin-GFP, transfected with Rnd3 siRNA and reconstituted with WT Rnd3 (WT), AIIA Rnd3 (AIIA) or S240A Rnd3 (S240A). Represented are the best-fit single exponential curves from one of the experiments (g) and tension (initial recoils) measured after ablation (h).

Data represent mean ± S.E.M. for at least three individual experiments (n=3) (c,e,f) *p<0.05; **p<0.01, ***P<0.001, ****P<0.0001, one-way ANOVA, Dunnett's multiple comparisons test (c,e,f) and Student's t-test (h).

Scale bars: 10 μm

Figure 4: ROCK-1 phosphorylates Rnd3 to support junctional Rho signalling.

(a) Confluent MCF-7 cells were fixed with methanol and stained for ROCK-1, NMIIA and E-cadherin. Representatives are confocal images acquired at the apical junctions of the cells.

(b) HEK293T cells expressing GFP-Rnd3 were treated with either PBS or Y-27632 (30 μM, 1 hour). Rnd3 was immunoprecipitated by GFP-trap and lysates were immunoblotted for GFP and phospho-serine.

(c) MCF-7 cells transfected with Rnd3 siRNA and reconstituted with GFP-tagged WT Rnd3 (WT), AIIA Rnd3 (AIIA), S240A Rnd3 (S240A) were treated with either PBS or Y-27632 (30 μM, 1 hour). The ratio between mean fluorescence intensity at junctions and cytoplasm was obtained using ImageJ.

(d) MCF-7 cells were transfected with GFP-Rnd3 and treated with either PBS (Ctrl) or Y-27632 (30 μM, 1 hour). Fluorescence recovery after photobleaching was performed on the junctional pool of GFP-Rnd3. Solid lines are best-fit mono-exponential curves and vertical lines represent the S.E.M. Mobile fraction (Mf) values were obtained by non-linear regression analysis.

(e-f) Confluent MCF-7 cells were treated with either PBS (Ctrl) or Y-27632 (30 μM, 1 hour), fixed with methanol and stained for p190B Rho GAP (e) or fixed with TCA and stained for RhoA (f). The fluorescence intensity at cell junctions was quantitated by linescan analysis.

(g,h) GFP-AHPH distribution in MCF-7 cells treated with either PBS (Ctrl) or Y-27632 (30 μM, 1 hour), and imaged by spinning disc confocal microscopy (g). Junctional/Cytoplasmic fluorescence intensity ratio of GTP-Rho was calculated by line-scan analysis (h).

(i) MCF-7 cells were transfected with non-targeting control siRNA (Ctrl) or with ROCK-1 siRNA (ROCK-1KD) and 48 hours post-transfection, treated with either

blebbistatin (100 μ M, 2 hours) alone (BLB) or in combination with ROCK-1 siRNA (ROCK-1 KD+BLB). Fluorescence intensity of p190B Rho GAP at cell junctions was quantitated by linescan analysis.
(j) MCF-7 cells were transfected with non-targeting control siRNA (Ctrl) or with ROCK-1 siRNA (ROCK-1KD) and 48 hours post-transfection, treated with either blebbistatin (100 μ M, 2 hours) alone (BLB) or in combination with ROCK-1 siRNA (ROCK-1 KD+BLB). Fluorescence intensity of RhoA at cell junctions was quantitated by linescan analysis.
Data represent mean $\pm$ S.E.M. of at least three individual experiments; **P<0.01, ***P<0.001, ****P<0.0001, one-way ANOVA, Dunnett's multiple comparisons test (c, i,j) and Student's t-test (d,e,f,h).
Scale bars: 10 μ m

Figure 5: Myosin II scaffolds ROCK-1 at the epithelial ZA.
(a-b) Confluent MCF-7 cells were treated with either DMSO (Ctrl) or blebbistatin (BLB) (100 μ M, 2 hours), fixed with methanol and stained for ROCK1.Representatives are confocal images acquired at the apical junctions of the cells (a). The fluorescence intensity at cell junctions was quantitated by linescan analysis (b).
(c) Fluorescence intensity of ROCK-1 at cell junctions measured in MCF-7 cells transduced with lentivirus encoding non-targeting control shRNA (Ctrl), NMIIA (IIAKD) and NMIIB (IIB KD) shRNA.
(d) HEK293T cells were transfected with GFP-ROCK-1 and treated with blebbistatin (BLB) (100 μ M, 2 hours). ROCK-1 was immunoprecipitated using GFP-TRAP and lysates were immunoblotted for NMIIA, NMIIB and GFP.
(e) HEK293T cells were transfected with GFP-FL NMIIA (full-length) or GFP-NMIIA-ROD and treated with Y-27632 (30 μ M, 1 hour). Immunoprecipitation was performed using GFP-TRAP and lysates were immunoblotted for ROCK-1 and GFP.
(f-g) MCF-7 cells were depleted of NMIIA using siRNA and then transfected with GFP only, GFP-full-length NMIIA (FL IIA), GFP-N93K mutant of NMIIA (N93K), or GFP-NMIIA-ROD (ROD). Methanol-fixed cells were stained for GFP and ROCK-1. Representatives are confocal images acquired at the apical junctions of the cells (g). The fluorescence intensity at cell junctions was quantitated by linescan analysis (f).
Data represent mean $\pm$ S.E.M. of three individual experiments (n=3), **P<0.01 and ****P<0.0001 Student's t-test (b) or one-way ANOVA, Dunnett's multiple comparisons test (c,f).

Scale bars: 10 μ m

Figure 6: Bistable properties of RhoA activation at cell-cell junctions.
(a) Activation and repression network model of GTP RhoA, ROCK-1, Rnd3, p190B RhoGAP and NMIIA. Arrows represent activation, T-junctions represent repression.
(b) Switching between states in the network model. The network shown in (a) was mathematically modelled as a system of pairwise activations and repressions. A NMIIA to ROCK-1 activation coefficient ($\mathrm{K}_{\mathrm{NMIIA}}^{\mathrm{ROCK1}}$), equivalent to the dissociation constant of NMIIA/ROCK-1 in a Hill model, of 0.5 was used with all other model constants as given in Table 1 in Materials and Methods. All concentrations were initialised to 1 at time t=0. In the figure active concentrations of all elements of the model are shown across time. At time t=200, the activation of ROCK-1 by Myosin IIA is turned off in the model.
(c) Effect of feedback from NMIIA to ROCK-1 on stable signaling outcomes from the network. Steady state levels of RhoA were determined in simulations in which the activation coefficient $\mathrm{K}_{\mathrm{NMIIA}}^{\mathrm{ROCK1}}$ was varied in the range 0 to 5, equivalent to a variation in the association constant (feedback strength) between >10 to 0.25 between these two molecules in a Hill model and all other constants as in Table 1 in Supplementary experimental procedure. For each model, a number of distinct initial concentrations of RhoA in the range 0 to 3.5, Rnd3 in the range 0 to 3.5, and all other concentrations 1 were run for t=0 to t=5000. Each was found to lead to one of two stable states, that is RhoA, ROCK-1 and NMIIA high and Rnd3 and p190B low or RhoA, ROCK-1 and NMIIA low and Rnd3 and p190B RhoGAP high. In the figure, the stable state (t=5000) concentrations of RhoA found for each K_{NMIIA}^{ROCK1} are shown.
(d-e') Immunofluorescence analysis of junctional RhoA localization in control and blebbistatin treated MCF-7 cells (d) and frequency distribution of junctional RhoA intensity under the same conditions (e). (e') Histograms were fitted to a double Gaussian function for control ($p<0.01$ double peak vs. single peak non linear regression; extra-sum-of squares F-test) and with a single Gaussian curve for blebbistatin treated cells (n.s. for double peak vs single peak non linear regression; extra-sum-of squares F-test). Scale bars: 50 μ m
(f) Computer simulations of the network in 3-dimension. A cell was modelled as a sphere of 5 μm radius where the surface represents the cell cortex and the interior volume the cytoplasm. The top panels correspond to the steady state distribution at the cortex for NMIIA, RhoA, ROCK-1, Rnd3 and p190B and a RhoGEF under conditions where myosin is unstable throughout the cell cortex. The bottom panels

correspond to a similar simulation but a ring of stable NMIIA was created at the equator of the sphere.

Supplementary Figure Legends

Supplementary Figure 1: Myosin II supports a stable Rho zone at the ZA

(a) Confluent MCF-7 cells fixed with TCA and stained for RhoA (green) and E-cadherin (red). Shown are representative confocal images acquired at the apical junctions of the cells and the corresponding merged image.

(b) Confluent MCF-7 cells transfected with GFP-AHPH and RFP-UtrCH, treated with vehicle control (Ctrl) or with Rho-inhibitor C3 Transferase (C3T, 1 μg/ml) for 3 hours and then imaged for GFP-AHPH and RFP-UtrCH distribution using a spinning disc confocal microscope.

(c) MCF-7 cells were co-transfected with GFP-AHPH and a ctrl siRNA (Ctrl) or a siRNA against E-cadherin (E-cad KD) and fixed 24 hours later with TCA. Cells were immunostained for GFP (GFAHPH), E-cadherin (E-cad) and ZO-1.Representative confocal images were acquired at the apical junctions of the cells.

(d) Lysates from MCF-7 cells transfected with control siRNA or E-cadherin siRNA were immunoblotted for E-cadherin and β-tubulin (loading control).

(e) MCF-7 cells were transfected with siRNA against E-cadherin (E-cad KD), NMIIA (NMIIA KD) or treated with blebbistatin (100 μ M, 2 hours) (BLB) were lysed and GTP-Rho was isolated using beads coated with the RBD domain of Rhotekin (as described in the supplementary experimental procedure). The lysates were immunoblotted for RhoA and β-tubulin (loading control).

(f) MCF-7 cells were treated with blebbistatin (100 μ M, 2 hours), fixed with methanol and immunostained for NMIIA or E-cadherin. Representative confocal images were acquired at the apical junctions of the cells.

(g) Caco2 and MDCK cells were grown till confluent, treated with blebbistatin (100 μ M, 2 hours), fixed with TCA and stained for RhoA. Representative confocal images were acquired at the apical junctions of the cells.

(h, i) Lysates from MCF-7 cells transduced with lentivirus encoding an empty vector control (Ctrl), shRNA-directed against NMIIA (h) or shRNA-directed against NMIIB (i) were immunoblotted for NMIIA, NMIIB and β-tubulin (loading control).

(j) GFP-AHPH and MRLC-mCherry localization at the apical junctions in live MCF-7 cells treated with blebbistatin (100 μ M, 2 hours) and imaged by spinning disc confocal microscopy.

Scale bars: 10 μ m

Supplementary Figure 2: p190B RhoGAP degrades the junctional Rho zone when NMII is inactivated.

(a-e) MCF-7 cells transduced with lentivirus encoding non-targeting control shRNA (Ctrl), NMIIA (IIAKD) or NMIIB (IIB KD) shRNA, or treated with DMSO (Ctrl) or blebbistatin (100 μ M, 2 hours) were fixed with methanol and stained for ECT2 (a), MgcRacGAP (RacGAP) (b) p190A Rho GAP (p190A), Myosin IIA and Myosin IIB (c-e). Representative confocal images were acquired at the apical junctions of the cells. Scale bars: 10 μ m

(f-g) Lysates from MCF-7 cells transduced with lentivirus encoding an empty vector control (Ctrl) or an shRNA-directed against NMIIA or an shRNA-directed against NMIIB (f) or treated with DMSO control (Ctrl) or blebbistatin (BLB, 100 μ M, 2 hours), (g) were immunoblotted for p190B Rho GAP and β -tubulin (loading control).
Scale bars: 10 μ m

Supplementary Figure 3: Rnd3 recruits p190B to the epithelial Zonula Adherens

(a-c) MCF-7 cells transduced with lentivirus encoding non-targeting control shRNA (Ctrl), NMIIA (IIAKD) or NMIIB (IIB KD) shRNA, and treated with DMSO (Ctrl) or blebbistatin (100 μ M, 2 hours) were fixed with TCA and stained for Rac1. Representative confocal images were acquired at the apical junctions.
(d) Lysates from wild type MCF-7 (Ctrl) and MCF-7 cells transfected with siRNA against Rac1 were immunoblotted for Rac1 and β -tubulin (loading control).
(e) Wild type MCF-7 and MCF-7 cells transfected with Rac siRNA were treated with DMSO (Ctrl) or with blebbistatin (BLB; 100 μ M, 2 hours) and fixed and stained for p190B Rho GAP.
(f) MCF-7 cells were left untreated (Ctrl) or treated with blebbistatin (BLB; 100 μ M, 2 hours) alone or in combination with Rac inhibitors EHT1864 (10 μM, 12 hours) or NSC23766 (50 μM, 12 hours), fixed with methanol and stained for p190B GAP.
(g) MCF-7 cells transduced with lentivirus encoding non-targeting control shRNA (Ctrl), NMIIA (IIAKD) or NMIIB (IIB KD) shRNA were transfected with the Raichu-Rac FRET biosensor and FRET measurements were performed as described in supplementary experimental procedure. Average emission ratios were calculated at

the apical junctions. Data represent mean ± S.E.M. of 60 contacts and the result is the representative of two independent experiments.
(h) MCF-7 cells were left untreated (Ctrl) or treated with blebbistatin (BLB) (100 μ M, 2 hours) alone or in combination with Src inhibitors SU6656 (10 μM) or PP2 (10 μM)) for 4 hours. Cells were fixed with methanol and stained for p190B GAP.
(i) Lysates from MCF-7 cells transfected with control siRNA or siRNA targeted against Rnd3 were immunoblotted for Rnd3 and β -tubulin (loading control).
(j,k) Control MCF-7 cells or MCF-7 cells transfected with siRNA against Rnd3 or Rnd1 and treated with blebbistatin (BLB; 100 μ M, 2 hours) were fixed with methanol and stained for p190B Rho GAP and E-cadherin. Representative confocal images were acquired at the apical junctions (j) and fluorescence intensity at cell junctions was quantitated by linescan analysis (k). Data represent mean ± S.E.M. of three individual experiments (n=3); ****P<0.0001, one-way ANOVA, Dunnett's multiple comparisons test
(l) Lysates from MCF-7 cells transfected with Rnd3siRNA along with GFP-tagged Rnd3 constructs (WT, AIIA, S240A, T55V) were immunoblotted for GFP and β -tubulin (loading control).
(m) MCF-7 cells transfected with Ctrl siRNA or Rnd3 siRNA and GFP, WT Rnd3 (WT), AIIA Rnd3 (AIIA), S240A Rnd3 (S240A), T55V Rnd3 (T55V) were treated with either DMSO (Ctrl) or blebbistatin (100 μ M, 2 hours), fixed with TCA and stained for RhoA.
Scale bars: 10 μ m

Supplementary Figure 4: ROCK-1 phosphorylates Rnd3 to support junctional Rho signaling.
(a) Confluent MCF-7 cells were fixed with methanol and stained for ROCK-2 and E-cadherin. Representative images were acquired at the apical junctions of the cells by confocal microscopy.
(b) MCF-7 cells transfected with Rnd3 siRNA and reconstituted with GFP tagged WT Rnd3 (WT), AIIA Rnd3 (AIIA), S240A Rnd3 (S240A) were treated with either PBS (Ctrl) or Y-27632 (30 μ M, 1 hour). Representatives images were acquired at the apical junctions of the cells by confocal microscopy.
(c) MCF-7 cells were transfected with ctrl siRNA (ctrl) or p190B Rho GAP siRNA and RhoA-FRET biosensor and then treated with Y-27632 (30 μ M, 1 hour). Average emission ratios were quantified at the apical junctions. Data represent mean ± S.E.M.

of three individual experiments (n=3), **P<0.01, one-way ANOVA, Dunnett's multiple comparisons test.

(d) Lysates from MCF-7 cells treated either with DMSO (ctrl) or Y-27632 (30 μM, 1 hour), or blebbistatin (BLB) (100 μM, 2 hours) and blotted for Rnd3 and β-tubulin (loading control).

(e) Lysates from MCF-7 cells transfected with control siRNA (ctrl) or ROCK-1 siRNA (ROCK-1 KD) and immunoblotted for ROCK-1, ROCK-2 and β-tubulin (loading control)

(f) MCF-7 cells were transfected with Ctrl siRNA or ROCK-1 siRNA (ROCK-1KD) and 48 hours post-transfection, treated with either blebbistatin (100 μM, 2 hours) alone (BLB) or in combination with ROCK-1 KD (ROCK-1 KD+BLB). Cells were fixed with methanol and stained for p190B Rho GAP or fixed with TCA and stained for Rho. Representative images were acquired at the apical junctions of the cells by confocal microscopy.

Scale bars: 10 μm

Supplementary Figure 5: Myosin II scaffolds ROCK-1 at the epithelial Zonula Adherens

(a-b) MCF-7 cells wild type (ctrl) and transduced with lentivirus encoding NMIIA (IIAKD) or NMIIB (IIB KD) shRNA were fixed with methanol and stained for ROCK-1, NMIIA and NMIIB. Representative images were acquired at the apical junctions of the cells by confocal microscopy.

(c-e) Lysates from MCF-7 cells transfected with non-targeting control siRNA (Ctrl) or NMIIA siRNA (c), Cdc42siRNA (d), or N-WASP siRNA (e) and immunoblotted for NMIIA, Cdc42 or N-WASP, respectively and β-tubulin (loading control)

(f) MCF-7 cells transfected with siRNA targeted against Cdc42 or N-WASP were fixed with methanol and stained for ROCK-1 and ZO-1. Representative images were acquired at the apical junctions of the cells by confocal microscopy.

(g) MCF-7 cells transfected with siRNA targeted against Cdc42 or N-WASP were fixed with TCA and stained for RhoA. Representative images were acquired at the apical junctions of the cells by confocal microscopy.

(h) MCF-7 cells transfected with siRNA targeted against Cdc42 or N-WASP were fixed with methanol and stained for p190B Rho GAP, E-cadherin or ZO-1. Representative images were acquired at the apical junctions of the cells by confocal microscopy.

Supplementary Figure 6: Bistable properties of RhoA activation at cell-cell junctions

(a) NMIIA to ROCK-1 activation coefficient and stable states. Using the activation and repression model and constants as described in Table 1 (Supplementary Information), time course plots for Rnd3 against RhoA are shown for three values for K_{NMIIA}^{ROCK1}: (left) $K_{NMIIA}^{ROCK1} = 2.3$; (center) $K_{NMIIA}^{ROCK1} = 1.4$; (right) K_{NMIIA}^{ROCK1}=0.5. In each, initial concentrations of RhoA and Rnd3 were set in a range between 0 to 3.5 and all other concentrations equal to unity. Simulations were run for t=0 to t=5000, with each line corresponding to a time course. Arrows denote the direction of increased time and red circles denote stable points.

(b) Convergence behaviour of Rnd3 and RhoA for varying NMIIA initial values. Using the model described in Experimental Procedures and constants as in Table 1 of Supplementary experimental procedures, the convergence behaviour for initial values of Rnd3 and RhoA in the range 0 to 3.5 were examined, with all other initial concentrations set to 1 apart from NMIIA which was allowed to take values 0, 1, 2, 3, 4 in distinct simulations. The red circles show the stable point concentrations for Rnd3 and RhoA that all initialisations converge towards. Each point in the plane then corresponds to an initialisation for Rnd3 and RhoA that will converge to one of the stable circles. Each line then denotes the boundary, for a given initial value of Myosin IIA, between those points in the plane that will converge to either the RhoA low/Rnd3 high state and the RhoA high/Rnd3 low state. For instance, the points above the red line correspond to those initial values of RhoA and Rnd3 that for an initial concentration of NMIIA of 4 will converge toward the RhoA low / Rnd3 high state over time (upper left red circle). Similarly, the points below the red line are those initial values of RhoA and Rnd3 that will converge to the RhoA high / Rnd3 low state (lower right red circle) given an initial NMIIA of 4. Note how increasing NMIIA initial concentration leads to a larger proportion of initial RhoA and Rnd3 values that will converge to the RhoA high / Rnd3 low state.

(c) A model for the sustenance of robust Rho zone at the epithelial Zonula Adherens.

Priya et al_Fig 1

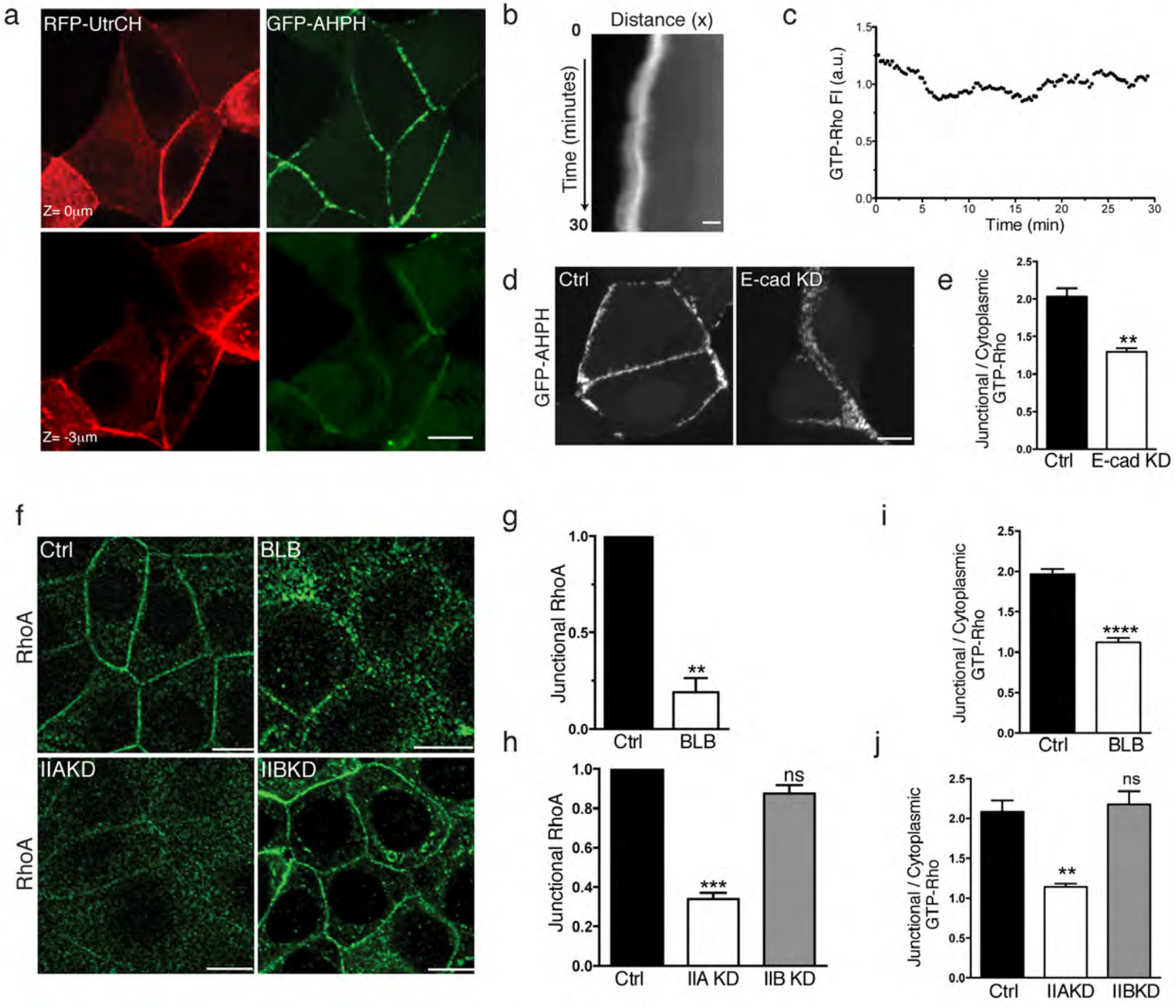

Priya et al_Fig 2

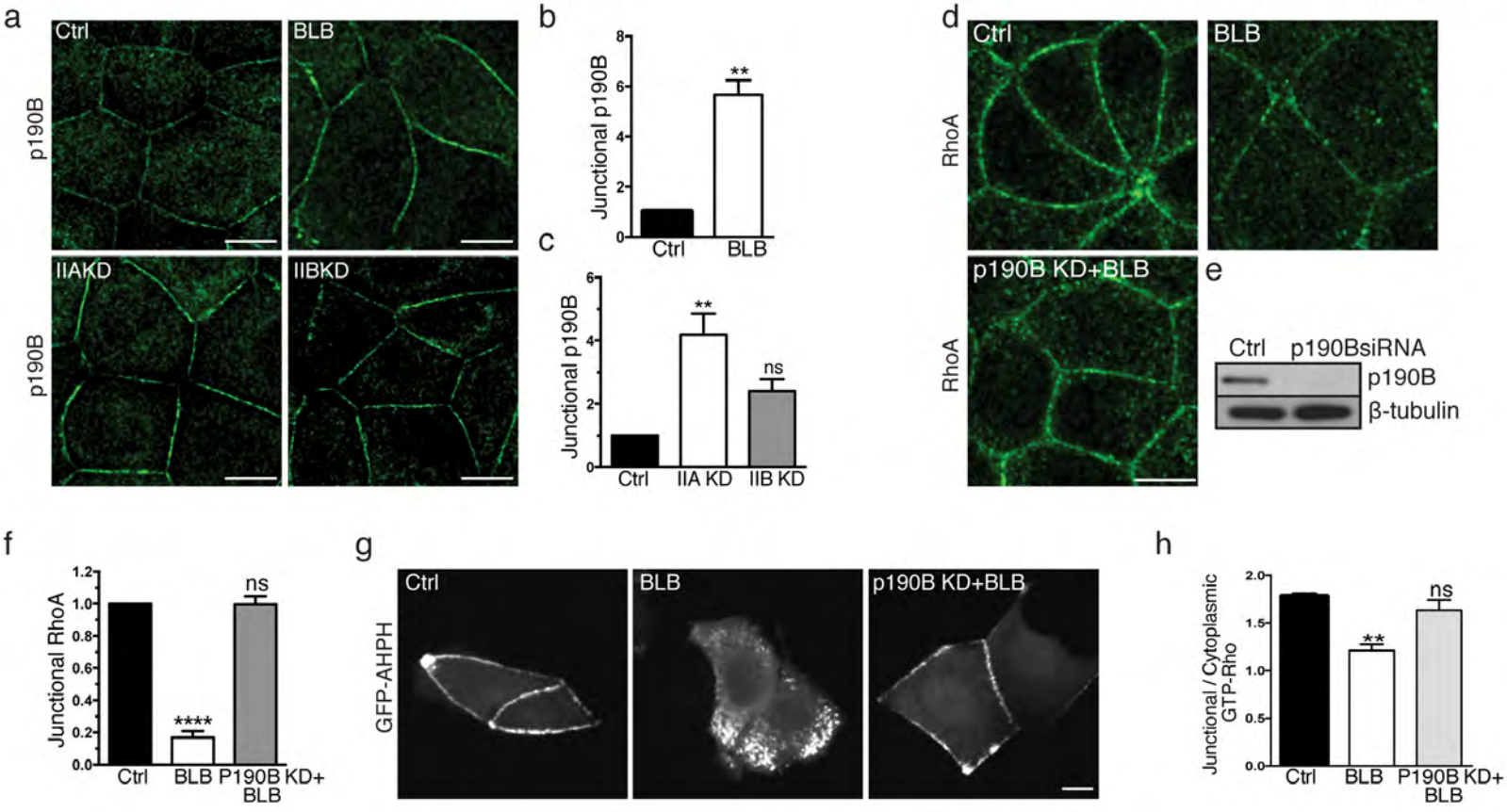

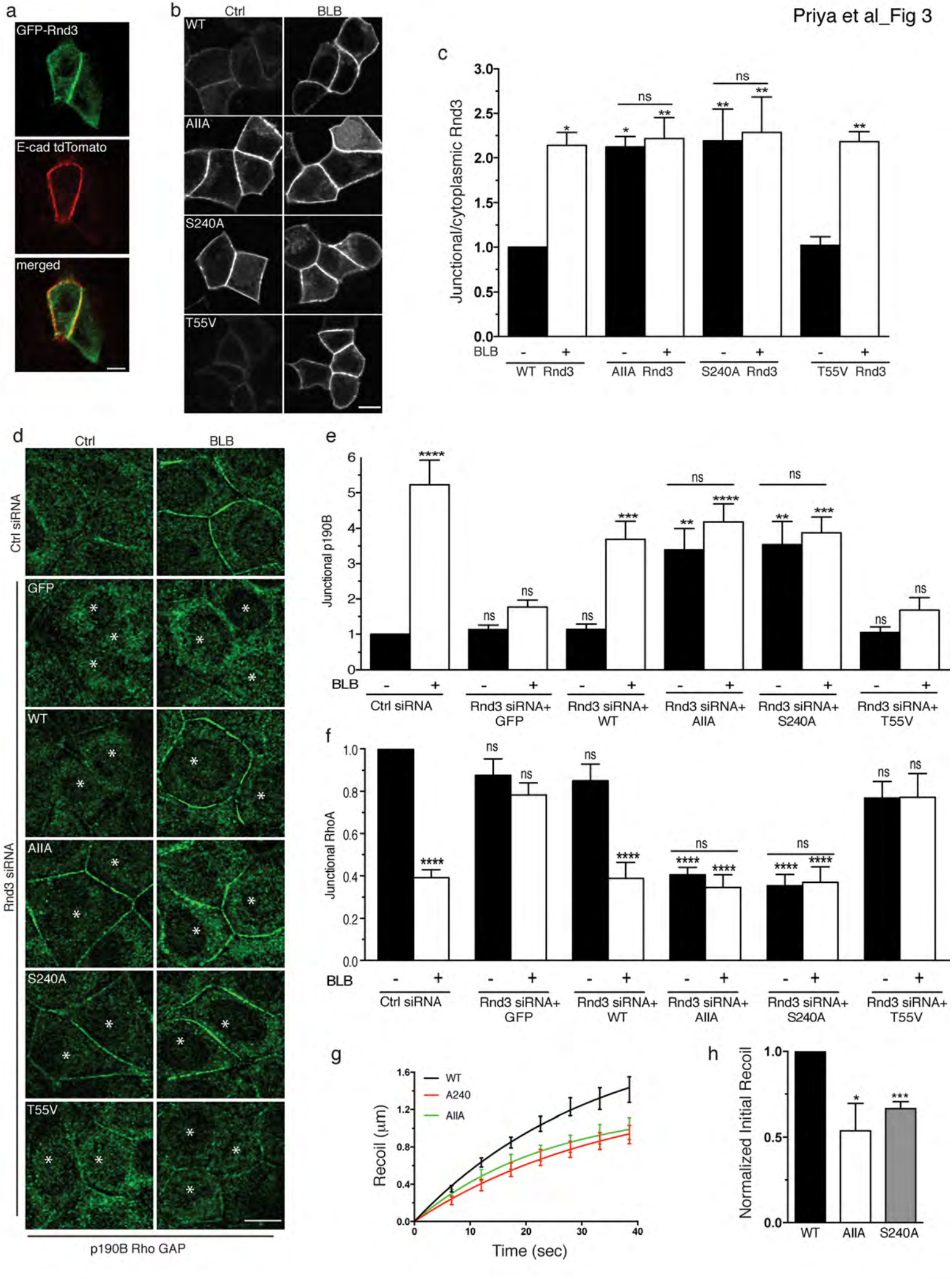
a
GFP-Rnd3
E-cad tdTomato
merged
b
Ctrl
BLB
WT
AIIA
S240A
T55V
c
Junctional/cytoplasmic Rnd3
3.0
2.5
2.0
1.5
1.0
0.5
0.0
ns
*
**
BLB
- + - + - + - +
WT Rnd3
AIIA Rnd3
S240A Rnd3
T55V Rnd3
d
Ctrl
BLB
Ctrl siRNA
Rnd3 siRNA
GFP
WT
AIIA
S240A
T55V
p190B Rho GAP
e
Junctional p190B
6
5
4
3
2
1
0
****
***
**
*
ns
BLB
- + - + - + - + - + - +
Ctrl siRNA
Rnd3 siRNA+ GFP
Rnd3 siRNA+ WT
Rnd3 siRNA+ AIIA
Rnd3 siRNA+ S240A
Rnd3 siRNA+ T55V
f
Junctional RhoA
1.0
0.8
0.6
0.4
0.2
0.0
****
ns
BLB
- + - + - + - + - + - +
Ctrl siRNA
Rnd3 siRNA+ GFP
Rnd3 siRNA+ WT
Rnd3 siRNA+ AIIA
Rnd3 siRNA+ S240A
Rnd3 siRNA+ T55V
g
Recoil (µm)
1.6
1.2
0.8
0.4
0.0
WT
A240
AIIA
0
10
20
30
40
Time (sec)
h
Normalized Initial Recoil
1.0
0.5
0.0
*
***
WT
AIIA
S240A

Priya et al_Fig 4

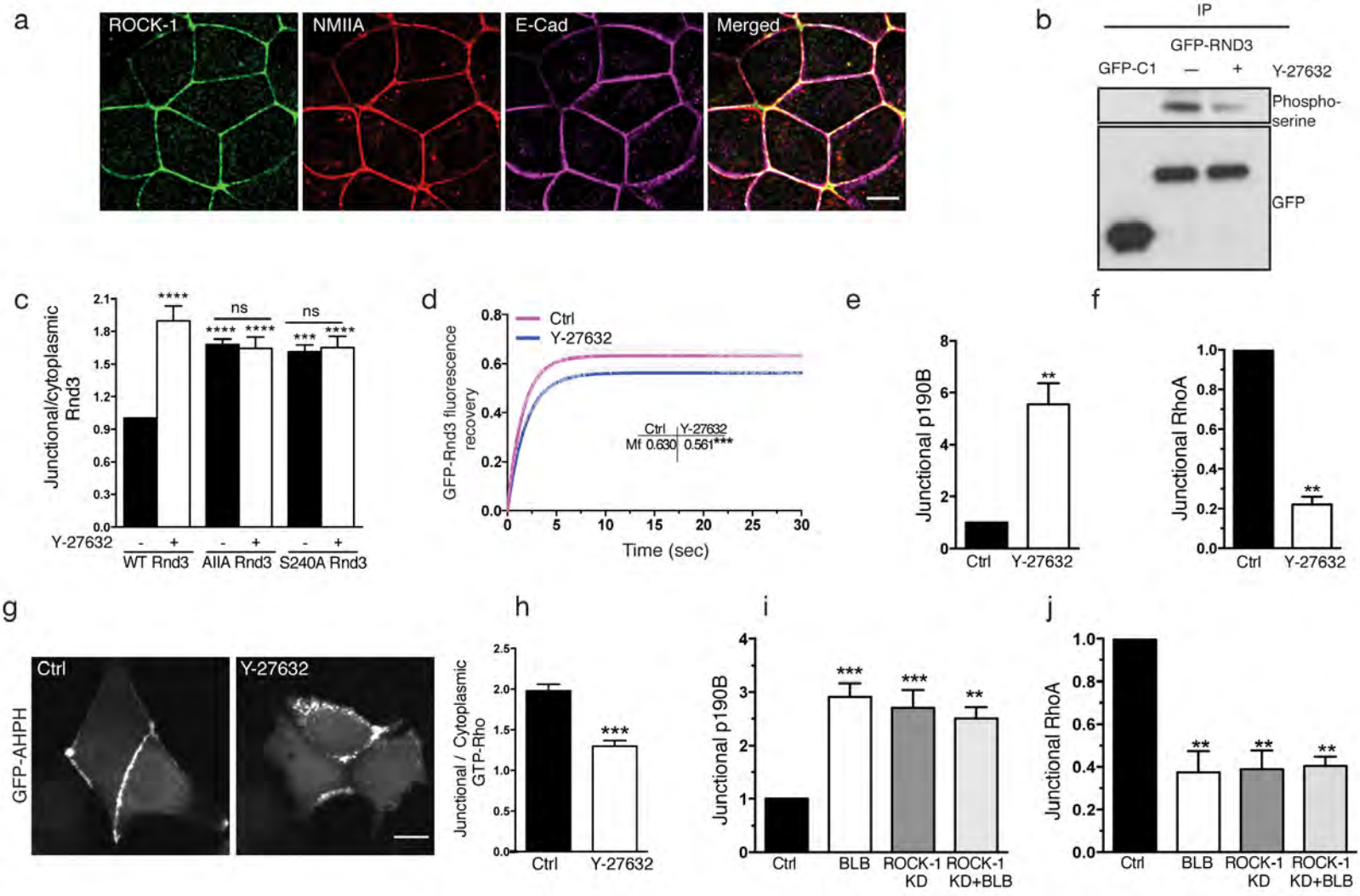

Priya et al_Fig 5

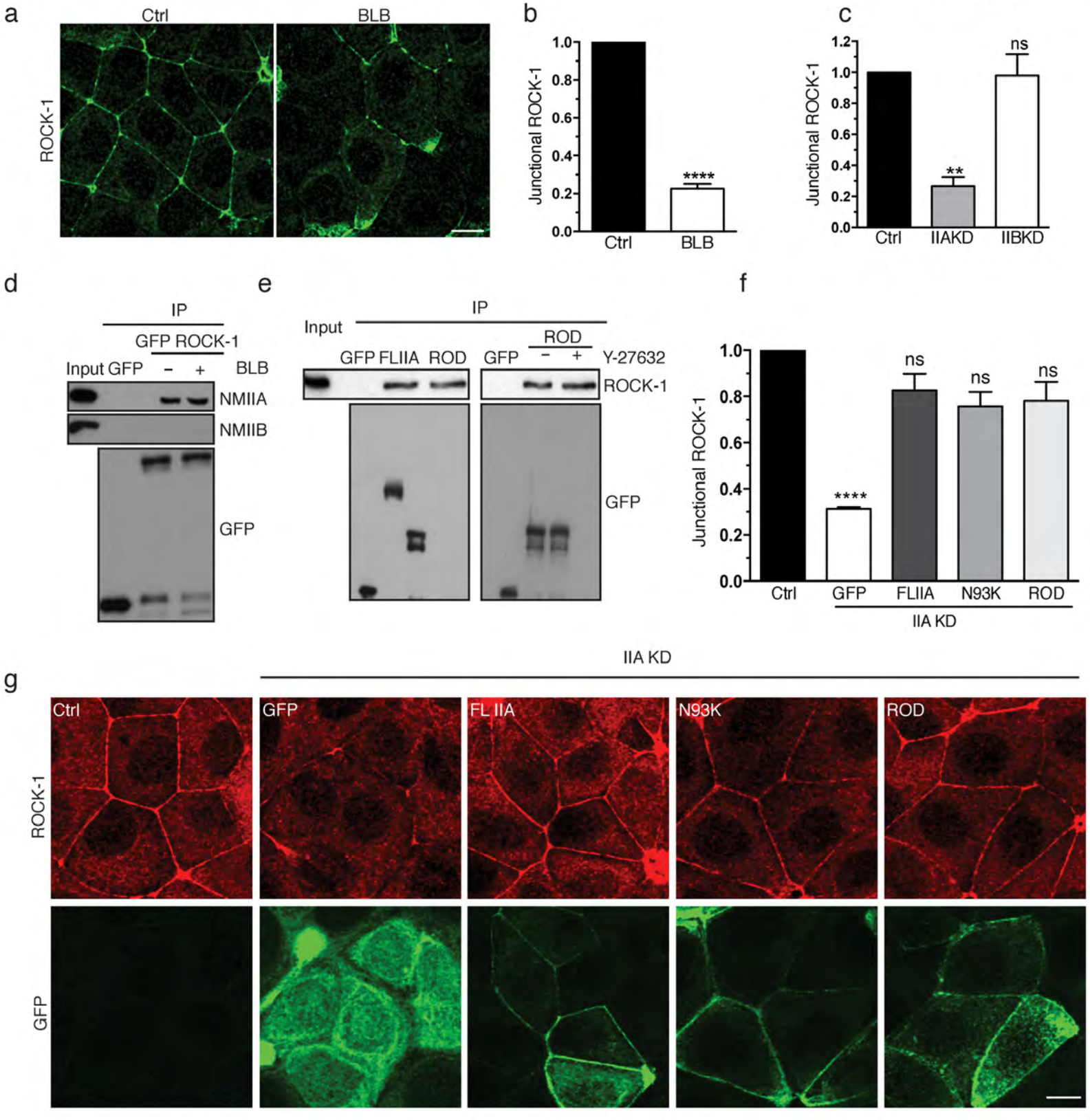

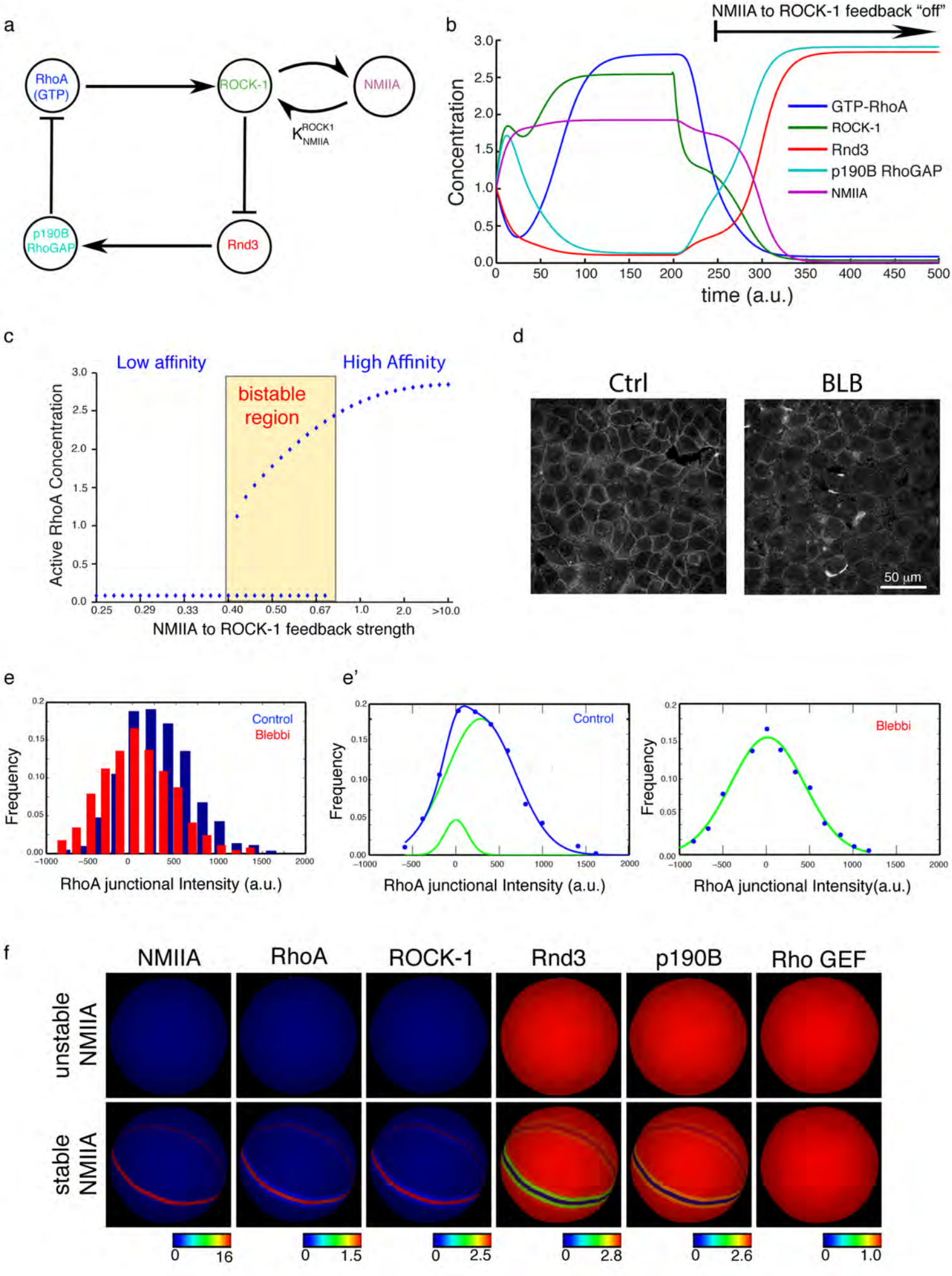
a
RhoA (GTP)
ROCK-1
NMIIA
K_{NMIIA}^{ROCK1}
p190B RhoGAP
Rnd3
b
NMIIA to ROCK-1 feedback "off"
Concentration
time (a.u.)
GTP-RhoA
ROCK-1
Rnd3
p190B RhoGAP
NMIIA
c
Low affinity
High Affinity
bistable region
Active RhoA Concentration
NMIIA to ROCK-1 feedback strength
d
Ctrl
BLB
50 μm
e
Control
Blebbi
Frequency
RhoA junctional Intensity (a.u.)
e'
Control
Blebbi
Frequency
RhoA junctional Intensity (a.u.)
RhoA junctional Intensity(a.u.)
f
NMIIA
RhoA
ROCK-1
Rnd3
p190B
Rho GEF
unstable NMIIA
stable NMIIA
0 16
0 1.5
0 2.5
0 2.8
0 2.6
0 1.0

Priya et al_Fig S1

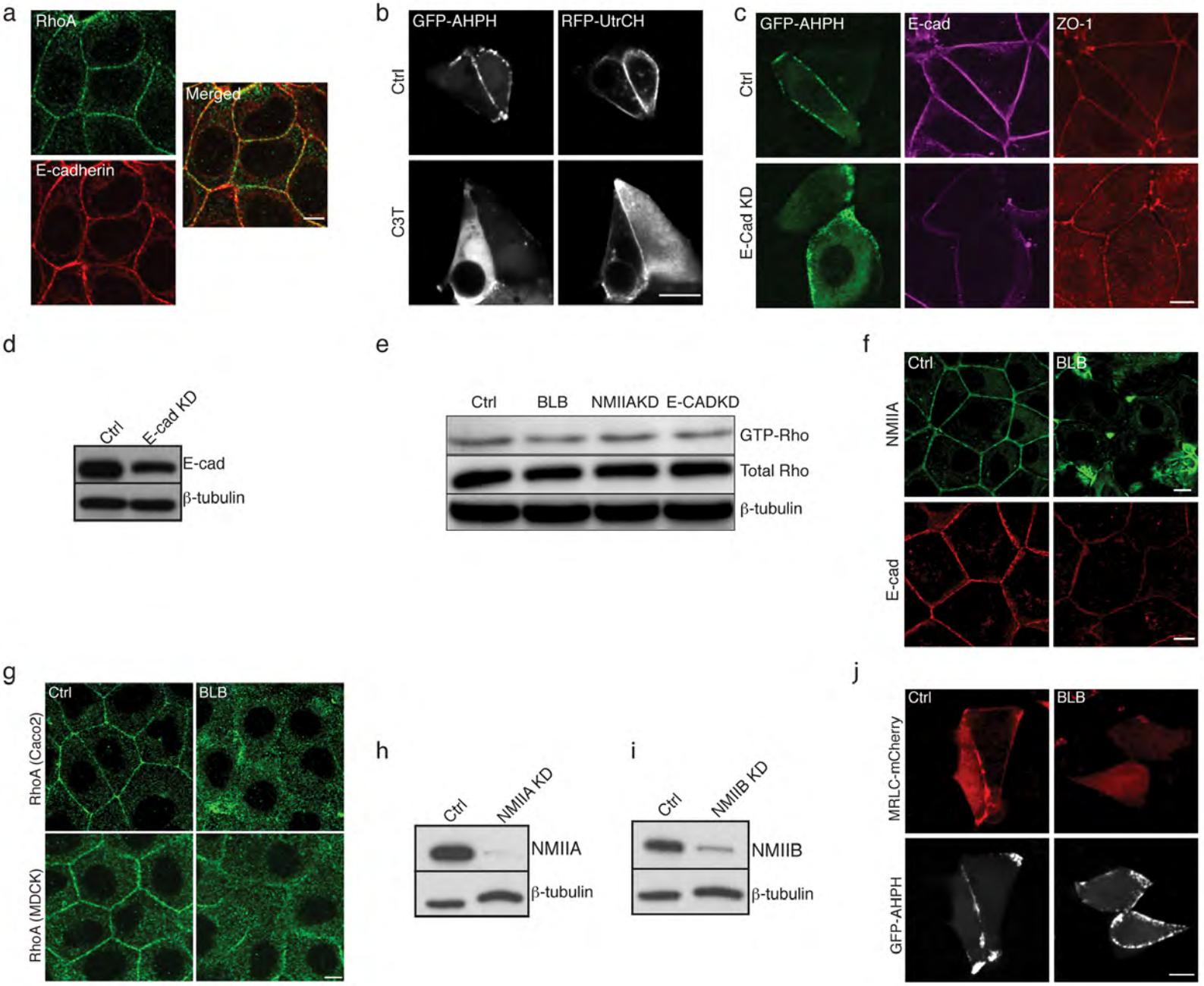

Priya et al_Fig S2

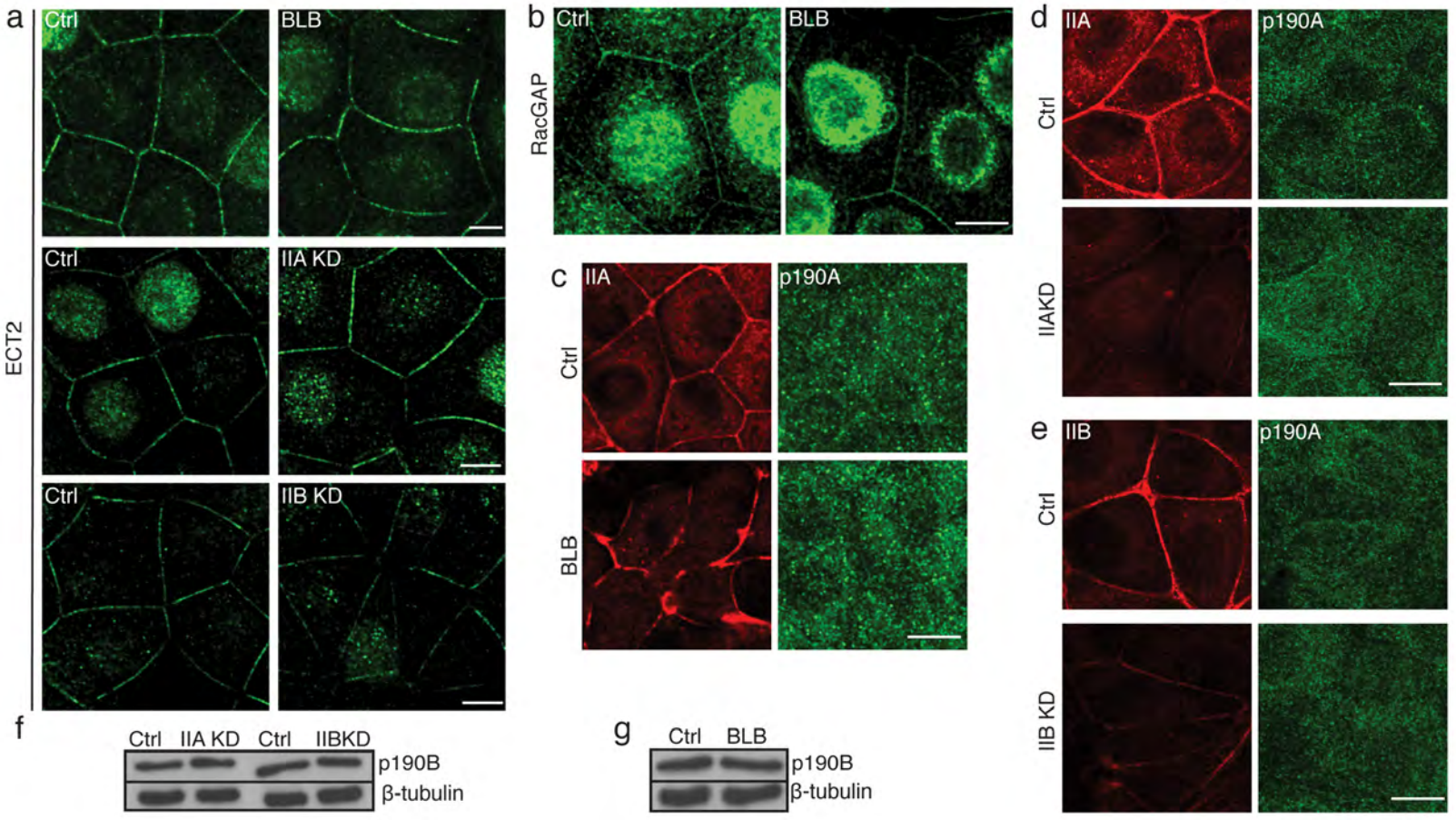

Priya et al_Fig S3

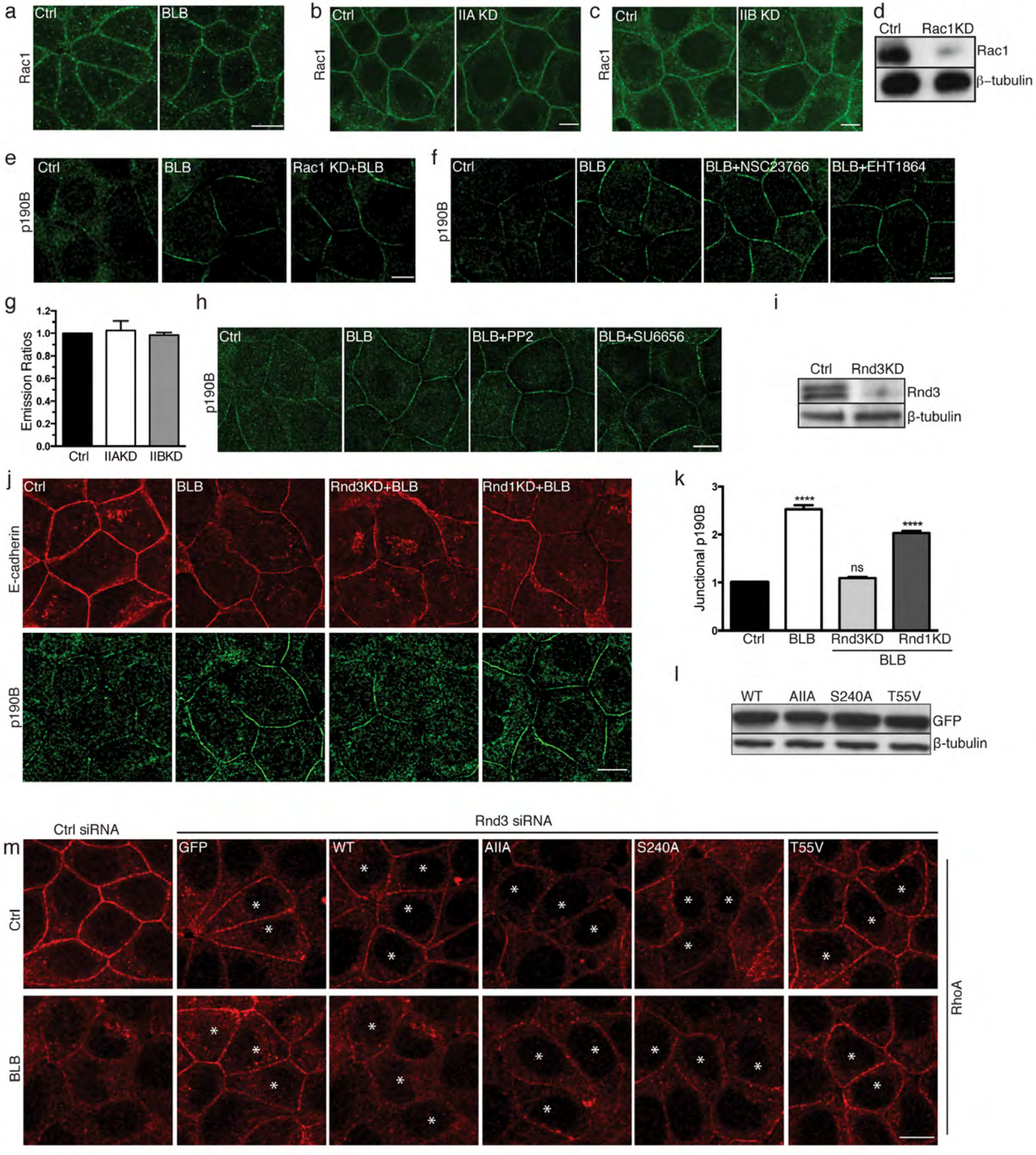

Priya et al_Fig S4

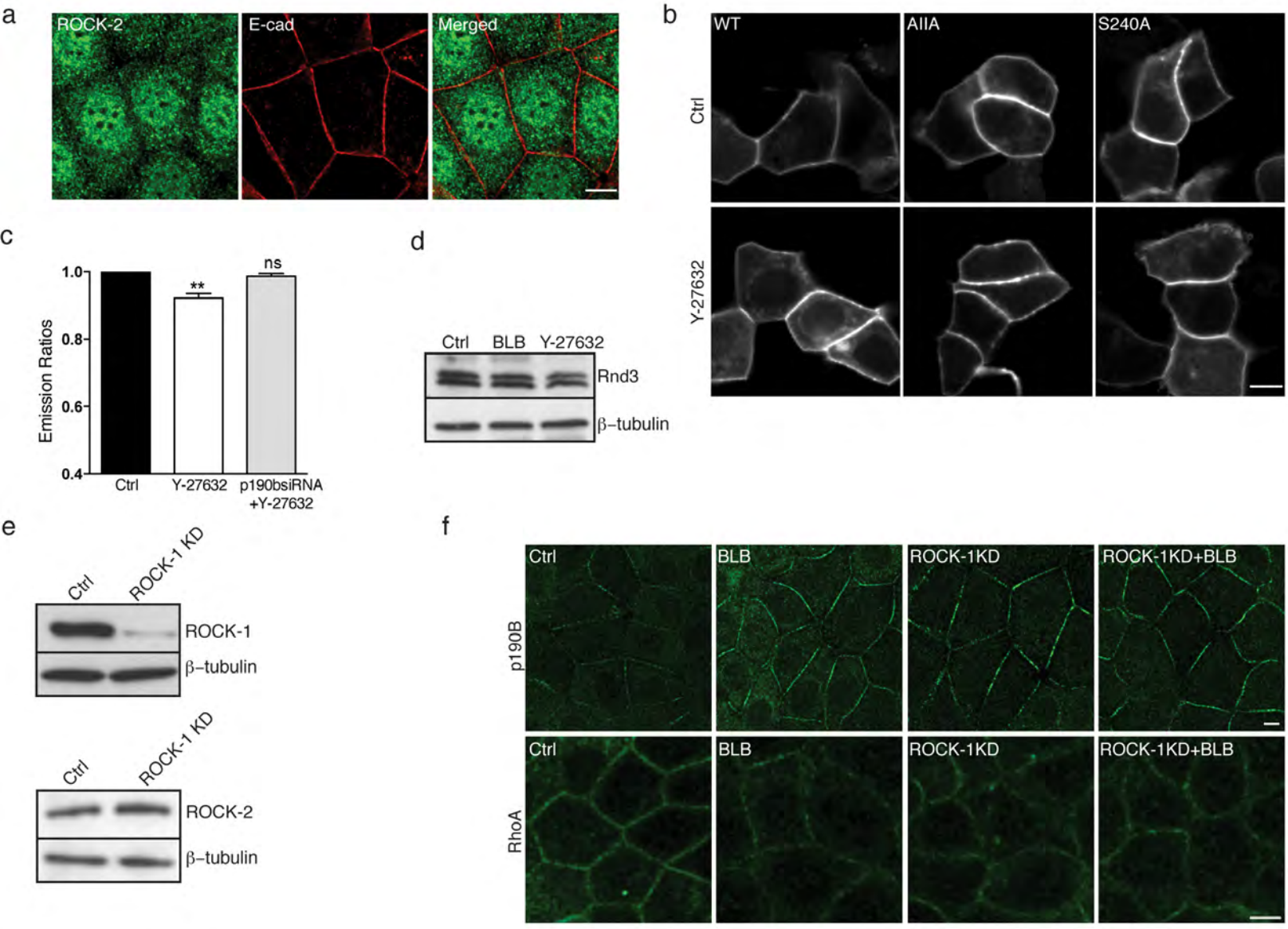

Priya et al_Fig S5

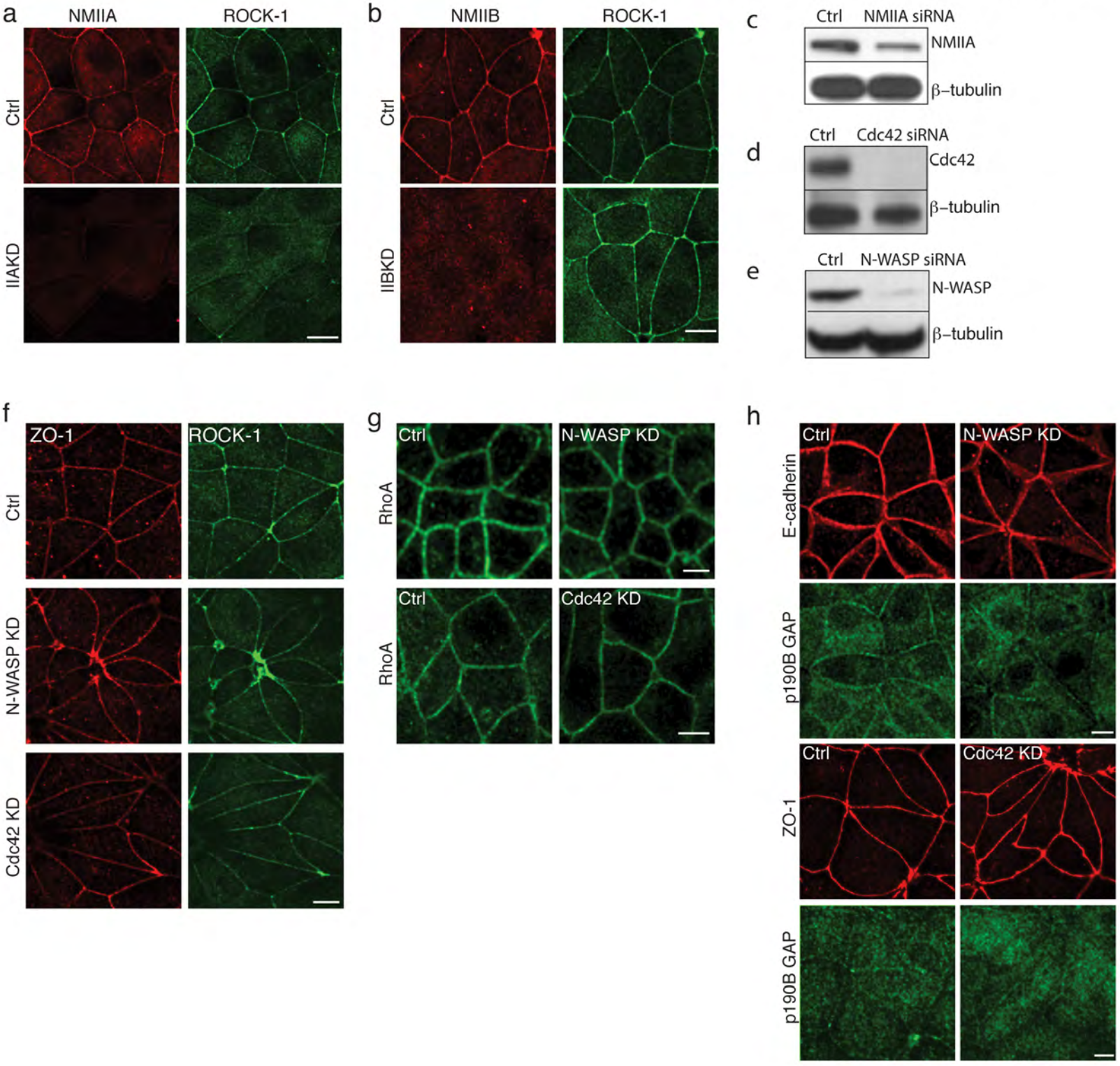

a

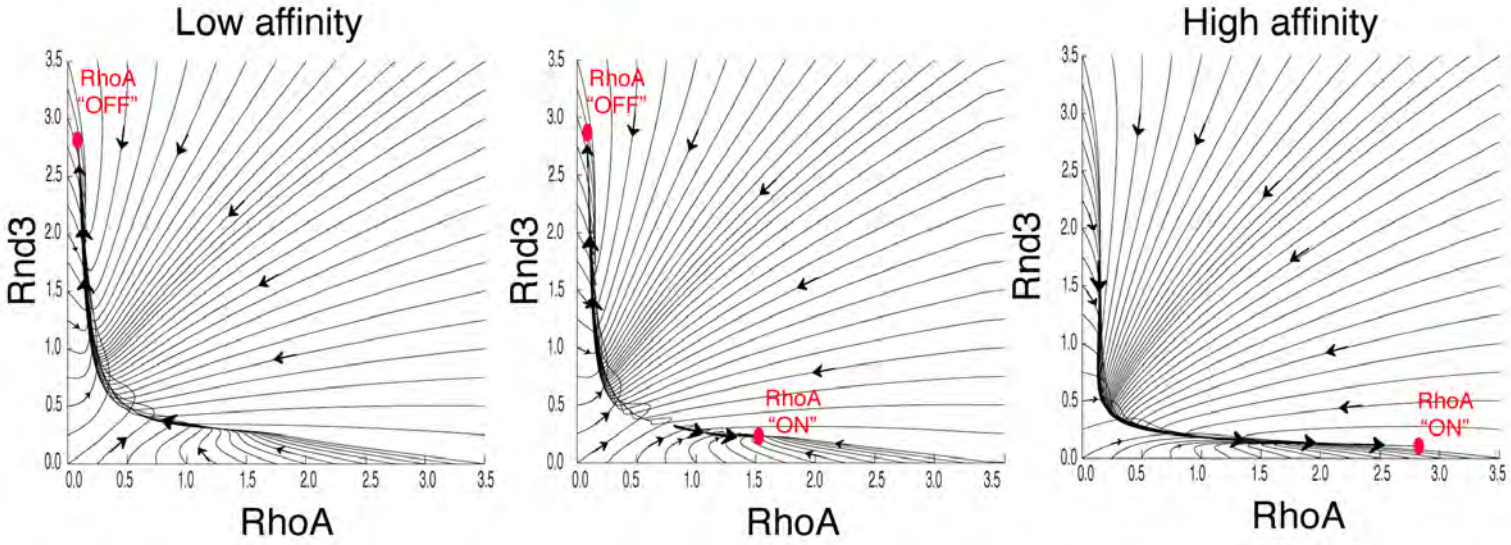
Low affinity
High affinity
RhoA "OFF"
RhoA "ON"
Rnd3
RhoA

b

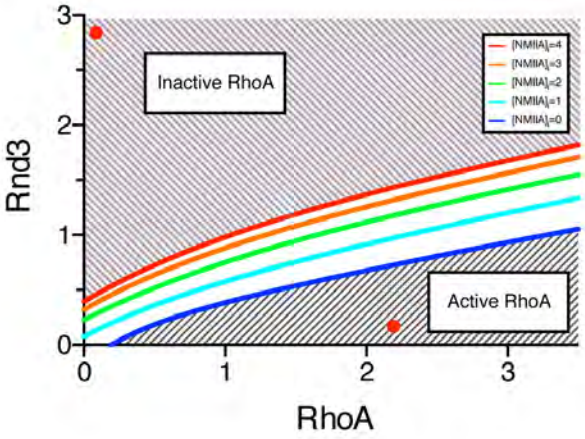
Inactive RhoA
Active RhoA
[NMIIA]=4
[NMIIA]=3
[NMIIA]=2
[NMIIA]=1
[NMIIA]=0
Rnd3
RhoA

c

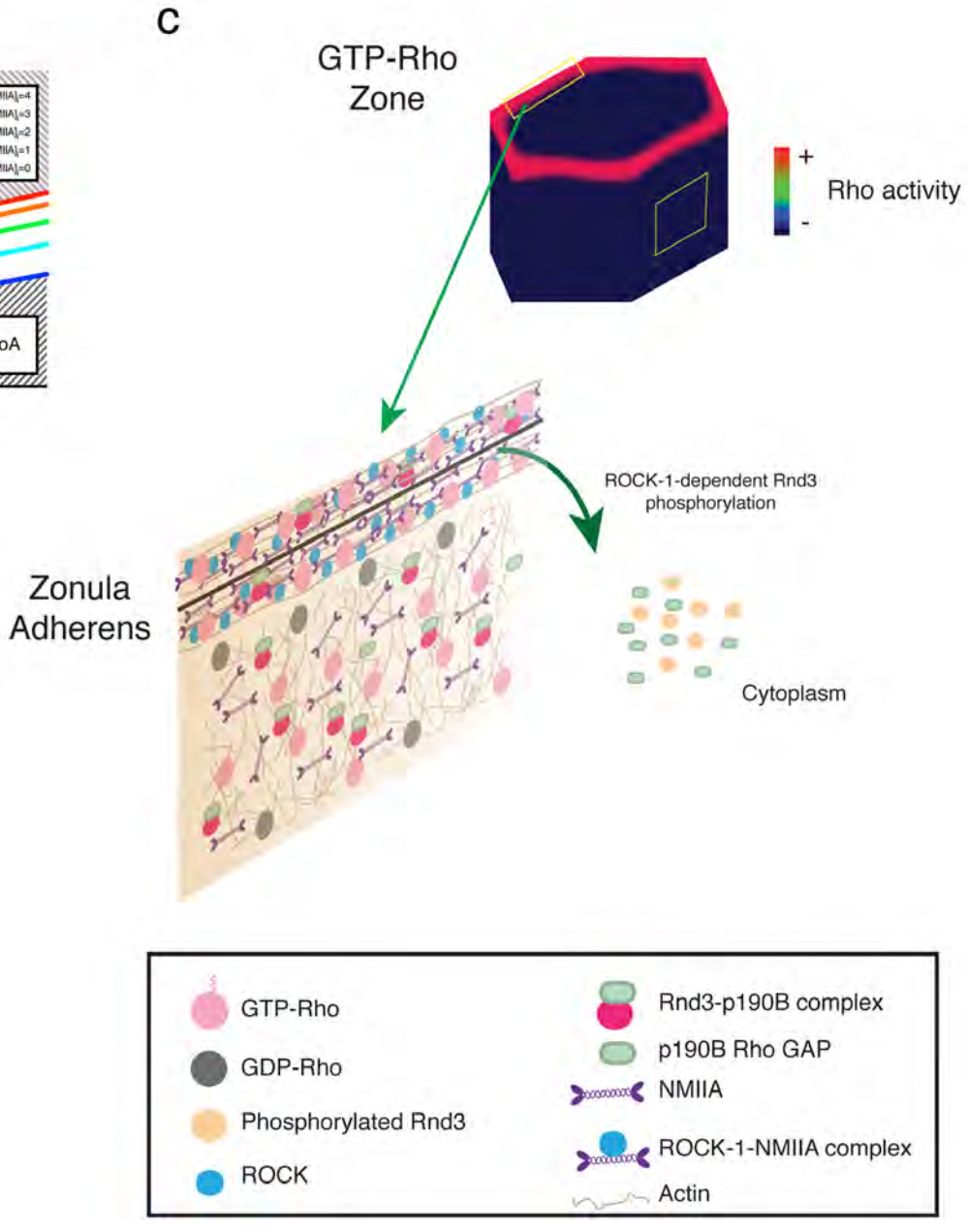
GTP-Rho Zone
Rho activity
+
-
ROCK-1-dependent Rnd3 phosphorylation
Zonula Adherens
Cytoplasm
GTP-Rho
GDP-Rho
Phosphorylated Rnd3
ROCK
Rnd3-p190B complex
p190B Rho GAP
NMIIA
ROCK-1-NMIIA complex
Actin

Supplementary Information

Methods

Cell culture, Transfection:

MCF-7, MDCK and HEK293T and Caco2 cells were grown in DMEM and RPMI media, respectively, supplemented with 10% FBS, 1% L-glutamine, 1% penicillin/streptomycin. All cell lines were maintained in low-doses of plasmocin (Invivogen) and routinely tested for the presence of mycoplasma. Cells were seeded at 30-40% confluency 48 hours before transfection with plasmids and siRNA, using Lipofectamine 2000 (Invitrogen) or RNAimax (Invitrogen), respectively according to manufacturer's recommendations. For live-cell experiments, cells were cultured on 29 mm glass-bottom dishes (Shengyou Biotechnology) and imaged in clear Hank's balanced salt solution supplemented with 5% FBS, 10 mM HEPES (pH 7.4) and 5mM $CaCl_2$.

siRNA and shRNA:

NMIIA and NMIIB were depleted using lentiviral shRNA, produced and transduced as described previously [1, 2]. For reconstitution experiments with human Rnd3 and NMIIA, siRNA sequences were designed against their UTR regions using Invitrogen Block-iT RNAi designer. Smartpool siRNA (Dharmacon) were used to deplete Rac1, p190BRhoGAP, ROCK-1, Rnd1, E-cadherin and N-WASP. Cdc42 siRNA (#sc-29256) has been described previously [3]. The relevant sequences of siRNA are shown in Supplementary Table 1.

Antibodies and Inhibitors:

Primary antibodies used in this study were: (1) mouse monoclonal antibody (mAb) HECD-1 against the ectodomain of E-cadherin (1:50; a gift from Peggy Wheelock, University of Nebraska, Omaha, NE; with the permission of M. Takeichi); (2) rabbit polyclonal antibody (pAb) for non-muscle myosin IIA heavy chain (1:1000; #PRB-440P, Covance); (3) rabbit pAb for non-muscle myosin IIB heavy chain (1:1000; #PRB-445P, Covance); (4) rabbit pAb (1:2000; #A-6455) and mouse mAb (1:200; #A-1120) against GFP (Molecular Probes/Invitrogen); (5) rabbit pAb (1:300; #61-7300, Invitrogen) and (6) mouse mAb against human ZO-1(1:300, #33-9100, Invitrogen); (7) mouse mAbs against RhoA (1:100; Santa Cruz Biotechnology, #sc418), (8) rabbit pAb against Ect2 (1:50; Millipore; #07-1364), (9) MKLP1(#sc: 22793, 1:50) and (10) RacGAP1(cat #sc:98617, 1:50) (SantaCruz Biotechnology Inc); mouse mAbs against (11) p190A (cat #610150, 1:50) and (12) p190B (#611612, 1:50) (BD Biosciences); (13) mouse mAb against β-tubulin (1:500, #T4026, Sigma-Aldrich); (14) rabbit pAb against ROCK-1 (1:300, Abcam ,#AB134181); (15) rabbit pAb to ROCK-2 (1:100, Abcam, # AB71598); (16) mouse anti-ROCK-2 mAb (1:300,BD Biosciences,

#610623,); (17) mouse mAb Anti-Rac1 (1:200, Millipore, #05-389); (18) mouse mAb against GFP (1:1,000; Roche; #11814460001, mixture of clones 7.1 and 13.1); (19) mouse mAb against actin (1:100; Millipore; # MAB1501, clone number C4); (20) rabbit mAb antibody 30D10 against N-WASP (1:50; Cell Signaling Technologies; #4848; (21) rat mAb E-Cadherin (ECCD-2) (1:500, Invitrogen, #13-1900,); and (22) mouse mAb Anti-Cdc42 (1:300, BD biosciences, # 610928).).

Secondary antibodies were species-specific antibodies conjugated with AlexaFluor 488, 594 or 647 (Invitrogen) (1:500) for immunofluorescence, or with horseradish peroxidase (Bio-Rad Laboratories) (1:5000) for immunoblotting.

Cells were treated with Blebbistatin (#US1203390-5MG, Merck; 100 µM, 2 hours) or Y-27632 (# Y0503, Sigma; 30 µM, 1 hour). To inhibit Rac activity, cells were treated with 10 µM EHT1864 (#3872, Bio-Scientific) or 50 µM NSC23766 (#2161, Bio-Scientific) for 12 hours. To inhibit Src activity, cells were treated with 10 µM SU6656 (#572635, MERCK) or 10 µM PP2 (#529573, MERCK) for 4 hours [4].For inhibition of Rho activity, cells were treated with 1 µgm/µl of cell permeable Rho Inhibitor (C3T based; #CT04-A, Jomar Bioscience) for 2-3 hours [5].

Plasmids:

FLAG-tagged RND3 mutants (WT, AIIA, S240A, T55V) were a kind gift from Anne Ridley, (King's College London) and were described previously [6].These constructs were used as template for PCR-amplification and were subsequently cloned into pEGFP-C1 (Clontech) using EcoR1 and Kpn1 restriction sites. To generate mCherry-tagged version of these Rnd3 constructs, the GFP tag was replaced in this vector by mCherry from pmCherry-C1 (Clontech) using Age1 and BsrG1 restriction sites. GFP-p190BRhoGAP was generated by PCR from cDNA obtained from MCF-7 cells and cloned into pEGFP-C1 using EcoR1 and Kpn1 sites. GFP-Myosin IIA ROD was a kind gift from Thomas Egelhoff (Cleveland Clinic, USA). GFP-ROCK1 construct was generated by PCR-amplifying mouse ROCK1 using FLAG-tag mouse ROCK1 (a kind gift from Michael Samuel, Centre for Cancer Biology, Uni of South Australia) as a template and cloned into pEGFP-C1 (Clontech) using Sac1 and Kpn1 restriction sites. Raichu- Rac FRET biosensors was a kind gift from M. Matsuda (Kyoto University, Japan). pTriEx–RhoA biosensor WT was obtained from Addgene (#12150). GFP-AHPH location Rho biosensor was a kind gift from Michael Glotzer (Uni of Chicago, USA) [7, 8]. GFP-Myosin IIA (#11347, Addgene) and GFP-Myosin N93K have been described previously [2].E-cad-EGFP and E-cad-tdTomato have been described previously [2, 9 10]. MRLC1-mCherry was obtained by cloning MRLC1 (# 35680, Addgene) into pLL5.0 cherry [1] by PCR using SacI and BamHI restriction sites.

Immunofluorescence microscopy and live-cell imaging:

Cells were fixed with ice-cold methanol in -20 °C for 5 minutes or with 4% paraformaldehyde in cytoskeleton stabilization buffer (10 mM PIPES at pH 6.8, 100 mM KCl, 300 mM sucrose, 2 mM

EGTA and 2 mM $MgCl_2$) on ice for 15 minutes or with freshly-prepared 10% TCA on ice for 15 minutes (for Rho staining). TCA fixed cells were subsequently washed three times with 30mM glycine. Both PFA and TCA fixed cells were permeabilized with 0.25% triton X-100 for 5 minutes at room temperature. Confocal images were acquired with a Zeiss 510 or a Zeiss 710 Meta laser-scanning confocal microscope. Background correction, contrast adjustment and Z-projections of raw data images were performed with ImageJ.

Live cell imaging (of GFP- and mCherry-Rnd3) was performed with cells incubated in movie-media (Hank's balanced salt solution supplemented with 5% FBS, 10 mM HEPES pH 7.4 and 5mM $CaCl_2$) on a Zeiss 510 Meta laser-scanning confocal microscope. The mean grey values of fluorescence intensity from junctions and cytoplasm were obtained using ImageJ and their ratio was used for statistical analysis.

For representation purpose, images were processed in ImageJ by using the function smooth, applying a median filter of one pixel radius, or despeckle, as appropriate. Where necessary, background subtraction was performed using rolling-ball background subtraction function in Image J. Control and test images were processed identically.

RhoA location biosensor (GFPAHPH) image acquisition and analysis:

Cell grown on glass bottom dishes and expressing GFP-AHPH were imaged in a Zeiss inverted spinning disk confocal microscope equipped with a 63x 1.3 NA multi-immersion immersion objective (Zeiss), a CSU=X1-A Yokogawa spinning disk unit, and two Roper Evolve EMCCD 512x512 cameras. Z-stacks were acquired with a Z-displacement of 0.2 µm and images were acquired with a digital resolution of 0.2 µm. Quantitative analysis of fluorescence intensity at contacts was performed using the line scan function of ImageJ. A line of ~20 µm in length (15 pixels thick) was drawn starting from a cell-cell contact and orthogonal to it. Numerical values for the fluorescence intensity profile along this line were obtained for at least 100 contacts per condition per experiment using the Multiplot Plot feature of ImageJ and plotted in. Profiles were then averaged and fitted to the equation:

$$Y(x) = Y_0 + (1 - Y_0) * e^{(-k*x^{\alpha})}$$

where α was chosen as a shared parameter for the different conditions that were evaluated. To measure GTP-Rho accumulation at junctions the ratio at the ZA [Y(x=0 µm)] and its adjacent cytoplasmic region [Y(x=1 µm)] away was calculated for at least three independent experiments and the average values together with the standard errors of means were reported as indicated in the corresponding figure legends.

Frequency analysis of RhoA intensity at junctions:

To acquire a large dataset of cell-cell junctions, wide-view Z-stacks (300x300x10 µm) of cells immunolabeled for RhoA and E-cadherin were acquired using a PLAN-Apochromat 40x Oil Objective. Then, quantitative analysis of fluorescence intensity at contacts was performed using the line scan function of ImageJ. A line of 10 µm in length (0.6 µm thick) was positioned orthogonal to, and centered upon, each cell-cell contact labeled with E-cadherin in every field of view. Numerical values for the RhoA fluorescence intensity profile along this line were obtained using the Plot Profile feature of ImageJ. Average profiles were then fitted to a Gaussian curve centered at zero. For each line scan profile, average intensities for pixels at a distance $-1.2<x<1.2$ µm from the center (junction) were calculated. In order to correct for background, we subtracted the corresponding average Rho fluorescence in the apical pole of cell (its average intensities for pixels located at distances $X<-1.2$ µm and $x>1.2$ µm). Corrected intensities (background subtracted) were then plotted as an histogram and fitted to a single or double peak Gaussian functions using the Peak Fitter function in Matlab [11]. This approach allowed us to identify Rho labelling at the junctions that is higher than elsewhere in the apical region. As Rho staining at the apical pole of cells was of variable intensity, corrected intensities for single junctions could also acquire negative values, especially when their Rho content was reduced.

GFP-TRAP pull-down assays:

HEK293T cells growing on 10cm dishes were transfected with relevant constructs using Lipofectamine 2000 and processed for immunoprecipitation analysis 48 hours post-transfection. Cells were scrapped in pre-chilled tubes in 1 ml 1X TBS and centrifuged for 2 minutes for 1500xg to remove the TBS. Lysis buffer (600 µl) containing 50mM Tris, pH 7.5, 1% NP-40, 300 mM Nacl, Protease inhibitor cocktail (#138467, Roche), 1 mM Sodium orthovanadate, 20 mM Sodium Fluoride, 3mM EDTA, 10mM ATP, 5mM $MgCl_2$ was added to the cell pellet. Cells were incubated on ice for 30 minutes, with a brief vortex once every 10 minutes, and then centrifuged at 15,000xg for 30 minutes. The cleared 550 µl of supernatants were loaded with pre-blocked GFP-TRAP beads (GFP-Bond, Protein Expression facility, The University of Queensland, Australia) (50ul of 50% bead-slurry) and allowed to incubate on a rotating wheel overnight in 4°C. The beads were then washed three times with wash buffer (50mM Tris pH 7.5, 1% NP-40, 500 mM NaCl) and protease inhibitor cocktail. The samples were eluted in 1X Laemmli buffer and processed for western blotting. For detection of Rnd3 phosphorylation levels, a phosphatase inhibitor cocktail (Cell Signaling, #5872) was added to the lysis and wash buffers and all the steps were performed as mentioned above. The samples were resolved on a 8-12% polyacrylamide gel, transferred to nitrocellulose membranes, and then blocked with 5% milk in TBST. The blots were washed thrice with TBST, incubated with anti-Phosphoserine Antibody (#AB1603, MERCK) in 3% BSA. This was

followed by three washes with TBST and incubation with secondary antibody in 5% milk (TBST) for 1 hour.

GTP-Rho Pull down assays:

GTP-Rho pulldown assays were performed with RhoA Pulldown Activation Assay Kit (#BK036, Cytoskeleton Inc) according to the manufacturer's instructions. MCF-7 cells were grown in 10cm dishes for 4-5 days and transfected with siRNA against E-cadherin or siRNA against NMIIA. The cells were then incubated in DMEM with 0.5% FBS for 24 hours followed by serum-starvation for another 24 hours. On the day of lysis, cells were treated with blebbistatin (100 µM, 2 hrs) followed by stimulation with 20% serum for 30 minutes. The cells were then washed with ice-cold PBS, lysed quickly and processed for pulldown assay according to the manufacturer's instructions.

FRET microscopy

MCF-7 cells transduced with lentivirus encoding NMIIA shRNA and NMIIB shRNA were grown on 29 mm glass-bottom dishes and transiently transfected with Raichu-Rac biosensor or pTriEx–RhoA biosensor as indicated in the corresponding figure legend. FRET measurements and analysis were performed 48 hours after transfection as described previously[5].Briefly, live-cell imaging was performed at 37 °C on a LSM710 Zeiss confocal microscope equipped with a 63x oil Immersion objective (Plan Apochromat 63x 1.4 NA, Zeiss, Jena, GER). Images were acquired by sequential line acquisition. The acceptor (A) channel was imaged using 514 nm laser line for excitation and emission was collected in the acceptor emission range (BP 530-590 nm). Donor and FRET channels were acquired using 458nm laser line and emission was collected in the donor emission region (BP 470-490 nm) and acceptor emission region (BP 530-590 nm), respectively. When needed, mCherry fluorescence signal was collected using a 561 nm laser line and a 580-620 nm band pass emission filter.

Laser Nanoscissors:

MCF-7 cells transduced with lentivirus encoding E-cadherin-EGFP [2] were transfected with mCherry-Rnd3 WT, AIIA and S240A. Cells were processed for experiments twenty-four hours post transfection. Laser nanoscissors experiment was performed on a LSM 510 meta Zeiss confocal microscope equipped with a 37° C heating stage. Images (95.1 x 95.1 µm) were acquired with a 63X objective (1.4 NA oil Plan Apochromat immersion lens) with 1.5X zoom. A constant ROI, with the longer axis parallel to the cell-cell contact was ablated with a Ti:sapphire laser (Chameleon Ultra, Coherent Scientific) tuned to 790nm, 30 iterations, and 25% transmission. Time-lapse images were acquired before (2 frames, 5.28 sec) and after (7 frames, 43.6 sec) ablation. Image analysis was done as described previously [12].

FRAP:

MCF-7 cells were co-transfected with GFP-Rnd3 and with siRNA targeted against the UTR region of Rnd3. Images (47.5x47.5 μm) were acquired on a LSM 510 meta Zeiss confocal microscope equipped with a 37 °C heating stage, with a 63X objective (1.4 NA oil Plan Apochromat immersion lens) and 3X zoom. A constant ROI was drawn in the center of cell-cell contact and was bleached to 70-80% with a 790nm laser at 33%, 1 iteration. Time-series images were acquired before (3 frames, ~311 ms) and after (247 frames, 38.8 s). To obtain FRAP profiles; a constant ROI at the bleached region of GFP-Rnd3 was drawn and the mean grey value were obtained at each time point. The fluorescence intensities obtained were normalized to the average pre-bleach values and fitted to a monoexponential function in the GraphPad Prism software.

Supplementary Table 1:

Sequences of siRNA used in the study

Target gene	Vendor, Catalogue number	siRNA sequences
Human ROCK1	Thermo Scientific, HumanROCK1 (6093) SMARTpool siRNA sequences	5'-GCCAAUGACUUACUUAGGA-3' 5'-GAGAUGAGCAAGUCAAUUA-3' 5'-GAAGAAACAUUCCCUAUUC-3' 5'-GGACACAGCUGUAAGAUUG-3'
Human P190B Rho GAP	Thermo Scientific, ON-TARGETplus Human ARHGAP5 (394) SMARTpool siRNA sequence	5'-GUACGAAUUUGCAACCAUA-3' 5'-GCUGAUACAACCACAAUUA-3' 5'-GAUCAUGGCCGCUUAAGAU-3' 5'-GGAAUCAGUUAAACACAAU-3'
Human RND1	Thermo Scientific, ON-TARGETplus Human RND1 (27289) SMARTpool siRNA sequence	5'-GGAUCUCCCUACUACGAUA-3' 5'-GAGCUUAGUCUCUGGGAUA-3' 5'-AGACAGACCUGCGAACAGA-3' 5'- CAGAAGAGCCCUGUCCGAA-3'
Human RAC1	Thermo Scientific, ON-TARGETplus Human RAC1 (5879) SMARTpool siRNA sequence	5'-GUGAUUUCAUAGCGAGUUU-3' 5'-GUAGUUCUCAGAUGCGUAA-3' 5'-AUGAAAGUGUCACGGGUAA-3' 5'-GAACUGCUAUUUCCUCUAA-3'
RND3 siRNA	Invitrogen, Custom siRNA	5'-UAAGCCUCUGGUAUACAUGACUUUG-3' 5'-AUGAGUAUCCUCUCAAACGCCUCCU-3'
Myosin IIA UTR	Invitrogen, Custom siRNA	5'-UAUAGCCAGGACCUGAACCUGGAUC-3' 5'-UUUAGAAUCAGGAGGGAGACAGCGG-3'
Human N-WASP	Thermo Scientific, ON-TARGETplus Human N-WASP(NM003941) SMARTpool siRNA sequence	5'-CCAGAAAUCACAACAAAUA-3′ 5'-CAGCAGAUCGGAACUGUAU-3 5'-UAGAGAGGGUGCUCAGCUA-3′ 5'-GGUGUUGCUUGUCUUGUUA-3′
Human E-cadherin	Thermo Scientific, ON-TARGETplus Human CDH1 (NM_004360) SMARTpool siRNA sequence	5'-GGCCUGAAGUGACUCGUAA-3′ 5'-GAGAACGCAUUGCCACAUA-3′ 5'-GGGACAACGUUUAUUACUA-3′ 5'-GACAAUGGUUCUCCAGUUG-3′

Supplementary Videos:

Video 1:

GFP-AHPH localizes at the zonula adherens of epithelial cells.

AZ-stacks of GFP-AHPH and RFP-UtrCH acquired by spinning disc confocal microscopy.

Video 2:

GFP-AHPH exhibits stability on the time scale of minutes.

Time-lapse imaging of GFP-APHPH (transfected in MCF-7 cells) acquired over a span of 30 minutes.

Video 3:

ROCK-1 inhibition causes accumulation of p190B Rho GAP at the cell-cell junctions.

MCF-7 cells were transfected with GFP-p190B RhoGAP and time-lapsed imaging was performed briefly before and after addition of Y-27632 (30 μM) (20-minutes post-treatment).

4.2 Dissecting the role of Rho signaling in oncogenic epithelial extrusion

The results presented in the previous section establish that in epithelial monolayers, Rho signaling exhibits bistability. Also, it implies that, by exploiting the myosin-ROCK feedback loop, cells can actually tune Rho activity (either ON or OFF) efficiently depending on the physiological cues. This gives rise to an important question: at cellular levels, when and why does Rho need to be turned OFF? There is enough evidence in the literature supporting the role of active Rho in cellular processes (Bement et al., 2006; Burkel et al., 2012; Miller and Bement, 2009; Piekny et al., 2005; Ratheesh et al., 2012; Tse et al., 2012; Wolfe and Glotzer, 2009). However, epithelial morphogenesis relies on the extensive rearrangement of actomyosin cytoskeleton, of which Rho is a prime modulator. So to facilitate these dynamic changes, Rho activity must be downregulated at certain stages, probably by exploiting the balance between upstream Rho regulators, GEFs and GAPs.

In order to understand the relevance of Rho inactivation, I used apical epithelial cell-extrusion as a model system, as described previously (Hogan et al., 2009; Slattum et al., 2009; Wu et al., 2014b). It is a process utilized by epithelial cells to preserve epithelial homeostasis, maintain barrier functions and modulate morphogenetic events (Eisenhoffer and Rosenblatt, 2013; Gu and Rosenblatt, 2012; Katoh and Fujita, 2012). The process involves expulsion of a minority of cells from the monolayer, driven by apoptosis (Rosenblatt et al., 2001; Eisenhoffer et al., 2012; Kuipers et al., 2014), over-crowding (Eisenhoffer et al., 2012) or expression of an oncogene (Hogan et al., 2009; Leung and Brugge, 2012; Wu et al., 2014b) The molecular pathways required for cell-extrusion have been the focus of intense studies. Strikingly, actomyosin generated junctional contractility plays a decisive role in this process of epithelial oncogenic extrusion (Wu et al., 2014b). Epithelial cells establish disparate regions of tension within their cell-cell junctions: the ZA acts as a site of high contractile tension, while lateral junctions display a much lower tension (Wu et al., 2014b). This higher apical tension is essential for epithelial integration as when this is depleted, cells tend to leave the monolayer and extrude (Wu et al., 2014b). Of note, it's established that an active Rho is required to maintain apical junctional tension in epithelial monolayers (research chapter 2).

Given above observations, I hypothesized that inhibition of Rho activity via p190B Rho GAP at the apical cadherin junctions leads to loss of apical tension and thus facilitates oncogenic extrusion (Fig 4.2.1). To test this hypothesis, I performed mosaic expression of oncogenic Ras (HRasV12) in the

MCF-7 cells and asked whether depleting p190B GAP can affect this process. Expression of HRasV12 leads to a significant increase in the percentage of extruding cells (Fig 4.2.2 a).

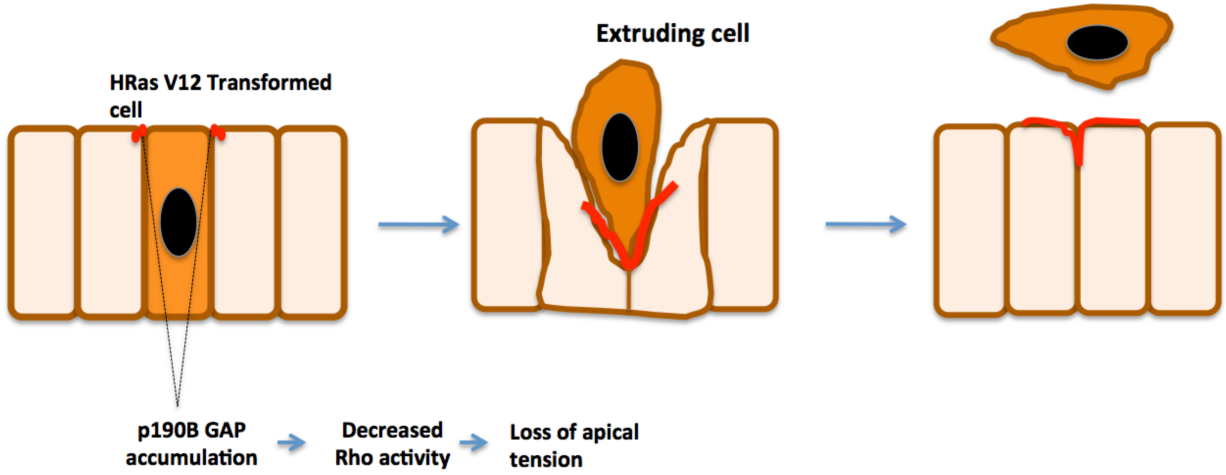

Fig 4.2.1 Schematic indicating the proposed role of Rho signaling in apical oncogenic extrusion.

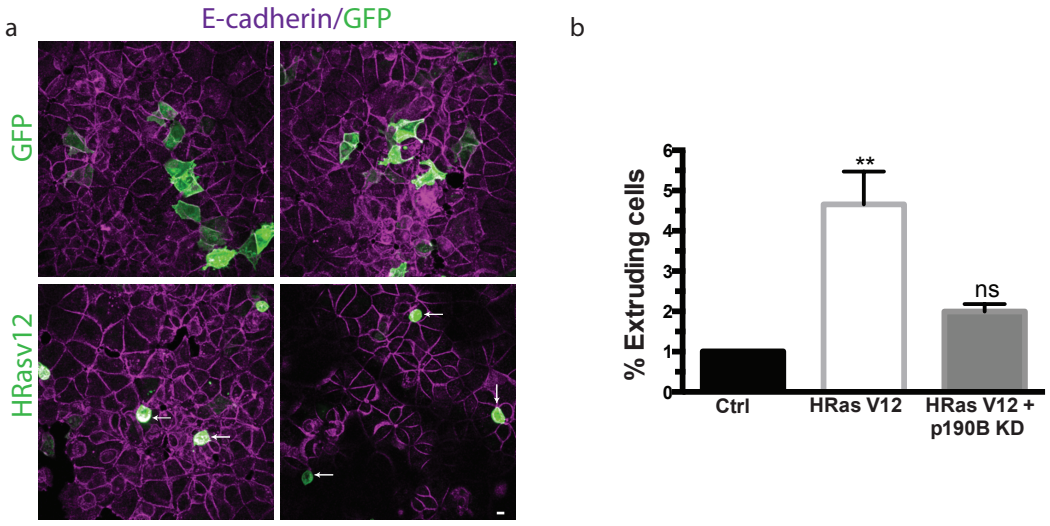

Fig 4.2.2 p190B is essential for oncogenic extrusion. (a) MCF-7 cell monolayer with mosaic expression of control (GFP only) and HRasV12 cells, stained for E-cadherin and GFP. Arrow indicates the extruding cells. (b) Quantification of HRasV12-expressing cells undergoing extrusion in control or p190B depleted cell. Data represent mean ± S.E.M calculated from n = 3 independent experiments; ns, not significant; ** P < 0.01, Student's t-test. Scale bar =10 µm

Interestingly p190B GAP is required for this process as depletion of p190B GAP led to a sharp decrease in the number of Ras-transformed extruding cells (Fig 4.2.2 b. This suggests that p190B GAP activity is critical for cells to extrude. One way to envisage how this might happen is that the

GAP activity of p190B will suppress Rho signaling at the ZA, apical junctional tension will consequently be reduced, thus enabling cells to extrude.

To test this hypothesis, I used laser-ablation to measure junctional tension along the interface of WT-WT vs. WT-HRasV12 transfected cells. Junctional tension was significantly less at the heterologous contacts between WT-HRasV12 cells compared to WT-WT cells (Fig 4.2.3). This indicates that indeed apical junctional tension is compromised at contacts of presumptive extruding cells, as observed earlier (Wu et al., 2014b). Strikingly, depletion of p190B GAP abolished this phenotype and junctional tension at the heterologous contacts was similar to the WT-WT cells (Fig 4.2.3). These results strongly establish that p190B GAP is required to reduce the apical tension during oncogenic extrusion.

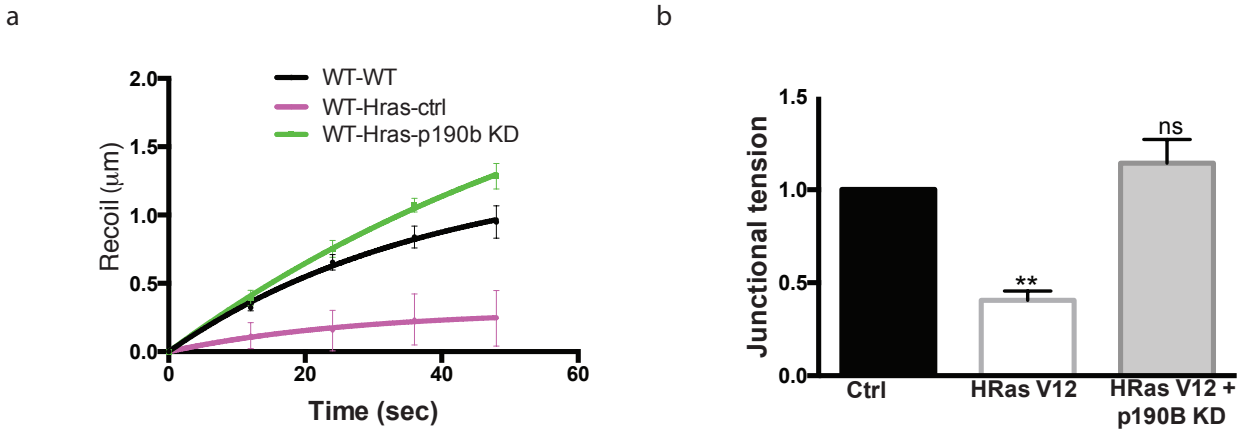

Fig 4.2.3 p190B reduces apical tension at the interface of WT-HRas cells (a) Best-fit single exponential curves of apical junctions recoil (a) and tension (b) at the interface of heterologous contacts in the indicated conditions. Data represent mean ± S.E.M calculated from n = 3 independent experiments; ns, not significant; ∗∗ P < 0.01, Student's t-test.

Since p190B GAP function is crucial for oncogenic extrusion, it indicates that the HRasV12-transfected cells might exploit its activity/localization to decrease Rho activity and thus exhibits reduced apical tension. So, to further dissect this, I aimed to characterize the distribution of p190B GAP and Rho at the heterologous contacts between WT-HRasV12 transfected cells. For this, I performed mosaic expression of HRasV12 in MCF-7 cells monolayer, fixed them and studied for Rho and p190B GAP localization.

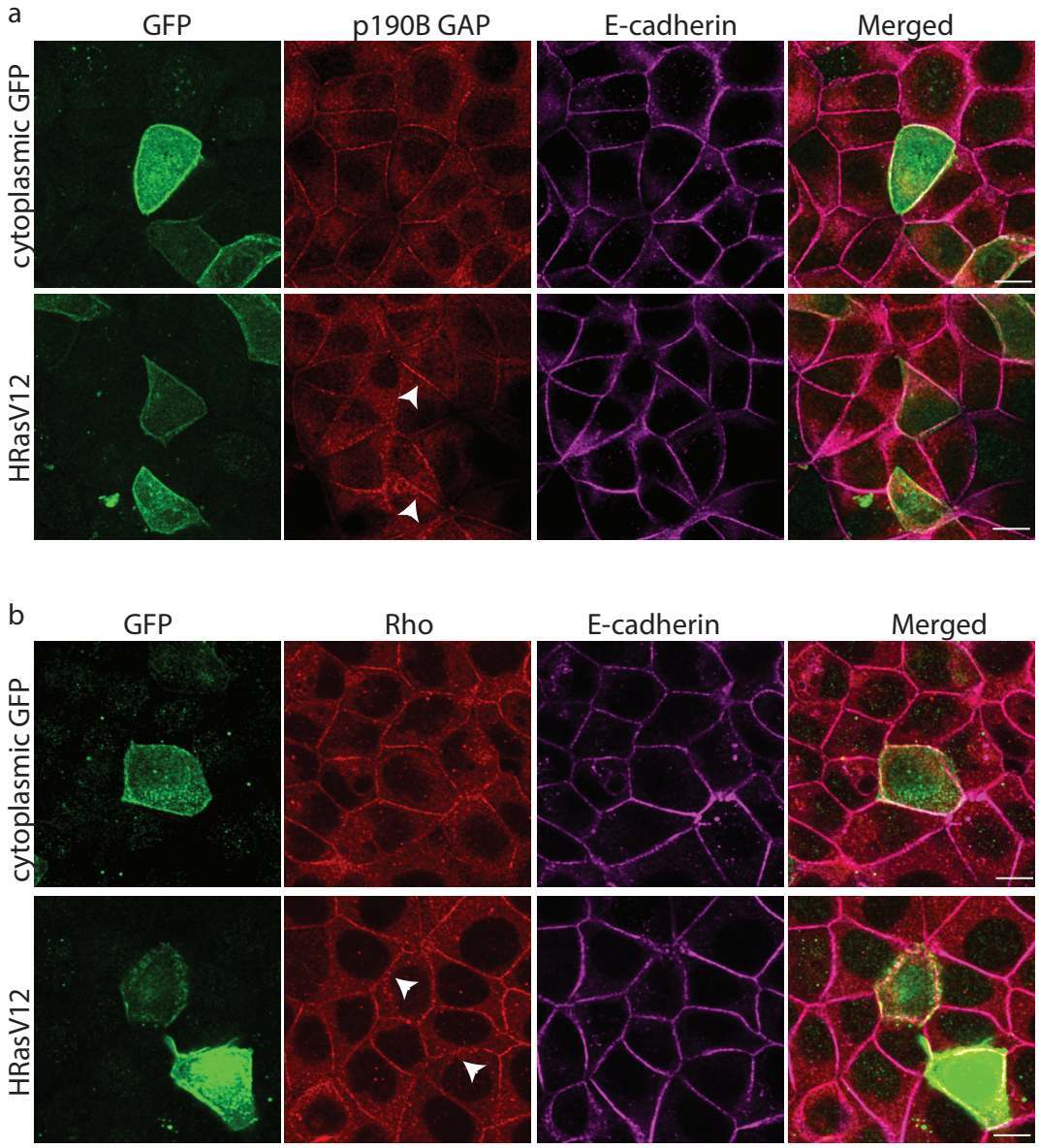

Fig 4.2.4 Rho and p190B GAP localization in the extruding cells. Confluent MCF-7 cells with mosaic expression of GFP only or HRasV12, fixed with methanol and stained for p190B GAP (a) fixed with TCA and stained for Rho along with E-cadherin, and GFP. Scale bar=10 µm

As shown in Fig 4.2.4, preliminary results indicate that at the heterologous contacts, Rho localization appeared to get disrupted (arrows) (Fig 4.2.4 b) and this was accompanied by an increase in the junctional accumulation of p190B GAP (Fig 4.2.4 a). However, the experiment proved to be technically challenging to reproduce the results because of the heterogeneous phenotype of the extruding cells. When studied closely, I found out that the process of HRasV12 oncogenic extrusion in epithelia can be broadly characterized into three stages, and each stage is identified by a distinct shape of the presumptive extruding cell (Fig 4.2.5). The initial stage where the transformed cell is still in monolayer (stage 1); the middle stage in which the HRasV12 cell slightly lifts up from the monolayers and appears to be elongated (stage 2); and finally stage 3,

where the cell is completely extruded from the monolayer. Also, other studies have illustrated that epithelial cells extrusion is a multi-step complex process, with each step exhibiting distinct phenotype (Kuipers et al., 2014)

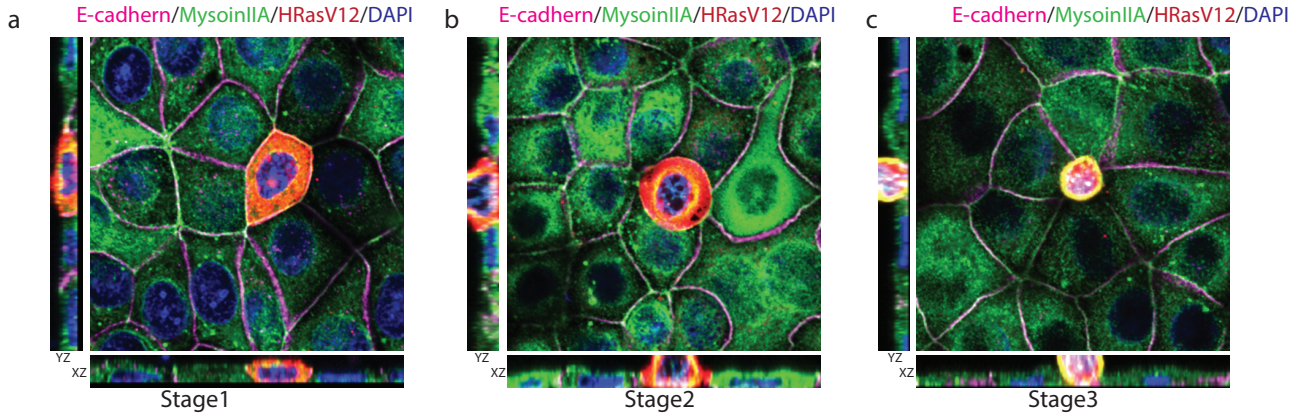

Fig 4.2.5 Different stages of oncogenic extrusion identified in MCF-7 cells. Confluent MCF-7 cells with mosaic expression of HRasV12, fixed with methanol and stained for E-cadherin, Myosin IIA, GFP and DAPI. Representative are confocal images from different stages of extrusion.

It is entirely possible that the component of Rho signaling pathways might get re-distributed only at a certain stage of oncogenic extrusion, but the sheer heterogeneity of the cells makes it hard to isolate that particular stage. Thus to better characterize the modulation of Rho-signaling elements during oncogenic extrusion, it will be useful to exploit an inducible system to control Ras expression, as used by other (Hogan et al., 2009). These are exciting possibilities and are part of on-going work.

4.2.1: References

Bement, W.M., A.L. Miller, and G. von Dassow. 2006. Rho GTPase activity zones and transient contractile arrays. *BioEssays.* 28:983-993.

Bos, J.L., H. Rehmann, and A. Wittinghofer. 2007. GEFs and GAPs: critical elements in the control of small G proteins. *Cell*. 129:865-877.

Braga, V.M., and A.S. Yap. 2005. The challenges of abundance: epithelial junctions and small GTPase signalling. *Curr Opin Cell Biol*. 17:466-474.

Brieher, W.M., and A.S. Yap. 2013. Cadherin junctions and their cytoskeleton(s). *Curr Opin Cell Biol*. 25:39-46.

Brouns, M.R., S.F. Matheson, and J. Settleman. 2001. p190 RhoGAP is the principal Src substrate in brain and regulates axon outgrowth, guidance and fasciculation. *Nat Cell Biol*. 3:361-367.

Burkel, B.M., H.A. Benink, E.M. Vaughan, G. von Dassow, and W.M. Bement. 2012. A Rho GTPase signal treadmill backs a contractile array. *Dev Cell*. 23:384-396.

Bustos, R.I., M.A. Forget, J.E. Settleman, and S.H. Hansen. 2008. Coordination of Rho and Rac GTPase Function via p190B RhoGAP. *Curr Biol*. 18:1606-1611.

Chardin, P. 2006. Function and regulation of Rnd proteins. *Nat Rev Mol Cell Biol*. 7:54-62.

Eisenhoffer, G.T., P.D. Loftus, M. Yoshigi, H. Otsuna, C.B. Chien, P.A. Morcos, and J. Rosenblatt. 2012. Crowding induces live cell extrusion to maintain homeostatic cell numbers in epithelia. *Nature*. 484:546-549.

Eisenhoffer, G.T., and J. Rosenblatt. 2013. Bringing balance by force: live cell extrusion controls epithelial cell numbers. *Trends Cell Biol*. 23:185-192.

Even-Ram, S., A.D. Doyle, M.A. Conti, K. Matsumoto, R.S. Adelstein, and K.M. Yamada. 2007. Myosin IIA regulates cell motility and actomyosin-microtubule crosstalk. *Nat Cell Biol*. 9:299-309.

Ferrell, J.E., Jr. 2002. Self-perpetuating states in signal transduction: positive feedback, double-negative feedback and bistability. *Curr Opin Cell Biol*. 14:140-148.

Gu, Y., and J. Rosenblatt. 2012. New emerging roles for epithelial cell extrusion. *Curr Opin Cell Biol*. 24:865-870.

Guillot, C., and T. Lecuit. 2013. Mechanics of epithelial tissue homeostasis and morphogenesis. *Science*. 340:1185-1189.

Gumbiner, B.M. 2005. Regulation of cadherin-mediated adhesion in morphogenesis. *Nat Rev Mol Cell Bio*. 6:622-634.

Harris, T.J.C., and U. Tepass. 2010. Adherens junctions: from molecules to morphogenesis. *Nat Rev Mol Cell Bio*. 11:502-514.

Hogan, C., S. Dupre-Crochet, M. Norman, M. Kajita, C. Zimmermann, A.E. Pelling, E. Piddini, L.A. Baena-Lopez, J.P. Vincent, Y. Itoh, H. Hosoya, F. Pichaud, and Y. Fujita. 2009. Characterization of the interface between normal and transformed epithelial cells. *Nat Cell Biol*. 11:460-467.

Katoh, H., and Y. Fujita. 2012. Epithelial homeostasis: elimination by live cell extrusion. *Current biology .* 22:R453-455.

Kovacs, E.M., M. Goodwin, R.G. Ali, A.D. Paterson, and A.S. Yap. 2002. Cadherin-directed actin assembly: E-cadherin physically associates with the Arp2/3 complex to direct actin assembly in nascent adhesive contacts. *Current biology* .12:379-382.

Kovacs, E.M., S. Verma, R.G. Ali, A. Ratheesh, N.A. Hamilton, A. Akhmanova, and A.S. Yap. 2011. N-WASP regulates the epithelial junctional actin cytoskeleton through a non-canonical post-nucleation pathway. *Nat Cell Biol*. 13:934-U400.

Kuipers, D., A. Mehonic, M. Kajita, L. Peter, Y. Fujita, T. Duke, G. Charras, and J.E. Gale. 2014. Epithelial repair is a two-stage process driven first by dying cells and then by their neighbours. *Journal of cell science*. 127:1229-1241.

Lee, C.S., C.K. Choi, E.Y. Shin, M.A. Schwartz, and E.G. Kim. 2010. Myosin II directly binds and inhibits Dbl family guanine nucleotide exchange factors: a possible link to Rho family GTPases. *J Cell Biol*. 190:663-674.

Leerberg, J.M., G.A. Gomez, S. Verma, E.J. Moussa, S.K. Wu, R. Priya, B.D. Hoffman, C. Grashoff, M.A. Schwartz, and A.S. Yap. 2014. Tension-Sensitive Actin Assembly Supports Contractility at the Epithelial Zonula Adherens. *Curr Biol*. 24:1689-1699.

Leung, C.T., and J.S. Brugge. 2012. Outgrowth of single oncogene-expressing cells from suppressive epithelial environments. *Nature*. 482:410-413.

McCormack, J., N.J. Welsh, and V.M. Braga. 2013. Cycling around cell-cell adhesion with Rho GTPase regulators. *J Cell Sci*. 126:379-391.

Miller, A.L., and W.M. Bement. 2009. Regulation of cytokinesis by Rho GTPase flux. *Nat Cell Biol*. 11:71-77.

Munjal, A., and T. Lecuit. 2014. Actomyosin networks and tissue morphogenesis. *Development*. 141:1789-1793.

Niessen, C.M., D. Leckband, and A.S. Yap. 2011. Tissue organization by cadherin adhesion molecules: dynamic molecular and cellular mechanisms of morphogenetic regulation. *Physiol Rev*. 91:691-731.

Nishimura, T., and M. Takeichi. 2009. Remodeling of the adherens junctions during morphogenesis. *Current topics in developmental biology*. 89:33-54.

Oinuma, I., K. Kawada, K. Tsukagoshi, and M. Negishi. 2012. Rnd1 and Rnd3 targeting to lipid raft is required for p190 RhoGAP activation. *Mol Biol Cell*. 23:1593-1604.

Piekny, A., M. Werner, and M. Glotzer. 2005. Cytokinesis: welcome to the Rho zone. *Trends Cell Biol*. 15:651-658.

Piekny, A.J., and M. Glotzer. 2008. Anillin is a scaffold protein that links RhoA, actin, and myosin during cytokinesis. *Curr Biol*. 18:30-36.

Priya, R., A.S. Yap, and G.A. Gomez. 2013. E-cadherin supports steady-state Rho signaling at the epithelial zonula adherens. *Differentiation.* 86:133-140.

Ratheesh, A., G.A. Gomez, R. Priya, S. Verma, E.M. Kovacs, K. Jiang, N.H. Brown, A. Akhmanova, S.J. Stehbens, and A.S. Yap. 2012. Centralspindlin and alpha-catenin regulate Rho signalling at the epithelial zonula adherens. *Nat Cell Biol*. 14:818-828.

Ratheesh, A., and A.S. Yap. 2012. A bigger picture: classical cadherins and the dynamic actin cytoskeleton. *Nat Rev Mol Cell Bio*. 13:673-679.

Riento, K., N. Totty, P. Villalonga, R. Garg, R. Guasch, and A.J. Ridley. 2005. RhoE function is regulated by ROCK I-mediated phosphorylation. *Embo Journal*. 24:1170-1180.

Riou, P., S. Kjaer, R. Garg, A. Purkiss, R. George, R.J. Cain, G. Bineva, N. Reymond, B. McColl, A.J. Thompson, N. O'Reilly, N.Q. McDonald, P.J. Parker, and A.J. Ridley. 2013. 14-3-3 proteins interact with a hybrid prenyl-phosphorylation motif to inhibit G proteins. *Cell*. 153:640-653.

Rosenblatt, J., M.C. Raff, and L.P. Cramer. 2001. An epithelial cell destined for apoptosis signals its neighbors to extrude it by an actin- and myosin-dependent mechanism. *Current biology .* 11:1847-1857.

Schock, F., and N. Perrimon. 2002. Molecular mechanisms of epithelial morphogenesis. *Annu Rev Cell Dev Biol*. 18:463-493.

Shewan, A.M., M. Maddugoda, A. Kraemer, S.J. Stehbens, S. Verma, E.M. Kovacs, and A.S. Yap. 2005. Myosin 2 is a key Rho kinase target necessary for the local concentration of E-cadherin at cell-cell contacts. *Mol Biol Cell*. 16:4531-4542.

Slattum, G., K.M. McGee, and J. Rosenblatt. 2009. P115 RhoGEF and microtubules decide the direction apoptotic cells extrude from an epithelium. *J Cell Biol*. 186:693-702.

Smith, A.L., M.R. Dohn, M.V. Brown, and A.B. Reynolds. 2012. Association of Rho-associated protein kinase 1 with E-cadherin complexes is mediated by p120-catenin. *Mol Biol Cell*. 23:99-110.

Smutny, M., H.L. Cox, J.M. Leerberg, E.M. Kovacs, M.A. Conti, C. Ferguson, N.A. Hamilton, R.G. Parton, R.S. Adelstein, and A.S. Yap. 2010. Myosin II isoforms identify distinct functional modules that support integrity of the epithelial zonula adherens. *Nat Cell Biol*. 12:696-702.

Smutny, M., S.K. Wu, G.A. Gomez, S. Mangold, A.S. Yap, and N.A. Hamilton. 2011. Multicomponent analysis of junctional movements regulated by myosin II isoforms at the epithelial zonula adherens. *PLoS One*. 6:e22458.

Takeichi, M. 2014. Dynamic contacts: rearranging adherens junctions to drive epithelial remodelling. *Nat Rev Mol Cell Biol*. 15:397-410.

Tse, Y.C., M. Werner, K.M. Longhini, J.C. Labbe, B. Goldstein, and M. Glotzer. 2012. RhoA activation during polarization and cytokinesis of the early Caenorhabditis elegans embryo is differentially dependent on NOP-1 and CYK-4. *Mol Biol Cell*. 23:4020-4031.

Wennerberg, K., M.A. Forget, S.M. Ellerbroek, W.T. Arthur, K. Burridge, J. Settleman, C.J. Der, and S.H. Hansen. 2003. Rnd proteins function as RhoA antagonists by activating p190 RhoGAP. *Curr Biol*. 13:1106-1115.

Wolfe, B.A., and M. Glotzer. 2009. Single cells (put a ring on it). *Genes Dev*. 23:896-901.

Wu, M.H., Y.A. Chen, H.H. Chen, K.W. Chang, I.S. Chang, L.H. Wang, and H.L. Hsu. 2014a. MCT-1 expression and PTEN deficiency synergistically promote neoplastic multinucleation through the Src/p190B signaling activation. *Oncogene*. 33(43):5109-20

Wu, S.K., G.A. Gomez, M. Michael, S. Verma, H.L. Cox, J.G. Lefevre, R.G. Parton, N.A. Hamilton, Z. Neufeld, and A.S. Yap. 2014b. Cortical F-actin stabilization generates apical-lateral patterns of junctional contractility that integrate cells into epithelia. *Nat Cell Biol*. 16:167-178.

Yuce, O., A. Piekny, and M. Glotzer. 2005. An ECT2-centralspindlin complex regulates the localization and function of RhoA. *J Cell Biol*. 170:571-582.

Chapter 5: Discussion and Future Implications

Epithelial cells are tightly interlinked to each other via specialized adhesive structures called intercellular junctions. These junctions can display the dual properties of plasticity and stability: at steady state they provide strong cohesive strength to the cells, while during morphogenetic events, they transform into highly dynamic entities (Takeichi, 2014; Niessen et al., 2011). This enables epithelia to adopt various shapes and sizes and undergo extensive rearrangement like bending and constriction (Guillot and Lecuit, 2013; Takeichi, 2014). The adherens junction is a prominent feature of many epithelia. It is a cadherin-based cell-cell adhesion junction, supported by an extensive actomyosin network. At the apical zone of the cells, it organizes itself into a tight ring like structure, referred as the zonula adherens (ZA). This ring-like structure of the ZA accumulates dense clusters of E-cadherin decorating the actomyosin cables (Meng and Takeichi, 2009; Takeichi, 2014). The intracellular domain of E-cadherin associates with this actomyosin network via linkers like α-catenin (Meng and Takeichi, 2009; Takeichi, 2014). This actomyosin network is an intrinsically dynamic highly contractile structure, which acts in concert with the E-cadherin complex to dictate various morphogenetic events (Brieher and Yap, 2013; Guillot and Lecuit, 2013; Munjal and Lecuit, 2014). The coordinated action of ZA and actomyosin network in response to developmental cues is an outcome of many signaling events, primarily modulated by a class of powerful molecular switches called Rho GTPases (Braga and Yap, 2005; McCormack et al., 2013; Niessen et al., 2011; Ratheesh et al., 2013; Ratheesh and Yap, 2012).

Rho GTPases are master regulators of cell physiology which, depending on the cellular context, are capable of fine-tuning their activity in a defined spatio-temporal manner (McCormack et al., 2013; Ratheesh et al., 2013). This is facilitated by a subset of upstream regulators: GEFs promote the exchange of GDP to GTP thus activating Rho; GAPs inactivate Rho by catalyzing the GTP hydrolysis; and GDIs sequester the GDP-bound Rho. Once activated, they initiate actomyosin remodeling via downstream effectors like ROCK and formins, which ultimately translate into a relevant biological outcome like migration, epithelial polarity or sustained adhesion (Bishop and Hall, 2000; Etienne-Manneville and Hall, 2002; Jaffe and Hall, 2005). Indeed, Rho GTPases have been shown to influence almost every aspect of junctional biogenesis; e.g. formation, maturation and disassembly (McCormack et al., 2013).

We have come a long way since the initial studies suggesting that Rho GTPases support cadherin-junctions. However, cadherin junction assembly and maintenance is a multi-step complex process,

utilizing a plethora of cytoskeletal regulators, not all of which respond to the same GTPase. Also, complexity lies in the fact that the same GTPase at a given point in time can coordinate opposing cellular processes by switching its activation state, by indulging in cross-talk or by exploiting different downstream effectors, depending on the cellular context (Braga and Yap, 2005; McCormack et al., 2013; Niessen et al., 2011; Ratheesh et al., 2013). The challenge lies in understanding how these multiple events are organized to ensure physiological interplay between cadherin and Rho.

The work presented here aimed to address some of the above issues by unraveling very basic important questions pertaining to Rho signaling at junctions: how Rho GTPase supports cadherin junctions and what are the upstream factors required to maintain this GTPase cycle. Accordingly, I have dissected the precise molecular pathways by which RhoA supports the overall architecture of ZA and maintains junctional tension (Research chapter 2). Also, I have documented that E-cadherin facilitates junctional Rho activity by orchestrating the upstream Rho activators: ECT2 and centralspindlin complex (Research chapter 3). Finally, I have identified a novel feedback regulation anchored via ROCK and myosin-IIA; which ensures sustained production of GTP-Rho, thus ensuring the robustness of junctional Rho signaling (Research chapter 4). These findings advance our understanding of the interplay between Rho GTPase and cadherin junctions.

In this chapter, I will discuss my research findings pertaining to each chapter in detail, with a perspective on existing literature and the future implications

5.1 A novel role for Rho-GEF ECT2: from cell-division to cell-adhesion

The last two decades has seen an increasing number of studies that outline the significance of Rho GTPases for epithelial integrity and junctional biology in various model systems (Ratheesh et al., 2012; Simoes Sde et al., 2014; Smith et al., 2012; Smutny et al., 2011; Terry et al., 2011). Despite that, a great deal of knowledge is lacking about the upstream regulatory elements and downstream pathways, which determine the outcome of junctional Rho signaling.

Given the above literature, I aimed to precisely dissect the functional impact of Rho signaling on the zonula adherens (Research chapter 2). By the time that I embarked upon these studies, preliminary data in the laboratory had already strongly suggested that ECT2 might be the relevant GEF for Rho at ZA. However, this was not a mainstream observation in the literature. Instead, multiple studies had confirmed its role as a Rho-GEF at the cytokinetic furrow and suggest that it

principally localizes in the nucleus during interphase and is found at the cortex only during cell division (Fields and Justilien, 2010; Hara et al., 2006; Yuce et al., 2005).

So, I started with characterizing the location of ECT2 in monolayers of breast epithelial cells during interphase. Using immunofluorescence and live-cell imaging, I observed that ECT2 does get recruited to junctions, along with a prominent nuclear localization. This was in contrary to previous reports suggesting that ECT2 exclusively resides in the nucleus during interphase. The discrepancy can be because most of those studies were done on single cells or embryos and not on the monolayer of cells. Indeed, others have also reported junctional association of ECT2 (Liu et al., 2004) Also, the fact that ECT2 harbors a PH domain known to have affinity for membrane-lipids, suggested that it might directly associate with plasma-membrane, as shown elsewhere (Chalamalasetty et al., 2006; Su et al., 2011).

Further by using a lentivirus mediated knockdown approach, I demonstrated that ECT2 depletion led to the dispersion of E-cadherin at the apical zone of the cells and a significant reduction in the junctional cadherin staining. Also, I measured FRAP of GFP E-cadherin and found out that ECT2 depletion or treating the cells with a pharmacological inhibitor of Rho led to significant reduction in the mobile fraction and half-time of recovery, indicating faster turnover of apical E-cadherin. Thus, Rho-ECT2 signaling maintains the stability of cadherin at apical junctions. These deleterious effects of ECT2 KD on the ZA were mediated specifically by myosin IIA (not by IIB), as junctional actin and myosin IIB remain unperturbed in these cells. ECT2 KD led to reduction in junctional myosin IIA and GFP-myosin IIA could rescue the E-cad phenotype. Also, depletion of myosin IIA led to destabilization of E-cadherin as assessed by FRAP. Of note, the effect of ECT2 KD on ZA was very much similar to myosin IIA KD (Smutny et al., 2010). These results indicate that ECT2 support cadherin organization by indirectly recruiting myosin IIA at the ZA via activation of Rho. Myosin IIA then supports E-cadherin clustering and stabilization. This is in agreement with previous findings from our lab suggesting that the Rho-ROCK pathway supports ZA integrity by specifically regulating junctional myosin IIA localization while myosin IIB is modulated by Rap1 GTPase. (Shewan et al., 2005; Smutny et al., 2010).

Strikingly, in these studies, inhibition of Rho activity by ECT2 depletion perturbed the ZA, but not tight junctions. However, Rho GTPases have been implicated in the organization of tight junctions (McCormack et al., 2013; Terry et al., 2011). This discrepancy can be explained by the increasingly evident notion that Rho GTPases can modulate specific junctions by exploiting unique upstream activators, in this case GEFs. Indeed, Terry *et al* have shown that p114 Rho GEF is required for

tight junction assembly and its barrier function by activating Rho. Junctional protein cingulin directs the association of p114 Rho GEF with tight junctions and loss of p114 Rho GEF led to warped staining of ZO-1 without affecting adherens junctions (Terry et al., 2011). In contrast to this, ECT2 associates with α-catenin to localize specifically at zonula adherens and support its functions, with insignificant impact on tight junctions (Ratheesh and Yap, 2012). Thus, these finding contribute to the growing understanding that a common Rho GTPase can exploit the action of specific GEFs to generate a spatially restricted Rho signaling and functional outcomes.

Myosin, along with actin, generates tensile forces at the cell junctions, which act in concert with cadherin to modulate epithelial patterning during disease and development (Gomez et al., 2011). Since ECT2 depletion led to the loss of cortical myosin IIA, I questioned whether the ECT2-Rho pathway affects junctional tension. Indeed, using a femtosecond laser to cut the junctions and measuring instantaneous recoil as a measure of tension, I have demonstrated that an active ECT2-Rho signaling is required to maintain functional tension. Depletion of ECT2 or its downstream target by C3-T or myosin RNAi led to significant reductions in tension.

Further, using a 3-dimensional cyst culture that allows formation of polarized cysts, I have shown that ECT2 is required for morphogenesis. As compared to controls, Caco2 cells depleted of ECT2 were unable to form fully formed cysts with proper lumen in the center. Also, E-cadherin organization in these structures was grossly disrupted with less concentration at the junctions. This suggests that the Rho-ECT2 pathway is indeed required for cadherin organization in a more physiologically relevant model like cyst culture. ECT2 has been implicated in establishing epithelial polarity by interacting with Par6/Par3 complex (Liu et al., 2004; Liu et al., 2006), but interestingly I could not observe any dominant alteration in polarity upon ECT2 depletion in Caco2 cells. This inconsistency can be explained by the type of model system used (MDCK vs CaCO2) and the kind of maneuver used. Liu *et al* relied on the use of dominant negative and constitutively forms of ECT2 (compare to the shRNA mediated knockdown of ECT2 employed here) for their studies, which has its own limitation of off-target effects and bypassing the endogenous regulatory mechanisms. Nonetheless, both studies speak to the argument that ECT2 supports morphogenesis in 3-D cyst cultures, probably via different pathways depending on the cellular context. Due to the limited time frame of my thesis, I was not able to expand more on the cyst-study, but it remains an exciting possibility in the future.

Overall, these results have identified a novel role for Rho-GEF ECT2 out of the ‘small cytokinetic window’. Multiple studies have established its importance as a Rho-GEF for cell division. But the

work presented here suggests that ECT2 is essential for the overall architecture and function of ZA in tinterphase epithelial cells. I have demonstrated that ECT2 specifically localizes to ZA and signals to myosin IIA (the downstream effector of Rho) to support ZA integrity and junctional tension.

With this perspective, an important issue is what determines ECT2 localization at the ZA? Our lab has shown that α-catenin can act as a cortical anchor for MgcRacGAP (upstream activator of ECT2), thereby supporting ECT2 junctional association. However, α-catenin extensively co-localizes with E-cadherin throughout the lateral surface of the cell, while ECT2 localization was found to be mostly apical. This suggests that alternate mechanisms might exist to spatially restrict ECT2 at the apical junctions. One of the most favorable candidates is Anillin, a multidomain protein that acts as an anchor to orchestrate Rho-signaling during cell-division (Piekny and Maddox, 2010). It was initially identified as an actin-binding protein and has been shown to regulate the localization of ECT2, CS, myosin and Rho, almost all the components of the junctional Rho-pathway during cell-division. Whether Anillin regulates ECT2 localization at junctions remains an interesting question.

Also, at steady-state ECT2 remains in an inactive auto-inhibited form by interaction of its c-terminus with N-terminus. During cytokinesis, binding to MgcRacGAP relieves this in a phosphorylation dependent manner (discussed in detail in section 1.8.2). We still don't know whether some of these modifications are relevant for ECT2 activity at junctions. This will require the identification of junctional ECT2 modifications by exploiting phospho-specific antibodies. Also, kinases like CDK1 and Plk1 control the GEF activity/localization of ECT2 during cell division. Since these kinases are very tightly regulated in a cell-cycle dependent manner, this warrants the search for 'new' regulator of ECT2 phosphorylation in interphase cells.

5.2 E-cadherin and Rho signaling: a reciprocal interaction

Cadherin based junctions are required to maintain the overall integrity of epithelial tissue. They regulate a variety of cellular processes like establishment of polarity, junctional biogenesis, cell sorting, and tissue formation (Brieher and Yap, 2013). Given these varied and profound outcomes, a key issue has been to understand how classical cadherins exert these functions. Indeed, cadherin-based receptors have been established to act as a spot for the convergence of various signal transduction pathways (Braga, 2002; Niessen et al., 2011; Wheelock and Johnson, 2003; Yap and

Kovacs, 2003). By virtue of being adhesion receptors, they can directly initiate signaling reactions by homophilic ligation of cadherin ectodomain or drive juxtacrine signaling by bringing two plasma-membranes together. The signaling pathways emanating from cadherin-based junctions involve kinases (e.g Src, MAPK) and Wnt signaling and Rho family GTPases.

Rho GTPases are known to influence cadherin-based junctions. Interestingly, cadherins also can modulate the spatiotemporal activity and localization of these GTPases (Braga and Yap, 2005; Wheelock and Johnson, 2003). This functional cooperativity enables these junctions to modulate a variety of cellular processes and thus needs to be understood in detail. So, using a combination of lentivirus mediated knockdown and rescue approaches, I aimed to address the impact of E-cadherin on GTP-Rho at junctions (Research chapter 3).

In breast epithelial monolayers (MCF-7), depletion of cadherin displaces Rho from junctions, which can be restored by expression of a RNAi resistant GFP-E-cadherin. Of note, in a recent publication we have shown that treating with pharmacological inhibitor C3-T significantly reduced the amount of junctions Rho, implying that junctional Rho staining can be used as proxy for its activity (Ratheesh et al., 2012). Given this, my observation hints that E-cadherin supports GTP-Rho. In fact, using an activity-based Rho FRET biosensor, I found that cadherin depletion leads to loss of junctional Rho activity. How could cadherin support Rho GTPase? One immediate hypothesis will be by modulating its upstream regulators, GEF or GAP, as these molecules are largely responsible for the activity state of Rho. Indeed, cadherin depletion led to the loss of junctional Rho-GEF ECT2 and its upstream activator centralspindlin complex. Further, in all these maneuvers cell-cell contacts remained intact as identified by ZO-1 staining, suggesting that the Rho signaling at junctions require the presence of cadherins.

Strikingly, the findings reported here contrast with the earlier observation where it was shown that the assembly of cadherin junctions suppress Rho signaling while triggering Rac1 and Cdc42 (Noren et al., 2001). However, the discrepancy in the outcomes can by explained by the fact that the experimental maneuvers employed by those study are different from ours. Noren *et al* used acute methods like calcium switch and 'artificial' cadherin ligation (which broadly mimics 'de novo' junction assembly), while our studies were performed on steady-state mature junctions. Noren *et al* further proved that cadherin engagement dampens Rho signaling by the activation of p190RhoGAP (Noren et al., 2003). Rac GTPase, in response to cadherin signaling, has been shown to trigger p190RhoGAP activity and its localization at ZA via p120 catenin (Wildenberg et al., 2006). However a recent study from our lab indicates that at steady-state ZA, α-catenin can anchor

centralspindlin, which inhibits Rac activity and prevents p190BRhoGAP from junctional association (Ratheesh et al., 2012). These conflicting observations highlight the complexity of Rho signaling and strengthen the notion that a common GTPase can exist in alternate states by utilizing different effectors during various stages of junctional biogenesis (in this case formation vs. maintenance).

Further to this, careful analysis of Rho localization at junctions revealed that apart from its distribution at the lateral cell surface, it selectively concentrates with cadherins at the ZA. Also, ECT2 and centralspindlin showed preferential localization at the apical junctions. What is the functional relevance of this 'restricted' Rho zone at ZA? I hypothesized that this spatially constrained zone of Rho signaling locally activates its downstream effectors (e.g. myosin IIA) and generates high concentration of cadherin at the apical zone (vs. lateral), thus generating the ZA. By performing FRAP studies on the apical vs. lateral pool of GFP-E-cadherin, I observed that indeed these two pools of cadherin are distinct and show different recovery patterns. Apical E-cadherin recovered to a lesser extent, with a low speed of recovery while basal E-cadherin recovered to greater extent and the recovery speed was higher than the apical (as reflected in the half time and mobile fraction values). This was a very intriguing novel observation, which suggests that E-cadherin organizes itself into two differentially stabilized pools. Strikingly, these regional differences in the apical vs. lateral pool of cadherin was largely abolished when Rho signalling was perturbed by various maneuver; by inhibiting GTP-Rho, by deleting upstream activator ECT2 or by removing the downstream effector myosin IIA. These results affirm that local activation of myosin IIA via ECT2-Rho pathways is necessary to generate a stabilized and restricted pool of cadherin at the apical zone, referred as ZA.

Recently we have shown that the cadherin-catenin complex can biochemically associate with upstream Rho regulators like ECT2 and centralspindlin as they were found to be present in the same complex (Ratheesh et al., 2012). This led me to ask that can E-cadherin directly influence the recruitment of Rho and its upstream activator at the ZA? I attempted to address this issue by exploiting 'receptor-clustering' mechanism. For this I used a fusion protein consisting of the IL2 receptor α-subunit ectodomain (also called TAC) fused to the transmembrane and cytoplasmic domains of E-cadherin (Miranda et al., 2001) and induced E-cadherin clustering using TAC antibody. However, the results were not conclusive as the experiment had many technical limitations, mostly pertaining to the fixation methods used for Rho and ECT2. Due to the time-constraints of my candidature, I was not able to further trouble-shoot this experiment, but it remains an exciting possibility for the future.

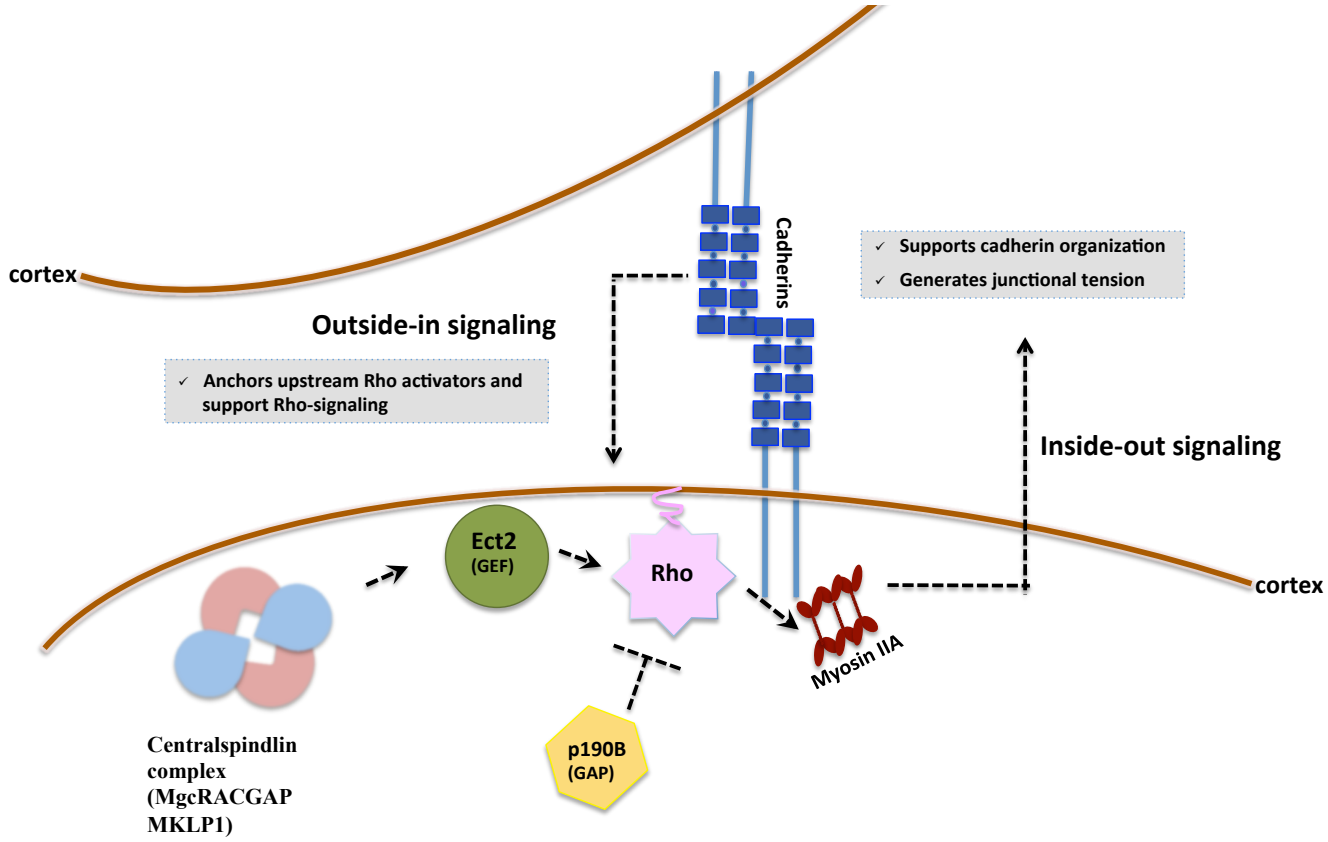

Fig 5.1 Signaling nexus between Rho and E-cadherin at epithelial zonula adherens. ECT2-Rho mediated activation of myosin IIA leads to cadherin clustering, stabilization and generates junctional tension. In-turn E-cadherin anchors upstream Rho activators ECT2 and centralspindlin to maintain the GTPase cycle.

Overall, the findings presented here speak to the notion that cadherins and Rho GTPase interacts cooperatively to generate a signaling nexus comprised of 'inside-out' signaling (e.g. Rho GTPase supports adhesion by modulating actomyosin cytoskeleton) and 'out-side-in' signaling (cadherins influence spatiotemporal activity of Rho GTPase) (Fig 5.1).

5.3 A myosin-mediated feedback loop ensure robustness of junctional Rho signaling

The work presented in the first two research chapters establishes that the ZA can be defined as a spatially confined zone of high Rho activity. Here, the Rho GEF ECT2 act in concert with centralspindlin to ensures proper activation of Rho (Priya et al., 2013; Ratheesh et al., 2012). Since Rho GTPases are implicated in myriad cellular functions, their activity should be tightly controlled in a precise spatio-temporal fashion. Indeed, it is increasingly becoming apparent that Rho-GTPase signaling is a multi-faceted event, which requires the co-ordination of various regulatory elements (apart from the classical GEF-GAP pathway) to produce a relevant biological response (Bement et al., 2006; Guilluy et al., 2011; McCormack et al., 2013). However, we still do not know what are these precise circuitry elements that generate an integrated picture of Rho signaling. Accordingly, in this study, I aimed to dissect the molecular components required to confine and strengthen Rho signaling at the epithelial zonula adherens (ZA).

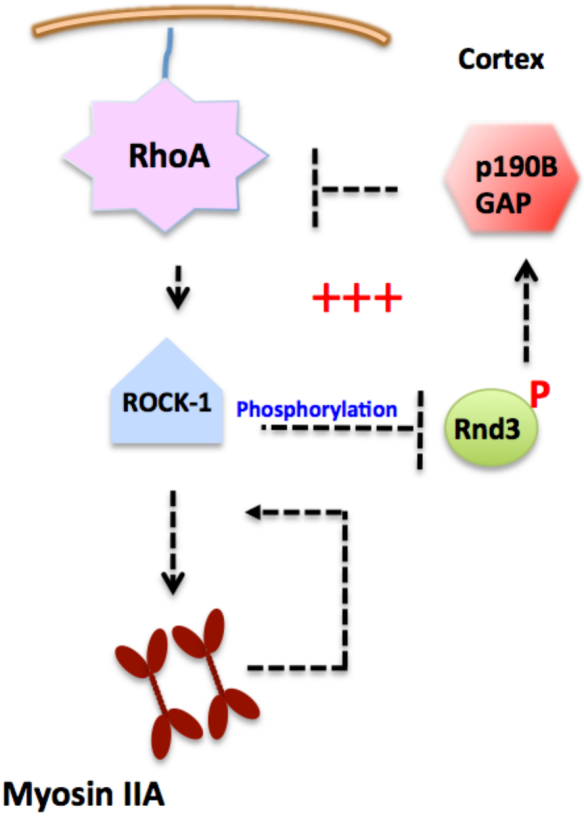

Fig 5.2 Myosin-ROCK feedback loop sustains junctional GTP-Rho.

Once GTP loaded, Rho mediates its biological functions via various effector proteins (Bustelo et al., 2007). Previously, we identified non-muscle myosin IIA (NMIIA) as a downstream target of Rho at the epithelial zonula adherens (Shewan et al., 2005; Smutny et al., 2010). NMIIA along with actin forms the contractile actomyosin network and is the prime modulator of cellular processes involving mechanical forces and tension (Gomez et al., 2011; Munjal and Lecuit, 2014; Vicente-Manzanares et al., 2009). Accordingly, in this chapter I have proposed that myosin itself can act to orchestrate a feedback loop that is required to maintain GTP-Rho levels at ZA. This is achieved by two interlocking feedback loops intersecting at ROCK-1. In the first loop, ROCK-1 supports Rho by inhibiting the junctional association of the Rho-antagonist Rnd3, which thus prevents the GAP,

p190B, from localizing to junctions. In the second loop, myosin localizes ROCK-1 to the ZA via its rod domain (Fig 5.2). Together, this whole cascade ensures that Rho-zone at the ZA remains spatially focused and stable over time.

My studies reveal that myosin inhibition/depletion leads to a significant reduction in junctional Rho localization by enriching the GAP, p190B at the ZA. As Rho protein extensively distributes throughput the lateral junctions and the apical pole of the cells, to better characterize GTP-Rho distribution I used a GFP-AHPH location Rho-biosensor (obtained from the c-terminus of anillin) (Piekny and Glotzer, 2008; Tse et al., 2012).This showed a prominent concentration as a sharp band at the ZA and indeed, this was the most evident location of the biosensor in cells. Myosin inhibition led to an extensive redistribution of the GTP-Rho over the apical pole of the cells, and along with junctional Rho staining, this could also be restored by p190B GAP depletion. This implies that myosin is required to concentrate GTP-Rho zone at junctions by inhibiting the localization of p190B GAP. Further, I have found that Rnd3 is required to localize p190B GAP (and thus inhibit Rho) in a phosphorylation dependent manner. A phospho-deficient mutant of Rnd3 constitutively localizes to junctions and prevents Rho from signaling by constitutively recruiting p190B to junctions. This phosphorylation of Rnd3 is mediated by ROCK-1, as inhibition of ROCK-1 led to the loss of Rnd3 phosphorylation and induced its junctional association. This implies that in steady state, ROCK-1 prevents Rnd3 junctional localization by phosphorylating it, and thus supports GTP-Rho levels. Lastly, I found that myosin contributes to junctional GTP-Rho by scaffolding ROCK-1 at epithelial cadherin junctions, independent of its head-domain functions. In summary, the results presented here identify a novel feedback loop anchored via myosin IIA required to sustain and define GTP-Rho at cadherin junctions.

Previously we reported that blocking microtubules (MT) dynamics led to increased junctional association of p190B GAP via the Rac GTPase(Ratheesh et al., 2012). At cadherin junctions, MgcRacGAP blocks Rac activity and thus prevents p190B GAP recruitment. Blocking MT dynamics by nocodazole perturbed MgcRacGAP localization, thus activating Rac and inducing p190B localization (Ratheesh et al., 2012). However, Rac GTPase does not seem to affect p190B junctional localization when myosin was displaced from junctions. In fact, myosin relies on the action of another GTPase: Rnd3 to modulate p190B GAP localization. Rnd3 has been shown to act as a Rho antagonist in various systems (Riento et al., 2003; Wennerberg et al., 2003) and stimulates the GAP activity of p190B *in vitro* (Wennerberg et al., 2003). Of note, Rac needs to be activated for localizing p190B (Bustos et al., 2008), and we have reported previously that blocking MT dynamics by nocodazole leads to enhanced Rac activity and thus enables Rac to localize p190B at the ZA

(Ratheesh et al., 2012). However, I didn't observe any increase in Rac activity or localization when myosin was inhibited or depleted, thus further confirming the notion that Rac does not mediate the cross-talk between myosin II and p190B Rho GAP. Also, unlike nocodazole, blebbistatin didn't affect MgcRacGAP localization and thus Rac activity was not changed. Overall, these current findings agree with our earlier observations that to sustain GTP-Rho levels, p190B junctional localization should be prevented. How might Rac and Rnd3 co-ordinate at cadherin junctions to regulate p190B localization? I don't have any data to suggest that Rac and Rnd3 independently modulate p190B GAP localization. The fact that both Rac and Rnd3 bind to the middle domain of p190B makes it difficult to isolate the effect of the two GTPases (Bustos et al., 2008).Also, this might be a reflection of the differential upstream regulation of these GTPases; extended analysis of p190B Rho GAP binding with Rac1 and Rnd3 will be needed in the future to resolve this issue. However, these distinct regulatory effects of Rac and Rnd 3 suggest that p190B constitutes a key point of integration – i.e. it can respond to several important upstream signals to repress Rho signaling.

I have illustrated that ROCK-1 supports Rho signaling at epithelial cadherin junctions by phosphorylating and thus inhibiting another small GTPase Rnd3. Cross-talk between small GTPases is a fundamental process behind regulation of various cellular functions and mostly happens on the level of activity, expression levels or downstream signaling (Boulter et al., 2012; Guilluy et al., 2011).Rnd proteins (basically Rnd1 and Rnd3) have been shown to affect cell morphology by antagonizing Rho, either via activating the GAP p190 or by inhibiting the ROCK-1 (Riento et al., 2003; Wennerberg et al., 2003).I could not see any effect on p190B localization when Rnd1 was depleted, thus indicating the prevalent contribution of Rnd3 for p190B localization. Also, p190b recruitment seems to be the favored mode of Rho inhibition as Rnd3 depletion did not affect ROCK-1 localization.

Interestingly, the results presented here identify that NMIIA (and not NMIIB) supports GTP-Rho zone at ZA. This is in accordance with our previous findings that the junctional accumulation of NMIIA responds to Rho signaling while Rap1 is the upstream regulator for NMIIB (Smutny et al., 2010).Further, ROCK-1 junctional association was sensitive to the loss of NMIIA but not NMIIB and only NMIIA was found to be present in the immunoprecipitates of ROCK-1, suggesting that NMIIA selectively can scaffold ROCK-1 at cadherin junctions. Although I cannot ignore the fact that these two paralogues are differentially expressed inside MCF-7 cells (Smutny et al., 2010),still the findings reported here complement the growing idea that despite sharing significant sequence similarity, NMII paralogues exhibit unique functions and can be subjected to distinct upstream

regulatory pathways (Betapudi, 2010; Sandquist and Means, 2008; Smutny et al., 2010; Wang et al., 2009).

Indeed, its been shown in other systems that ROCK kinase can specifically regulate phosphorylation of NMIIA, rather than NMIIB and ROCK inhibition phenotype is exactly similar to NMIIA (but not NMIIB) depletion (Sandquist et al., 2006). How is this achieved, considering that both NMII isoforms share the same regulatory light chain (RLC)? Based on our current findings, one can envisage that once activated, ROCK-1 can induce similar levels of phosphorylation on NMIIA and NMIIB associated RLC, but NMIIA-RLC phosphorylation would be greatly enhanced as NMIIA specifically can bind and scaffold ROCK-1. Further to this, the rod domain of NMIIA has been implicated in these isoform specific functions, mostly because it exhibits greater dissimilarity in sequence between different paralogues (Conti and Adelstein, 2008; Heissler and Manstein, 2013; Vicente-Manzanares et al., 2009); can harbour unique regulatory modifications like phosphorylation (Rosenberg and Ravid, 2006) and has been shown to mediate interactions with exclusive binding partners (Li and Bresnick, 2006). Indeed, I also found out that the rod domain of NMIIA was capable of mediating junctional localization of ROCK-1, thus reinforcing the idea that the rod domain contributes to paralogue -specific functions.

Also, it's worth mentioning here that these findings argue for a novel regulatory feature of myosin. The conventional wisdom considers myosin as a motor-protein, which binds to filamentous actin and generates forces/contractile structures. However, there have been few studies recently speculating that it also contributes to signaling cascades (Conti and Adelstein, 2008; Kuo et al., 2011; Lee et al., 2010; Shin et al., 2014), but the detailed mechanistic details have been missing. The results presented here illustrate an active role of myosin in sustaining junctional Rho signaling by localizing ROCK-1 at apical cadherin junctions and thus mediating a feedback loop leading to the inhibition of GAP.

Intriguingly, while ROCK-1 localized specifically at apical cadherin junctions, myosin is also present elsewhere in the cells apart from at the ZA, including an extensive distribution throughout the lateral surface of the cells (Wu et al., 2014). How then can then myosin spatially recruit ROCK-1 at the apical junctions, when it is present so extensively? Further study will be necessary to answer this question. One possibility might be that the stability of myosin differs in the apical vs. lateral junctions. Interestingly, apical cadherin junctions exhibit significantly higher contractile tension (Wu et al., 2014)and accumulate a stable, immobile pool of E-cadherin locally (Priya et al., 2013)as compared to the lateral cadherin junctions. This fits well with the presumption that a

steady-stable pool of myosin at apical junctions will be more efficient in generating high tension locally and concentrating E-cadherin at these sites. I have not tested these ideas experimentally, but it does predict that at apical cadherin junctions, myosin might be stabilized and thus can bind and recruit ROCK-1 much more efficiently. This leads to a localized accumulation of ROCK-1 at the ZA, which by inhibiting p190B, leads to the formation of a sharp active zone of Rho.

GTP-Rho zones have been implicated in various physiological processes like wound-healing and cytokinesis (Bement et al., 2006; Benink and Bement, 2005; Piekny et al., 2005; Simon et al., 2013). The focusing and stabilization of these zones have been shown to depend on the anchoring functions of actin filaments, and a proper balance of GEF and GAP activity to maintain the GTPase flux and GTPase cross-talk (Benink and Bement, 2005; Miller and Bement, 2009; Miller et al., 2008). Strikingly, using the GFP-AHPH location Rho biosensor, we could visualize a highly concentrated, stable zone of GTP-Rho at the apical junctions of interphase epithelial cells, which persisted for tens of minutes. Earlier, we identified that the Rho GEF ECT2 pool at the ZA is highly dynamic with a half time of ~3-4 seconds, indicating the transient nature of its junctional association (Ratheesh et al., 2012). Such a short-lived interaction won't be able to generate a persistent zone of active Rho at ZA, thus warranting the need of other mechanisms.

Indeed, this study reveals that myosin IIA; the downstream effector of Rho sustains and spatially restrains the Rho zone at epithelial cadherin junctions. NMIIA functions as a signaling module, which acts by antagonizing the localization of p190B GAP at the ZA. This helps in sustaining the active Rho by increasing its lifetime. The intrinsic GTP-hydrolysis half-time of Rho is ~ 30 minutes, which is reduced to ~ 0.4 seconds by the GAP activity of p190B (Zhang and Zheng, 1998). This implies that in the absence of p190B GAP activity, half-time of GTP-Rho will increase to 30 minutes and thus produces a stable GTP-Rho zone. Though the possibility that other GAPs might be functional at the ZA cannot be excluded, the data presented here suggest that p190B GAP is the prominent GAP inhibiting Rho when NMIIA was depleted. This asserts the significance of inhibiting p190B GAP localization via myosin II to sustain GTP-Rho zone at the ZA.

This pathway also identifies the contribution of Rho-Rnd3 cross talk in focusing the Rho-zone at the ZA. Further, myosin/ROCK depletion led to the loss of Rho activity, as assessed by FRET biosensor and localization studies. Of note, in a recent paper by Reyes et al, it was shown that depleting Anillin, a protein known to anchor/activate Rho and its regulators during cytokinesis, led to the broadening of the Rho-zone at intercellular junctions (Reyes et al., 2014). These observations imply that the activation state of Rho is essential to confine it spatially and ZA might act as a 'sink'

that generates and thus sustains an active Rho zone by utilizing its components like myosin IIA. Here I envisage that myosin initiates a feedback loop, which creates a self-amplification machinery. Thus even an initial 'weak' accumulation of GTP-Rho signal (mediated by the GEF ECT2) can be rapidly and efficiently amplified. This confers robustness to junctional Rho signaling, making it less sensitive to the fluctuations inside the cells. Also, this adds to the growing notion that effectors of Rho signaling pathway can act both upstream and downstream of Rho, thus creating a feedback loop to strengthen the output signal (Ivetic and Ridley, 2004; Kitzing et al., 2007; Tang et al., 2012).

Further, the numerical simulations predicted that the signaling network I have unraveled has the tendency to exhibit bistability. Bistability is a phenomenon inherent to essential cellular pathways like the cell cycle or cell differentiation. A bistable system rests in two steady states and is capable of transforming an initial trigger to a sustained signal, which ultimately translates into a biological response (Bhalla and Iyengar, 2001; Ferrell, 2002). Indeed, we identified that in steady-state epithelial monolayer, junctional Rho can be categorized into two states; ON and OFF and the myosin to ROCK feedback loop skews the Rho activity towards ON state. This further asserts that the myosin to ROCK loop is necessary to maintain Rho in its GTP-loaded state. Also, the notion that Rho signaling exhibits bistability has great implications for Rho biology during morphogenetic processes. Physiological events like cytokinesis, extrusion and wound healing rely on the active remodeling of actomyosin based cellular structures, of which Rho is the master regulator. The bistability makes Rho signaling facile and amenable to morphogenetic cues. Also, by exploiting the myosin to ROCK feedback loop, cells can potentially tune the state of Rho activity quickly, thus enabling them to co-operate well with the changes in the cell-environment.

In conclusion, my findings indicate the presence of a novel signaling cascade that assures the sustenance of a stable GTP-Rho zone at the ZA. Considering that an active Rho is required for such myriad cellular functions, whether some of the components and mechanism of this pathway is shared by other cellular processes remains an exciting question for the future.

5.4 References

Bement, W.M., A.L. Miller, and G. von Dassow. 2006. Rho GTPase activity zones and transient contractile arrays. *BioEssays* .28:983-993.

Benink, H.A., and W.M. Bement. 2005. Concentric zones of active RhoA and Cdc42 around single cell wounds. *J Cell Biol*. 168:429-439.

Betapudi, V. 2010. Myosin II motor proteins with different functions determine the fate of lamellipodia extension during cell spreading. *PLoS One*. 5:e8560.

Bhalla, U.S., and R. Iyengar. 2001. Robustness of the bistable behavior of a biological signaling feedback loop. *Chaos*. 11:221-226.

Bishop, A.L., and A. Hall. 2000. Rho GTPases and their effector proteins. *Biochemical Journal*. 348:241-255.

Boulter, E., S. Estrach, R. Garcia-Mata, and C.C. Feral. 2012. Off the beaten paths: alternative and crosstalk regulation of Rho GTPases. *Faseb J*. 26:469-479.

Braga, V.M. 2002. Cell-cell adhesion and signalling. *Curr Opin Cell Biol*. 14:546-556.

Braga, V.M., and A.S. Yap. 2005. The challenges of abundance: epithelial junctions and small GTPase signalling. *Curr Opin Cell Biol*. 17:466-474.

Brieher, W.M., and A.S. Yap. 2013. Cadherin junctions and their cytoskeleton(s). *Curr Opin Cell Biol*. 25:39-46.

Bustelo, X.R., V. Sauzeau, and I.M. Berenjeno. 2007. GTP-binding proteins of the Rho/Rac family: regulation, effectors and functions in vivo. *BioEssays.* 29:356-370.

Bustos, R.I., M.A. Forget, J.E. Settleman, and S.H. Hansen. 2008. Coordination of Rho and Rac GTPase Function via p190B RhoGAP. *Curr Biol*. 18:1606-1611.

Chalamalasetty, R.B., S. Hummer, E.A. Nigg, and H.H. Sillje. 2006. Influence of human Ect2 depletion and overexpression on cleavage furrow formation and abscission. *J Cell Sci*. 119:3008-3019.

Conti, M.A., and R.S. Adelstein. 2008. Nonmuscle myosin II moves in new directions. *J Cell Sci*. 121:11-18.

Etienne-Manneville, S., and A. Hall. 2002. Rho GTPases in cell biology. *Nature*. 420:629-635.

Ferrell, J.E., Jr. 2002. Self-perpetuating states in signal transduction: positive feedback, double-negative feedback and bistability. *Curr Opin Cell Biol*. 14:140-148.

Fields, A.P., and V. Justilien. 2010. The guanine nucleotide exchange factor (GEF) Ect2 is an oncogene in human cancer. *Adv Enzyme Regul*. 50:190-200.

Gomez, G.A., R.W. McLachlan, and A.S. Yap. 2011. Productive tension: force-sensing and homeostasis of cell-cell junctions. *Trends Cell Biol*. 21:499-505.

Guillot, C., and T. Lecuit. 2013. Mechanics of epithelial tissue homeostasis and morphogenesis. *Science*. 340:1185-1189.

Guilluy, C., R. Garcia-Mata, and K. Burridge. 2011. Rho protein crosstalk: another social network? *Trends Cell Biol*. 21:718-726.

Hara, T., M. Abe, H. Inoue, L.R. Yu, T.D. Veenstra, Y.H. Kang, K.S. Lee, and T. Miki. 2006. Cytokinesis regulator ECT2 changes its conformation through phosphorylation at Thr-341 in G2/M phase. *Oncogene*. 25:566-578.

Heissler, S.M., and D.J. Manstein. 2013. Nonmuscle myosin-2: mix and match. *Cell Mol Life Sci*. 70:1-21.

Ivetic, A., and A.J. Ridley. 2004. Ezrin/radixin/moesin proteins and Rho GTPase signalling in leucocytes. *Immunology*. 112:165-176.

Jaffe, A.B., and A. Hall. 2005. Rho GTPases: biochemistry and biology. *Annu Rev Cell Dev Biol*. 21:247-269.

Kitzing, T.M., A.S. Sahadevan, D.T. Brandt, H. Knieling, S. Hannemann, O.T. Fackler, J. Grosshans, and R. Grosse. 2007. Positive feedback between Dia1, LARG, and RhoA regulates cell morphology and invasion. *Genes Dev*. 21:1478-1483.

Kuo, J.C., X. Han, C.T. Hsiao, J.R. Yates, 3rd, and C.M. Waterman. 2011. Analysis of the myosin-II-responsive focal adhesion proteome reveals a role for beta-Pix in negative regulation of focal adhesion maturation. *Nat Cell Biol*. 13:383-393.

Lee, C.S., C.K. Choi, E.Y. Shin, M.A. Schwartz, and E.G. Kim. 2010. Myosin II directly binds and inhibits Dbl family guanine nucleotide exchange factors: a possible link to Rho family GTPases. *J Cell Biol*. 190:663-674.

Li, Z.H., and A.R. Bresnick. 2006. The S100A4 metastasis factor regulates cellular motility via a direct interaction with myosin-IIA. *Cancer Res*. 66:5173-5180.

Liu, X.F., H. Ishida, R. Raziuddin, and T. Miki. 2004. Nucleotide exchange factor ECT2 interacts with the polarity protein complex Par6/Par3/protein kinase Czeta (PKCzeta) and regulates PKCzeta activity. *Mol Cell Biol*. 24:6665-6675.

Liu, X.F., S. Ohno, and T. Miki. 2006. Nucleotide exchange factor ECT2 regulates epithelial cell polarity. *Cellular signalling*. 18:1604-1615.

McCormack, J., N.J. Welsh, and V.M. Braga. 2013. Cycling around cell-cell adhesion with Rho GTPase regulators. *J Cell Sci*. 126:379-391.

Meng, W.X., and M. Takeichi. 2009. Adherens Junction: Molecular Architecture and Regulation. *Csh Perspect Biol*. 1.

Miller, A.L., and W.M. Bement. 2009. Regulation of cytokinesis by Rho GTPase flux. *Nat Cell Biol*. 11:71-77.

Miller, A.L., G. von Dassow, and W.M. Bement. 2008. Control of the cytokinetic apparatus by flux of the Rho GTPases. *Biochem Soc Trans*. 36:378-380.

Miranda, K.C., T. Khromykh, P. Christy, T.L. Le, C.J. Gottardi, A.S. Yap, J.L. Stow, and R.D. Teasdale. 2001. A dileucine motif targets E-cadherin to the basolateral cell surface in Madin-Darby canine kidney and LLC-PK1 epithelial cells. *J Biol Chem*. 276:22565-22572.

Munjal, A., and T. Lecuit. 2014. Actomyosin networks and tissue morphogenesis. *Development*. 141:1789-1793.

Niessen, C.M., D. Leckband, and A.S. Yap. 2011. Tissue organization by cadherin adhesion molecules: dynamic molecular and cellular mechanisms of morphogenetic regulation. *Physiol Rev*. 91:691-731.

Noren, N.K., W.T. Arthur, and K. Burridge. 2003. Cadherin engagement inhibits RhoA via p190RhoGAP. *J Biol Chem*. 278:13615-13618.

Noren, N.K., C.M. Niessen, B.M. Gumbiner, and K. Burridge. 2001. Cadherin engagement regulates Rho family GTPases. *J Biol Chem*. 276:33305-33308.

Piekny, A., M. Werner, and M. Glotzer. 2005. Cytokinesis: welcome to the Rho zone. *Trends Cell Biol*. 15:651-658.

Piekny, A.J., and M. Glotzer. 2008. Anillin is a scaffold protein that links RhoA, actin, and myosin during cytokinesis. *Curr Biol*. 18:30-36.

Piekny, A.J., and A.S. Maddox. 2010. The myriad roles of Anillin during cytokinesis. *Semin Cell Dev Biol*. 21:881-891.

Priya, R., A.S. Yap, and G.A. Gomez. 2013. E-cadherin supports steady-state Rho signaling at the epithelial zonula adherens. *Differentiation.*86:133-140.

Ratheesh, A., G.A. Gomez, R. Priya, S. Verma, E.M. Kovacs, K. Jiang, N.H. Brown, A. Akhmanova, S.J. Stehbens, and A.S. Yap. 2012. Centralspindlin and alpha-catenin regulate Rho signalling at the epithelial zonula adherens. *Nat Cell Biol*. 14:818-828.

Ratheesh, A., R. Priya, and A.S. Yap. 2013. Coordinating Rho and Rac: the regulation of Rho GTPase signaling and cadherin junctions. *Progress in molecular biology and translational science*. 116:49-68.

Ratheesh, A., and A.S. Yap. 2012. A bigger picture: classical cadherins and the dynamic actin cytoskeleton. *Nat Rev Mol Cell Bio*. 13:673-679.

Reyes, C.C., M. Jin, E.B. Breznau, R. Espino, R. Delgado-Gonzalo, A.B. Goryachev, and A.L. Miller. 2014. Anillin regulates cell-cell junction integrity by organizing junctional accumulation of Rho-GTP and actomyosin. *Current biology.*24:1263-1270.

Riento, K., R.M. Guasch, R. Garg, B. Jin, and A.J. Ridley. 2003. RhoE binds to ROCK I and inhibits downstream signaling. *Mol Cell Biol*. 23:4219-4229.

Rosenberg, M., and S. Ravid. 2006. Protein kinase Cgamma regulates myosin IIB phosphorylation, cellular localization, and filament assembly. *Mol Biol Cell*. 17:1364-1374.

Sandquist, J.C., and A.R. Means. 2008. The C-terminal tail region of nonmuscle myosin II directs isoform-specific distribution in migrating cells. *Mol Biol Cell*. 19:5156-5167.

Sandquist, J.C., K.I. Swenson, K.A. Demali, K. Burridge, and A.R. Means. 2006. Rho kinase differentially regulates phosphorylation of nonmuscle myosin II isoforms A and B during cell rounding and migration. *J Biol Chem*. 281:35873-35883.

Shewan, A.M., M. Maddugoda, A. Kraemer, S.J. Stehbens, S. Verma, E.M. Kovacs, and A.S. Yap. 2005. Myosin 2 is a key Rho kinase target necessary for the local concentration of E-cadherin at cell-cell contacts. *Mol Biol Cell*. 16:4531-4542.

Shin, E.Y., C.S. Lee, C.Y. Yun, S.Y. Won, H.K. Kim, Y.H. Lee, S.J. Kwak, and E.G. Kim. 2014. Non-Muscle Myosin II Regulates Neuronal Actin Dynamics by Interacting with Guanine Nucleotide Exchange Factors. *PLoS One*. 9.

Simoes Sde, M., A. Mainieri, and J.A. Zallen. 2014. Rho GTPase and Shroom direct planar polarized actomyosin contractility during convergent extension. *J Cell Biol*. 204:575-589.

Simon, C.M., E.M. Vaughan, W.M. Bement, and L. Edelstein-Keshet. 2013. Pattern formation of Rho GTPases in single cell wound healing. *Mol Biol Cell*. 24:421-432.

Smith, A.L., M.R. Dohn, M.V. Brown, and A.B. Reynolds. 2012. Association of Rho-associated protein kinase 1 with E-cadherin complexes is mediated by p120-catenin. *Mol Biol Cell*. 23:99-110.

Smutny, M., H.L. Cox, J.M. Leerberg, E.M. Kovacs, M.A. Conti, C. Ferguson, N.A. Hamilton, R.G. Parton, R.S. Adelstein, and A.S. Yap. 2010. Myosin II isoforms identify distinct functional modules that support integrity of the epithelial zonula adherens. *Nat Cell Biol*. 12:696-702.

Smutny, M., S.K. Wu, G.A. Gomez, S. Mangold, A.S. Yap, and N.A. Hamilton. 2011. Multicomponent analysis of junctional movements regulated by myosin II isoforms at the epithelial zonula adherens. *PLoS One*. 6:e22458.

Su, K.C., T. Takaki, and M. Petronczki. 2011. Targeting of the RhoGEF Ect2 to the Equatorial Membrane Controls Cleavage Furrow Formation during Cytokinesis. *Dev Cell*. 21:1104-1115.

Takeichi, M. 2014. Dynamic contacts: rearranging adherens junctions to drive epithelial remodelling. *Nat Rev Mol Cell Biol*. 15:397-410.

Tang, A.T., W.B. Campbell, and K. Nithipatikom. 2012. ROCK1 feedback regulation of the upstream small GTPase RhoA. *Cellular signalling*. 24:1375-1380.

Terry, S.J., C. Zihni, A. Elbediwy, E. Vitiello, I.V.L.C. San, M.S. Balda, and K. Matter. 2011. Spatially restricted activation of RhoA signalling at epithelial junctions by p114RhoGEF drives junction formation and morphogenesis. *Nat Cell Biol*. 13:159-U120.

Tse, Y.C., M. Werner, K.M. Longhini, J.C. Labbe, B. Goldstein, and M. Glotzer. 2012. RhoA activation during polarization and cytokinesis of the early Caenorhabditis elegans embryo is differentially dependent on NOP-1 and CYK-4. *Mol Biol Cell*. 23:4020-4031.

Vicente-Manzanares, M., X. Ma, R.S. Adelstein, and A.R. Horwitz. 2009. Non-muscle myosin II takes centre stage in cell adhesion and migration. *Nat Rev Mol Cell Biol*. 10:778-790.

Wang, Y., X.R. Zheng, N. Riddick, M. Bryden, W. Baur, X. Zhang, and H.K. Surks. 2009. ROCK isoform regulation of myosin phosphatase and contractility in vascular smooth muscle cells. *Circulation research*. 104:531-540.

Wennerberg, K., M.A. Forget, S.M. Ellerbroek, W.T. Arthur, K. Burridge, J. Settleman, C.J. Der, and S.H. Hansen. 2003. Rnd proteins function as RhoA antagonists by activating p190 RhoGAP. *Curr Biol*. 13:1106-1115.

Wheelock, M.J., and K.R. Johnson. 2003. Cadherin-mediated cellular signaling. *Curr Opin Cell Biol*. 15:509-514.

Wildenberg, G.A., M.R. Dohn, R.H. Carnahan, M.A. Davis, N.A. Lobdell, J. Settleman, and A.B. Reynolds. 2006. p120-catenin and p190RhoGAP regulate cell-cell adhesion by coordinating antagonism between Rac and Rho. *Cell*. 127:1027-1039.

Wu, S.K., G.A. Gomez, M. Michael, S. Verma, H.L. Cox, J.G. Lefevre, R.G. Parton, N.A. Hamilton, Z. Neufeld, and A.S. Yap. 2014. Cortical F-actin stabilization generates apical-lateral patterns of junctional contractility that integrate cells into epithelia. *Nat Cell Biol*. 16:167-178.

Yap, A.S., and E.M. Kovacs. 2003. Direct cadherin-activated cell signaling: a view from the plasma membrane. *J Cell Biol*. 160:11-16.

Yuce, O., A. Piekny, and M. Glotzer. 2005. An ECT2-centralspindlin complex regulates the localization and function of RhoA. *J Cell Biol*. 170:571-582.

Zhang, B., and Y. Zheng. 1998. Regulation of RhoA GTP hydrolysis by the GTPase-activating proteins p190, p50RhoGAP, Bcr, and 3BP-1. *Biochemistry*. 37:5249-5257.

6. Appendix 1

Research article published in Nature Cell Biology

nature cell biology

Centralspindlin and α-catenin regulate Rho signalling at the epithelial zonula adherens

Aparna Ratheesh[1,4,6], Guillermo A. Gomez[1,4], Rashmi Priya[1], Suzie Verma[1], Eva M. Kovacs[1], Kai Jiang[2], Nicholas H. Brown[3], Anna Akhmanova[2], Samantha J. Stehbens[1,5] and Alpha S. Yap[1,6]

The biological impact of Rho depends critically on the precise subcellular localization of its active, GTP-loaded form. This can potentially be determined by the balance between molecules that promote nucleotide exchange or GTP hydrolysis. However, how these activities may be coordinated is poorly understood. We now report a molecular pathway that achieves exactly this coordination at the epithelial zonula adherens. We identify an extramitotic activity of the centralspindlin complex, better understood as a cytokinetic regulator, which localizes to the interphase zonula adherens by interacting with the cadherin-associated protein, α-catenin. Centralspindlin recruits the RhoGEF, ECT2, to activate Rho and support junctional integrity through myosin IIA. Centralspindlin also inhibits the junctional localization of p190 B RhoGAP, which can inactivate Rho. Thus, a conserved molecular ensemble that governs Rho activation during cytokinesis is used in interphase cells to control the Rho GTPase cycle at the zonula adherens.

Rho family GTPases are fundamental regulators of cell behaviour that are active in their GTP-loaded state[1]. This state is determined by the action of guanosine nucleotide exchange factors (GEFs) that catalyse GTP-loading, and GTPase-activating proteins (GAPs) that stimulate Rho proteins to convert bound GTP to GDP (refs 2,3). The biological impact of Rho also depends on the precise subcellular site where Rho–GTP is expressed[4–7]. This is exemplified by cytokinesis, where Rho accumulates at the contractile furrow and regulates actomyosin-based processes necessary for cell division[6,8,9]. Importantly, the precise spatio-temporal control of this Rho zone contributes to orderly cell division[3,8].

Interphase epithelial cells concentrate Rho at their cell–cell junctions[5,10]. Rho signalling is necessary for cell–cell integrity[11,12] and this is probably mediated by the actomyosin cytoskeleton. Potential Rho effectors at junctions include non-muscle myosin II (ref. 13) and regulators of actin dynamics, such as formins[14]. However, the molecular mechanism that controls Rho–GTP at junctions is poorly understood. Formally, coordinate regulation of the GEF and GAP limbs of its GTPase cycle can control the spatial expression of the Rho–GTP signal[3,12]. However, for this to occur there must be mechanisms that spatially coordinate the localization of relevant RhoGEFs and RhoGAPs to cadherin junctions. We now report that this involves an extramitotic action of the centralspindlin complex, a key regulator of Rho signalling during cytokinesis[9].

RESULTS

The zonula adherens is a microtubule-dependent Rho zone

We began by comparing the subcellular distribution of RhoA and E-cadherin in interphase MCF-7 mammary epithelial monolayers. E-cadherin distributed extensively throughout the lateral surfaces of the cells, forming both a prominent apical ring denoting the zonula adherens[15] and puncta throughout the lateral surface below the zonula adherens[13,16] (Fig. 1a,b). Conspicuous RhoA staining[5] was also evident at the cell–cell contacts (Fig. 1a), concentrating at the zonula adherens (Fig. 1a,b). This suggested that the zonula adherens might represent a Rho zone in interphase epithelial cells, akin to that of the cytokinetic furrow[3,17].

C3-transferase (C3T) reduced the amount of junctional Rho (Fig. 1c,d), implying that a significant proportion of it was likely to be in the GTP-loaded state. We investigated this using a fluorescence resonance energy transfer (FRET)-based Rho–GTP biosensor[4] which, like endogenous Rho, distributed in the cytoplasm and concentrated at cell–cell junctions (Fig. 1e). However, greater energy transfer (indicating Rho–GTP) was detected at the junctions (Fig. 1f) and

[1]Division of Molecular Cell Biology, Institute for Molecular Bioscience, The University of Queensland, St Lucia, Brisbane 4072, Queensland, Australia. [2]Cell Biology, Faculty of Science, Utrecht University, Padualaan 8, 3584 CH, Utrecht, The Netherlands. [3]Gurdon Institute and Department of Physiology, Development and Neuroscience, Cambridge University, Tennis Court Rd, Cambridge CB2 1QN, UK. [4]These authors contributed equally to this work. [5]Present address: Department of Cell and Tissue Biology, University of California, San Francisco, San Francisco, California 94143, USA.
[6]Correspondence should be addressed to A.R. or A.S.Y. (e-mail: aparnaratheesh@gmail.com or a.yap@uq.edu.au)

Received 7 October 2011; accepted 25 May 2012; published online 1 July 2012; DOI: 10.1038/ncb2532

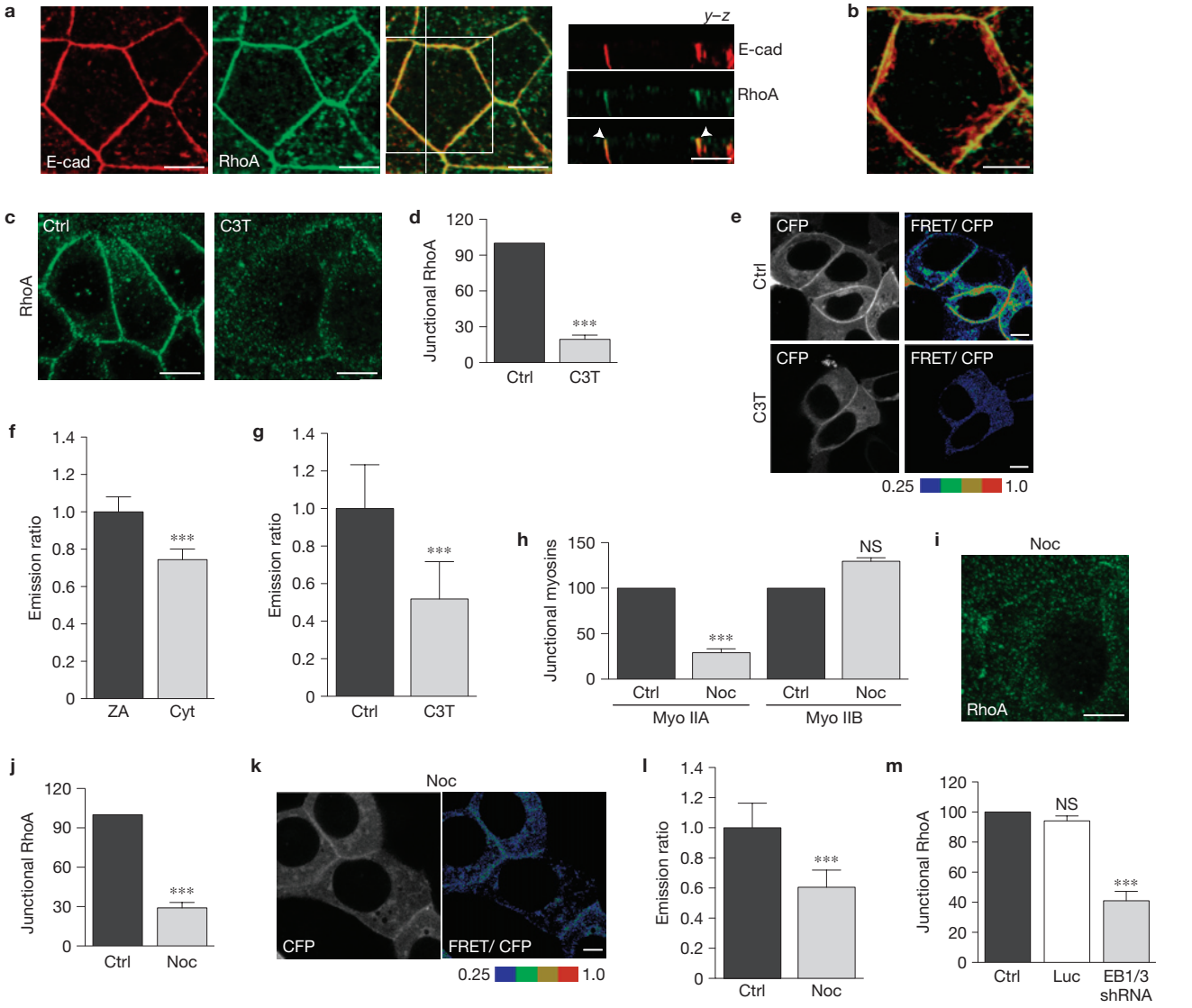

Figure 1 The zonula adherens is a microtubule-dependent Rho zone. (**a**,**b**) E-cadherin (E-cad, red) and RhoA (green) at apical junctions in TCA-fixed MCF-7 monolayers. *y*–*z* views (taken at the vertical line) are shown in (**a**) and the magnification (outlined in the square) shows E-cadherin and RhoA at the zonula adherens in a maximum-intensity projection (**b**). The arrowheads indicate the zonula adherens (**a**). (**c**,**d**) RhoA in confluent MCF-7 cells treated with C3T (0.25 μg ml^{-1}, 1 h) or glycerol (vehicle, Ctrl). Representative apical confocal images are shown (**c**) with junctional RhoA fluorescence intensity (**d**). $n = 30$; $^{***}P < 0.0001$; Student's *t*-test. (**e**–**g**) Rho–GTP measured using a RhoA FRET biosensor in MCF-7 cells treated as in **c**,**d**. Representative images of CFP and the ratio of FRET/CFP are shown (**e**). (**f**,**g**) Average emission ratios were determined at the zonula adherens (ZA) and the cytoplasm (Cyt) of control cells (**f**) and at the zonula adherens of control and C3T-treated (**g**) cells. $n = 26$; $^{***}P < 0.0001$; Student's *t*-test. (**h**) Fluorescence intensity of myosin (Myo) IIA and IIB at cell junctions in MCF-7 cells treated with dimethylsulphoxide (Ctrl) or nocodazole (Noc, 100 nM, 3 h). $n = 25$; $^{***}P < 0.001$; NS, not significant; Student's *t*-test. (**i**,**j**) RhoA in control and nocodazole-treated cells. A representative apical confocal image is shown (**i**) with junctional RhoA fluorescence intensity (**j**). $n = 30$; $^{***}P < 0.001$; NS, not significant; Student's *t*-test. (**k**,**l**) Effect of nocodazole on Rho–GTP in confluent MCF-7 cells. CFP and ratio of FRET/CFP representative images are shown (**k**) with average emission ratios quantified at the apical junctions (**l**). $n = 40$; $^{***}P < 0.001$; Student's *t*-test. (**m**) Junctional Rho in MCF-7 cells transfected with pECFP–C1 (Ctrl) or with pSUPER constructs containing shRNAs against luciferase (Luc) or EB1 + EB3 (EB1/3 shRNA). $n = 15$; $^{***}P < 0.001$; one-way analysis of variance (ANOVA), Dunnett's *post hoc* test. Heat colour scales in **e** and **k** for FRET/CFP emission ratios are shown. Data are control normalized means ± s.e.m. pooled from three individual experiments. Scale bars: 10 μm (**a**,**c**,**i**); 5 μm (**b**,**e**,**k**).

this was reduced by C3T (Fig. 1e,g). Thus, cadherin-based cell–cell junctions are prominent sites of Rho signalling in interphase epithelial cells. Mechanisms must then exist to ensure that Rho is activated, and maintained in an active state, at those junctions.

Previously we demonstrated that cadherin junctions and their associated cytoskeleton are influenced by dynamic microtubules[18]. In particular, nocodazole, used at a concentration (100 nM) that blocks microtubule plus-end dynamics without depolymerizing the lattice[19,20], prevented the junctional accumulation of myosin IIA, but not that of myosin IIB (Fig. 1h and Supplementary Fig. S1a). As myosin IIA, but not myosin IIB (ref. 13), requires Rho signalling to concentrate at the zonula adherens[13,21], this suggested that dynamic microtubule plus-ends might also regulate Rho. Indeed, nocodazole substantially reduced both junctional Rho (Fig. 1i,j) and Rho–GTP (Fig. 1k,l). Junctional Rho

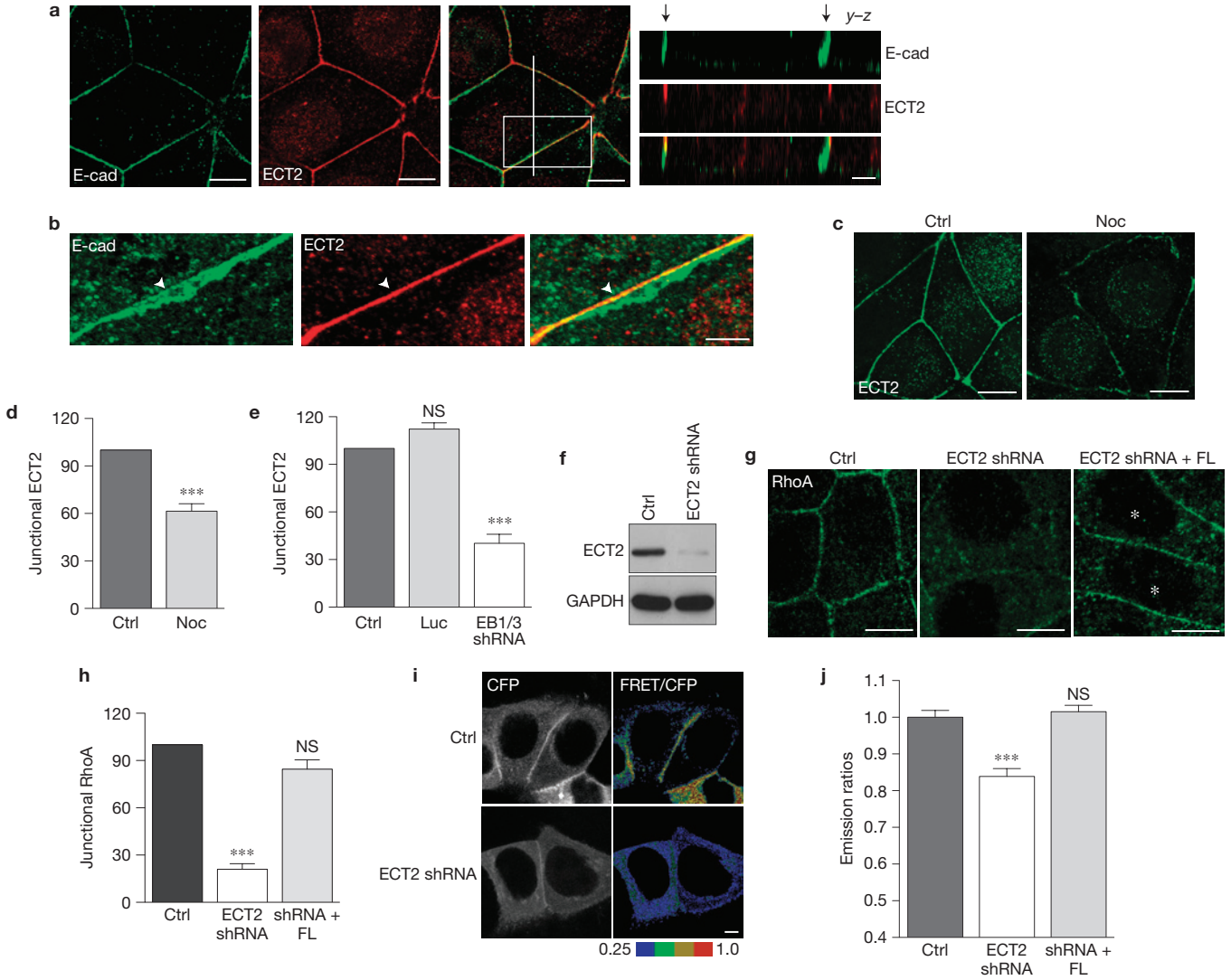

Figure 2 ECT2 is a junctional RhoA GEF. (**a**,**b**) E-cadherin (E-cad, green) and ECT2 (red) in confluent MCF-7 cells. Representative confocal images at the zonula adherens (**a**) and *y*–*z* views (taken at the vertical line) illustrating the distribution of proteins along the *z* axis of cells. The arrows indicate the apices of cell–cell contacts. (**b**) Magnification of the outlined area in **a** shows E-cadherin and ECT2 at the zonula adherens in a maximum-intensity projection. The arrowheads indicate the zonula adherens. (**c**,**d**) ECT2 in confluent MCF-7 cells treated with or without nocodazole (Noc and Ctrl). Representative apical confocal images are shown (**c**) with junctional ECT2 fluorescence intensity (**d**). $n = 30$; $^{***}P < 0.001$; Student's *t*-test. (**e**) Junctional ECT2 in MCF-7 cells transfected with pECFP–C1 (Ctrl) or with pSUPER constructs containing shRNAs against luciferase (Luc) or EB1 + EB3 (EB1/3 shRNA). $n = 15$; $^{***}P < 0.001$; NS, not significant; one-way ANOVA, Dunnett's *post hoc* test. (**f**) ECT2 and GAPDH (loading control) immunoblots of lysates from MCF-7 cells infected with lentivirus bearing an empty vector control (Ctrl) or an shRNA directed against ECT2 (ECT2 shRNA). (**g**,**h**) Rho immunofluorescence in control (Ctrl), ECT2 knockdown cells, and ECT2 knockdown cells transiently expressing shRNA-resistant EGFP–ECT2 (ECT2 shRNA + FL). Representative apical confocal images are shown (**g**) with junctional RhoA fluorescence intensity (**h**). The asterisks mark cells transfected with EGFP–ECT2. $n = 15$; $^{***}P < 0.001$; NS, not significant; one-way ANOVA, Dunnett's *post hoc* test. (**i**,**j**) Rho–GTP measured with a RhoA FRET biosensor in control (Ctrl), ECT2 knockdown and ECT2 knockdown cells expressing RNAi-resistant ECT2 (shRNA +FL). Representative images of CFP and ratio of FRET/CFP are shown (**i**) with average emission ratios quantified at the apical junctions (**j**). $n = 43$; $^{***}P < 0.001$; NS, not significant; Student's *t*-test. Data represent control-normalized means ± s.e.m. pooled from three individual experiments. Scale bars: 10 μm (**a**,**b**,**c**,**g**); 5 μm (**i**). Uncropped images of blots are shown in Supplementary Fig. S8.

(Fig. 1m and Supplementary Fig. S1b) and myosin IIA (Supplementary Fig. S1c) were also decreased when dynamic microtubule plus ends were independently perturbed by depletion of end-binding (EB) proteins 1 and 3 (Supplementary Fig. S1b)[22,23]. The zonula adherens thus seemed to be a microtubule-dependent Rho zone.

ECT2 activates Rho signalling at the zonula adherens

We then examined the cellular localization of microtubule-sensitive RhoGEFs. Strikingly, ECT2 (Fig. 2a,b), but not GEF-H1 (not shown), was stained at junctions in interphase MCF-7 cells. ECT2 is a RhoGEF best understood to operate during mitosis, where it localizes to the contractile furrow (Supplementary Fig. S2a) and activates Rho[9,24,25]. With some exceptions[26], it is reported to be a nuclear protein during interphase[24], although these studies were generally performed in isolated cells that did not make adhesive contacts with one another. We found that although nuclear staining was detectable in confluent MCF-7 cells, ECT2 also clearly localized at cell–cell contacts (Fig. 2a), an observation that we confirmed in Caco-2

and MDCK cells[26] (Supplementary Fig. S2b). Furthermore, ECT2 selectively localized to the zonula adherens within contacts (Fig. 2a,b). The specificity of this staining pattern was confirmed by ECT2 RNA-mediated interference (RNAi; Supplementary Fig. S2c,e) and further corroborated by transiently expressed GFP–ECT2, which also localized to cell–cell contacts (Supplementary Fig. S2d). Of note, the amount of junctional ECT2 staining was reduced by both nocodazole (Fig. 2c,d) and EB1/3 short hairpin RNA (shRNA; Fig. 2e). Thus, ECT2 was an attractive candidate to mediate microtubule-dependent Rho signalling at the zonula adherens.

To investigate this, we depleted ECT2 in MCF-7 cells by lentiviral shRNA (Fig. 2f). Both junctional Rho (Fig. 2g,h) and Rho–GTP (Fig. 2i,j) were reduced by ECT2 knockdown. Furthermore, both parameters were restored by expression of an RNAi-resistant transgene (Fig. 2g–j), indicating that the changes in Rho signalling were due to loss of ECT2 itself. Junctional Rho was similarly reduced when ECT2 was depleted by short interfering RNA (siRNA; Supplementary Fig. S2e,f). Together, these findings identify ECT2 as a major activator of Rho signalling at the zonula adherens.

ECT2 signalling regulates zonula adherens integrity and apical junction tension

The zonula adherens is a specialized adhesive junction that supports epithelial cohesion and apical contractility[27]. Its integrity requires Rho signalling to the actomyosin cytoskeleton[13,28].

We found that ECT2 supports the zonula adherens. When compared with controls, ECT2-deficient cells failed to concentrate E-cadherin into the apical ring of the zonula adherens (Fig. 3a,b and Supplementary Fig. S2g), although cadherin clusters remained at the lateral contacts (Fig. 3a). In contrast, tight junctions persisted in ECT2-knockdown cells (Supplementary Fig. S3a,b), indicating a relatively selective effect on the zonula adherens. As neither total nor surface levels of E-cadherin were altered by ECT2 knockdown (Supplementary Fig. S3c), we postulated that the defect arose from failure of surface cadherin to be concentrated in an apical junctional structure. To investigate this, we expressed E-cadherin–EGFP in cadherin RNAi cells[29] and measured fluorescence recovery after photobleaching (FRAP) in the apical region. ECT2 knockdown and C3T both decreased the immobile fraction and the half-time of recovery ($t_{1/2}$; Fig. 3c and Supplementary Table S1), indicating more rapid turnover of apical E-cadherin. This implies that ECT2–Rho signalling stabilizes E-cadherin mobility at the apical junctional zone.

To better understand how ECT2 stabilizes cadherin, we then examined its effects on the junctional cytoskeleton. Surprisingly, F-actin staining at the zonula adherens was not altered by ECT2 RNAi or by C3T (Supplementary Fig. S3d,e). However, ECT2 RNAi depleted myosin IIA, but not myosin IIB, from apical junctions (Fig. 3d,e). Myosin IIA depletion perturbs the zonula adherens in a very similar manner to ECT2 RNAi (ref. 13) and, indeed, myosin IIA shRNA also increased apical E-cadherin–EGFP mobility (Fig. 3c and Supplementary Table S1). These findings thus suggested that ECT2 supports zonula adherens integrity through myosin IIA. If so, we predicted that junctional integrity might be restored in ECT2 shRNA cells if the amount of myosin IIA at the junctions could be increased. Indeed, the intensity of the E-cadherin fluorescence signal was increased in ECT2 knockdown cells by expression of GFP–myosin IIA (Fig. 3f,g). As Rho is necessary for myosin IIA to concentrate at the zonula adherens[13] and acute treatment with C3T displaced myosin IIA, but not ECT2, from junctions (Fig. 3h,i), ECT2 presumably recruits myosin IIA indirectly by activating Rho.

The coordination of actomyosin contractility with cadherin adhesion can also generate tension at the zonula adherens[30], which influences cell–cell movements and patterning within epithelia[31,32]. To determine whether ECT2 signalling affects junctional tension, we used a femtosecond laser to cut junctions and measured the instantaneous recoil of their vertices as an index of tension[32]. Junctional tension was reduced by ECT2 knockdown and also when its downstream targets were inhibited by C3T and myosin IIA RNAi (Fig. 3j,k and Supplementary Fig. S3f).

Overall, these findings identify an extra-mitotic role for ECT2 to support cell–cell interactions between interphase epithelial cells. We propose that selective localization of ECT2 to the zonula adherens promotes local Rho signalling. This ultimately signals to recruit and activate myosin IIA (refs 13,21), which stabilizes apical cadherin to preserve the integrity of the zonula adherens and support junctional tension.

The centralspindlin complex mediates microtubule-dependent junctional localization of ECT2

To better understand how dynamic microtubules influence junctional ECT2 we measured FRAP of junctional GFP–ECT2 expressed in ECT2 RNAi cells (Fig. 4a). Nocodazole reduced the immobile fraction, without significantly affecting $t_{1/2}$, suggesting that dynamic microtubules might influence cortical binding of ECT2 at junctions. In parallel, we screened ECT2 immunoprecipitates by mass spectrometry to identify potential junctional binding partners (not shown). Amongst these we found the kinesin, MKLP1, a component of the centralspindlin complex, which also contains MgcRacGAP, a direct binder of ECT2 (ref. 33). During cytokinesis centralspindlin localizes ECT2 to activate Rho at the contractile furrow[9,25] and we therefore wondered whether it might play a similar role at the zonula adherens during interphase.

Indeed, both MgcRacGAP and MKLP1 localized to microtubule-dense MCF-7 cell–cell junctions, as well as in nuclei, as has been previously reported in isolated cells[34] (Fig. 4b and Supplementary Fig. S4a). Of note, like ECT2 (Fig. 2a), both centralspindlin components selectively concentrated with E-cadherin in the zonula adherens (shown for MgcRacGAP in Fig. 4b). RNAi of either protein abolished its junctional staining (Supplementary Fig. S4b,c) and junctional localization was further confirmed by GFP-tagged MgcRacGAP and MKLP1 (Supplementary Fig. S4d). Centralspindlin is thus a junctional constituent in interphase MCF-7 cells.

We then used RNAi (Supplementary Fig. S4b) to assess whether centralspindlin affected junctional ECT2 and Rho signalling. MgcRacGAP or MKLP1 siRNA substantially reduced junctional ECT2 (Fig. 4c,d) but not its total expression (Fig. 4e), whereas ECT2 RNAi did not affect junctional centralspindlin (Supplementary Fig. S4e). This suggested that centralspindlin influences the junctional localization of ECT2, analogous to its action during cytokinesis[9,25]. Furthermore, the amount of junctional Rho was reduced by either MKLP1 or MgcRacGAP knockdown (Fig. 4f,g) and the amount of Rho–GTP was reduced by MgcRacGAP depletion (Fig. 4h). Myosin IIA was also selectively lost from junctions in centralspindlin-depleted cells (Fig. 4i and Supplementary Fig. S4f). Supporting a central role for centralspindlin in junctional signalling, the integrity of the zonula adherens was

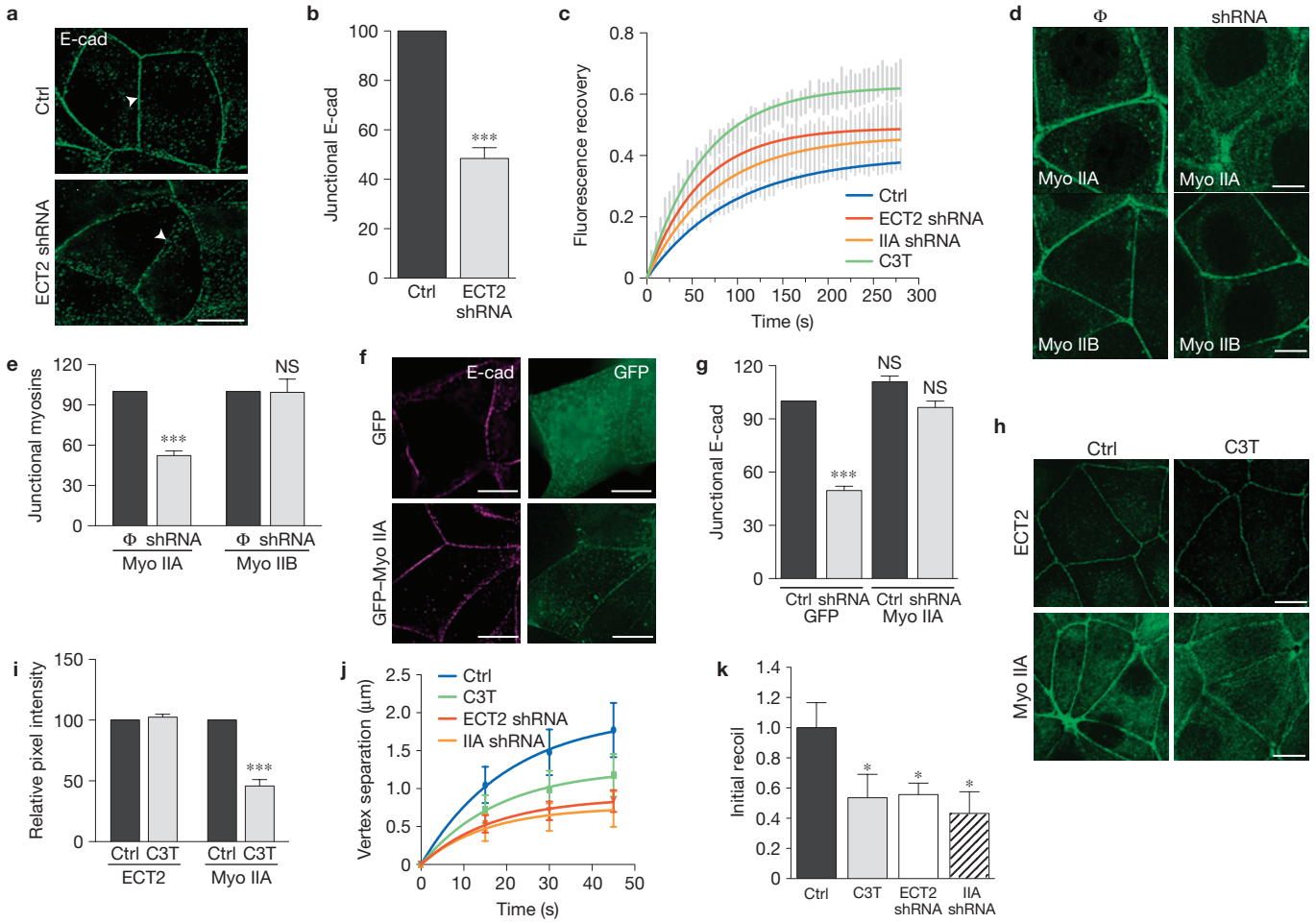

Figure 3 ECT2 is necessary for zonula adherens integrity and junctional tension. (**a**,**b**) E-cadherin (E-cad) immunostaining in control (Ctrl) and ECT2 knockdown (ECT2 shRNA) cells imaged by wide-field deconvolution microscopy (in **a**, the arrowheads indicate apical junctional regions). Peak junctional fluorescence intensity (**b**) was measured by line scan analysis. $n = 25$; $^{***}P < 0.001$; Student's t-test. (**c**) FRAP was performed for E-cadherin–GFP (expressed in MCF-7 cells depleted of endogenous E-cadherin by RNAi; Ctrl) or also treated with C3T or RNAi against ECT2 (ECT2 shRNA) or myosin IIA (IIA shRNA). The vertical lines represent means ± s.e.m. and solid lines are best-fit single exponential curves ($n = 11$). (**d**,**e**) Junctional myosin IIA or myosin IIB in control (Φ) and ECT2 knockdown (shRNA) cells. Representative images are shown (**d**) with junctional myosin fluorescence intensity (**e**). $n = 20$; $^{***}P < 0.001$; NS, not significant; Student's t-test. (**f**,**g**) Control (Ctrl) and ECT2 knockdown cells transfected with either pEGFP–C1 (GFP) or EGFP–MyoIIA (GFP–Myo IIA) were fixed and stained for E-cadherin (E-cad; magenta) and GFP (green). Representative apical epi-illumination images in ECT2 knockdown cells are shown (**f**) with junctional E-cadherin fluorescence intensity (**g**). $n = 17$; $^{***}P < 0.001$; NS, not significant; one-way ANOVA, Dunnett's *post hoc* test. (**h**,**i**) ECT2 and myosin IIA (Myo IIA) staining in MCF-7 cells treated with glycerol (vehicle control, Ctrl) or C3T (0.25 μg ml^{-1}, 1 h). Representative confocal images are shown (**h**) with junctional fluorescence intensities (**i**). $n = 20$; $^{***}P < 0.001$; Student's t-test. (**j**,**k**) Junctional tension was measured by laser nanoscissors in control (Ctrl) MCF-7 cells and cells treated with C3T or RNAi against ECT2 or myosin IIA. Vertex displacement (**j**) and initial recoil (**k**) are shown. The error bars in **j** represent means ± s.e.m. and solid lines are best-fit single exponential curves and in **k** means ± s.e.m. of data. $n = 12$; $^{*}P < 0.05$; t-test. Unless otherwise stated, data are control-normalized mean ± s.e.m. pooled from three individual experiments. Scale bars, 10 μm.

perturbed in both MKLP1 and MgcRacGAP knockdown cells (Fig. 4j and Supplementary Fig. S4f). Interestingly, junctional localization of centralspindlin was reduced by 100 nM nocodazole (Fig. 4k,l), making it an attractive candidate to mediate the microtubule-dependent localization of ECT2 to junctions. Indeed, the nocodazole sensitivity of junctional ECT2 was abolished by MgcRacGAP RNAi (Fig. 4m). Overall, these data implicate centralspindlin in localizing ECT2 to the zonula adherens.

α-catenin localizes ECT2 to the zonula adherens through centralspindlin

Binding to centralspindlin alone did not readily explain the specific localization of ECT2 to the zonula adherens. We were thus interested to also identify α-catenin in our ECT2 interaction screen (not shown), a finding confirmed by reciprocal co-immunoprecipitation analysis (Fig. 5a). E-cadherin also co-precipitated with ECT2 and α-catenin (Fig. 5a) suggesting that these proteins might exist in a complex. Consistent with this, ECT2, α-catenin and E-cadherin co-localized, principally at the zonula adherens (Fig. 5b and Supplementary Fig. S5a). We then depleted α-catenin by siRNA (Supplementary Fig. S5b) and examined cells after 24 h, when junctional α-catenin was significantly diminished, but cell–cell contacts remained intact (Fig. 5b). The amount of junctional ECT2 (Fig. 5b,c) and the biochemical association of E-cadherin with ECT2 (Fig. 5d) were both significantly reduced in α-catenin knockdown cells. Thus, α-catenin also contributes to the junctional localization of ECT2.

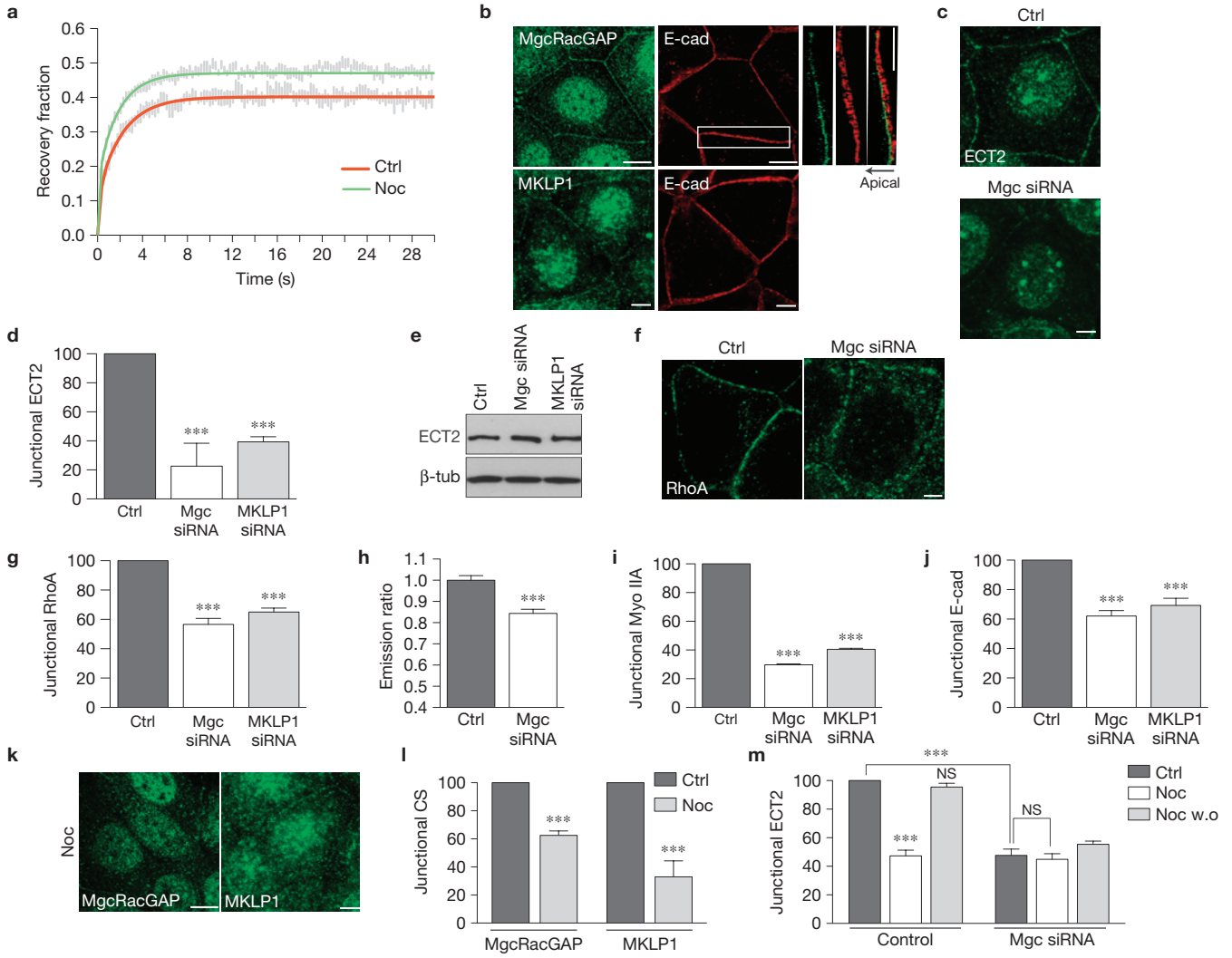

Figure 4 Centralspindlin regulates junctional ECT2–Rho signalling. (**a**) FRAP of GFP–ECT2 expressed in MCF-7 cells depleted of endogenous ECT2 and treated with dimethylsulphoxide (vehicle control, Ctrl) or nocodazole (Noc). The vertical lines represent means ± s.e.m. ($n = 9$) and the solid lines are best-fit double exponential curves. (**b**) E-cadherin (E-cad, red) and either MgcRacGAP or MKLP1 (green) in MCF-7 monolayers. The magnifications (taken from the outlined area) show E-cadherin and MgcRacGAP at the zonula adherens in a maximum-intensity projection (the direction of the arrow indicates basal to apical). (**c**–**e**) ECT2 in MCF-7 cells transfected with siRNAs against MgcRacGAP (Mgc siRNA), MKLP1 (MKLP1 siRNA) or with scrambled siRNA (Ctrl). Representative confocal images are shown (**c**) with junctional ECT2 fluorescence intensity (**d**). $n = 25$; $^{***}P < 0.001$; one-way ANOVA, Dunnett's *post hoc* test. (**e**) Lysates from control, MgcRacGAP knockdown and MKLP1 knockdown cells immunoblotted for ECT2 and β-tubulin (β-tub). (**f**–**j**) RhoA, myosin IIA, E-cadherin and Rho–GTP in control (Ctrl), MgcRacGAP knockdown or MKLP1 knockdown cells. Representative images of RhoA staining at the apical junctions are shown (**f**) with junctional RhoA (**g**), Rho–GTP (**h**), Myo IIA (**i**) and E-cad (**j**). For RhoA (**g**), Myo IIA (**i**) and E-cad (**j**), $n = 20$; $^{***}P < 0.001$; one-way ANOVA, Dunnett's *post hoc* test and for Rho–GTP (**h**), $n = 59$; $^{***}P < 0.001$; Student's *t*-test. (**k**,**l**) MgcRacGAP or MKLP1 in MCF-7 cells treated with nocodazole. Representative confocal images are shown (**k**) with junctional MgcRacGAP and MKLP1 (CS) fluorescence intensity (**l**). $n = 30$; $^{***}P < 0.001$; Student's *t*-test. (**m**) MCF-7 cells were transfected with siRNA against MgcRacGAP or scrambled (control) siRNA and were incubated with 100 nM nocodazole (3 h) or dimethylsulphoxide (Ctrl), after which nocodazole was washed out and cells were allowed to recover (Noc w.o, 1 h). ECT2 staining was quantified by line scan analysis. $n = 15$; $^{***}P < 0.001$; NS, not significant; one-way ANOVA, Bonferroni *post hoc* test, to compare across all data sets. Unless otherwise stated, data are control-normalized mean ± s.e.m. pooled from three individual experiments. Scale bars, 10 μm (**c**, and **b**,**k** for MgcRacGAP); 5 μm (**f**, and **b**,**k** for MKLP1). Uncropped images of blots are shown in Supplementary Fig. S8.

We then examined whether centralspindlin was involved in the interaction between α-catenin and ECT2. MgcRacGAP immunoprecipitated with both E-cadherin and α-catenin (Fig. 6a) and MgcRacGAP knockdown significantly reduced the amount of ECT2 that co-immunoprecipitated with α-catenin (Fig. 6b), without affecting the E-cadherin–α-catenin interaction (Fig. 6c). This implied that centralspindlin serves as an intermediate to localize ECT2 to α-catenin at the zonula adherens. Consistent with this, α-catenin knockdown substantially reduced the amount of both junctional MgcRacGAP and MKLP1 (Fig. 6d,e) but MgcRacGAP knockdown had only a minor impact on the amount of junctional α-catenin (Fig. 6f,g) probably owing to loss of the mature zonula adherens. Furthermore, nocodazole reduced the level of interaction between MgcRacGAP and α-catenin (Fig. 6h), suggesting that

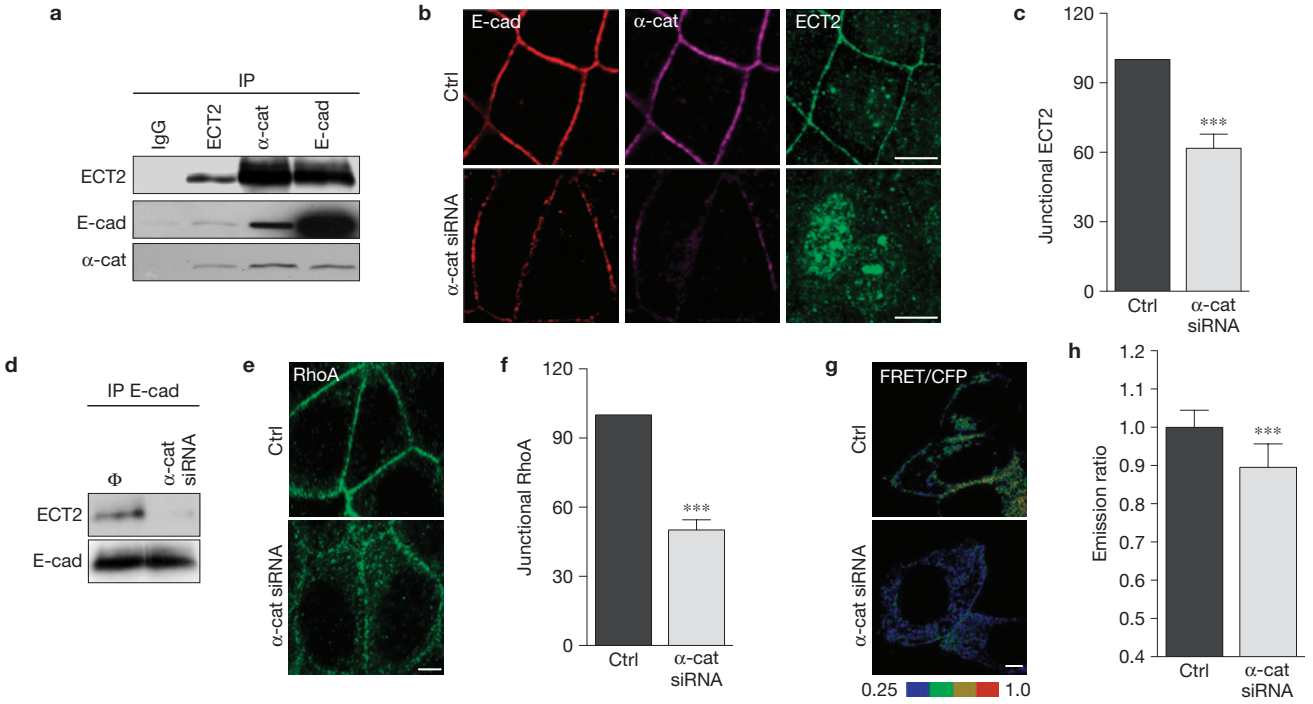

Figure 5 α-catenin mediates the junctional retention of ECT2. (**a**) Immunoprecipitates (IP) of ECT2, E-cadherin (E-cad) or α-catenin (α-cat) were immunoblotted for ECT2, E-cadherin and α-catenin. Rabbit IgG was the negative immunoprecipitation control. (**b**,**c**) MCF-7 cells transfected with SMARTpool siRNA against α-catenin (α-cat siRNA) or non-targeting siRNA pools (Ctrl) were fixed and stained for E-cadherin (red), α cat (magenta) and ECT2 (green). Representative apical confocal images are shown (**b**) with junctional ECT2 fluorescence intensity (**c**). $n = 25$; $^{***}P < 0.001$; Student's t-test. (**d**) Immunoprecipitates of E-cadherin (IP E-cad) from MCF-7 cells transfected with SMARTpool siRNA against α-catenin or non-targeting siRNA pools (Φ) were immunoblotted for ECT2 and E-cadherin. (**e**,**f**) Control and α-catenin knockdown (α cat kd) cells were fixed and stained for RhoA. Representative apical confocal images are shown (**e**) with junctional RhoA fluorescence intensity (**f**). $n = 25$; $^{***}P < 0.001$; Student's t-test. (**g**,**h**) MCF-7 cells transfected simultaneously with a Rho FRET biosensor and a SMARTpool siRNA against α-catenin or non-targeting siRNA pools (Ctrl) were imaged by live-cell confocal microscopy after 36 h. Representative images of the ratio of FRET/CFP are shown (**g**) and average emission ratios were quantified at the apical junctions (**h**). $n = 46$; $^{***}P < 0.0001$; Student's t-test. Data represent control-normalized mean ± s.e.m. pooled from three individual experiments. Scale bars: 10 μm (**b**); 5 μm (**e**,**g**). Uncropped images of blots are shown in Supplementary Fig. S8.

dynamic microtubules might regulate this interaction to support junctional ECT2.

To better characterize the molecular basis of these interactions, we expressed GFP-tagged α-catenin mutants in HEK293 cells (Fig. 6i and Supplementary Fig S5d). Both endogenous ECT2 and MgcRacGAP consistently co-precipitated with full-length α-catenin and with amino-terminal fragments of α-catenin (1–290, 1–507), but not with a carboxy-terminal fragment (507–906). Thus, the N terminus of α-catenin seems to mediate its association with centralspindlin and ECT2. We therefore conclude that α-catenin serves as a cortical anchor for centralspindlin at the zonula adherens, to thereby support the ECT2–Rho signalling pathway.

This model further predicted that α-catenin would influence junctional Rho signalling. Indeed, the amounts of junctional Rho (Fig. 5e,f), Rho–GTP (Fig. 5g,h) and myosin IIA, but not myosin IIB (Supplementary Fig. S5c), were reduced in α-catenin knockdown cells.

Centralspindlin inhibits the junctional recruitment of p190B RhoGAP

Finally, we investigated whether centralspindlin might also influence junctional Rho by regulating its inactivation, as the spatial expression of Rho–GTP is influenced by the localized action of RhoGAPs as well as by RhoGEFs (refs 3,35). We focused on p190RhoGAP, which has been implicated in cadherin junctions[36,37] and in regulating Rho signalling at the cytokinetic furrow[35,38,39]. Two members of this protein family exist in mammals[40,41] and both p190A RhoGAP and p190B RhoGAP were detected in MCF-7 cells (Fig. 7f). In control MCF-7 monolayers, staining for both these proteins was predominantly cytoplasmic, with little apparent at junctions (Fig. 7a). Strikingly, however, junctional p190B RhoGAP, but not p190A RhoGAP, became evident after nocodazole treatment (Fig. 7b,c). This suggested that dynamic microtubules might specifically inhibit the junctional accumulation of p190B RhoGAP.

As dynamic microtubules support the junctional localization of the centralspindlin complex, we then investigated whether centralspindlin influenced junctional p190B RhoGAP. Indeed, junctional p190B RhoGAP staining was significantly increased by either MgcRacGAP or MLKP1 knockdown but not by ECT2 RNAi (Fig. 7d,e). Together, these data suggested that the microtubule-dependent localization of centralspindlin at the zonula adherens might also promote junctional Rho–GTP by blocking recruitment of p190B RhoGAP, as well as through local activation of Rho by ECT2.

We investigated this by examining whether the increased p190B RhoGAP contributed to the reduced Rho found at junctions in nocodazole-treated cells. This hypothesis predicted that reducing

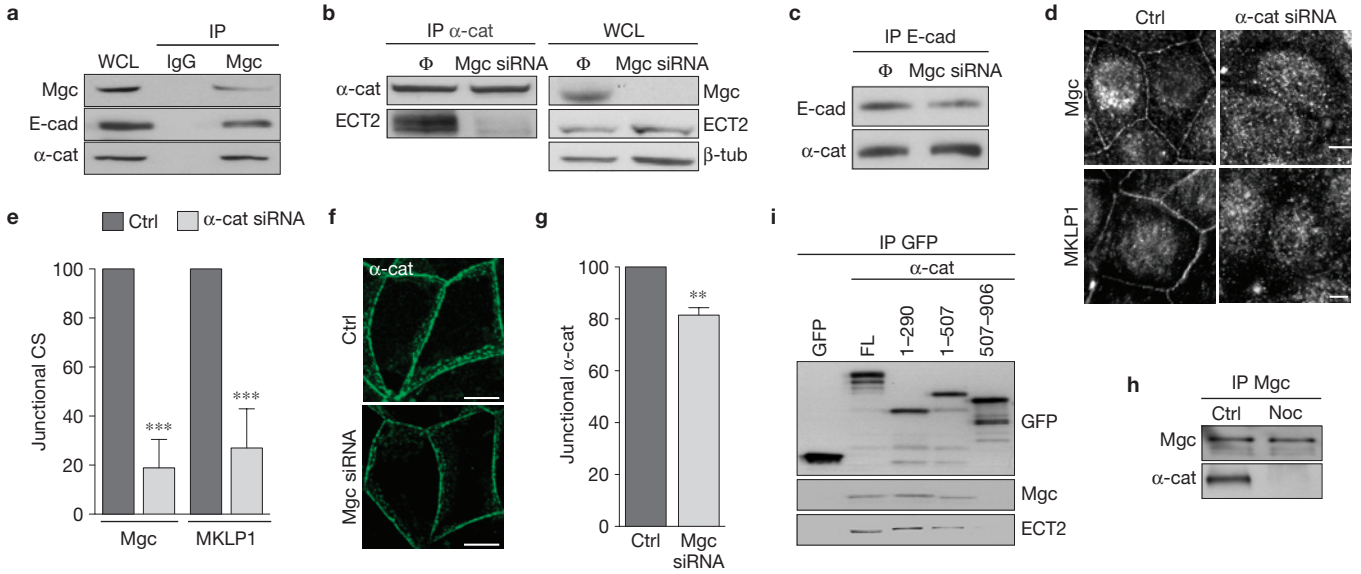

Figure 6 α-catenin mediates the junctional retention of centralspindlin. (**a**) Whole-cell lysates from MCF-7 cells (WCL) and MgcRacGAP immunoprecipitates immunoblotted for MgcRacGAP (Mgc), E-cadherin (E-cad) and α-catenin (α-cat). Rabbit IgG (IgG) was the negative immunoprecipitation control. (**b**) α-catenin immunoprecipitates (IP α-cat) from control (Φ) and MgcRacGAP siRNA knockdown cells (Mgc siRNA) were immunoblotted for α-catenin (α cat) and ECT2. Whole cell lysates (WCL) from control and MgcRacGAP knockdown cells were immunoblotted for MgcRacGAP, ECT2 and β-tubulin. (**c**) E-cadherin immunoprecipitates (IP E-cad) from control (Φ) and MgcRacGAP knockdown cells immunoblotted for E-cadherin and α-catenin. (**d**,**e**) MgcRacGAP or MKLP1 in MCF-7 cells transfected with SMARTpool siRNA against α-catenin (α-cat siRNA) or non-targeting siRNA pools (Ctrl). Representative apical confocal images are shown (**d**) with junctional MgcRacGAP and MKLP1 (CS) (**e**). $n = 25$; $^{***}P < 0.001$; Student's t-test. (**f**,**g**) α-catenin (green) in MCF-7 cells transfected with siRNAs against MgcRacGAP or scrambled (Ctrl) siRNA. Representative apical confocal images are shown (**f**) with junctional α-catenin fluorescence intensity (**g**). $n = 25$; $^{**}P < 0.005$; Student's t-test. (**h**) MgcRacGAP immunoprecipitates from control (Ctrl) and nocodazole (Noc)-treated MCF-7 cells immunoblotted for MgcRacGAP and α-catenin. (**i**) GFP-tagged full-length (FL) α-catenin or truncation mutants were transiently expressed in HEK293 cells, isolated by GFP-Trap and then immunoblotted for GFP, MgcRacGAP or ECT2. The mutants are illustrated in Supplementary Fig. S5d. Data represent control-normalized mean ± s.e.m. pooled from three individual experiments. Scale bars: 10 μm (**f** and **d** for MgcRacGAP); 6 μm (**d** for MKLP1). Uncropped images of blots are shown in Supplementary Figs S8 and S9.

p190B RhoGAP should decrease the impact of nocodazole on junctional Rho. Accordingly, we selectively depleted p190B RhoGAP by siRNA (Fig. 7f). Nocodazole reduced junctional Rho and Rho–GTP in cells transfected with control siRNAs (Fig. 7g–i), exactly as it did in untransfected cells (Fig. 1i–l). Strikingly, however, nocodazole did not reduce junctional Rho (Fig. 7g,h) or Rho–GTP (Fig. 7i) to the same level in p190B RhoGAP knockdown cells as it did in control cells. This implies that p190B RhoGAP contributed to the inhibition of Rho by nocodazole.

p190B RhoGAP contains a GTP–Rac binding domain that regulates its cortical recruitment[40]. As cell–cell contacts can be sites of Rac signalling[7], we therefore investigated whether p190B RhoGAP was recruited to junctions in response to Rac. Indeed, the junctional accumulation of p190B RhoGAP induced by nocodazole was reduced by the expression of dominant-negative Rac (N17; Fig. 7j) or treatment with the Rac inhibitor NSC 23766 (Supplementary Fig. S6b). Furthermore, a p190B RhoGAP mutant lacking the Rac-interaction domain[40] did not localize to junctions in nocodazole-treated cells (Supplementary Fig. S6a). Thus, the nocodazole-induced recruitment of p190B RhoGAP seems to require Rac signalling. Potentially, then, the microtubule–centralspindlin pathway may block p190B RhoGAP recruitment by inhibiting junctional Rac. Indeed, using a Raichu-Rac FRET biosensor we found that junctional GTP–Rac was increased both by nocodazole and MgcRacGAP knockdown (Fig. 7k and Supplementary Fig. S6c). Together, these results suggest that centralspindlin may inhibit junctional p190B RhoGAP recruitment by reducing the level of junctional Rac signalling.

DISCUSSION

In sum, our findings identify the epithelial zonula adherens as a Rho zone that is an interphase equivalent of the Rho zone of the cytokinetic furrow[8,9]. Like the cytokinetic furrow, the Rho zone of the zonula adherens serves to concentrate actomyosin, acting through myosin IIA to maintain the integrity of the junction itself. Remarkably, Rho signalling at the zonula adherens is controlled by many of the same molecules that regulate Rho at the cytokinetic furrow. The key role is played by the centralspindlin complex, which supports the junctional Rho zone by regulating both the activation and inactivation limbs of the GTPase cycle: it activates Rho by recruiting the RhoGEF ECT2 and prevents Rho inhibition by blocking the junctional recruitment of p190B RhoGAP (Supplementary Fig. S7). Recruitment of ECT2 may reflect its known direct interaction with MgcRacGAP (refs 9,25) and we postulate that centralspindlin blocks p190B RhoGAP recruitment by directly or indirectly inhibiting junctional Rac (ref. 40). Of note, both ECT2 and p190 RhoGAP have also been implicated in Rho regulation at the cytokinetic furrow[9,25,35,39], although other GAPs, including MgcRacGAP itself[3], may also contribute. Thus, the Rho zone of the zonula adherens reflects the action during interphase of a conserved molecular ensemble that can translate coordinated regulation of the Rho GTPase cycle into spatial expression of an active Rho signal at the junction.

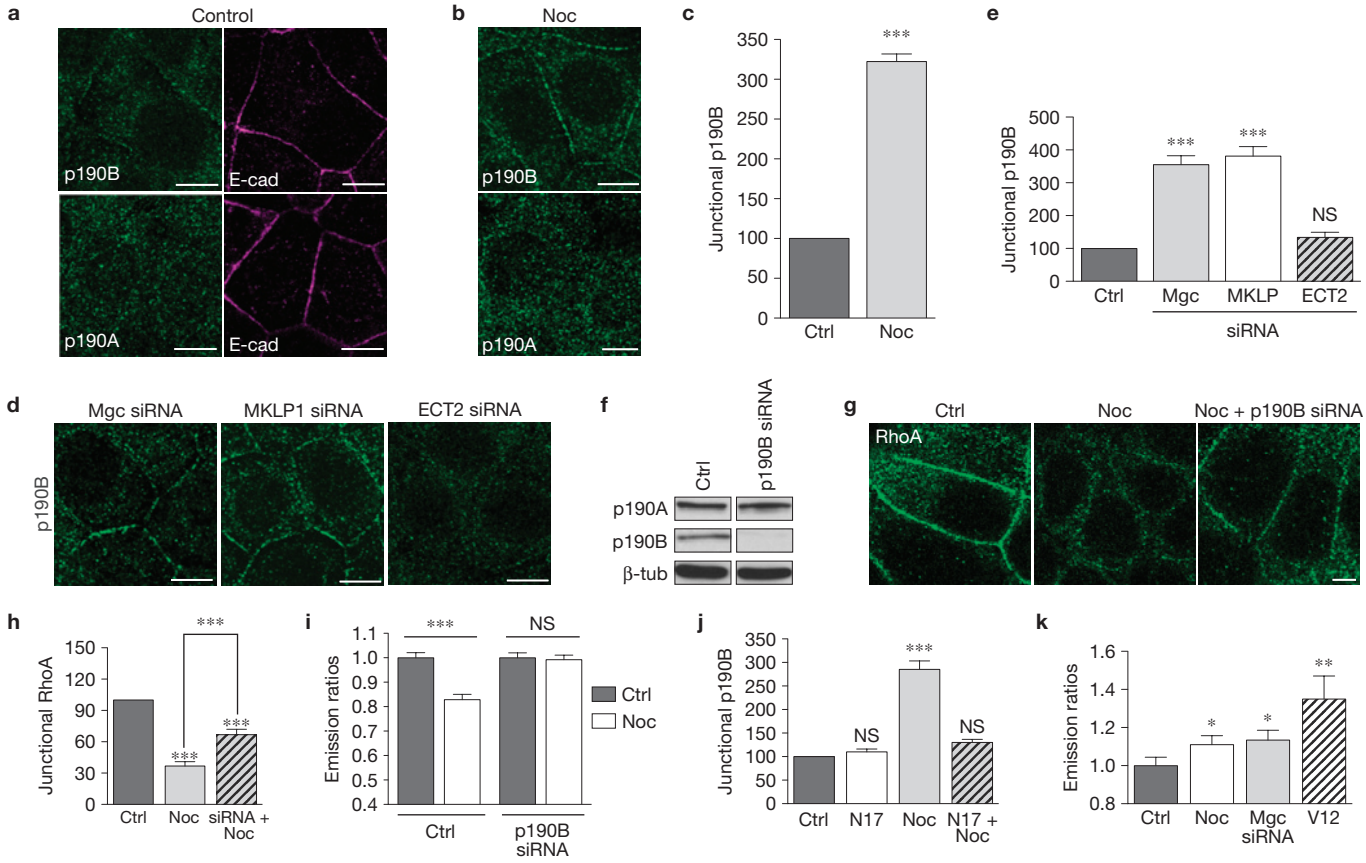

Figure 7 Centralspindlin inhibits the junctional recruitment of p190B RhoGAP. (**a**–**c**) E-cadherin (E-cad, magenta) and either p190A RhoGAP (p190A) or p190B RhoGAP (p190B, green) in control (**a**) and nocodazole (Noc; 100 nM, 3 h)-treated MCF-7 cells (**b**). Representative apical confocal images are shown (**a**,**b**) with junctional p190B in control and nocodazole-treated cells (**c**). $n = 60$; $^{***}P < 0.001$; Student's t-test. (**d**,**e**) p190B RhoGAP in MCF-7 cells transfected with siRNAs against MgcRacGAP (Mgc siRNA), MKLP1 (MKLP siRNA) or scrambled (Ctrl) siRNA, or infected with lentivirus bearing an shRNA directed against ECT2 (ECT2 shRNA). Representative apical junction images (**d**) and junctional p190B RhoGAP fluorescence intensity (**e**) are shown. $n = 25$; $^{***}P < 0.001$; NS, not significant; one-way ANOVA, Dunnett's *post hoc* test. (**f**) Whole-cell lysates from MCF-7 cells transfected with non-targeting siRNA pools (Ctrl) or SMARTpool siRNA against p190B RhoGAP (p190B siRNA) immunoblotted for p190A RhoGAP, p190B RhoGAP or β-tubulin. (**g**–**i**) Junctional Rho or Rho–GTP in control and p190B RhoGAP knockdown cells incubated with or without nocodazole. Representative Rho images are shown (**g**) with junctional fluorescence intensity (**h**). $n = 25$; $^{***}P < 0.001$; NS, not significant; one-way ANOVA, Bonferroni *post hoc* test, to compare across all data sets. Rho–GTP (**i**) was measured using a transiently expressed Rho FRET biosensor. $n = 50$; $^{***}P < 0.001$; Student's t-test. (**j**) Junctional p190B RhoGAP in MCF-7 cells transfected with EGFP pcDNA3.1 (Ctrl) or GFP–N17 Rac1 DN-pcDNA3.1 (N17), then treated with nocodazole. $n = 25$; $^{***}P < 0.001$; NS, not significant; one-way ANOVA, Dunnett's *post hoc* test. (**k**) Junctional Rac–GTP was measured with a wild-type Raichu-Rac biosensor in control (Ctrl) cells or cells treated with nocodazole (100 nM, 3 h), MgcRacGAP siRNA or a constitutively active Raichu-Rac mutant (V12). $n = 30$; $^{*}P < 0.05$; Student's t-test. Data are control-normalized mean ± s.e.m. pooled from three individual experiments. Scale bars, 10 μm. Uncropped images of blots are shown in Supplementary Fig. S9.

From this perspective, a key issue is what localizes centralspindlin to the zonula adherens. Here we found that α-catenin supports the cortical binding of centralspindlin, and thereby ECT2, at the zonula adherens. This implies that α-catenin can influence cadherin biology by regulating Rho signalling at the zonula adherens. Consistent with this, α-catenin knockdown reduced both Rho signalling and the cortical recruitment of myosin IIA. Of note, too, these effects were observed under conditions of incomplete α-catenin depletion; at later times after siRNA transfection, cells detached from one another, a more extreme phenotype that may reflect the other pathways by which α-catenin can affect cadherin function[42,43]. Thus, Rho regulation may be a relatively sensitive effect of α-catenin on cadherin biology. Interestingly, *Drosophila* α-catenin has been reported to associate with Rho itself[10], suggesting that multiple mechanisms may exist to allow α-catenin to regulate Rho signalling at cadherin junctions.

It was striking that both centralspindlin and ECT2 selectively localized to the zonula adherens. Moreover, ECT2 and the centralspindlin complex seemed to selectively support zonula adherens integrity, whereas tight junctions remained morphologically intact in ECT2 and centralspindlin knockdown cells. In contrast, p114 RhoGEF, which is recruited to tight junctions through an association with cingulin[44], supports tight junctions but not cadherin-based adhesive junctions. Different GEFs may then control different pools of Rho to support different junctions within the apical junctional complex and elsewhere in the contact zone between cells. Such a conclusion is consistent with the general paradigm that the action of specific GEFs may allow the common Rho signal to be used for different functional outcomes[1,40]. Furthermore, although α-catenin was necessary to localize centralspindlin and ECT2 to the zonula adherens, it is noteworthy that α-catenin also distributes with E-cadherin more extensively outside

the zonula adherens itself. Thus, centralspindlin is unlikely to associate constitutively with α-catenin. Instead, other as yet unknown factors must collaborate to confer specificity for this interaction on the pool of α-catenin associated with the zonula adherens itself.

Finally, our experiments also identify a role for dynamic microtubules to affect Rho signalling at the zonula adherens, apparently by influencing the capacity of the junctional cortex to bind ECT2. Dynamic microtubules seemed to regulate the association between centralspindlin and α-catenin, but not the catenin–cadherin interaction (not shown). The detailed mechanism responsible for this effect remains to be clarified. During cytokinesis it has been proposed that centralspindlin mediates the microtubule-dependent delivery of ECT2 to cytokinetic furrows[45]. Cell–cell junctions are regions that interact with and regulate microtubules[15,46,47], including a subpopulation that extend with their dynamic plus-ends directed towards the junctional cortex[18]. Such dynamic microtubules could facilitate the delivery of centralspindlin by microtubule-dependent transport[48] or by serving as diffusional traps[47] at the cortex. However, so far we have been unable to demonstrate microtubule-dependent transport of centralspindlin or ECT2 (not shown). Alternatively, dynamic microtubules might affect the binding of centralspindlin to α-catenin indirectly, through cortical signalling[49]. These signals may include post-translational modifications, such protein phosphorylation, which influences ECT2 activation and its interaction with centralspindlin during cytokinesis[50]. Whether some of these pathways are also reused at the zonula adherens will be an important issue for future research. □

METHODS

Methods and any associated references are available in the online version of the paper.

Note: Supplementary Information is available in the online version of the paper

ACKNOWLEDGEMENTS

We thank our laboratory colleagues for their support and advice, all our colleagues who provided gifts of reagents, and R. Saint who first suggested we think about ECT2. This work was financially supported by the Human Frontiers Science Program, the National Health and Medical Research Council of Australia, Australian Research Council, and the Oncology Children's Foundation. Confocal microscopy was performed at the IMB/ACRF Cancer Biology Imaging Facility, established with the generous support of the Australian Cancer Research Foundation.

AUTHOR CONTRIBUTIONS

A.R., S.J.S., A.A. and A.S.Y. conceived the project, A.R., G.A.G., R.P., S.V. and N.H.B. conducted experiments, E.M.K. and K.J. generated reagents, A.R., G.A.G. and A.S.Y. analysed the data and A.R. and A.S.Y. wrote the paper.

COMPETING FINANCIAL INTERESTS

The authors declare no competing financial interests.

Published online at www.nature.com/doifinder/10.1038/ncb2532
Reprints and permissions information is available online at www.nature.com/reprints

1. Jaffe, A. B. & Hall, A. Rho GTPases: Biochemistry and biology. *Annu. Rev. Cell. Dev. Biol.* **21,** 247–269 (2005).
2. Bos, J. L., Rehmann, H. & Wittinghofer, A. GEFs and GAPs: critical elements in the control of small G proteins. *Cell* **129,** 865–877 (2007).
3. Miller, A. L. & Bement, W. M. Regulation of cytokinesis by Rho GTPase flux. *Nat. Cell Biol.* **11,** 71–77 (2009).
4. Pertz, O., Hodgson, L., Klemke, R. L. & Hahn, K. M. Spatiotemporal dynamics of RhoA activity in migrating cells. *Nature* **440,** 1069–1072 (2006).
5. Yonemura, S., Hirao-Minakuchi, K. & Nishimura, Y. Rho localization in cells and tissues. *Exp. Cell Res.* **295,** 300–314 (2004).
6. Yoshizaki, H. *et al.* Activity of Rho-family GTPases during cell division as visualized with FRET-based probes. *J. Cell Biol.* **162,** 223–232 (2003).
7. Yamada, S. & Nelson, W. J. Localized zones of Rho and Rac activities drive initiation and expansion of epithelial cell–cell adhesion. *J. Cell Biol.* **178** (2007).
8. Bement, W. M., Miller, A. L. & von Dassow, G. Rho GTPase activity zones and transient contractile arrays. *Bioessays* **28,** 983–993 (2006).
9. Yuce, O., Piekny, A. & Glotzer, M. An ECT2-central spindlin complex regulates the localization and function of RhoA. *J. Cell Biol.* **170,** 571–582 (2005).
10. Magie, C. R., Pinto-Santini, D. & Parkhurst, S. M. Rho1 interacts with p120ctn and α-catenin, and regulates cadherin-based adherens junction components in Drosophila. *Development* **129,** 3771–3782 (2002).
11. Takaishi, K., Sasaki, T., Kotani, H., Nishioka, H. & Takai, Y. Regulation of cell–cell adhesion by Rac and Rho small G proteins in MDCK cells. *J. Cell Biol.* **139,** 1047–1059 (1997).
12. Braga, V. M. M., Machesky, L. M., Hall, A. & Hotchin, N. A. The small GPTases rho and rac are required for the formation of cadherin-dependent cell–cell contacts. *J. Cell Biol.* **137,** 1421–1431 (1997).
13. Smutny, M. *et al.* Myosin II isoforms identify distinct functional modules that support integrity of the epithelial zonula adherens. *Nat. Cell Biol.* **12,** 696–702 (2010).
14. Carramusa, L., Ballestrem, C., Zilberman, Y. & Bershadsky, A. D. Mammalian diaphanous-related formin Dia1 controls the organization of E-cadherin-mediated cell–cell junctions. *J. Cell Sci.* **120,** 3870–3882 (2007).
15. Meng, W., Mushika, Y., Ichii, T. & Takeichi, M. Anchorage of microtubule minus ends to adherens junctions regulates epithelial cell–cell contacts. *Cell* **135,** 948–959 (2008).
16. Kametani, Y. & Takeichi, M. Basal-to-apical cadherin flow at cell junctions. *Nat. Cell Biol.* **9,** 92–98 (2007).
17. Wolfe, B. A. & Glotzer, M. Single cells (put a ring on it). *Genes Dev.* **23,** 896–901 (2009).
18. Stehbens, S. J. *et al.* Dynamic microtubules regulate the local concentration of E-cadherin at cell–cell contacts. *J. Cell Sci.* **119,** 1801–1811 (2006).
19. Jordan, M. A. & Wilson, L. Use of drugs to study role of microtubule assembly dynamics in living cells. *Methods Enzymol.* **298,** 252–276 (1998).
20. Perez, F., Diamantopoulos, G. S., Stalder, R. & Kreis, T. E. CLIP-170 highlights growing microtubule ends *in vivo*. *Cell* **96,** 517–527 (1999).
21. Shewan, A. M. *et al.* Myosin 2 is a key rho kinase target necessary for the local concentration of E-Cadherin at cell–cell contacts. *Mol. Biol. Cell* **16,** 4531–4532 (2005).
22. Komarova, Y. *et al.* Mammalian end binding proteins control persistent microtubule growth. *J. Cell Biol.* **184,** 691–706 (2009).
23. Komarova, Y. *et al.* EB1 and EB3 control CLIP dissociation from the ends of growing microtubules. *Mol. Biol. Cell* **16,** 5334–5345 (2005).
24. Tatsumoto, T., Xie, X., Blumenthal, R., Okamoto, I. & Miki, T. Human ECT2 is an exchange factor for Rho GTPases, phosphorylated in G2/M phases, and involved in cytokinesis. *J. Cell Biol.* **147,** 921–928 (1999).
25. Somers, W. G. & Saint, R. A RhoGEF and Rho family GTPase-activating protein complex link the contractile ring to cortical microtubules at the onset of cytokinesis. *Dev. Cell* **4,** 29–39 (2003).
26. Liu, X. F., Ishida, H., Raziuddin, R. & Miki, T. Nucleotide exchange factor ECT2 interacts with the polarity protein complex Par6/Par3/protein kinase Czeta (PKCzeta) and regulates PKCzeta activity. *Mol. Cell. Biol.* **24,** 6665–6675 (2004).
27. Sawyer, J. M. *et al.* Apical constriction: a cell shape change that can drive morphogenesis. *Dev. Biol.* **341,** 5–19 (2010).
28. Miyake, Y. *et al.* Actomyosin tension is required for correct recruitment of adherens junction components and zonula occludens formation. *Exp. Cell Res.* **312,** 1637–1650 (2006).
29. Smutny, M. *et al.* Multicomponent analysis of junctional movements regulated by myosin II isoforms at the epithelial zonula adherens. *PLoS One* **6,** e22458 (2011).
30. Kasza, K. E. & Zallen, J. A. Dynamics and regulation of contractile actin-myosin networks in morphogenesis. *Curr. Opin. Cell Biol.* **23,** 30–38 (2011).
31. Monier, B., Pelissier-Monier, A., Brand, A. H. & Sanson, B. An actomyosin-based barrier inhibits cell mixing at compartmental boundaries in Drosophila embryos. *Nat. Cell Biol.* **12,** 60–65 (2009).
32. Fernandez-Gonzalez, R., Simoes Sde, M., Roper, J. C., Eaton, S. & Zallen, J. A. Myosin II dynamics are regulated by tension in intercalating cells. *Dev. Cell* **17,** 736–743 (2009).
33. Mishima, M., Kaitna, S. & Glotzer, M. Central spindle assembly and cytokinesis require a kinesin-like protein/RhoGAP complex with microtubule bundling activity. *Dev. Cell* **2,** 41–54 (2002).
34. Hirose, K., Kawashima, T., Iwamoto, I., Nosaka, T. & Kitamura, T. MgcRacGAP is involved in cytokinesis through associating with mitotic spindle and midbody. *J. Biol. Chem.* **276,** 5821–5828 (2001).
35. Mikawa, M., Su, L. & Parsons, S. J. Opposing roles of p190RhoGAP and Ect2 RhoGEF in regulating cytokinesis. *Cell Cycle* **7,** 2003–2012 (2008).
36. Wildenberg, G. A. *et al.* p120-catenin and p190RhoGAP regulate cell–cell adhesion by coordinating antagonism between Rac and Rho. *Cell* **127,** 1027–1039 (2006).
37. Noren, N. K., Arthur, W. T. & Burridge, K. Cadherin engagement inhibits RhoA via p190RhoGAP. *J. Biol. Chem.* **278,** 13615–13618 (2003).
38. Manchinelly, S. A. *et al.* Mitotic down-regulation of p190RhoGAP is required for the successful completion of cytokinesis. *J. Biol. Chem.* **285,** 26923–26932 (2010).

39. Su, L., Pertz, O., Mikawa, M., Hahn, K. & Parsons, S. J. p190RhoGAP negatively regulates Rho activity at the cleavage furrow of mitotic cells. *Exp. Cell Res.* **315,** 1347–1359 (2009).
40. Bustos, R. I., Forget, M. A., Settleman, J. E. & Hansen, S. H. Coordination of Rho and Rac GTPase function via p190B RhoGAP. *Curr. Biol.* **18,** 1606–1611 (2008).
41. Burbelo, P. D. *et al.* p190-B, a new member of the Rho GAP family, and Rho are induced to cluster after integrin cross-linking. *J. Biol. Chem.* **270,** 30919–30926 (1995).
42. Scott, J. A. & Yap, A. S. Cinderella no longer: alpha-catenin steps out of cadherin's shadow. *J. Cell Sci.* **119,** 4599–4605 (2006).
43. Lien, W. H., Klezovitch, O. & Vasioukhin, V. Cadherin-catenin proteins in vertebrate development. *Curr. Opin. Cell Biol.* **18,** 499–506 (2006).
44. Terry, S. J. *et al.* Spatially restricted activation of RhoA signalling at epithelial junctions by p114RhoGEF drives junction formation and morphogenesis. *Nat. Cell Biol.* **13,** 159–166 (2011).
45. Saint, R. & Somers, W. G. Animal cell division: a fellowship of the double ring? *J. Cell Sci.* **116,** 4277–4281 (2003).
46. Bellett, G. *et al.* Microtubule plus-end and minus-end capture at adherens junctions is involved in the assembly of apico-basal arrays in polarised epithelial cells. *Cell Motil. Cytoskeleton* **66,** 893–908 (2009).
47. Stehbens, S. J., Akhmanova, A. & Yap, A. S. Microtubules and cadherins: a neglected partnership. *Front. Biosci.* **14,** 3159–3167 (2009).
48. Akhmanova, A., Stehbens, S. J. & Yap, A. S. Touch, grasp, deliver and control: functional cross-talk between microtubules and cell adhesions. *Traffic* **10,** 268–274 (2009).
49. Rodriguez, O. C. *et al.* Conserved microtubule-actin interactions in cell movement and morphogenesis. *Nat. Cell Biol.* **5,** 599–609 (2003).
50. Wolfe, B. A., Takaki, T., Petronczki, M. & Glotzer, M. Polo-like kinase 1 directs assembly of the HsCyk-4 RhoGAP/Ect2 RhoGEF complex to initiate cleavage furrow formation. *PLoS Biol.* **7,** e1000110 (2009).

METHODS

Cell culture and transfection. MCF-7, MDCK and HEK293T cells were cultured in DMEM; Caco2 cells were cultured in RPMI media. Cells were transfected using Lipofectamine 2000 (Invitrogen) for expression constructs or with Lipofectamine RNAiMAX (Invitrogen) for RNAi oligonucleotides according to the manufacturer's instructions and analysed 24–48 h after transfection.

Plasmids. The following were gifts: EGFP–ECT2 (R. Saint, Australian National University, Australia); CYK4–EGFP and MKLP1–EGFP (M. Glotzer, University of Chicago, USA); GFP–N17 Rac1-DN (ref. 51; A. Hall, UCL, UK); Raichu-Rac FRET biosensors[52] (M. Matsuda, Kyoto University, Japan); and Flag–p190B RhoGAP (WT) and Flag–p190B ΔRBS (ΔRBS; ref. 40; S. Hansen, Harvard Medical School, USA). pTriEx–RhoA biosensor WT (ref. 4) was obtained from Addgene; pSuper-based simultaneous EB1 and EB3 shRNA vectors, the control vector (expressing luciferase-specific shRNA; ref. 23); and EGFP–Myosin IIA (GFP-Myo IIA) and Ecad–GFP (refs 13,29) have been described previously. Full-length mouse α-catenin was initially cloned into pEGFP–C2 vector and mouse α-catenin deletion mutants were cloned into pEGFP–C1 vector using EcoRI and SalI sites. Truncation mutants were created by PCR mutagenesis based on the secondary structure of α-catenin.

Mass Spectrometry. Mass spectrometry was performed as previously described[53].

siRNA and shRNA knockdowns. A lentivirus-based shRNA system[54,55] was used to deplete ECT2 in MCF-7 cells. The lentivirus expression vector LentiLox pLL5.0 (backbone pLL3.7) and the third-generation packaging constructs pMDLg/pRRE, RSV–Rev and pMD.G were gifts from J. Bear[55] (UNC Chapel Hill, USA). Algorithms from Dharmacon were used to predict sequences that would lead to silencing of human ECT2 (NM_018098). Predicted sequences were used to design shRNAs containing a stem loop sequence based on previous studies[56], and these were cloned into pLL5.0 yielding pLL5.0 Cherry–shECT2. In brief, shRNA was cloned downstream of the U6 promoter (HpaI and XhoI) into a modified version of pLL5.0 carrying a soluble cherry as a reporter gene (pLL5.0 Cherry–shECT2). To reconstitute full-length ECT2 in the same vector, the ECT2 coding sequence was amplified and cloned into the BsrGI site of pLL5.0 Cherry–shECT2 (pLL5.0 mCherry–shRNA resistant ECT2). Alternatively, to reconstitute GFP-tagged shRNA-resistant ECT2 in an ECT2 knockdown background, the mCherry reporter was replaced by a sequence encoding GFP from pEGFP–C1 and then the ECT2 coding sequence was cloned into the vector using EcoR1 and BamH1 sites (pLL5.0 GFP–shRNA resistant ECT2).

The generation and titre of lentivirus stocks has been described previously[13]. MCF-7 cells were infected with lentiviral particles at a multiplicity of infection of 10 per cell as described previously[13] and used within the first week after infection. siRNA and shRNA sequences are shown in Supplementary Table S2.

Antibodies, immunoprecipitations and inhibitors. Primary antibodies used in this study are shown in Supplementary Table S3. Secondary antibodies were species-specific antibodies conjugated with AlexaFluor 488, 594 or 647 (Invitrogen; 1:500) and F-actin was stained with AlexaFluor 488–phalloidin or 594–phalloidin (1:1,000 dilution; Invitrogen).

For each immunoprecipitation assay, ~2 mg of total protein was used, and 2 μg of antibody and 20 ml packed slurry of Protein A or 15 ml packed slurry of GFP-Trap coupled to agarose beads (Chromotek) were added. Surface trypsin sensitivity assays were carried out as described previously[57].

Nocodazole (Sigma Aldrich) was used at 100 nM and the Rho inhibitor CT04 (Cytoskeleton) was used at 0.250 μg ml^{-1}. The Rac inhibitor NSC 23766 (Sigma Aldrich) was used at 50 μM.

Immunofluorescence microscopy. Cells were fixed with 10% TCA on ice for 15 min for RhoA staining or with 4% paraformaldehyde in PBS at 22 °C for 20 min for F-actin staining, and were then permeabilized with 0.25% Triton-X100 in PBS for 5 min at room temperature. Otherwise, cells were fixed with ice-cold methanol for 5 min on ice.

Wide-field images were acquired with either an IX81 Olympus epi-illumination microscope (×60 and ×100, 1.4 numerical aperture (NA) objectives) and a Hamamatsu Orca-1 ER camera driven by Metamorph imaging software (version 7; Universal Imaging) or a Personal Deltavision deconvolution microscope (Applied Precision, ×60, 1.4 NA objectives) and a Roper Coolsnap HQ2 monochrome camera. Confocal images were captured with a Zeiss 510 or a Zeiss 710 Meta laser-scanning confocal microscope, and z-stacks were processed with ImageJ (National Institutes of Health) software. Background correction, contrast adjustment and z-projections of raw data images were performed with ImageJ, Imaris (Bitplane) or Photoshop (Adobe).

Quantification of fluorescence intensity at contacts. The fluorescence intensity at contacts was quantified using the line scan function in ImageJ as described earlier[13]. Up to 50 contacts were measured, derived from three different experiments. To quantify MgcRacGAP or MKLP1 at contacts (Supplementary Fig. S4e), the number of contacts that were positive for the protein was normalized to the total number of contacts. Up to 180 contacts were counted in each experiment and the data from three different experiments were pooled. Data were normalized to control values.

FRET microscopy. MCF-7 cells were transiently transfected with the following constructs; RhoA biosensor[4]; RhoA biosensor with either pLL5.0 Cherry–shECT2 or pLL5.0 mCherry–shRNA-resistant ECT2; Raichu-Rac biosensors[52]. For siRNA experiments, the biosensor was co-transfected with the indicated siRNA and FRET measurements were performed 48 h after transfection. Cells were imaged live at 37 °C by confocal microscopy and images were acquired on an LSM 710 Zeiss confocal microscope equipped with a ×63 oil immersion objective (Plan Apochromat ×63 1.4 NA, Zeiss). Donor and FRET channels were recorded by scanning using a 458 nm laser line and collecting the emission in the donor emission region (BP 470–490 nm) and acceptor emission region (BP 530–590 nm), respectively. In addition, crosstalk and acceptor channels were collected using the 514 nm laser line for excitation and collecting the emission in the donor and acceptor emission regions. Where necessary, a third scan was included to acquire the mCherry fluorescence signal (mCherry channel) using a 561 nm laser line and fluorescence signal was collected in the region 590–620 nm.

A modified version of the FRET emission ratio method[4] was used to calculate this parameter on a pixel-by-pixel basis. The FRET index was calculated for every image as the average (FRET/donor) emission ratio for pixels located in the selected regions of interest (ROIs). FRET values were calculated for the cell–cell junctions and cytosolic regions independently and were normalized to the value corresponding to the average FRET emission ratio value observed at the cell–cell contacts in control conditions. Data presented are mean FRET emission ratios calculated across the different images and their standard errors.

FRAP. FRAP experiments were performed either on an LSM 510 or LSM 710 meta Zeiss confocal microscope with a heated stage maintained at 37 °C. Images were acquired using a ×63 objective, 1.4 NA oil Plan Apochromat immersion lens at ×4 digital magnification.

To assess E-cadherin dynamics, a vector that allows simultaneous expression of a shRNA specific for human E-cadherin and full-length mouse E-cadherin–EGFP (E-cad–GFP; ref. 29) and pLL5.0 Cherry–shECT2 were introduced into MCF-7 cells by lentivirus and cells analysed after 24 h. A constant ROI in the centre of the cell–cell contact was bleached to ~70% with a 488 nm laser at 100%. Time-lapse images were acquired before and after photobleaching with an interval of ~5 s per frame for a total of 280 s. Image analysis was performed using ImageJ. To calculate FRAP profiles, a ROI at the bleached GFP–E-cadherin area was marked and the plug-in FRAP profiler (McMaster University) was applied to obtain fluorescence intensity profiles, $F(t)$. Fluorescence intensities were normalized to prebleach values $F(-t)$ and fitted to the equation:

$$\text{Fluorescence recovery} = \frac{F(t)-F(0)}{F(-t)} = Mf \cdot \left(1 - e^{\frac{\ln 2 \cdot t}{t_{1/2}}}\right)$$

where $F(t)$ is the average fluorescence of the ROI, Mf is the mobile fraction, $t_{1/2}$ is the half-time of recovery and t is time in seconds.

ECT2 dynamics were assessed using EGFP–ECT2 expressed with ECT2 shRNA by lentiviral infection. A constant circular ROI in the centre of the cell–cell contact was bleached to ~70% with 488 and 405 nm lasers at 100%. Time-lapse images of the same were acquired before (20 frames, 5 s) and after (210 frames, 50 s) photobleaching with an interval of ~250 ms per frame. Image analysis was performed using ImageJ. To calculate FRAP profiles, a ROI at the bleached GFP–ECT2 area was marked and its average fluorescence intensity was determined at every time point. Fluorescence intensities were normalized to average prebleach values $F(-t)$ and fitted to the double exponential equation:

$$\text{Fluorescence recovery} = \frac{F(t)-F(0)}{F(-t)} = Mf \cdot \left[f_{\text{fast}} \cdot \left(1 - e^{\frac{\ln 2 \cdot t}{t^{\text{fast}}_{1/2}}}\right)\right] + Mf \cdot \left[f_{\text{slow}} \cdot \left(1 - e^{\frac{\ln 2 \cdot t}{t^{\text{slow}}_{1/2}}}\right)\right]$$

where $F(t)$ is the average fluorescence of the ROI, Mf is the mobile fraction, f_{fast} and f_{slow} are weighting factors for fast and slow mobile components, $t^{\text{fast}}_{1/2}$ and $t^{\text{slow}}_{1/2}$ their

DOI: 10.1038/ncb2532

respective half-times and t is time in seconds. A numerical solution of the above equation for Fluorescence recovery = 0.5 was applied to obtain the global half-time for ECT2 recovery.

Laser nanoscissors. Ablation experiments were performed on an LSM 510 meta Zeiss confocal microscope at 37 °C. Images were acquired using a ×63 objective, 1.4 NA oil Plan Apochromat immersion lens at ×1.5 digital magnification, with the pinhole adjusted to 3 Airy units to obtain optical sections 2 µm thick. Time-lapse images were acquired before (3 frames) and after (4 frames) ablation with an interval of 15 s per frame. For ablation, a Ti:sapphire laser (Chameleon Ultra, Coherent Scientific) tuned to 790 nm was used to ablate cell contacts identified with E-cadherin–GFP fluorescence emission. A constant ROI was marked for each experiment and ablated with 30 iterations of a 790 nm laser with 50% transmission. GFP fluorescence intensity was determined before and after the induced ablation using a 488 nm laser for excitation and a 500–550 nm emission filter.

51. Ridley, A. J., Paterson, H. F., Johnston, C. L., Diekmann, D. & Hall, A. The small GTP-binding protein rac regulates growth factor-induced membrane ruffling. *Cell* **70,** 401–410 (1992).
52. Itoh, R. E. *et al.* Activation of rac and cdc42 video imaged by fluorescent resonance energy transfer-based single-molecule probes in the membrane of living cells. *Mol. Cell. Biol.* **22,** 6582–6591 (2002).
53. Grigoriev, I. *et al.* STIM1 is a MT-plus-end-tracking protein involved in remodelling of the ER. *Curr. Biol.* **18,** 177–182 (2008).
54. Rubinson, D. A. *et al.* A lentivirus-based system to functionally silence genes in primary mammalian cells, stem cells and transgenic mice by RNA interference. *Nat. Genet.* **33,** 401–406 (2003).
55. Vitriol, E. A., Uetrecht, A. C., Shen, F., Jacobson, K. & Bear, J. E. Enhanced EGFP-chromophore-assisted laser inactivation using deficient cells rescued with functional EGFP-fusion proteins. *Proc. Natl Acad. Sci. USA* **104,** 6702–6707 (2007).
56. Reynolds, A. *et al.* Rational siRNA design for RNA interference. *Nat. Biotechnol.* **22,** 326–330 (2004).
57. Verma, S. *et al.* Arp2/3 activity is necessary for efficient formation of E-cadherin adhesive contacts. *J. Biol. Chem.* **279,** 34062–34070 (2004).

DOI: 10.1038/ncb2532

nature cell biology

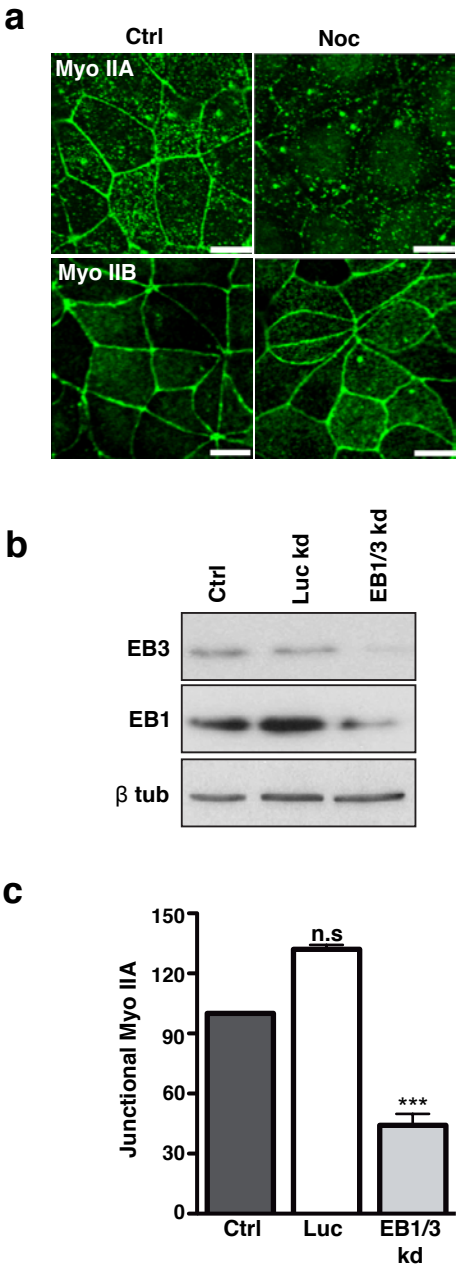

Figure S1 Dynamic microtubules selectively support junctional localization of myosin IIA but not myosin IIB. (a) Confluent MCF-7 cells were treated with DMSO (Ctrl) or nocodazole (Noc, 100nM, 3h), fixed and stained for myosin IIA (Myo IIA) or myosin IIB (Myo IIB). Representative apical confocal images are shown. (b) MCF-7 cells were transfected with pECFP-C1 (Ctrl) or with pSUPER constructs containing shRNAs encoding RNAi against Luciferase (Luc) or EB1 + EB3 (EB1/3) and whole cell lysates were prepared after 48 hours. Lysates were immunoblotted for EB1, EB3 and b-tubulin (b-tub). (c) MCF-7 cells were transfected with pECFP-C1 or with pSUPER constructs containing shRNAs encoding RNAi against Luciferase (Luc) or EB1 + EB3. Junctional myosin IIA (Myo IIA) in CFP-positive cells was quantified by linescan analysis; data represent mean ± S.E.M. pooled from three individual experiments (n=15), ***P<0.001; One way Anova, Dunnett's post hoc test. Scale bar: 10 μm.

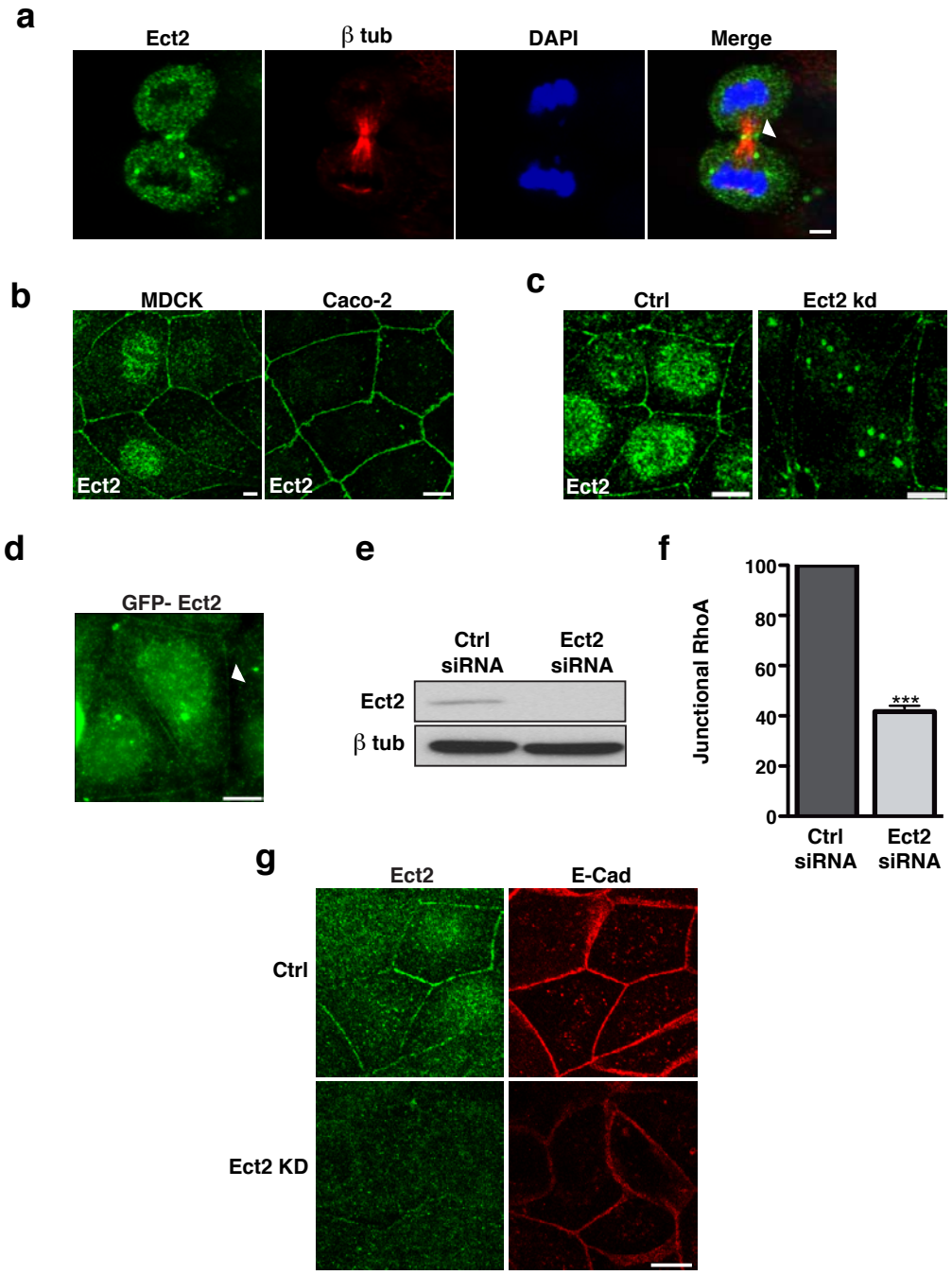

Figure S2 Ect2 localization and knockdown. (a) MCF-7 cells stained for Ect2 (green), β-tubulin (β-tub, red) and DAPI to detect Ect2 at the cytokinetic furrow. Representative images of cells undergoing cytokinesis are shown. (b) Caco-2 and MDCK cells were fixed and stained for Ect2 (green). Representative apical confocal images are shown. (c) Ect 2 staining in MCF-7 cells infected with lentivirus bearing an empty vector control (Ctrl) or an shRNA-directed against Ect2 (Ect2 kd). Representative apical confocal images are shown. (d) MCF-7 cells were transiently transfected with an expression construct encoding EGFP-Ect2. Cells were fixed and stained for GFP 36-48h-post transfection. Arrowheads indicate accumulation of the transgene at junctions. (e) Lysates from MCF-7 cells transfected with SMARTpool siRNA against Ect2 (Ect2 siRNA) or non-targeting siRNA pools (Ctrl siRNA) were immunoblotted for Ect2 and β-tubulin (β-tub). (f) MCF-7 cells transfected with SMARTpool siRNA against Ect2 (Ect2 siRNA) or non-targeting siRNA pools (Ctrl siRNA) were fixed and stained for RhoA and fluorescence intensity of RhoA at cell junctions was quantitated by linescan analysis. Data represent mean ± S.E.M. pooled from three individual experiments (n=25), ***P<0.001; One way Anova, Dunnett's post hoc test. (g) E-cadherin (E-Cad,red) and Ect2 (green) immunostaining in Control (Ctrl) and Ect2 knockdown (Ect2 KD) cells imaged by wide-field deconvolution microscopy. Scale bars: a,b,d 5 μm; c,g 10 μm.

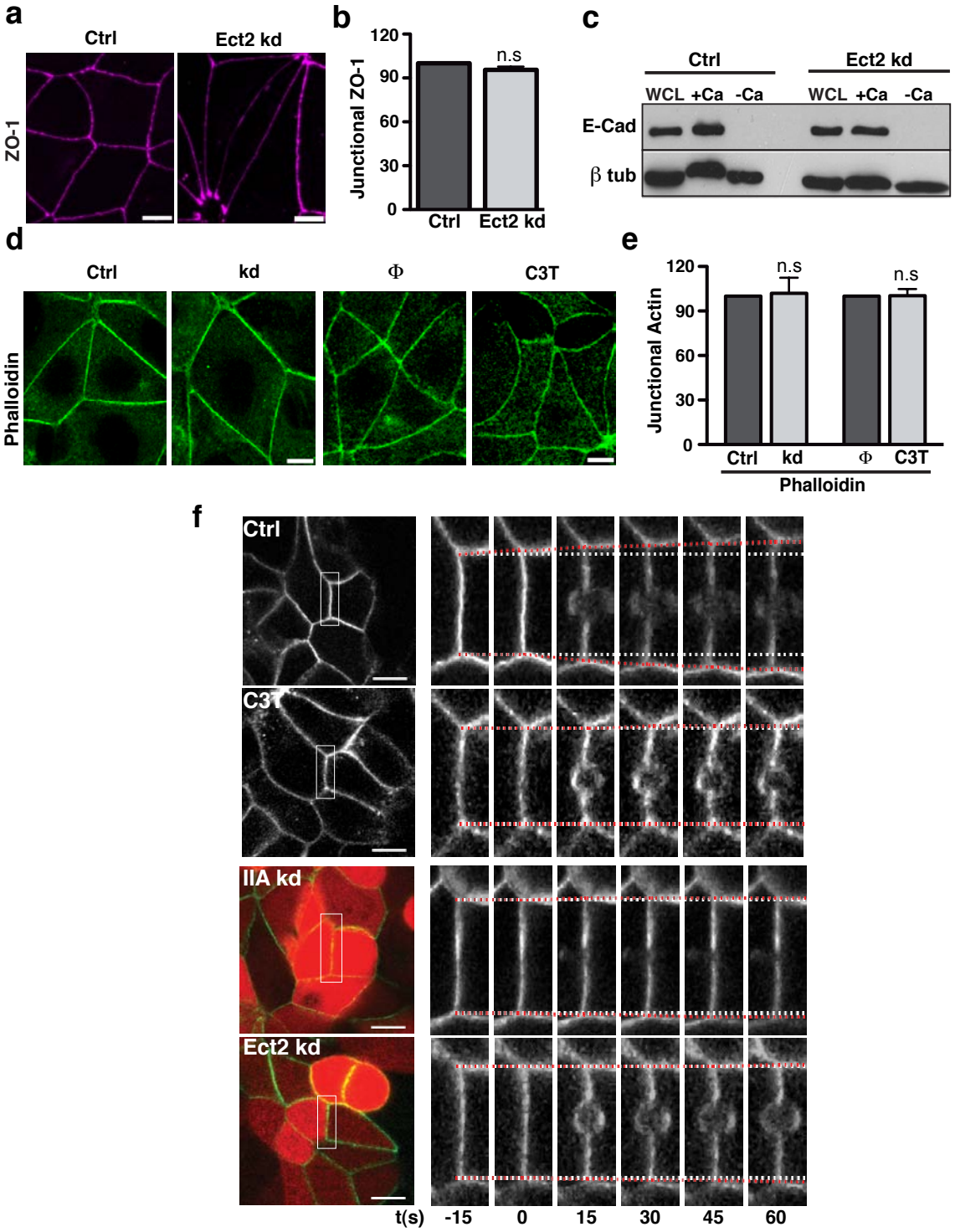

Figure S3 Ect2 knockdown does not affect tight junctions or total and surface expression levels of E-Cadherin. (a-b) Immunostaining for Zona occludens protein 1 (ZO-1) in control (Ctrl) and Ect2 knockdown (Ect2kd) cells. Representative apical confocal images were taken (a) and junctional ZO-1 was quantitated by linescan analysis (b). Data represent mean ± S.E.M. pooled from three individual experiments (n= 25, n.s. Student's *t*-test). (c) Surface expression of E-cadherin was measured using surface trypsin protection assays in control (Ctrl) and Ect2 knockdown (Ect2kd) cells. Cells were lysed immediately (WCL) or after trypsinisation in the presence (+Ca) or absence (–Ca) of extracellular Ca^{2+} . Lysates were immunoblotted for E-Cadherin (E-Cad) and β-tubulin (β-tub). (d,e) Control (Ctrl) and Ect2 knockdown (kd) cells and cells treated with glycerol (vehicle control, Φ) or C3T (0.25μg/ml) for an hour were fixed and stained for F-actin (phalloidin). Representative confocal images were taken (d) and junctional F-actin was quantified by linescan analysis (e). Data represent mean ± S.E.M. pooled from three individual experiments (n=17); n.s. no statistically significant difference was identified by Student's *t*-test). (f) Junctional tension was measured by laser nanoscissors in control (Ctrl) MCF7 cells and cells treated with C3-T (C3T) or RNAi to Ect2 (Ect2 kd) or Myosin IIA (IIA kd). Representative confocal images were taken at various time points before and after ablation. The region of ablation is indicated in each case. Scale bars: 10 μm.

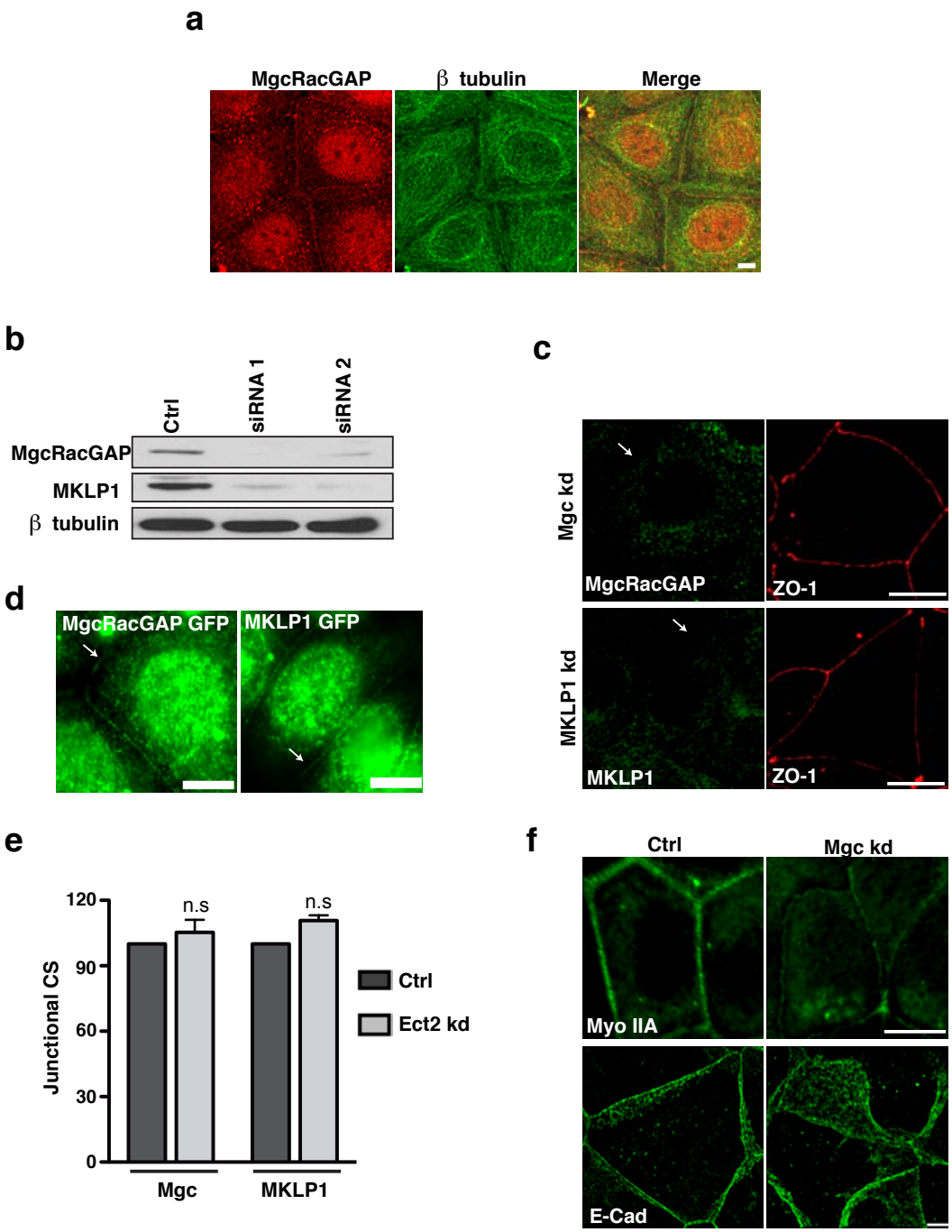

Figure S4 Centralspindlin and the zonula adherens. (a) MCF-7 cells were fixed and stained for MgcRacGAP (MgcRacGAP, red) and b-tubulin (b-tub, green) Representative apical confocal images were taken. (b) Lysates from MCF-7 cells transfected with two different siRNAs (siRNA1 and siRNA2) each against MgcRacGAP (MgcRacGAP) or MKLP1 (MKLP1) or with scrambled siRNA (Ctrl) were immunoblotted for MgcRacGAP or MKLP1 and β-tubulin (β-tub). (c) MCF-7 cells were transfected with siRNAs against MgcRacGAP (Mgc kd), MKLP1 (MKLP1 kd) or with scrambled siRNA (Ctrl). Cells were fixed after 48 hours and stained for MgcRacGAP (MgcRacGAP) or MKLP1 and ZO-1. Representative apical confocal images were taken. Arrows indicate lack of junctional staining for MgcRacGAP or MKLP1 in knockdown cells. (d) MCF-7 cells were transiently transfected with expression constructs encoding MgcRacGAP-EGFP (MgcRacGAP GFP) or MKLP1-EGFP (MKLP1 GFP). Cells were fixed and stained for GFP 36-48h-post transfection. Arrows indicate accumulation of the transgene at junctions. (e) Junctional MgcRacGAP and MKLP1 were immunostained in control (Ctrl) and Ect2 knockdown (Ect2 kd) cells. Data represent the percentage of contacts that stained for MgcRacGAP (Mgc) or MKLP1 normalised to the total number of contacts. Data represent mean ± S.E.M. pooled from three individual experiments (n=60; n.s. no statistically significant difference was identified by Student's *t*-test). (f) MCF-7 cells were transfected with siRNA against MgcRacGAP (Mgc kd). Cells were fixed after 48 hours and stained for myosin IIA (Myo IIA) and E-Cadherin (E-Cad). Representative apical confocal images were taken. Scale bars: a,d 5μm; d 10 μm ; f Myo IIA 10 μm, E-Cad 5 μm.

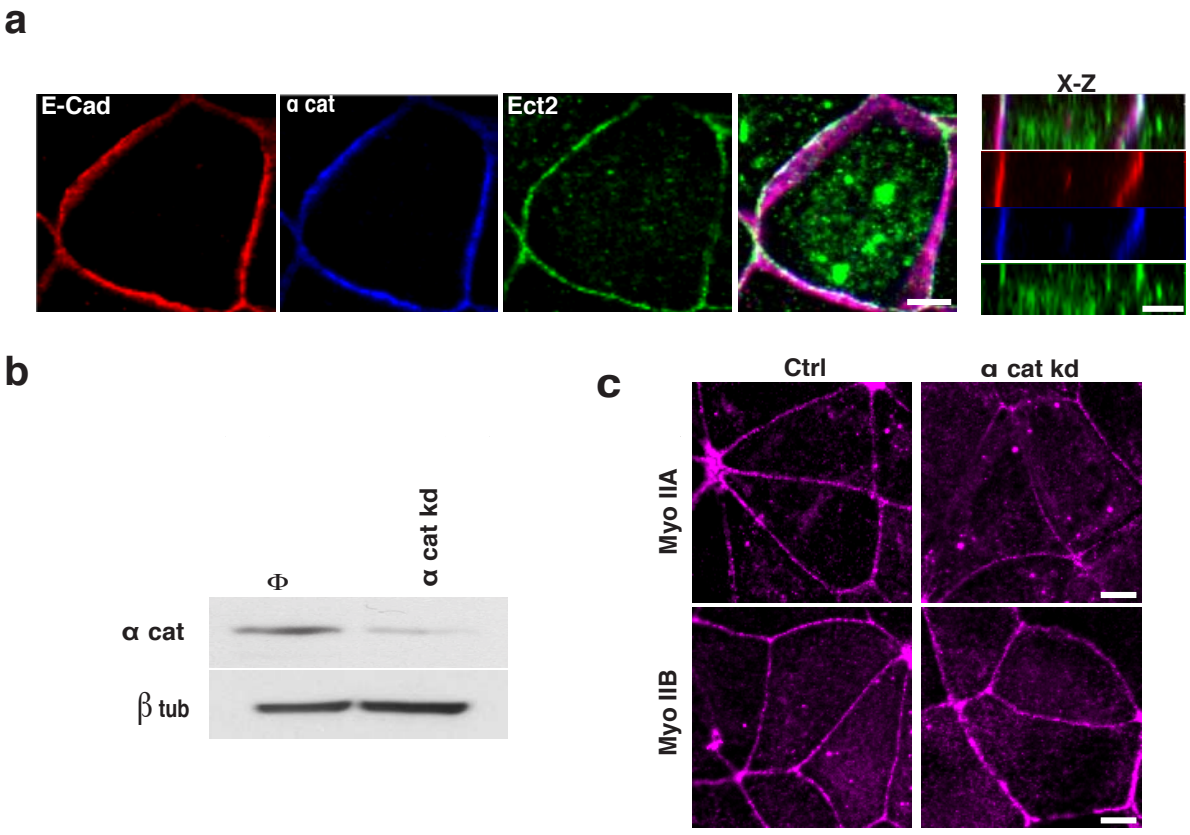

Figure S5 Impact of α-catenin on Ect2 at the zonula adherens. (a) Magnified image of MCF-7 cells fixed and stained for E-Cadherin (E-Cad, red), α- catenin (α cat , blue) and Ect2 (green). Representative confocal images were taken at the ZA and the distribution of proteins along the *z*-axis of cells is represented in *x–z* views. (b) Lysates from MCF-7 cells transfected with SMARTpool siRNA against α- catenin (α cat kd) or non-targeting siRNA pools (Φ) were immunoblotted for α- catenin (α cat) and β-tubulin (β-tub). (c) MCF-7 cells transfected with SMARTpool siRNA against α- catenin (α cat kd) or non-targeting siRNA pools (Ctrl) were fixed and stained for Myosin IIA (Myo IIA) or Myosin IIB(Myo IIB). Representative confocal images were taken. (d) Schematic representation of full length a-catenin (FL) and the constructs used. The positions of the VH1, VH2, VH3 domains are indicated. Scale bars: a 5 μm; c 10 μm.

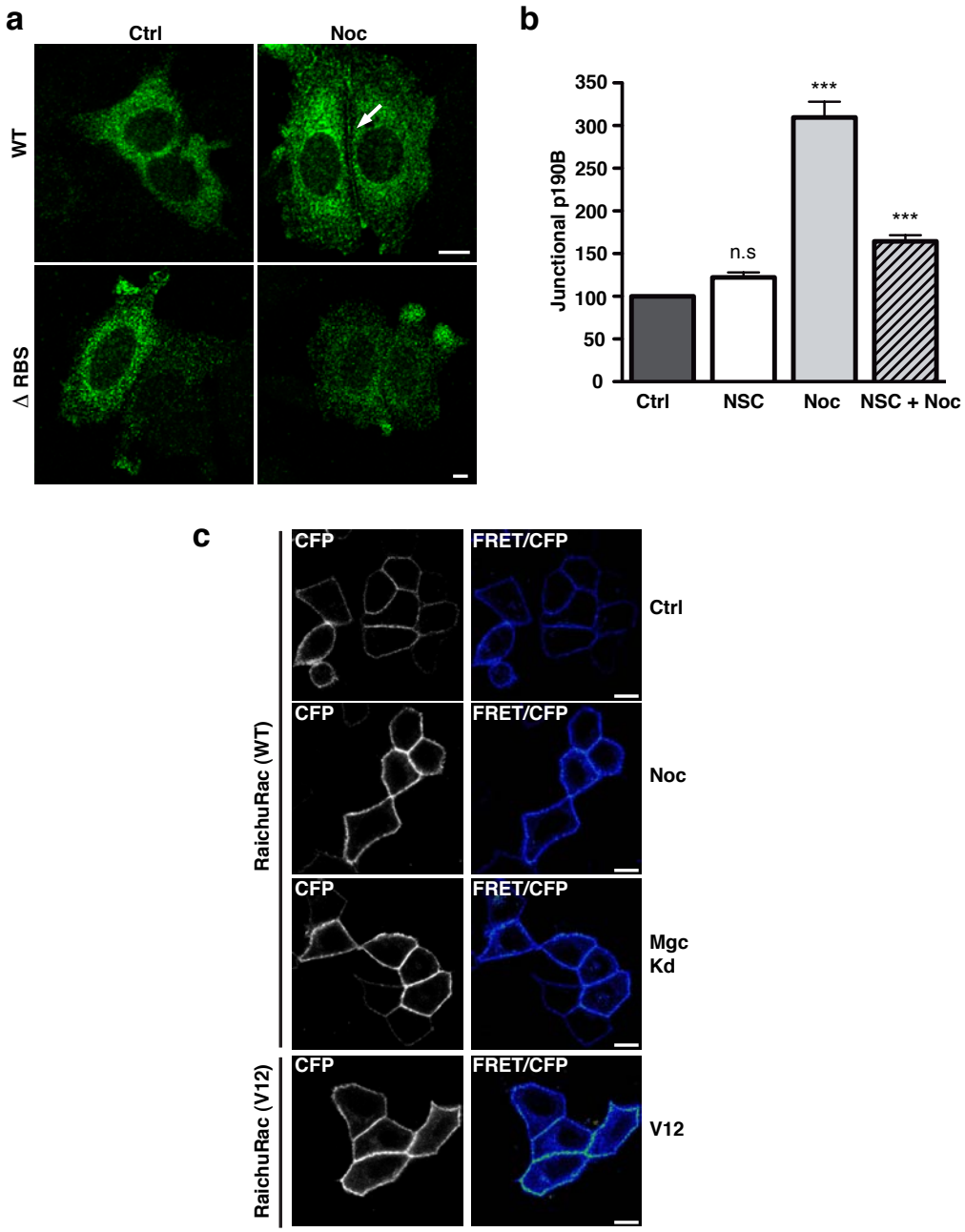

Figure S6 Nocodazole-induced recruitment of p190 B RhoGAP requires Rac signaling. (a) MCF-7 cells were transfected with either Flag-p190B RhoGAP (WT) or Flag-p190BΔRBS (DRBS) and then treated with DMSO (vehicle control, Ctrl) or Nocodazole (Noc). Cells were fixed and stained for FLAG. Representative apical confocal images were taken. Arrow indicates increase in junctional p190B in Nocodazole treated cells. (b) MCF-7 cells were treated with DMSO (Ctrl), Nocodazole alone (100nM,3h, Noc), NSC 23766 alone (50μM, 12h, NSC) or NSC 23766 and Nocodazole (Nocodazole was added in the last three hours of NSC incubation, Noc + NSC). Junctional p190 B RhoGAP was quantitated by linescan analysis. Data represent mean ± S.E.M. pooled from three individual experiments (n=25; ***P<0.001; One way Anova, Dunnett's post hoc test). (c) Junctional Rac-GTP was measured by using a Raichu-Rac biosensor expressed in control (Ctrl) cells or cells treated with nocodazole (Noc), MgcRacGAP RNAi (Mgc kd) or a transiently expressed constitutively-active Rac mutant (V12). Representative images of CFP and ratio of FRET/CFP are shown. Scale bars: a, c 10μm,

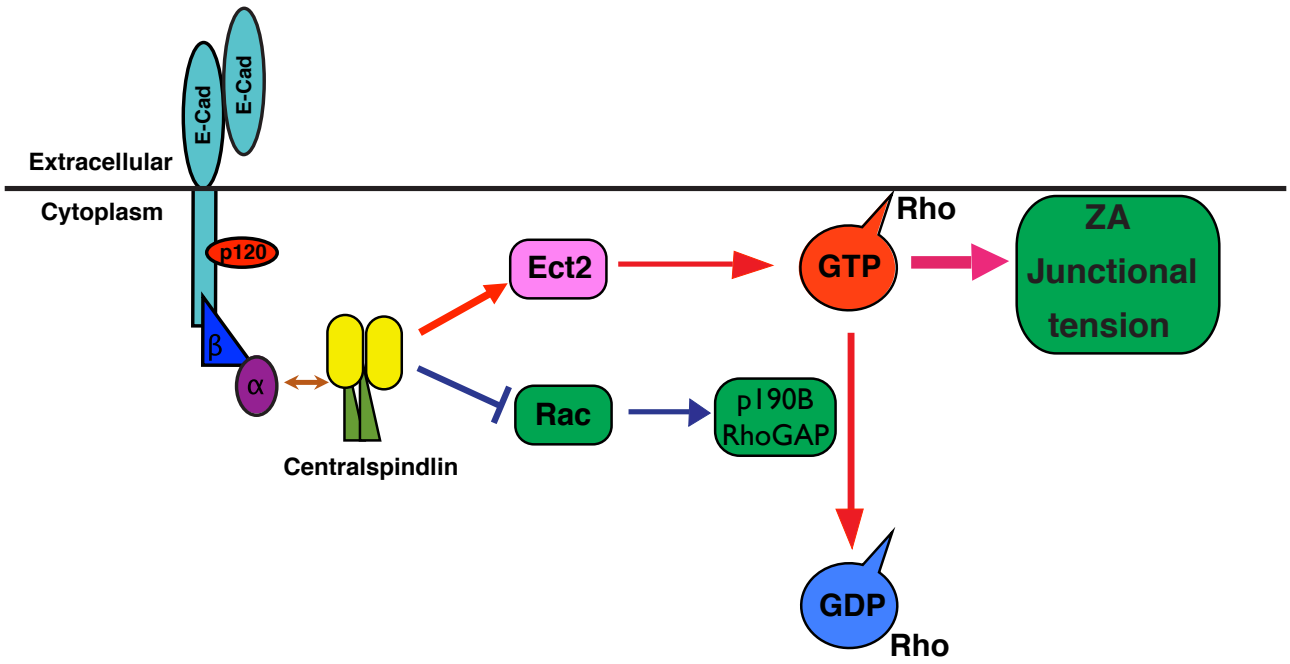

Figure S7 A model for coordination of Rho regulation at the zonula adherens by centralspindlin.

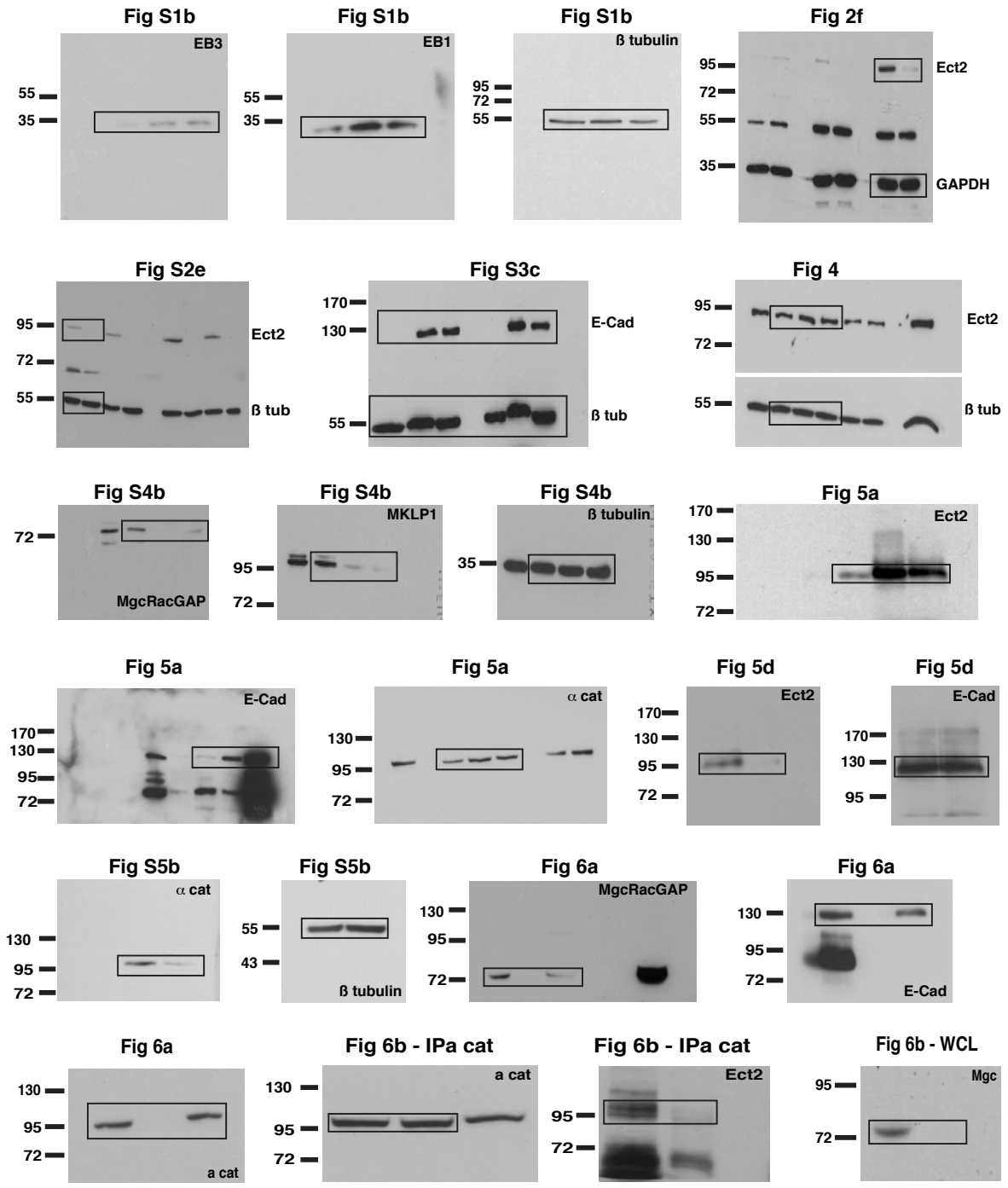

Figure S8 Uncropped Western Blots related to figures S1b, 2f, S2e, S3c, 4, S4b, 5a, 5d, s5b, 6a, 6b.

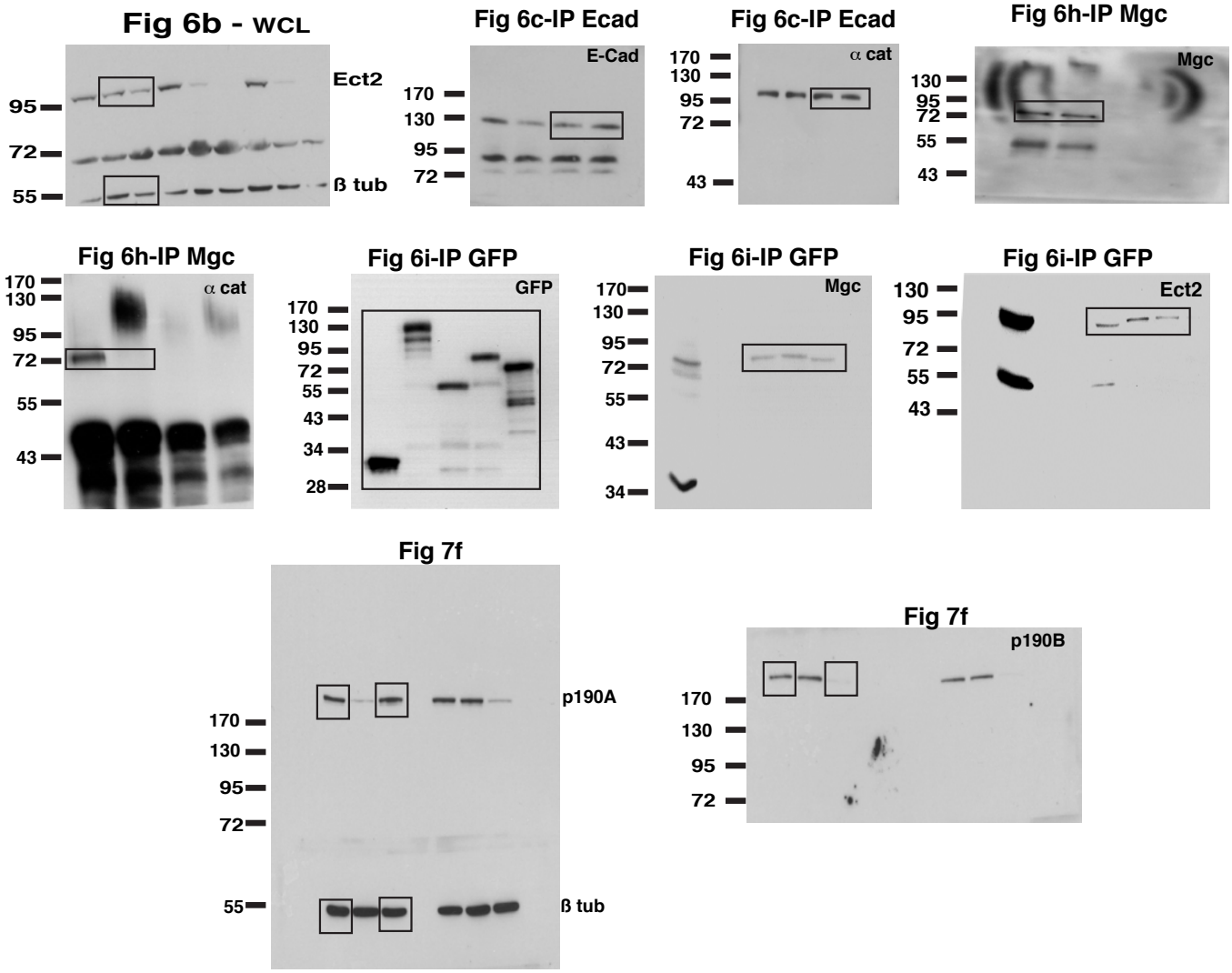

Figure S9 Uncropped Western Blots related to figures 6b, 6c, 6h, 6i, 7f.

Table S1 FRAP analysis of E-cadherin-GFP in control, Ect2 KD, Myosin IIA KD, and C3 transferase-treated cells. Fluoresence recovery after photobleaching E-cadherin-GFP expressed in E-cadherin knock-down cells treated with or without Ect2 RNAi, Myosin IIA RNAi or C3-transferase. Fluoresence recovery parameters are shown.

Table S2 List of siRNA and shRNA sequences. DNA sequences used for RNAi experiments. siRNAs were commercially-available oligonucleotide pools.

Table S3 Primary antibodies for immunofluorescence and western blotting. Details of primary antibodies used in these experiments: species, sources and dilutions used.

7. Appendix 2

Review Article accepted in the journal Current Topics in Developmental Biology; *in press*

CHAPTER THREE

Active Tension: The Role of Cadherin Adhesion and Signaling in Generating Junctional Contractility

Rashmi Priya, Alpha S. Yap[1]
Division of Cell Biology and Molecular Medicine, Institute for Molecular Bioscience, The University of Queensland, Brisbane, Queensland, Australia
[1]Corresponding author: e-mail address: a.yap@uq.edu.au

Contents

Abstract

In this chapter, we discuss the cell biology of contractility at cell–cell junctions. As discussed elsewhere in this volume, contractile forces play key roles in development and tissue homeostasis. Here, we review our understanding of the cellular mechanisms that functionally and physically link cadherin adhesion to the actomyosin contractile apparatus of the cell. Focusing on epithelia, we argue that E-cadherin junctions can be

Current Topics in Developmental Biology, Volume 112
ISSN 0070-2153
http://dx.doi.org/10.1016/bs.ctdb.2014.11.016

considered as active mechanical agents, which contribute to the assembly of actomyosin at the junctional cortex itself. This reflects cortical signaling, notably that regulated by the Rho GTPase, coordinated with actin regulation at junctions. The product, contractile tension at junctions, can then be regarded as an emergent property of a complex dynamical system that integrates adhesion with the cytoskeleton.

1. INTRODUCTION

Cell–cell interactions have long been recognized to participate in the genesis and homeostasis of tissue organization. Adhesive interactions between cells influence patterning in the early embryo and counteract forces that tend to disrupt tissue integrity (Levine, Lee, Kintner, & Gumbiner, 1994; Takeichi, 2014). These adhesive interactions have commonly been envisaged as passive resistance elements that respond to large-scale forces acting on organisms and tissues. Increasingly, we have come to realize that many of the forces that act upon cell–cell adhesions are generated by the neighboring cells themselves (Gomez, McLachlan, & Yap, 2011; Luo et al., 2013). Effectively, cells pull upon each other and cell–cell adhesion systems serve to mechanically couple the contractile apparatuses of neighboring cells together (Maitre et al., 2012). This is best understood for epithelia where a dominant adhesion system is mediated by E-cadherin. Mechanical coupling of contractility to E-cadherin adhesion is reflected in contractile tension within junctions that scales-up to tissue level patterns of tension (Fernandez-Gonzalez, Simoes Sde, Roper, Eaton, & Zallen, 2009; Martin, Gelbart, Fernandez-Gonzalez, Kaschube, & Wieschaus, 2010; Rauzi, Verant, Lecuit, & Lenne, 2008). Adhesion can effectively convert the isolated contractile apparatus of a single cell into a supracellular contractile network. This is implicated in both local cellular rearrangements and tissue-level morphogenesis (Martin, 2010).

At the cellular level, contractility is predominantly generated by the actomyosin system, involving the interaction of F-actin microfilaments with myosin II motors (Vicente-Manzanares, Ma, Adelstein, & Horwitz, 2009). Mechanistically, a key question is how cadherin molecular systems physically interact with actomyosin to couple adhesion and contractility. However, cadherin adhesion also contributes to the biogenesis of actomyosin at cell–cell junctions (Ladoux et al., 2010; Shewan et al., 2005). This entails the recruitment of cytoskeletal regulators to the junctional cortex, responding to cortical signals that are often influenced by cadherin adhesion

itself (Ratheesh & Yap, 2012). Thus, the integration of adhesion and contractility not only reflects the passive association of cadherins with the cytoskeleton but also involves an *active* role of adhesion in establishing the junctional cytoskeleton (Kovacs, Goodwin, Ali, Paterson, & Yap, 2002; Kovacs et al., 2011; Priya, Yap, & Gomez, 2013; Shewan et al., 2005; Smutny et al., 2011). In this chapter, we review our growing understanding of how this comes about. A recurring theme in this discussion is the emerging role that contractile tension itself can play in regulating actomyosin at cell–cell junctions.

2. THE CONTRACTILE APPARATUS: ACTOMYOSIN

Actomyosin constitutes the principal contractile apparatus in nonmuscle cells, as well as in muscle (Fernandez-Gonzalez & Zallen, 2009; Kasza & Zallen, 2011; Fig. 1). Contractility is generated by the physical interaction of the myosin II head domains with actin filaments. In the best-understood model, force is generated by the ability of myosin II to slide actin filaments once the motor is activated by phosphorylation of its regulatory light chain (RLC) (Craig, Smith, & Kendrick-Jones, 1983; Matsumura, 2005). myosin II activation also entails the assembly of Myosin motors into antiparallel minifilaments that can each consist of 10–30 individual myosins (Heissler & Manstein, 2013; Niederman & Pollard, 1975). This antiparallel orientation allows minifilaments to slide F-actin inward, thereby generating contractility (Fig. 1B). Importantly, the organization of the actin filaments with which myosin interacts can influence contractile output (Reymann et al., 2012). This is exemplified by the alignment of myosin minifilaments with parallel actin filaments that is found in the sarcomeres of muscle cells. Something similar has also been observed at epithelial cell–cell junctions (Ebrahim et al., 2013). However, Myosin minifilaments can also act upon actin filaments that are organized into less well organized, nonparallel networks; under these latter circumstances, contractility can aggregate F-actin and even induce filament turnover (as will be discussed further below) (Haviv, Gillo, Backouche, & Bernheim-Groswasser, 2008; Reymann et al., 2012).

The functional impact of actomyosin is demonstrated by the observation that morphogenetic events, such as germ-band extension during *Drosophila* development, are perturbed when components of myosin II are depleted from embryos (Bertet, Sulak, & Lecuit, 2004) This is thought to reflect local

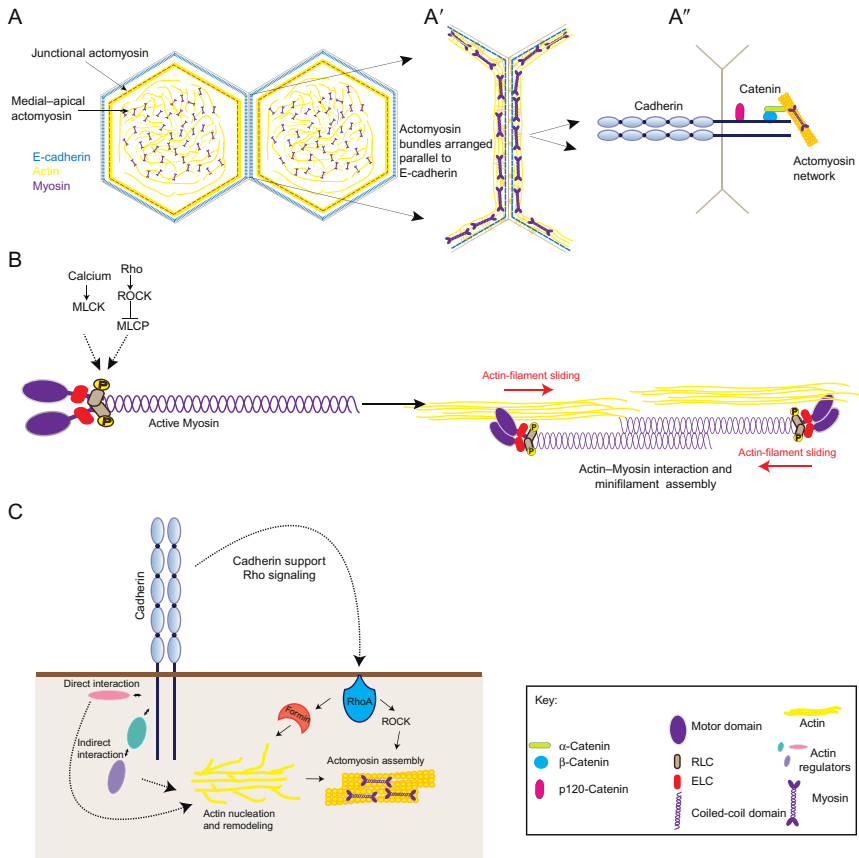

Figure 1 The contractile apparatus at junctions and its biogenesis. (A) Spatial relation of actomyosin network with cadherin junctions. F-actin and myosin form a mesh at the apical pole of the cells (medial–apical network) and also orient themselves parallel to the junctions (junctional actomyosin). (A′) The contractile cortices of neighboring cells are mechanically coupled through association with the cadherin–catenin complex (A″). (For clarity, this coupling is illustrated only for junctional actomyosin.) (B) Kinases (ROCK and MLCK) activate myosin by phosphorylating its RLC. This leads to association of myosin with F-actin and minifilament assembly (which is also controlled by heavy chain phosphorylation). (C) Cadherin ligation recruits actin regulators directly or indirectly via adaptor proteins to modulate local actin assembly and remodeling. Cadherin can also scaffold upstream Rho activators and thus support Rho signaling, which further mediates actomyosin assembly via its effectors.

cellular rearrangements that are driven by contractile coupling to cadherin cell junctions. Consistent with this, a number of patterns of myosin II networks are found to mechanically associate with junctions in tissues and cultured epithelial cells. One pattern involves myosin II networks located

at the apical poles of epithelial cells (often described as medial–apical networks; Martin, Kaschube, & Wieschaus, 2009); these commonly display pulsatile contractions which are transmitted to junctions. As well, myosin II accumulates at cell–cell junctions themselves, typically decorating F-actin bundles that circumscribe the apical junctions (Shewan et al., 2005; Smutny et al., 2010; Wu et al., 2014; Fig. 1A). These also contribute to contractile tension in junctions. But the latter appear to manifest as a line tension in the apical junctions rather than the pulsatile fluctuations seen with medial–apical networks. In both these systems, active myosin must physically interact with the cadherin adhesion system to allow force to be transmitted to, and through, junctions. This involves both cell-signaling pathways that regulate the activity and localization of myosin II and association of myosin-bound actin filaments with the cadherin complex (Fig. 1C).

2.1. The role of cadherin signaling in myosin II regulation

As noted in the preceding text, myosin II is regulated by a variety of cellular signals. In the best-characterized model, phosphorylation of the RLC (at Thr18 and Ser19) promotes F-actin binding and actin-induced ATPase activity (Heissler & Manstein, 2013); it also allows myosins to assemble into minifilaments (Sellers, 1991). Monophosphorylation of Ser19 is sufficient to stimulate myosin ATPase activity, motor activity, and minifilament assembly, although these can be further enhanced by additional phosphorylation of Thr18 (Julian & Olson, 2014). These combined effects promote actin filament sliding and therefore contractility. RLC phosphorylation is, in turn, determined by the balance between the action of kinases and myosin light-chain phosphatase (MLCP; Julian & Olson, 2014; Schofield & Bernard, 2013). A number of kinases can directly phosphorylate RLC, including myosin light-chain kinase (MLCK), which commonly responds to changes in intracellular Ca^{2+} levels that can activate contractility (Heissler & Manstein, 2013). Rho kinase (ROCK) is another Ser/Thr kinase that mediates signaling downstream of the small GTPase, Rho, a major regulator of cellular contractility (Riento & Ridley, 2003). Although ROCK can directly phosphorylate myosin *in vitro*, within cells its major impact may occur indirectly. In contrast to MLCK, ROCK can also inhibit the action of MLCP, thereby preventing RLC dephosphorylation (Amano et al., 1996; Kimura et al., 1996; Totsukawa et al., 2000).

Both MLCK and ROCK participate in building the contractile cytoskeleton at cadherin junctions (Smutny et al., 2010). In the case of ROCK,

this appears to reflect an E-cadherin-based Rho signaling pathway (which will be discussed in greater detail below). Thus, myosin II can be recruited to sites of adhesion when E-cadherin alone is ligated, which is isolated from other juxtacrine pathways that may come into effect when cell surfaces come into contact with one another (Shewan et al., 2005). This implies that cadherin adhesion itself can provide an instructive cue to recruit myosin II. Myosin recruitment to cadherin adhesions is disrupted when ROCK is inhibited, implying that ROCK serves in a cadherin-dependent signaling pathway to activate myosin II (Shewan et al., 2005). Similarly, junctional myosin II levels are reduced when ROCK is inhibited (Smutny et al., 2010). Consistent with the role of ROCK as a major mediator of Rho signaling (Riento & Ridley, 2003), junctional myosin II and contractile tension are also reduced when Rho signaling itself is blocked or the molecular mechanisms that activate Rho at junctions are disrupted (Ratheesh et al., 2012). The ability of myosin activation to promote junctional localization of the motor likely reflects the increased F-actin binding that accompanies RLC phosphorylation, as junctional myosin II is lost when junctional F-actin is reduced (Leerberg et al., 2014; Verma et al., 2012). MLCK is also necessary for E-cadherin adhesion to recruit myosin II (Shewan et al., 2005; Smutny et al., 2010), and intracellular calcium signaling is increased at junctions when cells make contacts with one another (Nigam, Rodriguez-Boulan, & Silver, 1992). However, what relationship this has to cadherin signaling has yet to be determined. As well, it is likely that many other signaling pathways impinge to influence the biogenesis and contractile activity of actomyosin at junctions.

Interestingly, mammalian cells have three myosin II paralogs (A–C) (Vicente-Manzanares et al., 2009), in contrast to the single myosin II possessed by invertebrates, and different sets of signaling pathways may influence individual myosin II paralogs at cadherin junctions in mammalian cells. For example, although both myosin IIA and myosin IIB were found at the zonulae adherente (ZA) in cultured MCF7 cells, a breast epithelial cell line, inhibition of Rho-ROCK signaling reduced the junctional accumulation of myosin IIA to a significantly greater extent than it did myosin IIB accumulation (Smutny et al., 2010). In contrast, myosin IIB localization was preferentially sensitive to Src and Rap1 activity (Smutny et al., 2010). Thus, multiple signaling pathways may determine the ability of different myosin paralogs to recruit to, and exert contractile force upon, cadherin-based cell–cell junctions.

2.2. F-actin mediates the association of myosin motors with cadherin adhesion

For activated myosin to generate contractile force upon junctions, molecular mechanisms are necessary to physically link myosin II to the cadherin adhesion complex. To date, there is no convincing evidence that myosin II interacts directly with cadherins or their associated proteins. Instead, it is probable that the mechanical coupling is achieved through the actin filaments with which the myosins interact. Junctional myosin is reduced, and contractile tension compromised, when the assembly of actin filaments is decreased at the junctions, either by drugs that disrupt F-actin or when regulators of F-actin dynamics are perturbed (Leerberg et al., 2014; Verma et al., 2012; Wu et al., 2014). This implies that cortical F-actin also contributes to localizing myosin II to the junctions.

How cadherin complexes associate with F-actin is an active and controversial area which has been reviewed in detail elsewhere (Ratheesh & Yap, 2012). For the purposes of the present discussion, it is sufficient to emphasize the following points. A number of actin-binding proteins can associate with E-cadherin and potentially serve to couple adhesion complexes to cortical F-actin (Fig. 2A). These include α-catenin, undoubtedly the most extensively discussed candidate, and also proteins such as vinculin, cortactin, and myosin VI. The reason(s) for this variety have yet to be resolved. Importantly, there is increasing evidence that contractile tension may influence the activity of some of these proteins. For example, α-catenin can directly associate with F-actin. Despite this, early efforts failed to reconstitute a minimal quaternary complex consisting of the cadherin cytoplasmic tail, β- and α-catenin bound to purified actin filaments (Drees, Pokutta, Yamada, Nelson, & Weis, 2005; Yamada, Pokutta, Drees, Weis, & Nelson, 2005). Those studies were performed in solution using purified proteins. However, it has recently been reported that the minimal cadherin–catenin complex will bind stably to actin filament when force is applied. Kinetic analysis of bond dissociation indicated that the interaction could be explained by a catch-bond model, where force strengthened the bond between cadherin/catenin and F-actin (Buckley et al., 2014).

α-Catenin can also interact indirectly with F-actin, through the recruitment of proteins such as vinculin (Choi et al., 2012; Rangarajan & Izard, 2012; Watabe-Uchida et al., 1998). Although other proteins may contribute (Peng, Cuff, Lawton, & DeMali, 2010), the junctional recruitment of vinculin is dominantly mediated by α-catenin (Huveneers et al., 2012; Leerberg et al., 2014). This effect is also force dependent, being decreased when myosin is

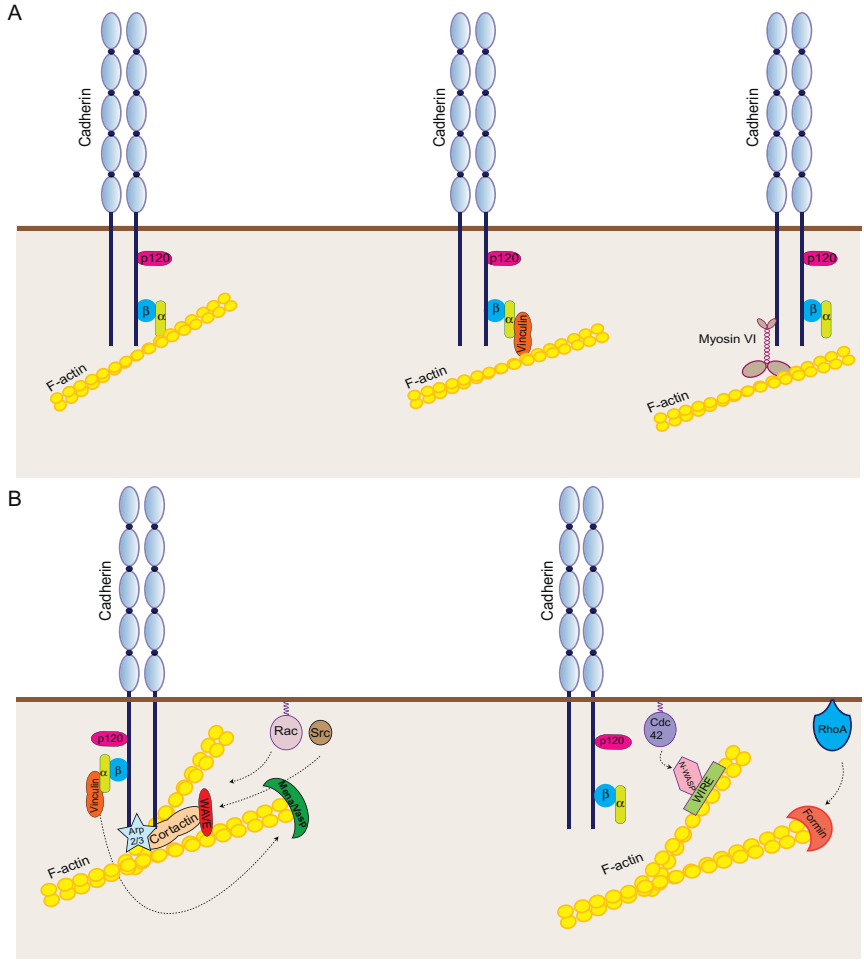

Figure 2 Cadherin and actin cooperativity. (A) The core cadherin–catenin complex is composed of cadherin, β-catenin, α-catenin, and p120-catenin. This core complex associates with actin in various ways: direct binding of α-catenin to F-actin; α-catenin binds to proteins such as vinculin which can interact with F-actin; myosin VI can directly associate with the cytoplasmic domain of cadherin and thus mediates the interaction of cadherin and F-actin. (For clarity, one of the cadherin dimers is drawn without its associated core catenins.) (B) Actin assembly and remodeling at junctions is an outcome of multiple overlapping pathways. WAVE-Arp2/3 responds to Rac signaling and nucleates actin assembly at junctions. Cortactin can directly bind WAVE and Arp2/3 and thus promote actin nucleation by scaffolding these regulators at cadherin junctions. Cortactin can also be phosphorylated by Src kinases. Further, Mena-VASP is recruited to cadherin junctions via vinculin to promote postnucleation elongation of actin filaments. N-WASP acts downstream of Cdc42 and binds to F-actin via the WIP family protein, WIRE. This promotes actin stability and organization. Rho-mediated activation of formins promotes elongation of preexisting filaments and also contributes to actin assembly by nucleation.

inhibited (Leerberg et al., 2014; Yonemura, Wada, Watanabe, Nagafuchi, & Shibata, 2010). An attractive notion is that contractile tension alters the molecular conformation of α-catenin to reveal or promote its vinculin-binding capacity. This concept was first suggested by evidence that an epitope near the vinculin-binding domain of α-catenin is revealed in a force-dependent fashion within cells (Yonemura et al., 2010). Recently, it was demonstrated that the vinculin-binding domain of α-catenin became unfolded when isolated molecules were stretched using magnetic tweezers. This promoted binding of vinculin, which then stabilized α-catenin in its open conformation (Yao et al., 2014). Thus, it is possible that the number of sites for cadherin complexes to interact with F-actin may be modulated in response to the force acting upon those adhesion complexes. Similar, myosin VI, which can bind directly to the E-cadherin cytoplasmic tail and contribute to the organization of F-actin at junctions (Mangold, Norwood, Yap, & Collins, 2012; Mangold et al., 2011), can function as a tension-sensitive actin-based anchor (Altman, Sweeney, & Spudich, 2004; Chuan, Spudich, & Dunn, 2011). Overall, this implies that cadherin–actin binding may not be a static process, but one that can be tuned in response to the forces that act upon junctions.

The association of actin with myosin II not only influences the junctional recruitment of myosin but also affects cortical F-actin itself. Myosin can control F-actin organization both by crosslinking filaments and by aggregating filaments as they slide. Furthermore, contractile stresses can induce F-actin severing, which leads to actin disassembly and turnover (Reymann et al., 2012). Effectively, stress-induced turnover would constitute a mechanism that inherently limits the force that can be generated by actomyosin, as it would turn over the F-actin scaffolds that myosin II requires to generate force. This has been demonstrated to occur in polarized cultured epithelial cells where stress-induced F-actin turnover limits the tension that is generated in the lateral cell–cell junctions found below the apical ZA (Wu et al., 2014). What function might be served by limiting the contractile stresses that junctional actomyosin can generate? One possibility is that it limits the forces that lateral membranes can exert on the cytoplasm, thereby allowing hydrodynamic behavior to be coupled across cell boundaries to drive cellular flows during morphogenesis (He, Doubrovinski, Polyakov, & Wieschaus, 2014). Additionally, control of contractility at lateral junctions contributes to integrating cells within epithelia (Wu et al., 2014). This further implies that the morphogenetic impact of actomyosin may depend not only on the myosin II and its regulation but also on the F-actin networks with which it interacts.

3. CADHERINS AND BIOGENESIS OF THE JUNCTIONAL ACTIN CYTOSKELETON

As well as influencing signaling pathways that impinge on myosin, cadherin adhesion can influence the biogenesis of junctional actomyosin by regulating multiple aspects of the actin cytoskeleton itself. These include actin filament dynamics and also potentially actin filament organization. At the mechanistic level, they are likely to reflect both intermolecular interactions that recruit actin regulators to the junctional cortex and cell signaling at cadherin junctions.

3.1. The dynamic junctional actin cytoskeleton

F-actin at the cortex of cell–cell junctions is dynamic. FRAP studies suggest that actin filaments undergo turnover on time scales of tens of seconds (Kovacs et al., 2011; Smutny et al., 2010; Yamada et al., 2005). It is also likely that multiple pools of F-actin exist at junctions that have different degrees of stability (Cavey, Rauzi, Lenne, & Lecuit, 2008; Zhang et al., 2005). Nonetheless, the fact that filaments are highly dynamic implies that the maintenance of the overall F-actin content at cell–cell junctions involves ongoing assembly of filaments to replenish those that are being lost. Moreover, the disruption of actin homeostasis affects junctional integrity and contractile tension (Verma et al., 2012), as will be discussed further. This indicates that, although filament pools may differ in their stability, the regulation of filament dynamics is functionally important.

3.2. Actin assembly

The process of assembling actin filaments can be thought of as consisting of two stages. The first is actin filament nucleation, the energetically rate-limiting step of building filaments from monomers to trimers (Pollard, Blanchoin, & Mullins, 2000). The subsequent growth of filaments from trimers can occur by actin self-assembly, but this is relatively slow. Therefore, within cells, the postnucleation assembly (growth) of filaments is commonly accelerated by proteins such as Ena/VASP proteins and formins (Chesarone & Goode, 2009; Krause, Dent, Bear, Loureiro, & Gertler, 2003).

Consistent with the notion that actin assembly may contribute to the homeostasis of dynamic filaments, actin assembly, including nucleation itself, can be identified at E-cadherin-based cell–cell junctions themselves

(Kovacs et al., 2011; Tang & Brieher, 2012; Vasioukhin, Bauer, Yin, & Fuchs, 2000; Yamada et al., 2005). A number of proteins can mediate actin filament nucleation, and several of these have been identified at E-cadherin junctions (Fig. 2B). These include the Arp2/3 complex, which mediates the assembly of branched networks of actin filaments (Pollard et al., 2000; Ydenberg, Smith, Breitsprecher, Gelles, & Goode, 2011). Arp2/3 concentrates at E-cadherin junctions (Tang & Brieher, 2012; Verma et al., 2012), through an interaction with the scaffolding protein, cortactin, which can directly associate with Arp2/3 (Han et al., 2014; Weed & Parsons, 2001). In cultured epithelial cells, depletion of Arp2/3 or cortactin reduces actin assembly at junctions, decreases steady-state levels of F-actin, and leads to fragmentation of the apical ZA (Han et al., 2014; Verma et al., 2012). Of note, Arp2/3 depletion reduces contractile tension at junctions, as well as the junctional accumulation of myosin II (Verma et al., 2012). Therefore, the local generation of F-actin by Arp2/3 appears to contribute to junctional contractility, by generating actin filaments that promote junctional accumulation of myosin and which are themselves necessary for active myosin to generate force. Arp2/3 has little intrinsic activity and instead is stimulated by cell-signaling pathways that are mediated by proteins, particularly those of the WASP/WAVE family, which transduce signals from Cdc42 and Rac1, respectively (Insall & Machesky, 2009). Indeed, both N-WASP and WAVE2 are found at cell–cell junctions, and WAVE2 is necessary for actin assembly to occur there (Kovacs et al., 2011; Verma et al., 2012). Consistent with this, Rac1 can promote actin assembly at E-cadherin adhesions (Kraemer, Goodwin, Verma, Yap, & Ali, 2007). Therefore, Arp2/3 may serve to mediate Rac-dependent actin assembly at cadherin-based junctions.

In contrast to Arp2/3, members of the formin family promote nucleation of parallel actin filaments (Chesarone & Goode, 2009), which would be predicted to be favored for the generation of F-actin bundles. Two formin family members have been identified at cell–cell junctions, formin-1 in keratinocytes and mDia1 in human mammary epithelial cells. Formin-1 was reported to interact with α-catenin, which may be responsible for its junctional recruitment (Kobielak, Pasolli, & Fuchs, 2004), whereas how mDia1 localizes to junctions remains poorly understood, although it is likely to respond to Rho (Carramusa, Ballestrem, Zilberman, & Bershadsky, 2007). Formin activity is also tightly regulated in response to cellular context (Chesarone & Goode, 2009). Interestingly, formins can also respond to changes in cellular tension, potentially independent of other known signals

(Higashida et al., 2013), although whether this is relevant at junctions remains to be determined.

A growing list of other proteins also cooperates to promote actin nucleation at junctions. α-Actinin-4 appears to facilitate Arp2/3-based actin nucleation at E-cadherin adhesion in cultured mammalian epithelial cells (Tang & Brieher, 2012), and cortactin also has a weak capacity to nucleate filaments *in vitro* (Weed & Parsons, 2001). The major contribution of cortactin to junctional nucleation in cells may, however, be to recruit Arp2/3 and WAVE2 to the junctions (Han et al., 2014). The plethora of molecules that can support actin nucleation attests to the functional importance of actin filament homeostasis at junctions, although it is possible that these diverse nucleators serve different functions depending on cellular context.

Postnucleation actin assembly also plays an important part in F-actin homeostasis at cadherin junctions. This is exemplified by members of the Ena/VASP protein family, which vary in their number from *Drosophila* (where Enabled [Ena] is the only member) to mammalian cells (which have three: Mena, VASP, and EVL; Krause et al., 2003). *In vitro*, Ena/VASP proteins have been reported to have weak nucleating capacity, but in cells their primary function appears to be to promote postnucleation elongation at F-actin barbed ends (Barzik et al., 2005). They may achieve this by antagonizing capping protein (Bear et al., 2002), which inhibits F-actin elongation at the barbed ends, and/or by acting as processive actin polymerases (Hansen & Mullins, 2010). In mammalian epithelia, Mena/VASP proteins localize to E-cadherin junctions where they contribute to actin assembly (Scott et al., 2006; Vasioukhin et al., 2000). Interestingly, their recruitment to junctions appears to constitute a mechanism for tension-dependent regulation of actin assembly (Leerberg et al., 2014). Thus, actin assembly at adherens junctions was sensitive to tension, increasing when contractility was stimulated and decreasing when myosin II was inhibited. This entailed the tension-sensitive recruitment of Mena/VASP downstream of vinculin (Leerberg et al., 2014; Peng et al., 2010). Of note, this tension-sensitive actin assembly apparatus was necessary for sustained contractile stress to be generated at the apical ZA (Leerberg et al., 2014).

Together, these findings argue that both nucleation and postnucleation mechanisms may play important roles in actin assembly at cell–cell junctions. This is further attested by the diverse impacts of Arp2/3 and Mena/VASP proteins during development. Arp2/3 and its activator, WASP, were reported to promote E-cadherin endocytosis for junctional remodeling during *Drosophila* morphogenesis (Georgiou, Marinari, Burden, & Baum, 2008;

Leibfried, Fricke, Morgan, Bogdan, & Bellaiche, 2008). Arp2/3 also contributes to junctional maturation and maintenance in the *Caenorhabditis elegans* gastrointestinal epithelium, although in that system other adhesion molecules may play a greater role in their recruitment than cadherin (Bernadskaya, Patel, Hsu, & Soto, 2011). Although Mena/VASP proteins do not appear to be essential during development, their impact becomes more apparent in tissues that are under mechanical stress. For example, mouse embryos lacking all Mena/VASP proteins have a defective endothelial barrier, a tissue that experiences shear forces (Furman et al., 2007), while during *Drosophila* development the contribution of Ena is most evident during dynamic morphogenetic events where cell–cell junctions experience strong forces (Gates et al., 2007, 2009). Together, these observations imply that Ena/VASP proteins may especially contribute to strengthening junctions against stress, potentially by mediating tension-sensitive actin assembly (Leerberg et al., 2014).

3.3. Actin filament stability and junctional contractility

Conversely, what are the mechanisms that challenge junctional actin homeostasis by inducing actin filament turnover? Isolated actin filaments have an intrinsic tendency toward disassembly, which is favored at the pointed (minus) end compared with the barbed end. However, this intrinsic process is often quite slow compared with the turnover rates of actin filaments within cells. Thus, other molecular mechanisms must exist within cells to accelerate actin filament turnover and promote the remodeling of actin networks (Brieher & Yap, 2013). One of these is contractile stress driven by myosin II (Haviv et al., 2008; Medeiros, Burnette, & Forscher, 2006; Reymann et al., 2012). As noted earlier, in epithelial cells, stress-induced filament turnover can limit the contractile tension that is generated at the lateral junctions located below the ZA (Wu et al., 2014). This carries the important implication that mechanisms that allow filaments to resist, or compensate for, stress-induced turnover can influence the active stresses that cells generate at junctions.

Indeed, several such compensatory mechanisms have recently been identified. One is tension-sensitive actin assembly itself; of note, targeting of Mena/VASP to junctions could restore contractile tension at the ZA when vinculin was depleted (Leerberg et al., 2014). A second is N-WASP, a member of the WASP/WAVE protein family that is selectively localized at the ZA in mammalian epithelial cells (Kovacs et al., 2011; Wu et al., 2014).

Although best understood as a regulator of Arp2/3-mediated actin nucleation (Padrick & Rosen, 2010), N-WASP at the ZA appears to function to stabilize actin filaments (Kovacs et al., 2011). This contributes to sustaining contractile tension at this apical junction (Wu et al., 2014). The precise molecular mechanism that allows N-WASP to stabilize F-actin is less clear. It involves the WIP family protein, WIRE, which associates directly with the N-terminal of N-WASP (Kovacs et al., 2011). WIRE can bundle actin filaments (Kato & Takenawa, 2005), an observation that is consistent with increasing evidence that network organization critically influences the sensitivity of F-actin to stress-induced turnover (Reymann et al., 2012). Branched networks appear to be especially sensitive to myosin-induced turnover (Medeiros et al., 2006), perhaps because contractility is more prone to generate compressive forces that buckle F-actin and increase its sensitivity to severing by cofilin. Conversely, actin filaments that are tense, as occur in bundles such as stress fibers, are actually resistant to cofilin (Hayakawa, Tatsumi, & Sokabe, 2011). Whether N-WASP and WIRE stabilize filaments by promoting bundling has yet to be determined. However, it is noteworthy that other bundling proteins, such as α-actinin (Knudsen, Soler, Johnson, & Wheelock, 1995) are recruited to junctions and associate with E-cadherin complexes.

4. REGULATION OF CORTICAL SIGNALING BY CADHERIN ADHESION

In this section, we will consider how cortical signals are regulated at cadherin junctions to influence junctional contractility. We focus on the Rho family of small GTPases, which have diverse and profound contributions to cytoskeletal regulation (Etienne-Manneville & Hall, 2002). Indeed, the best-known members of this family—Rho, Rac, and Cdc42—have all been identified as active at cadherin junctions (Kim, Li, & Sacks, 2000; Ratheesh et al., 2012). For the purposes of the present discussion, we will concentrate on Rho, given its central role in regulating contractility, cadherin biology and in development.

4.1. Rho signaling and morphogenesis

Morphogenesis involves the coordinated self-assembly of cells into multilayered tissues that undergo deformations such as bending, folding, and tube formation to generate specialized three-dimensional structures (Guillot & Lecuit, 2013; Mammoto, Mammoto, & Ingber, 2013).

Rho contributes to many morphogenetic processes during development. Its role has often been identified by experiments that targeted its upstream regulators, thereby identifying Rho as a common effector in many developmental signaling pathways. For example, *DRhoGEF2* (an activator of Rho) is important for cell-shape changes required for gastrulation: deletion of DRhoGEF2 or expression of dominant-negative Rho caused gastrulation to fail in *Drosophila* embryos (Barrett, Leptin, & Settleman, 1997). The junctional localization of DRhoGEF2 protein also appears to be important for its developmental impact in *Drosophila*, as the transcription factor Twist induces the expression of a transmembrane protein, T48, that serves to concentrate RhoGEF2 at cell junctions. The subsequent stimulation of Rho signaling was necessary to initiate mesoderm invagination (Kolsch, Seher, Fernandez-Ballester, Serrano, & Leptin, 2007). This emphasizes the important role that spatial coordination of signaling plays in the developmental impact of Rho. Similarly, the transcription factor Snail acts through its target gene *folded gastrulation* (Fog) to promote Rho-ROCK activity for apical constriction during fly gastrulation (Mammoto et al., 2013).

Rho is also implicated in developmental processes where junction remodeling is coupled to morphogenesis. For example, during the process of germ-band extension in *Drosophila*, cells intercalate to extend the body axis (Guillot & Lecuit, 2013; Mammoto et al., 2013). Here, Rho-mediated activation of ROCK leads to polarized localization of myosin filaments at the junctional interface undergoing shrinkage and at the same time regulates the preferential localization and stability of adherens junction components at the growing interface (Bertet et al., 2004).

The close link among Rho signaling, contractility, and cell–cell junctions is also evident in vertebrates. In chick embryos, Rho, along with its downstream effector myosin, becomes concentrated at the apical surface of neural plate cells, and drugs that inhibited this cascade caused gross disruptions in neural plate morphogenesis (Kinoshita, Sasai, Misaki, & Yonemura, 2008). ROCK has been implicated in neural tube closure, as the neural folds failed to bend and close normally when ROCK-1 signaling was diminished at the apical surfaces of the neural plates (Nishimura & Takeichi, 2008; Wei et al., 2001). Although RhoA null-knockout mice are embryonic lethal (Thumkeo, Watanabe, & Narumiya, 2013), conditional gene targeting has revealed its role in a variety of developing tissues. For example, ROCK-mediated phosphorylation of myosin RLC is required for eyelid closure as gross defects in actin-filament organization, and loss of pRLC was observed in the eyelid epithelium of ROCK-1-knockout mice

(Shimizu et al., 2005). Similarly, using conditional knockout in the lens epithelium, Chauhan, Lou, Zheng, and Lang (2011) reported that mutual antagonism of Rho and Rac modulates apical constriction and the changes in cell width required for epithelial invagination. RhoA, via ROCK, generates active myosin and contractility, which is needed for apical constriction. Thus, when RhoA was deleted, lens pits were open in shape (Chauhan et al., 2011). In the neuroepithelium of mice, ablation of RhoA disrupts adherens junctions and apical–basal cell polarity, causing aberrant proliferation of neuronal progenitors and defects in organization of ventricular region (Herzog et al., 2011; Katayama et al., 2011). Similar defects were seen when the Rho effector, mDia, was disrupted (Thumkeo et al., 2011).

4.2. Rho and cadherin biology

Rho is also essential for the stability and integrity of cadherin-based junctions. Although three Rho family genes are found in mammals, much work has focused on RhoA, as disruption of RhoA signaling perturbs the integrity of cadherin-based adhesions (Braga, 2000; Braga, Machesky, Hall, & Hotchin, 1997; Priya et al., 2013; Ratheesh et al., 2012; Ratheesh & Yap, 2012; Shewan et al., 2005; Smith, Dohn, Brown, & Reynolds, 2012; Takaishi, Sasaki, Kotani, Nishioka, & Takai, 1997). Rho signaling can contribute to adherens junction integrity by stabilizing cadherin receptors, cytoskeleton organization, generation of tension, and possibly facilitating E-cadherin clustering (Braga, Betson, Li, & Lamarche-Vane, 2000; Priya et al., 2013; Ratheesh et al., 2012; Ratheesh, Priya, & Yap, 2013; Shewan et al., 2005; Smutny et al., 2010, 2011).

In the context of our present discussion, myosin II is a major downstream target for Rho to promote cadherin biology. The recruitment and activity of myosin II at junctions responded to the Rho pathway. Inhibition of Rho kinase signaling not only led to the loss of myosin II from junctions but also abolished its activity as suggested by the loss of MLC phosphorylation and decreased junctional staining of ppRLC (Shewan et al., 2005). Moreover, the phenotype observed after ROCK inhibition was very similar to that of myosin inhibition, namely, an inability to concentrate E-cadherin in junctions and reduced adhesion to cadherin-coated substrata (Shewan et al., 2005). These observations placed myosin II as a potent downstream effector that allows Rho to modulate cadherin adhesion (Shewan et al., 2005). Interestingly, as noted earlier, although both myosin IIA and myosin IIB can be found at apical ZA, the junctional concentration of myosin IIA

was more dependent on the Rho/ROCK pathway than that of myosin IIB and served to promote cadherin clustering and the concentration of E-cadherin at the apical ZA (Smutny et al., 2010). Thus, a Rho-ROCK-Myosin II pathway can play an integral role in supporting the integrity of the ZA.

However, to perform its biological functions, Rho must undergo a regulated activation/inactivation cycle facilitated by ancillary stimulatory and inhibitory proteins (Jaffe & Hall, 2005). The spatiotemporal activity of these regulatory molecules decides the site and timing of Rho signaling (Bement, Miller, & von Dassow, 2006). An important emerging theme here is the ability of cells to localize contiguous elements of signaling pathways to cadherin junctions. This is well illustrated by the Rho-ROCK pathway. Both active, GTP-loaded Rho and its immediate downstream mediator, Rho-activated kinase (ROCK), are found at cadherin junctions (Priya et al., 2013; Ratheesh et al., 2012; Smith et al., 2012; Figs. 3B and 4A). Inhibition of either Rho or ROCK decreases junctional contractility. Moreover, disruption of mechanisms that activate or recruit Rho or ROCK to junctions also compromises junctional contractility (Ratheesh et al., 2012). This implies that the local regulation of this signaling module plays an important role in regulating junctional actomyosin. Indeed, this notion is teleologically attractive, as it would provide a mechanism to focus contractility at junctions. The important mechanistic issue is how such junctional localization of Rho-ROCK signaling might be achieved.

4.3. Focusing Rho signaling at cell–cell junctions

One major paradigm for the spatial control of Rho signaling lies in the proteins that control its activation and inactivation at the plasma membrane (Etienne-Manneville & Hall, 2002). This reflects two broad processes: the control of Rho nucleotide status and the localization of active Rho at the plasma membrane.

Like other GTPases, the ability of Rho to mediate cellular regulation depends on its nucleotide-loaded status. Binding of GTP induces conformational changes that allow Rho to interact with, and regulate the activity of, downstream effectors (Bustelo, Sauzeau, & Berenjeno, 2007). In contrast, conversion of bound GTP to GDP, mediated by the intrinsic GTPase activity of Rho, disables its ability to interact with its effectors, thereby terminating its signaling. However, the intrinsic nucleotide turnover rate for Rho is slow (half-life of ~30 min), relative to many of the cellular processes that it

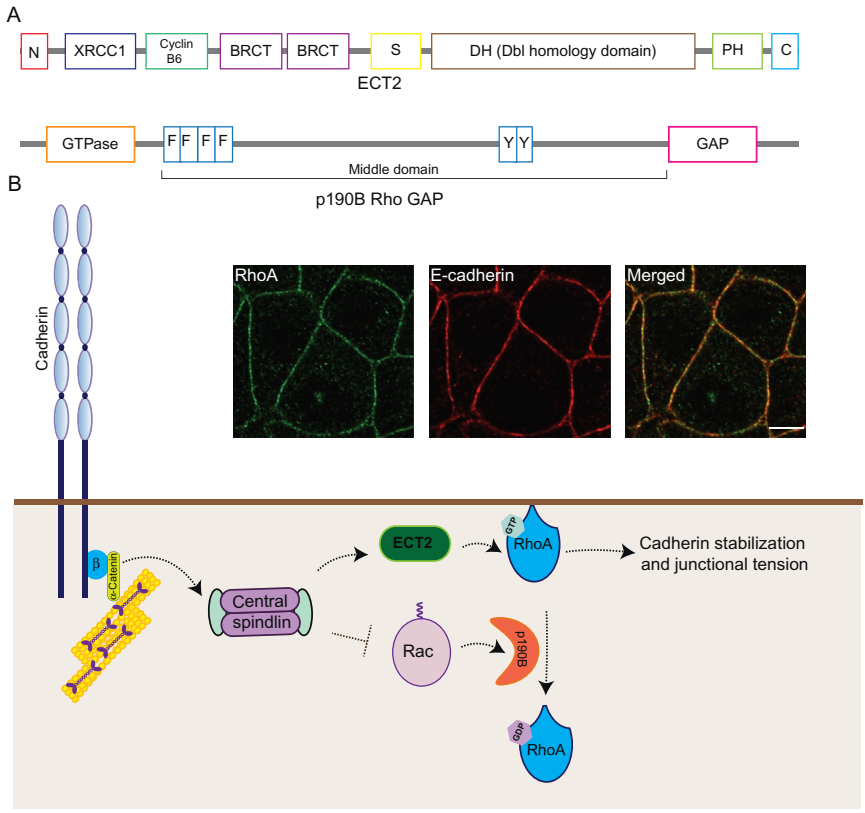

Figure 3 Junctional Rho regulation. (A) Domain structure of ECT2: N, amino-terminal; BRCT, BRAC1 C-terminal domain; XRCC1, X-ray repair complementing defective repair in Chinese hamster cells 1 domain; PH, pleckstrin-homology domain; C, carboxyl-terminal region; S, small central region. Domain structure of p190B Rho GAP: The N-terminus consists of a GTPase-like domain, followed by a relatively less well-characterized middle domain and a GAP domain at the C-terminus; FF, phosphorylation-regulated protein–protein interacting domain; Y, SH2 domain. (B) Rho signaling at the epithelial cadherin junctions. RhoA localizes to E-cadherin-based junctions as illustrated by immunofluorescence in MCF-7 cells. ECT2 acts as a GEF, which can activate Rho at epithelial cadherin junctions, while p190B Rho GAP is the GAP that can inhibit Rho activity. Junctional localization of ECT2 relies on the centralspindlin complex, which can also inhibit Rac and thus prevents p190B GAP localization. The GTP-Rho further supports cadherin stabilization and junctional tension via myosin-ROCK pathway. Scale bar = 10 μm.

controls (Zhang & Zheng, 1998). Instead, the nucleotide status of Rho is further regulated by two sets of proteins. Guanine nucleotide-exchange factors (GEFs) catalyze the exchange of GDP for GTP, thereby activating Rho, and GTPase-activating proteins (GAPs) stimulate nucleotide hydrolysis to

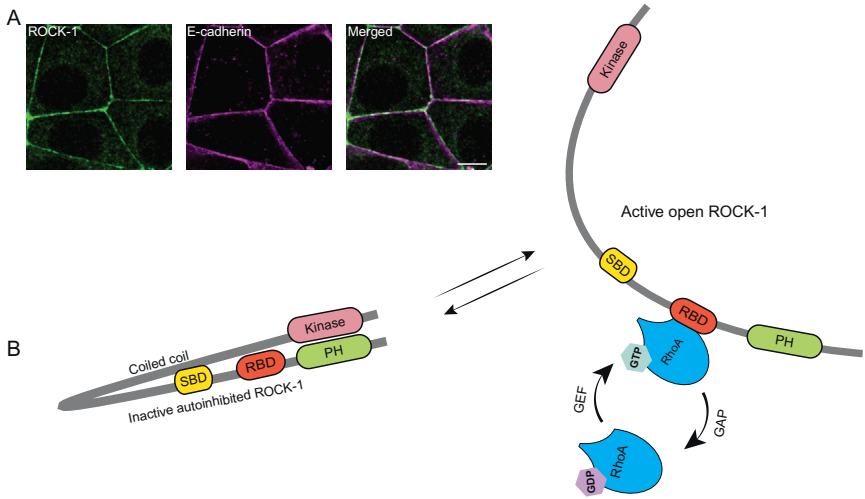

Figure 4 Rho kinase and cell–cell junctions. (A) ROCK-1 localizes to cadherin-based junctions as illustrated by immunofluorescence in MCF-7 cells. Scale bar = 10 μm. (B) The C-terminus of ROCK interacts with the kinase domain at the N-terminus leading to an autoinhibited conformation, which is inactive. Binding of GTP-Rho to the RBD (Rho-binding domain) disrupts this autoinhibition, resulting in an active ROCK. SBD, Shroom-binding domain; RBD, Rho-binding domain; PH, pleckstrin-homology domain.

GDP to inactivate Rho (Bos, Rehmann, & Wittinghofer, 2007; Etienne-Manneville & Hall, 2002).

In addition, Rho signaling typically occurs at cellular membranes. In the context of contractility, this allows GTP-Rho to ultimately activate the contractile apparatus at the cell cortex where it can interact with membrane proteins to control cell shape and motility. Accordingly, Rho bears a C-terminal CAAX box that serves as a lipid-binding membrane anchor. Conversely, inactivation of Rho signaling also involves its removal from the membrane. This is mediated by Guanine nucleotide dissociation inhibitors (GDIs) that extract Rho from membranes and sequester it in its GDP-bound state within the cytosol (Ridley, 2012).

Ultimately, the localized expression of Rho signaling at specific sites within cells is influenced by the action of these three sets of proteins. While it is likely that GDI function will also contribute, coordination of GEF and GAP activity is currently the best-understood way in which localized zones of Rho signaling can be established. Formally, one might envisage that a localized zone of GTP-Rho might be achieved at sites where GEF activity

predominates over GAP activity. Evidence for such a model has been identified during cell division, where Rho signaling is focused to support contractility at the cytokinetic furrow (Glotzer, 2005; Piekny, Werner, & Glotzer, 2005). To date, the GEFs and GAPs that regulate Rho signaling at cell–cell junctions are poorly understood. Surprisingly, however, one set involves proteins that are already implicated in cytokinesis, the GEF ECT2 and the GAP p190B RhoGAP (Fig. 3A).

4.4. ECT2

ECT2 belongs to the Dbl family of Rho GEFs and was first identified as a proto-oncogene (Chan et al., 1993). ECT2 is highly conserved across evolution, human ECT2 sharing a significant degree of similarity in its coding region with murine ECT2, *Let-21* (the ECT2 ortholog in *C. elegans*), and *XECT2* (*Xenopus* ECT2) (Fields & Justilien, 2010). ECT2 is composed of various structural domains, each with a distinct role (Fig. 3A). The N-terminal half contains many domains which are common to cell-cycle regulators while the C-terminal half is mainly responsible for the Rho-GEF catalytic activity (Tatsumoto, Xie, Blumenthal, Okamoto, & Miki, 1999). At the extreme N-terminus lies a XRCC1 domain, which shows sequence homology to human XRCC1, a protein involved in DNA repair. The major structural motif in the N-terminal half is a tandem array of BRCT repeats, which are highly conserved in proteins involved in DNA repair and cell-cycle checkpoint responses (Fields & Justilien, 2010). This BRCT motif can bind phosphorylated peptides (Manke, Lowery, Nguyen, & Yaffe, 2003), and it has been suggested that it can also bind to the C-terminal half of ECT2, leading to autoinhibition (discussed further below). The C-terminal half is the catalytic core of the protein and contains a tandem array of Dbl-homology (DH) and pleckstrin-homology (PH) domains (Tatsumoto et al., 1999). The extreme C-terminus region of ECT2 does not exhibit significant homology to any known protein domains or motifs (Fields & Justilien, 2010). The N- and C-terminal domains of ECT2 are separated by a small central S domain, which harbors two nuclear localization sequences that regulate the intracellular localization of ECT2 (Fields & Justilien, 2010).

ECT2 is best understood for its role in cytokinesis (Glotzer, 2005; Piekny et al., 2005; Wolfe & Glotzer, 2009; Wolfe, Takaki, Petronczki, & Glotzer, 2009; Yuce, Piekny, & Glotzer, 2005). RhoA plays the role of chief modulator in cytokinesis by initiating the formation of the contractile ring (Werner & Glotzer, 2008). This involves the Rho-mediated activation of

the actin assembly factor, formin, and phosphorylation of the RLC of myosin II. ECT2 acts as a primary GEF for Rho during cytokinesis. It ensures the correct localization and activation of Rho during cell division and is a crucial regulator for cytokinesis in all the metazoans analyzed to date (Werner & Glotzer, 2008; Yuce et al., 2005).

The profound contribution of ECT2 to cytokinesis has tended to obscure any potential extramitotic function that it may have. This, taken with its predominant localization in the nucleus of isolated interphase cells (the common system to study cytokinesis), has led to the notion that ECT2 may principally serve to regulate cytokinesis. Nonetheless, extramitotic functions for ECT2 are beginning to emerge. *Pebbles*, the *Drosophila* homolog of ECT2, contribute to mesoderm migration in the fly embryo (Schumacher, Gryzik, Tannebaum, & Muller, 2004; Smallhorn, Murray, & Saint, 2004), while ECT2 has been identified at the apical junctions of cultured mammalian epithelia when they are grown as monolayers (Liu, Ishida, Raziuddin, & Miki, 2004; Ratheesh et al., 2012). In the latter situation, ECT2 can interact with the Par6 apical polarity complex to influence apical–basal polarity (Liu, Ohno, & Miki, 2006). Additionally, it contributes to stimulating Rho signaling at the ZA. Depletion of ECT2 reduced GTP-Rho signaling at apical cadherin junctions. This was accompanied by loss of myosin II and a decrease in contractile tension at the junctions (Ratheesh et al., 2012). Thus, ECT2 represents one GEF that can support Rho signaling at cell–cell junctions.

4.5. p190 RhoGAP

The p190RhoGAP family comprises two members: p190A and p190B, which are widely expressed in human, rat, fly, and mouse (Chakravarty et al., 2000; Settleman, Narasimhan, Foster, & Weinberg, 1992). These proteins are encoded by separate genes and share 50% sequence homology (Ponik, Trier, Wozniak, Eliceiri, & Keely, 2013). Both contain three major structural features: an N-terminal GTP-binding domain (GBD), a large-middle domain responsible for various protein–protein interactions, and a C-terminal GAP domain (Tcherkezian & Lamarche-Vane, 2007; Fig. 3A). They show GAP activity toward RhoA, Rac 1, and Cdc42, with highest activity for RhoA (Settleman et al., 1992). Of note for this discussion, both p190 RhoGAPs have been identified at cadherin-based cell–cell junctions. p190A RhoGAP was found at N-cadherin-mediated cell–cell junctions, where its recruitment involved an association p120-ctn (Wildenberg et al., 2006). p190B RhoGAP can also be found at epithelial cell–cell junctions (Ratheesh et al., 2012).

Its junctional localization is especially interesting, as p190B has been implicated in regulating epithelial architecture both during morphogenesis and in disease. p190B is highly expressed in the terminal end buds of the mouse mammary gland and its deletion impairs ductal morphogenesis (Chakravarty, Hadsell, Buitrago, Settleman, & Rosen, 2003). On the other hand, overexpression of p190B caused complete disruption of mammary epithelial architecture (Vargo-Gogola, Heckman, Gunther, Chodosh, & Rosen, 2006). The precise expression of p190B activity thus seems to be critical for its impact on tissue organization. p190B is also overexpressed in mammary carcinomas, and its expression can influence mammary tumor progression in mouse models. Overexpression of p190B accelerated tumor development in an MMTV-Neu model system, while haploinsufficency for p190B retarded tumor development in this system (Heckman-Stoddard et al., 2009). Thus, p190B was necessary for epithelial morphogenesis but its overactivity might contribute to tumorigenesis. Given the close relationship between E-cadherin function and dysfunction during epithelial morphogenesis and tumorigenesis, respectively, this raises the interesting possibility that p190 might influence Rho signaling at junctions.

Indeed, both p190A and p190B have been implicated in regulating Rho signaling at junctions. Early studies demonstrated that acute engagement of Xenopus C-cadherin induced a transient decrease in Rho signaling through p190, although the precise paralog responsible was not identified (Noren, Arthur, & Burridge, 2003; Noren, Liu, Burridge, & Kreft, 2000). Subsequently, Wildenberg et al. (2006) reported that p190A RhoGAP could be recruited to N-cadherin-based adhesions through an association with p120-ctn, leading to local inactivation of the Rho-ROCK pathway. In epithelial cells, recruitment of p190B to apical cadherin junctions also contributes to inactivating Rho (Ratheesh et al., 2012). Therefore, both p190A and p190B RhoGAP may serve to inactivate Rho at cadherin junctions, perhaps with different contributions in different cellular contexts.

4.6. Coordinating GEF and GAP activity

Formally, it might be predicted that the generation of a Rho signaling zone would necessitate coordinated regulation of both GEF and GAP activities. Recruitment and/or activation of a GEF(s) would stimulate Rho signaling, while GAP activity would need to be simultaneously

antagonized to prevent the premature inactivation of Rho. This paradigm has already been developed for the Rho zone of the cytokinetic furrow (Mikawa, Su, & Parsons, 2008). Interestingly, a common mechanism—the centralspindlin complex—is also implicated in supporting the Rho zone at ZA (Fig. 3B).

Centralspindlin is an evolutionarily conserved protein complex, which was first identified at the central spindle of the mitotic apparatus. It is a tetrameric complex comprising a dimer of MKLP-1/ZEN-4, a member of the kinesin family of microtubule-binding proteins, and a dimer of hCYK-4/MgcRacGAP (Mishima, Kaitna, & Glotzer, 2002). It concentrates at the contractile furrow during cytokinesis, a process that reflects multiple molecular mechanisms (Glotzer, 2005; Somers & Saint, 2003). These include association with the microtubules of the central spindle, likely mediated by MKLP-1/ZEN-4, and binding of hCYK-4/MgcRacGAP to phosphoinositides at the inner leaflet of the plasma membrane (Glotzer, 2009). The junctional localization of centralspindlin at the ZA also requires dynamic microtubules and binding of centralspindlin to the N-terminus of α-catenin (Ratheesh et al., 2012). Importantly, depletion of centralspindlin reduced Rho signaling at the ZA and decreased junctional contractility (Ratheesh et al., 2012). Similar effects occurred when the mechanisms responsible for recruiting centralspindlin to junctions were perturbed. Thus, centralspindlin controls Rho signaling to support contractility at interphase cadherin junctions as it does to support the contractile furrow during cytokinesis. At the ZA, as well as in cytokinesis, localization of centralspindlin appears to be regulated through coincidence detection (Carlton & Cullen, 2005), where multiple mechanisms must coincide to ensure that centralspindlin is localized to the correct place with the cell with both spatial and temporal fidelity.

Once it is correctly localized to the cortex, centralspindlin can regulate Rho through ECT2. CYK-4/MgcRacGAP can bind directly to the N-terminal BRCT domain of ECT2, an interaction, which is responsible for recruiting ECT2 to the central spindle during cytokinesis (Yuce et al., 2005). In the absence of centralspindlin, ECT2 does not localize either to the central spindle during cell division or to the ZA of interphase epithelial monolayers (Ratheesh et al., 2012; Yuce et al., 2005). In cell division, this association is regulated by protein phosphorylation, as Polo-like kinase 1 (PLK1) phosphorylates CYK-4 to generate a phophoepitope that is recognized by the BRCT domain of ECT2 (Wolfe et al., 2009). This interaction may also serve to activate ECT2, by relieving its autoinhibitory

conformation. The C-terminus of ECT2 may also contribute to its cortical localization during cytokinesis (Su, Takaki, & Petronczki, 2011), but this also appears to be downstream of the influence of centralspindlin and protein phosphorylation by CDK1. Therefore, centralspindlin may lie at the top of a signaling pathway that activates Rho through ECT2 to support junctional contractility. However, what protein kinases may regulate centralspindlin and ECT2 at junctions remain to be identified.

In addition to promoting Rho activation at the ZA, centralspindlin can also antagonize the junctional accumulation of p190B RhoGAP, which increased when either MLKP1 or hCYK-4/MgcRacGAP was depleted. This accumulation of p190B contributed to the fall in junctional Rho signaling when centralspindlin was perturbed, as the change in Rho could be ameliorated by simultaneous depletion of p190B. Therefore, centralspindlin can support junctional Rho signaling by both recruiting a GEF and antagonizing an inactivator (Ratheesh et al., 2012).

How, then, does centralspindlin antagonize junctional p190B? One possibility is that centralspindlin blocks the mechanism responsible for recruiting p190B to junctions. One such recruitment mechanism is signaling by another Rho family GTPase, Rac, which can bind directly to p190B and promote its cortical localization (Bustos, Forget, Settleman, & Hansen, 2008; Wildenberg et al., 2006). Indeed, depletion of centralspindlin increased Rac signaling at junctions and inhibition of Rac blocked the junctional accumulation of p190B. Presumably, then, centralspindlin limits the junctional accumulation of p190B by dampening Rac signaling. Exactly how centralspindlin may inhibit junctional Rac signaling is not understood; however, CYK-4 itself is a candidate, as it possesses Rac GAP activity (Jantsch-Plunger et al., 2000). Interestingly, Rac signaling also promoted the recruitment of p190A RhoGAP to N-cadherin junctions (Wildenberg et al., 2006). However, this did not appear to involve direct binding of GTP-Rac to p190A. Instead, Rac-induced generation of reactive oxygen species promoted tyrosine phosphorylation of p190A and its associated protein, p120-RhoGAP, by inhibiting a protein tyrosine phosphatase (Noren et al., 2003). Whether centralspindlin may also participate in regulating the junctional recruitment of p190A RhoGAP has yet to be investigated.

4.7. Other mechanisms

While current experience with ECT2 and p190B illustrates the capacity for coordination of GEFS and GAPs, it is likely that other combinations of GEFs

and GAPs contribute to regulating junctional Rho signaling in other circumstances. Nor is control of the Rho GTPase cycle the only way in which its spatial expression can be influenced. Potentially, other Rho-binding proteins may contribute by limiting the diffusion of GTP-Rho and/or promoting its localization with GEFs and effectors. An interesting example is provided by anillin, a scaffolding protein that is found at the cytokinetic furrow and was also recently identified at cell–cell junctions (Piekny & Glotzer, 2008; Reyes et al., 2014). Anillin can bind directly to several proteins that regulate contractility, including Rho itself, ECT2, and myosin II (Piekny & Maddox, 2010). Depletion of anillin in Xenopus embryos perturbed the integrity of cadherin-based cell–cell junctions, associated with unstable bursts of GTP-Rho signaling at those junctions (Reyes et al., 2014). Whether that aberrant Rho signaling was responsible for the loss of junctional integrity remains to be determined.

4.8. Localizing ROCK to junctions

Spatial regulation of signaling is not confined to the upstream elements of the Rho signaling pathway. Instead, it is increasingly evident that it can extend to mediators of Rho signaling, including the ROCK itself. Consistent with the notion that coincidence detection can define the spatial rigor of Rho expression (Carlton & Cullen, 2005) ROCK localization is also determined by multiple mechanisms.

ROCK was among the first Rho effectors to have been identified. Two ROCK isoforms (ROCK-1 and ROCK-2) are found in mammalian cells (Amano, Nakayama, & Kaibuchi, 2010; Julian & Olson, 2014; Riento & Ridley, 2003). These share a broadly similar primary structure consisting of an N-terminal kinase domain, a central coiled-coil domain, and a C-terminal region which bears both the GTP-Rho-binding domain (RBD), and a lipid-binding PH domain (Fig. 4B). The kinase domain of both isoforms is highly conserved at the amino-acid level (92% identity), while overall they share 62% identity. GTP-bound Rho activates ROCK by altering its intramolecular conformation. In the absence of GTP-Rho, ROCK exists in an autoinhibited state where an intramolecular association between the C-terminal region and the N-terminal kinase domain inhibits ROCK activity. Binding of GTP-Rho to the RBD then releases this autoinhibitory conformation, thus activating the kinase (Fig. 4B; Amano et al., 2010; Riento & Ridley, 2003). As noted earlier, ROCK plays a canonical role in mediating the regulation of myosin II by Rho, including that at cadherin junctions.

Since the kinase domain is highly conserved between these two isoforms, it has often been assumed that they phosphorylate a similar range of substrates. However, it is increasingly apparent that they differ in their expression and protein–protein interactions, suggesting that they may have different biological functions (Amano et al., 2010; Sandquist & Means, 2008; Sandquist, Swenson, Demali, Burridge, & Means, 2006; Schofield & Bernard, 2013). Interestingly, these differences extend to their subcellular localization. ROCK-2 has been reported to localize in the cytoplasm, globally at the plasma membrane and also at the cleavage furrow during cytokinesis (Schofield & Bernard, 2013). In contrast, recent studies have reported the selective concentration of ROCK-1 at the apical junctions of epithelial cells (Smith et al., 2012). This suggests that mechanisms exist to selectively colocalize GTP-Rho with this key effector at cadherin junctions, thereby establishing a Rho-ROCK-signaling module at the junctions.

ROCK bears multiple binding domains that can influence its cortical localization. The PH domain appears to be necessary for its association with the membrane, but was not sufficient to confer concentration at cadherin junctions (Schofield & Bernard, 2013). Other coincident factors therefore appear to collaborate to concentrate ROCK at junctions. One of these is likely to be GTP-Rho itself, as deletion of the RBD generated a mutant ROCK that could associate with the membrane but was unable to concentrate at cadherin junctions (Simoes Sde, Mainieri, & Zallen, 2014).

There is also emerging evidence that junctional proteins themselves can contribute to localizing ROCK-1. One interesting role is played by the adaptor protein Shroom, which was first identified in a screen for mouse mutants that disrupted neural tube closure (Hildebrand & Soriano, 1999). Subsequent characterization identified a single Shroom gene in *Drosophila* and four Shroom isoforms (Shroom 1–4) in mammalian cells. Despite their number, many of these mammalian Shroom genes participate in regulating processes that involve contractility at junctions, including apical constriction in embryonic epithelia and junctional contractility in endothelia (Bolinger, Zasadil, Rizaldy, & Hildebrand, 2010; Hildebrand, 2005; Simoes Sde et al., 2014). Shroom is an actin-binding protein (Hildebrand & Soriano, 1999) that localizes to cell–cell junctions, including cadherin junctions through an association with the cadherin-associated protein, p120-catenin (p120-ctn) (Lang, Herman, Reynolds, Hildebrand, & Plageman, 2014). Its contribution to junctional contractility may reflect in part its ability to recruit both F-actin and myosin II to junctions (Hildebrand, 2005). However, an independent contribution to contractility comes from its additional ability to

interact directly with ROCK. The junctional accumulation of ROCK could be promoted or reduced by the expression or depletion of Shroom, respectively (Nishimura & Takeichi, 2008). Further, dominant-negative mutants of Shroom that disrupt the interaction between ROCK and endogenous Shroom perturb junctional tension and apical constriction (Nishimura & Takeichi, 2008).

Shroom may then collaborate with Rho in recruiting ROCK to junctions, an influence that appears to be closely tied to cell polarity (Simoes Sde et al., 2014). Not only does Shroom contribute to localizing ROCK at the ZA in epithelial cells that have undergone apical–basal polarization, but also it participates in regulating junctional signaling during planar polarization. This is demonstrated when *Drosophila* embryos undergo cellular rearrangements during axis elongation. At this stage, ROCK is not only accumulated at apical adherens junctions but also distributed in a planar polarized pattern to promote the remodeling of cell–cell junctions. Rho is necessary for this process, because of its ability to recruit ROCK to junctions, but Shroom also contributes by conferring planar polarized distribution on junctional ROCK (Simoes Sde et al., 2014).

Thus, the coordinated spatial localization of ROCK and Rho is a characteristic feature that contributes to contractility at cadherin junctions. It is likely that we have only begun to unravel the ways in which this coordination is established and how it affects contractility. For example, it remains to be determined whether the ability of p120-ctn to bind ROCK (Smith et al., 2012) is solely mediated by Shroom, or whether other interactions also participate. Furthermore, ROCK can also potentially feedback to influence Rho signaling by regulating p190 RhoGAPs. Both p190A and p190B are recruited to the plasma membrane by association with members of a family of atypical GTPases, Rnd1 and Rnd3, respectively (Oinuma, Kawada, Tsukagoshi, & Negishi, 2012; Wennerberg et al., 2003). These recruitment mechanisms are disrupted by ROCK, albeit by different molecular mechanisms (Riento et al., 2005). ROCK can phosphorylate p190A directly, thereby disrupting its interaction with Rnd1 (Mori et al., 2009). In contrast, ROCK does not appear to directly target p190B but, instead, phosphorylates Rnd3 to sequester it in the cytosol, preventing it from associating with the plasma membrane (Riento et al., 2005; Riou et al., 2013). By either pathway, ROCK antagonizes the membrane accumulation of p190, thereby potentially sustaining Rho signaling. However, whether these affect Rho signaling at cadherin junctions remains to be explored.

5. CLOSING COMMENTS

In conclusion, cell–cell junctions can be considered as active mechanical agents, where many molecular pathways are coordinated to ultimately integrate adhesion with the actomyosin contractile apparatus. The product, contractile tension at junctions, may then be regarded as the emergent property of an extremely complex system. An interesting challenge for the future will be to develop approaches to make sense of this complexity: defining the key architecture(s) of the system and parsing the rules that regulate it. One issue will be to understand whether (and if so, how) levels of tension may be regulated. It might be supposed, for example, that established tissues at homeostasis would display relatively stable levels of tension, compared with morphogenetically active tissues that are undergoing neighbor exchange or apical constriction. We will need to develop approaches to quantitatively characterize contractile tension in these different contexts as the basis for understanding their regulation. Finally, although we have focused on the basic cell biology of junctional contractility, what we learn is likely to have implications for understanding disease as well as development. It is interesting to note that a regulator of junctional Rho, such as p190B, is implicated in cancer. Whether this impact occurs through dysregulation of junctional contractility is an interesting, open question. Our growing understanding of the complex mechanisms that make junctions active mechanical agents then holds the promise of informing our understanding of cell biology in disease.

ACKNOWLEDGMENTS

Our work was supported by the National Health and Medical Research Council of Australia (1044041, 1037320) and an ANZ Trustees Ph.D. Scholarship in Medical Research to R. P.

REFERENCES

Altman, D., Sweeney, H. L., & Spudich, J. A. (2004). The mechanism of myosin VI translocation and its load-induced anchoring. *Cell*, *116*, 737–749.

Amano, M., Ito, M., Kimura, K., Fukata, Y., Chihara, K., Nakano, T., et al. (1996). Phosphorylation and activation of myosin by Rho-associated kinase (Rho-kinase). *The Journal of Biological Chemistry*, *271*(34), 20246–20249.

Amano, M., Nakayama, M., & Kaibuchi, K. (2010). Rho-kinase/ROCK: A key regulator of the cytoskeleton and cell polarity. *Cytoskeleton (Hoboken)*, *67*(9), 545–554. http://dx.doi.org/10.1002/cm.20472.

Barrett, K., Leptin, M., & Settleman, J. (1997). The rho GTPase and a putative RhoGEF mediate a signaling pathway for the cell shape changes in Drosophila gastrulation. *Cell*, *91*(7), 905–915. http://dx.doi.org/10.1016/S0092-8674(00)80482-1.

Barzik, M., Kotova, T. I., Higgs, H. N., Hazelwood, L., Hanein, D., Gertler, F. B., et al. (2005). Ena/VASP proteins enhance actin polymerization in the presence of barbed end capping proteins. *The Journal of Biological Chemistry*, *280*(31), 28653–28662.

Bear, J. E., Svitkina, T. M., Krause, M., Schafer, D. A., Maly, I. V., Chaga, O. Y., et al. (2002). Antagonism between Ena/VASP proteins and actin filament capping regulates fibroblast motility. *Cell*, *109*, 509–521.

Bement, W. M., Miller, A. L., & von Dassow, G. (2006). Rho GTPase activity zones and transient contractile arrays. *Bioessays*, *28*(10), 983–993.

Bernadskaya, Y. Y., Patel, F. B., Hsu, H. T., & Soto, M. C. (2011). Arp2/3 promotes junction formation and maintenance in the Caenorhabditis elegans intestine by regulating membrane association of apical proteins. *Molecular Biology of the Cell*, *22*(16), 2886–2899. http://dx.doi.org/10.1091/Mbc.E10-10-0862.

Bertet, C., Sulak, L., & Lecuit, T. (2004). Myosin-dependent junction remodelling controls planar cell intercalation and axis elongation. *Nature*, *429*(6992), 667–671. http://dx.doi.org/10.1038/Nature02590.

Bolinger, C., Zasadil, L., Rizaldy, R., & Hildebrand, J. D. (2010). Specific isoforms of Drosophila shroom define spatial requirements for the induction of apical constriction. *Developmental Dynamics*, *239*(7), 2078–2093. http://dx.doi.org/10.1002/dvdy.22326.

Bos, J. L., Rehmann, H., & Wittinghofer, A. (2007). GEFs and GAPs: Critical elements in the control of small G proteins. *Cell*, *129*(5), 865–877. http://dx.doi.org/10.1016/j.cell.2007.05.018.

Braga, V. (2000). Epithelial cell shape: Cadherins and small GTPases. *Experimental Cell Research*, *261*(1), 83–90. http://dx.doi.org/10.1006/excr.2000.5050, S0014-4827(00)95050-X [pii].

Braga, V. M., Betson, M., Li, X., & Lamarche-Vane, N. (2000). Activation of the small GTPase Rac is sufficient to disrupt cadherin-dependent cell-cell adhesion in normal human keratinocytes. *Molecular Biology of the Cell*, *11*(11), 3703–3721.

Braga, V. M., Machesky, L. M., Hall, A., & Hotchin, N. A. (1997). The small GTPases Rho and Rac are required for the establishment of cadherin-dependent cell-cell contacts. *The Journal of Cell Biology*, *137*(6), 1421–1431.

Brieher, W. M., & Yap, A. S. (2013). Cadherin junctions and their cytoskeleton(s). *Current Opinion in Cell Biology*, *25*(1), 39–46. http://dx.doi.org/10.1016/j.ceb.2012.10.010.

Buckley, C. D., Tan, J. L., Anderson, K. L., Hanein, D., Volkmann, N., Weis, W. I., et al. (2014). The minimal cadherin-catenin complex binds to actin filaments under force. *Science*, *346*, 1254211–1254218.

Bustelo, X. R., Sauzeau, V., & Berenjeno, I. M. (2007). GTP-binding proteins of the Rho/Rac family: Regulation, effectors and functions in vivo. *Bioessays*, *29*(4), 356–370. http://dx.doi.org/10.1002/bies.20558.

Bustos, R. I., Forget, M. A., Settleman, J. E., & Hansen, S. H. (2008). Coordination of Rho and Rac GTPase function via p190B RhoGAP. *Current Biology*, *18*(20), 1606–1611. http://dx.doi.org/10.1016/J.Cub.2008.09.019.

Carlton, J. G., & Cullen, P. J. (2005). Coincidence detection in phosphoinositide signaling. *Trends in Cell Biology*, *15*(10), 540–547. http://dx.doi.org/10.1016/j.tcb.2005.08.005.

Carramusa, L., Ballestrem, C., Zilberman, Y., & Bershadsky, A. D. (2007). Mammalian diaphanous-related formin Dia1 controls the organization of E-cadherin-mediated cell-cell junctions. *Journal of Cell Science*, *120*(21), 3870–3882. http://dx.doi.org/10.1242/Jcs.014365.

Cavey, M., Rauzi, M., Lenne, P. F., & Lecuit, T. (2008). A two-tiered mechanism for stabilization and immobilization of E-cadherin. *Nature*, *453*(7196), 751–756. http://dx.doi.org/10.1038/nature06953.

Chakravarty, G., Hadsell, D., Buitrago, W., Settleman, J., & Rosen, J. M. (2003). p190-B RhoGAP regulates mammary ductal morphogenesis. *Molecular Endocrinology*, *17*(6), 1054–1065. http://dx.doi.org/10.1210/me.2002-0428.

Chakravarty, G., Roy, D., Gonzales, M., Gay, J., Contreras, A., & Rosen, J. M. (2000). p190-B, a Rho-GTPase-activating protein, is differentially expressed in terminal end buds and breast cancer. *Cell Growth & Differentiation*, *11*(7), 343–354.

Chan, A. M., Fleming, T. P., McGovern, E. S., Chedid, M., Miki, T., & Aaronson, S. A. (1993). Expression cDNA cloning of a transforming gene encoding the wild-type G alpha 12 gene product. *Molecular and Cellular Biology*, *13*(2), 762–768.

Chauhan, B. K., Lou, M., Zheng, Y., & Lang, R. A. (2011). Balanced Rac1 and RhoA activities regulate cell shape and drive invagination morphogenesis in epithelia. *Proceedings of the National Academy of Sciences of the United States of America*, *108*(45), 18289–18294. http://dx.doi.org/10.1073/pnas.1108993108.

Chesarone, M. A., & Goode, B. L. (2009). Actin nucleation and elongation factors: Mechanisms and interplay. *Current Opinion in Cell Biology*, *21*(1), 28–37. http://dx.doi.org/10.1016/j.ceb.2008.12.001, S0955-0674(08)00198-1 [pii].

Choi, H. J., Pokutta, S., Cadwell, G. W., Bobkov, A. A., Bankston, L. A., Liddington, R. C., et al. (2012). αE-catenin is an autoinhibited molecule that coactivates vinculin. *Proceedings of the National Academy of Sciences of the United States of America*, *109*, 8576–8581. http://dx.doi.org/10.1073/pnas.1203906109.

Chuan, P., Spudich, J. A., & Dunn, A. R. (2011). Robust mechanosensing and tension generation by myosin VI. *Journal of Molecular Biology*, *405*(1), 105–112. http://dx.doi.org/10.1016/j.jmb.2010.10.010.

Craig, R., Smith, R., & Kendrick-Jones, J. (1983). Light-chain phosphorylation controls the conformation of vertebrate non-muscle and smooth muscle myosin molecules. *Nature*, *302*(5907), 436–439.

Drees, F., Pokutta, S., Yamada, S., Nelson, W. J., & Weis, W. I. (2005). Alpha-catenin is a molecular switch that binds E-cadherin-beta-catenin and regulates actin-filament assembly. *Cell*, *123*(5), 903–915.

Ebrahim, S., Fujita, T., Millis, B. A., Kozin, E., Ma, X., Kawamoto, S., et al. (2013). NMII forms a contractile transcellular sarcomeric network to regulate apical cell junctions and tissue geometry. *Current Biology*, *23*(8), 731–736. http://dx.doi.org/10.1016/j.cub.2013.03.039.

Etienne-Manneville, S., & Hall, A. (2002). Rho GTPases in cell biology. *Nature*, *420*(6916), 629–635. http://dx.doi.org/10.1038/nature01148.

Fernandez-Gonzalez, R., Simoes Sde, M., Roper, J. C., Eaton, S., & Zallen, J. A. (2009). myosin II dynamics are regulated by tension in intercalating cells. *Developmental Cell*, *17*(5), 736–743. http://dx.doi.org/10.1016/j.devcel.2009.09.003.

Fernandez-Gonzalez, R., & Zallen, J. A. (2009). Cell mechanics and feedback regulation of actomyosin networks. *Science Signaling*, *2*(101), pe78. http://dx.doi.org/10.1126/scisignal.2101pe78.

Fields, A. P., & Justilien, V. (2010). The guanine nucleotide exchange factor (GEF) ECT2 is an oncogene in human cancer. *Advances in Enzyme Regulation*, *50*(1), 190–200. http://dx.doi.org/10.1016/j.advenzreg.2009.10.010, S0065-2571(09)00067-3 [pii].

Furman, C., Sieminski, A. L., Kwiatkowski, A. V., Rubinson, D. A., Vasile, E., Bronson, R. T., et al. (2007). Ena/VASP is required for endothelial barrier function in vivo. *Journal of Cell Biology*, *179*(4), 761–775. http://dx.doi.org/10.1083/Jcb.200705002.

Gates, J., Mahaffey, J. P., Rogers, S. L., Emerson, M., Rogers, E. M., Sottile, S. L., et al. (2007). Enabled plays key roles in embryonic epithelial morphogenesis in Drosophila. *Development*, *134*(11), 2027–2039. http://dx.doi.org/10.1242/dev.02849.

Gates, J., Nowotarski, S. H., Yin, H., Mahaffey, J. P., Bridges, T., Herrera, C., et al. (2009). Enabled and Capping protein play important roles in shaping cell behavior during Drosophila oogenesis. *Developmental Biology*, *333*(1), 90–107. http://dx.doi.org/10.1016/j.ydbio.2009.06.030.

Georgiou, M., Marinari, E., Burden, J., & Baum, B. (2008). Cdc42, Par6, and aPKC regulate Arp2/3-mediated endocytosis to control local adherens junction stability. *Current Biology*, *18*(21), 1631–1638. http://dx.doi.org/10.1016/j.cub.2008.09.029.

Glotzer, M. (2005). The molecular requirements for cytokinesis. *Science*, *307*(5716), 1735–1739. http://dx.doi.org/10.1126/science.1096896, 307/5716/1735 [pii].

Glotzer, M. (2009). The 3Ms of central spindle assembly: Microtubules, motors and MAPs. *Nature Reviews Molecular Cell Biology*, *10*(1), 9–20. http://dx.doi.org/10.1038/nrm2609, nrm2609 [pii].

Gomez, G. A., McLachlan, R. W., & Yap, A. S. (2011). Productive tension: Force-sensing and homeostasis of cell-cell junctions. *Trends in Cell Biology*, *21*(9), 499–505. http://dx.doi.org/10.1016/j.tcb.2011.05.006.

Guillot, C., & Lecuit, T. (2013). Mechanics of epithelial tissue homeostasis and morphogenesis. *Science*, *340*(6137), 1185–1189. http://dx.doi.org/10.1126/science.1235249.

Han, S. P., Gambin, Y., Gomez, G. A., Verma, S., Giles, N., Michael, M., et al. (2014). Cortactin scaffolds Arp2/3 and WAVE2 at the epithelial zonula adherens. *Journal of Biological Chemistry*, *289*(11), 7764–7775. http://dx.doi.org/10.1074/Jbc.M113.544478.

Hansen, S. D., & Mullins, R. D. (2010). VASP is a processive actin polymerase that requires monomeric actin for barbed end association. *The Journal of Cell Biology*, *191*(3), 571–584. http://dx.doi.org/10.1083/jcb.201003014.

Haviv, L., Gillo, D., Backouche, F., & Bernheim-Groswasser, A. (2008). A cytoskeletal demolition worker: myosin II acts as an actin depolymerization agent. *Journal of Molecular Biology*, *375*(2), 325–330. http://dx.doi.org/10.1016/J.Jmb.2007.09.066.

Hayakawa, K., Tatsumi, H., & Sokabe, M. (2011). Actin filaments function as a tension sensor by tension-dependent binding of cofilin to the filament. *Journal of Cell Biology*, *195*(5), 721–727. http://dx.doi.org/10.1083/Jcb.201102039.

He, B., Doubrovinski, K., Polyakov, O., & Wieschaus, E. (2014). Apical constriction drives tissue-scale hydrodynamic flow to mediate cell elongation. *Nature*, *508*(7496), 392–396. http://dx.doi.org/10.1038/nature13070.

Heckman-Stoddard, B. M., Vargo-Gogola, T., McHenry, P. R., Jiang, V., Herrick, M. P., Hilsenbeck, S. G., et al. (2009). Haploinsufficiency for p190B RhoGAP inhibits MMTV-Neu tumor progression. *Breast Cancer Research*, *11*(4), R61. http://dx.doi.org/10.1186/bcr2352.

Heissler, S. M., & Manstein, D. J. (2013). Nonmuscle myosin-2: Mix and match. *Cellular and Molecular Life Sciences*, *70*(1), 1–21. http://dx.doi.org/10.1007/s00018-012-1002-9.

Herzog, D., Loetscher, P., van Hengel, J., Knusel, S., Brakebusch, C., Taylor, V., et al. (2011). The small GTPase RhoA is required to maintain spinal cord neuroepithelium organization and the neural stem cell pool. *Journal of Neuroscience*, *31*(13), 5120–5130. http://dx.doi.org/10.1523/Jneurosci. 4807-10.2011.

Higashida, C., Kiuchi, T., Akiba, Y., Mizuno, H., Maruoka, M., Narumiya, S., et al. (2013). F- and G-actin homeostasis regulates mechanosensitive actin nucleation by formins. *Nature Cell Biology*, *15*(4), 395–405. http://dx.doi.org/10.1038/ncb2693.

Hildebrand, J. D. (2005). Shroom regulates epithelial cell shape via the apical positioning of an actomyosin network. *Journal of Cell Science*, *118*(Pt 22), 5191–5203. http://dx.doi.org/10.1242/jcs.02626.

Hildebrand, J. D., & Soriano, P. (1999). Shroom, a PDZ domain-containing actin-binding protein, is required for neural tube morphogenesis in mice. *Cell*, *99*(5), 485–497. http://dx.doi.org/10.1016/S0092-8674(00)81537-8.

Huveneers, S., Oldenburg, J., Spanjaard, E., van der Krogt, G., Grigoriev, I., Akhmanova, A., et al. (2012). Vinculin associates with endothelial VE-cadherin junctions to control force-dependent remodeling. *The Journal of Cell Biology*, *196*(5), 641–652. http://dx.doi.org/10.1083/jcb.201108120.

Insall, R. H., & Machesky, L. M. (2009). Actin dynamics at the leading edge: From simple machinery to complex networks. *Developmental Cell*, *17*(3), 310–322. http://dx.doi.org/10.1016/J.Devcel.2009.08.012.

Jaffe, A. B., & Hall, A. (2005). Rho GTPases: Biochemistry and biology. *Annual Review of Cell and Developmental Biology*, *21*, 247–269. http://dx.doi.org/10.1146/annurev.cellbio.21.020604.150721.

Jantsch-Plunger, V., Gonczy, P., Romano, A., Schnabel, H., Hamill, D., Schnabel, R., et al. (2000). CYK-4: A Rho family gtpase activating protein (GAP) required for central spindle formation and cytokinesis. *The Journal of Cell Biology*, *149*(7), 1391–1404.

Julian, L., & Olson, M. F. (2014). Rho-associated coiled-coil containing kinases (ROCK): Structure, regulation, and functions. *Small GTPases*, *5*, e29846. http://dx.doi.org/10.4161/sgtp.29846.

Kasza, K. E., & Zallen, J. A. (2011). Dynamics and regulation of contractile actin-myosin networks in morphogenesis. *Current Opinion in Cell Biology*, *23*(1), 30–38. http://dx.doi.org/10.1016/j.ceb.2010.10.014.

Katayama, K. I., Melendez, J., Baumann, J. M., Leslie, J. R., Chauhan, B. K., Nemkul, N., et al. (2011). Loss of RhoA in neural progenitor cells causes the disruption of adherens junctions and hyperproliferation. *Proceedings of the National Academy of Sciences of the United States of America*, *108*(18), 7607–7612. http://dx.doi.org/10.1073/Pnas.1101347108.

Kato, M., & Takenawa, T. (2005). WICH, a member of WASP-interacting protein family, cross-links actin filaments. *Biochemical and Biophysical Research Communications*, *328*(4), 1058–1066. http://dx.doi.org/10.1016/j.bbrc.2005.01.058.

Kim, S. H., Li, Z., & Sacks, D. B. (2000). E-cadherin-mediated cell-cell attachment activates Cdc42. *The Journal of Biological Chemistry*, *275*, 36999–37005.

Kimura, K., Ito, M., Amano, M., Chihara, K., Fukata, Y., Nakafuku, M., et al. (1996). Regulation of myosin phosphatase by Rho and Rho-associated kinase (Rho-kinase). *Science*, *273*(5272), 245–248.

Kinoshita, N., Sasai, N., Misaki, K., & Yonemura, S. (2008). Apical accumulation of rho in the neural plate is important for neural plate cell shape change and neural tube formation. *Molecular Biology of the Cell*, *19*(5), 2289–2299. http://dx.doi.org/10.1091/Mbc.E07-12-1286.

Knudsen, K. A., Soler, A. P., Johnson, K. R., & Wheelock, M. J. (1995). Interaction of alpha-actinin with the cadherin/catenin cell-cell adhesion complex via alpha-catenin. *The Journal of Cell Biology*, *130*(1), 67–77.

Kobielak, A., Pasolli, H. A., & Fuchs, E. (2004). Mammalian formin-1 participates in adherens junctions and polymerization of linear actin cables. *Nature Cell Biology*, *6*(1), 21–30. http://dx.doi.org/10.1038/ncb1075.

Kolsch, V., Seher, T., Fernandez-Ballester, G. J., Serrano, L., & Leptin, M. (2007). Control of Drosophila gastrulation by apical localization of adherens junctions and RhoGEF2. *Science*, *315*(5810), 384–386. http://dx.doi.org/10.1126/Science.1134833.

Kovacs, E. M., Goodwin, M., Ali, R. G., Paterson, A. D., & Yap, A. S. (2002). Cadherin-directed actin assembly: E-cadherin physically associates with the Arp2/3 complex to direct actin assembly in nascent adhesive contacts. *Current Biology*, *12*(5), 379–382.

Kovacs, E. M., Verma, S., Ali, R. G., Ratheesh, A., Hamilton, N. A., Akhmanova, A., et al. (2011). N-WASP regulates the epithelial junctional actin cytoskeleton through a non-canonical post-nucleation pathway. *Nature Cell Biology*, *13*(8), 934–943. http://dx.doi.org/10.1038/Ncb2290.

Kraemer, A., Goodwin, M., Verma, S., Yap, A. S., & Ali, R. G. (2007). Rac is a dominant regulator of cadherin-directed actin assembly that is activated by adhesive ligation

independently of Tiam1. *American Journal of Physiology. Cell Physiology*, *292*(3), C1061–C1069.

Krause, M., Dent, E. W., Bear, J. E., Loureiro, J. J., & Gertler, F. B. (2003). ENA/VASP proteins: Regulators of the actin cytoskeleton and cell migration. *Annual Review of Cell and Developmental Biology*, *19*, 541–564. http://dx.doi.org/10.1146/Annurev.Cellbio.19.050103.103356.

Ladoux, B., Anon, E., Lambert, M., Rabodzey, A., Hersen, P., Buguin, A., et al. (2010). Strength dependence of cadherin-mediated adhesions. *Biophysical Journal*, *98*(4), 534–542. http://dx.doi.org/10.1016/j.bpj.2009.10.044.

Lang, R. A., Herman, K., Reynolds, A. B., Hildebrand, J. D., & Plageman, T. F. (2014). p120-Catenin-dependent junctional recruitment of Shroom3 is required for apical constriction during lens pit morphogenesis. *Development*, *141*(16), 3177–3187. http://dx.doi.org/10.1242/Dev.107433.

Leerberg, J. M., Gomez, G. A., Verma, S., Moussa, E. J., Wu, S. K., Priya, R., et al. (2014). Tension-sensitive actin assembly supports contractility at the epithelial zonula adherens. *Current Biology*, *24*(15), 1689–1699. http://dx.doi.org/10.1016/J.Cub.2014.06.028.

Leibfried, A., Fricke, R., Morgan, M. J., Bogdan, S., & Bellaiche, Y. (2008). Drosophila Cip4 and WASp define a branch of the Cdc42-Par6-aPKC pathway regulating E-cadherin endocytosis. *Current Biology*, *18*(21), 1639–1648. http://dx.doi.org/10.1016/j.cub.2008.09.063.

Levine, E., Lee, C. H., Kintner, C., & Gumbiner, B. M. (1994). Selective disruption of E-cadherin function in early Xenopus embryos by a dominant negative mutant. *Development*, *120*(4), 901–909.

Liu, X. F., Ishida, H., Raziuddin, R., & Miki, T. (2004). Nucleotide exchange factor ECT2 interacts with the polarity protein complex Par6/Par3/protein kinase Czeta (PKCzeta) and regulates PKCzeta activity. *Molecular and Cellular Biology*, *24*(15), 6665–6675.

Liu, X. F., Ohno, S., & Miki, T. (2006). Nucleotide exchange factor ECT2 regulates epithelial cell polarity. *Cellular Signalling*, *18*(10), 1604–1615. http://dx.doi.org/10.1016/j.cellsig.2006.01.007.

Luo, W., Yu, C. H., Lieu, Z. Z., Allard, J., Mogilner, A., Sheetz, M. P., et al. (2013). Analysis of the local organization and dynamics of cellular actin networks. *The Journal of Cell Biology*, *202*(7), 1057–1073. http://dx.doi.org/10.1083/jcb.201210123.

Maitre, J. L., Berthoumieux, H., Krens, S. F., Salbreux, G., Julicher, F., Paluch, E., et al. (2012). Adhesion functions in cell sorting by mechanically coupling the cortices of adhering cells. *Science*, *338*(6104), 253–256. http://dx.doi.org/10.1126/science.1225399.

Mammoto, T., Mammoto, A., & Ingber, D. E. (2013). Mechanobiology and developmental control. *Annual Review of Cell and Developmental Biology*, *29*(29), 27–61. http://dx.doi.org/10.1146/Annurev-Cellbio-101512-122340.

Mangold, S., Norwood, S. J., Yap, A. S., & Collins, B. M. (2012). The juxtamembrane domain of the E-cadherin cytoplasmic tail contributes to its interaction with Myosin VI. *Bioarchitecture*, *2*(5), 185–188. http://dx.doi.org/10.4161/bioa.22082.

Mangold, S., Wu, S. K., Norwood, S. J., Collins, B. M., Hamilton, N. A., Thorn, P., et al. (2011). Hepatocyte growth factor acutely perturbs actin filament anchorage at the epithelial zonula adherens. *Current Biology*, *21*(6), 503–507. http://dx.doi.org/10.1016/J.Cub.2011.02.018.

Manke, I. A., Lowery, D. M., Nguyen, A., & Yaffe, M. B. (2003). BRCT repeats as phosphopeptide-binding modules involved in protein targeting. *Science*, *302*(5645), 636–639.

Martin, A. C. (2010). Pulsation and stabilization: Contractile forces that underlie morphogenesis. *Developmental Biology*, *341*(1), 114–125. http://dx.doi.org/10.1016/J.Ydbio.2009.10.031.

Martin, A. C., Gelbart, M., Fernandez-Gonzalez, R., Kaschube, M., & Wieschaus, E. (2010). Integration of contractile forces during tissue invagination. *The Journal of Cell Biology*, *188*, 735–749.

Martin, A. C., Kaschube, M., & Wieschaus, E. F. (2009). Pulsed contractions of an actin-myosin network drive apical constriction. *Nature*, *457*(7228), 495–499. http://dx.doi.org/10.1038/nature07522.

Matsumura, F. (2005). Regulation of myosin II during cytokinesis in higher eukaryotes. *Trends in Cell Biology*, *15*(7), 371–377. http://dx.doi.org/10.1016/J.Tcb.2005.05.004.

Medeiros, N. A., Burnette, D. T., & Forscher, P. (2006). myosin II functions in actin-bundle turnover in neuronal growth cones. *Nature Cell Biology*, *8*(3), 215–226.

Mikawa, M., Su, L., & Parsons, S. J. (2008). Opposing roles of p190RhoGAP and ECT2 RhoGEF in regulating cytokinesis. *Cell Cycle*, *7*(13), 2003–2012.

Mishima, M., Kaitna, S., & Glotzer, M. (2002). Central spindle assembly and cytokinesis require a kinesin-like protein/RhoGAP complex with microtubule bundling activity. *Developmental Cell*, *2*(1), 41–54, doi: S1534580701001101 [pii].

Mori, K., Amano, M., Takefuji, M., Kato, K., Morita, Y., Nishioka, T., et al. (2009). Rho-kinase contributes to sustained RhoA activation through phosphorylation of p190A RhoGAP. *Journal of Biological Chemistry*, *284*(8), 5067–5076. http://dx.doi.org/10.1074/Jbc.M806853200.

Niederman, R., & Pollard, T. D. (1975). Human platelet myosin. II. In vitro assembly and structure of myosin filaments. *The Journal of Cell Biology*, *67*(1), 72–92.

Nigam, S. K., Rodriguez-Boulan, E., & Silver, R. B. (1992). Changes in intracellular calcium during the development of epithelial polarity and junctions. *Proceedings of the National Academy of Sciences of the United States of America*, *89*(13), 6162–6166.

Nishimura, T., & Takeichi, M. (2008). Shroom3-mediated recruitment of Rho kinases to the apical cell junctions regulates epithelial and neuroepithelial planar remodeling. *Development*, *135*(8), 1493–1502. http://dx.doi.org/10.1242/Dev.019646.

Noren, N. K., Arthur, W. T., & Burridge, K. (2003). Cadherin engagement inhibits RhoA via p190RhoGAP. *The Journal of Biological Chemistry*, *278*(16), 13615–13618. http://dx.doi.org/10.1074/jbc.C200657200.

Noren, N. K., Liu, B. P., Burridge, K., & Kreft, B. (2000). p120 Catenin regulates the actin cytoskeleton via rho family GTPases. *The Journal of Cell Biology*, *150*, 567–579.

Oinuma, I., Kawada, K., Tsukagoshi, K., & Negishi, M. (2012). Rnd1 and Rnd3 targeting to lipid raft is required for p190 RhoGAP activation. *Molecular Biology of the Cell*, *23*(8), 1593–1604. http://dx.doi.org/10.1091/Mbc.E11-11-0900.

Padrick, S. B., & Rosen, M. K. (2010). Physical mechanisms of signal integration by WASP family proteins. *Annual Review of Biochemistry*, *79*, 707–735. http://dx.doi.org/10.1146/annurev.biochem.77.060407.135452.

Peng, X., Cuff, L. E., Lawton, C. D., & DeMali, K. A. (2010). Vinculin regulates cell-surface E-cadherin expression by binding to beta-catenin. *Journal of Cell Science*, *123*(Pt 4), 567–577. http://dx.doi.org/10.1242/jcs.056432.

Piekny, A. J., & Glotzer, M. (2008). Anillin is a scaffold protein that links RhoA, actin, and myosin during cytokinesis. *Current Biology*, *18*(1), 30–36. http://dx.doi.org/10.1016/J.Cub.2007.11.068.

Piekny, A. J., & Maddox, A. S. (2010). The myriad roles of Anillin during cytokinesis. *Seminars in Cell and Developmental Biology*, *21*(9), 881–891. http://dx.doi.org/10.1016/j.semcdb.2010.08.002.

Piekny, A., Werner, M., & Glotzer, M. (2005). Cytokinesis: Welcome to the Rho zone. *Trends in Cell Biology*, *15*(12), 651–658. http://dx.doi.org/10.1016/j.tcb.2005.10.006, S0962-8924(05)00250-3 [pii].

Pollard, T. D., Blanchoin, L., & Mullins, R. D. (2000). Molecular mechanisms controlling actin filament dynamics in nonmuscle cells. *Annual Review of Biophysics and Biomolecular Structure*, *29*, 545–576.

Ponik, S. M., Trier, S. M., Wozniak, M. A., Eliceiri, K. W., & Keely, P. J. (2013). RhoA is down-regulated at cell-cell contacts via p190RhoGAP-B in response to tensional homeostasis. *Molecular Biology of the Cell*, *24*(11), 1688–1699. http://dx.doi.org/10.1091/Mbc.E12-05-0386.

Priya, R., Yap, A. S., & Gomez, G. A. (2013). E-cadherin supports steady-state Rho signaling at the epithelial zonula adherens. *Differentiation*, *86*(3), 133–140. http://dx.doi.org/10.1016/j.diff.2013.01.002.

Rangarajan, E. S., & Izard, T. (2012). The cytoskeletal protein α-Catenin unfurls upon binding to vinculin. *The Journal of Biological Chemistry*, *287*(22), 18492–18499. http://dx.doi.org/10.1074/jbc.M112.351023.

Ratheesh, A., Gomez, G. A., Priya, R., Verma, S., Kovacs, E. M., Jiang, K., et al. (2012). Centralspindlin and alpha-catenin regulate Rho signalling at the epithelial zonula adherens. *Nature Cell Biology*, *14*(8), 818–828. http://dx.doi.org/10.1038/ncb2532.

Ratheesh, A., Priya, R., & Yap, A. S. (2013). Coordinating Rho and Rac: The regulation of Rho GTPase signaling and cadherin junctions. *Progress in Molecular Biology and Translational Science*, *116*, 49–68. http://dx.doi.org/10.1016/B978-0-12-394311-8.00003-0.

Ratheesh, A., & Yap, A. S. (2012). A bigger picture: Classical cadherins and the dynamic actin cytoskeleton. *Nature Reviews. Molecular Cell Biology*, *13*(10), 673–679. http://dx.doi.org/10.1038/Nrm3431.

Rauzi, M., Verant, P., Lecuit, T., & Lenne, P. F. (2008). Nature and anisotropy of cortical forces orienting Drosophila tissue morphogenesis. *Nature Cell Biology*, *10*(12), 1401–1410. http://dx.doi.org/10.1038/ncb1798.

Reyes, C. C., Jin, M., Breznau, E. B., Espino, R., Delgado-Gonzalo, R., Goryachev, A. B., et al. (2014). Anillin regulates cell-cell junction integrity by organizing junctional accumulation of Rho-GTP and actomyosin. *Current Biology*, *24*(11), 1263–1270. http://dx.doi.org/10.1016/j.cub.2014.04.021.

Reymann, A. C., Boujemaa-Paterski, R., Martiel, J. L., Guerin, C., Cao, W. X., Chin, H. F., et al. (2012). Actin network architecture Can determine myosin motor activity. *Science*, *336*(6086), 1310–1314. http://dx.doi.org/10.1126/Science.1221708.

Ridley, A. J. (2012). Historical overview of Rho GTPases. *Rho GTPases: Methods and Protocols*, *827*, 3–12. http://dx.doi.org/10.1007/978-1-61779-442-1_1.

Riento, K., & Ridley, A. J. (2003). Rocks: Multifunctional kinases in cell behaviour. *Nature Reviews. Molecular Cell Biology*, *4*(6), 446–456. http://dx.doi.org/10.1038/nrm1128.

Riento, K., Totty, N., Villalonga, P., Garg, R., Guasch, R., & Ridley, A. J. (2005). RhoE function is regulated by ROCK I-mediated phosphorylation. *The EMBO Journal*, *24*(6), 1170–1180. http://dx.doi.org/10.1038/Sj.Emboj.7600612.

Riou, P., Kjaer, S., Garg, R., Purkiss, A., George, R., Cain, R. J., et al. (2013). 14-3-3 Proteins interact with a hybrid prenyl-phosphorylation motif to inhibit G proteins. *Cell*, *153*(3), 640–653. http://dx.doi.org/10.1016/j.cell.2013.03.044.

Sandquist, J. C., & Means, A. R. (2008). The C-terminal tail region of nonmuscle myosin II directs isoform-specific distribution in migrating cells. *Molecular Biology of the Cell*, *19*(12), 5156–5167. http://dx.doi.org/10.1091/mbc.E08-05-0533, E08-05-0533 [pii].

Sandquist, J. C., Swenson, K. I., Demali, K. A., Burridge, K., & Means, A. R. (2006). Rho kinase differentially regulates phosphorylation of nonmuscle myosin II isoforms A and B during cell rounding and migration. *The Journal of Biological Chemistry*, *281*(47), 35873–35883.

Schofield, A. V., & Bernard, O. (2013). Rho-associated coiled-coil kinase (ROCK) signaling and disease. *Critical Reviews in Biochemistry and Molecular Biology*, *48*(4), 301–316. http://dx.doi.org/10.3109/10409238.2013.786671.

Schumacher, S., Gryzik, T., Tannebaum, S., & Muller, H. A. J. (2004). The RhoGEF Pebble is required for cell shape changes during cell migration triggered by the Drosophila FGF

receptor Heartless. *Development*, *131*(11), 2631–2640. http://dx.doi.org/10.1242/Dev.01149.

Scott, J. A., Shewan, A. M., den Elzen, N. R., Loureiro, J. J., Gertler, F. B., & Yap, A. S. (2006). Ena/VASP proteins can regulate distinct modes of actin organization at cadherin-adhesive contacts. *Molecular Biology of the Cell*, *17*(3), 1085–1095. http://dx.doi.org/10.1191/Mbc.E05-07-0644.

Sellers, J. R. (1991). Regulation of cytoplasmic and smooth muscle myosin. *Current Opinion in Cell Biology*, *3*(1), 98–104.

Settleman, J., Narasimhan, V., Foster, L. C., & Weinberg, R. A. (1992). Molecular cloning of cDNAs encoding the GAP-associated protein p190: Implications for a signaling pathway from ras to the nucleus. *Cell*, *69*(3), 539–549.

Shewan, A. M., Maddugoda, M., Kraemer, A., Stehbens, S. J., Verma, S., Kovacs, E. M., et al. (2005). Myosin 2 is a key Rho kinase target necessary for the local concentration of E-cadherin at cell-cell contacts. *Molecular Biology of the Cell*, *16*(10), 4531–4542. http://dx.doi.org/10.1091/mbc.E05-04-0330.

Shimizu, Y., Thumkeo, D., Keel, J., Ishizaki, T., Oshima, H., Oshima, M., et al. (2005). ROCK-I regulates closure of the eyelids and ventral body wall by inducing assembly of actomyosin bundles. *The Journal of Cell Biology*, *168*(6), 941–953. http://dx.doi.org/10.1083/jcb.200411179.

Simoes Sde, M., Mainieri, A., & Zallen, J. A. (2014). Rho GTPase and Shroom direct planar polarized actomyosin contractility during convergent extension. *The Journal of Cell Biology*, *204*(4), 575–589. http://dx.doi.org/10.1083/jcb.201307070.

Smallhorn, M., Murray, M. J., & Saint, R. (2004). The epithelial-mesenchymal transition of the Drosophila mesoderm requires the Rho GTP exchange factor Pebble. *Development*, *131*(11), 2641–2651. http://dx.doi.org/10.1242/dev.01150, dev.01150 [pii].

Smith, A. L., Dohn, M. R., Brown, M. V., & Reynolds, A. B. (2012). Association of Rho-associated protein kinase 1 with E-cadherin complexes is mediated by p120-catenin. *Molecular Biology of the Cell*, *23*(1), 99–110. http://dx.doi.org/10.1091/Mbc.E11-06-0497.

Smutny, M., Cox, H. L., Leerberg, J. M., Kovacs, E. M., Conti, M. A., Ferguson, C., et al. (2010). myosin II isoforms identify distinct functional modules that support integrity of the epithelial zonula adherens. *Nature Cell Biology*, *12*(7), 696–702. http://dx.doi.org/10.1038/ncb2072.

Smutny, M., Wu, S. K., Gomez, G. A., Mangold, S., Yap, A. S., & Hamilton, N. A. (2011). Multicomponent analysis of junctional movements regulated by myosin II isoforms at the epithelial zonula adherens. *PLoS One*, *6*(7), e22458. http://dx.doi.org/10.1371/journal.pone.0022458.

Somers, W. G., & Saint, R. (2003). A RhoGEF and Rho family GTPase-activating protein complex link the contractile ring to cortical microtubules at the onset of cytokinesis. *Developmental Cell*, *4*, 29–39.

Su, K. C., Takaki, T., & Petronczki, M. (2011). Targeting of the RhoGEF ECT2 to the equatorial membrane controls cleavage furrow formation during cytokinesis. *Developmental Cell*, *21*(6), 1104–1115. http://dx.doi.org/10.1016/j.devcel.2011.11.003.

Takaishi, K., Sasaki, T., Kotani, H., Nishioka, H., & Takai, Y. (1997). Regulation of cell-cell adhesion by rac and rho small G proteins in MDCK cells. *The Journal of Cell Biology*, *139*(4), 1047–1059.

Takeichi, M. (2014). Dynamic contacts: Rearranging adherens junctions to drive epithelial remodelling. *Nature Reviews. Molecular Cell Biology*, *15*(6), 397–410. http://dx.doi.org/10.1038/nrm3802.

Tang, V. W., & Brieher, W. M. (2012). alpha-Actinin-4/FSGS1 is required for Arp2/3-dependent actin assembly at the adherens junction. *Journal of Cell Biology*, *196*(1), 115–130. http://dx.doi.org/10.1083/Jcb.201103116.

Tatsumoto, T., Xie, X. Z., Blumenthal, R., Okamoto, I., & Miki, T. (1999). Human ECT2 is an exchange factor for Rho GTPases, phosphorylated in G2/M phases, and involved in cytokinesis. *Journal of Cell Biology*, *147*(5), 921–927.

Tcherkezian, J., & Lamarche-Vane, N. (2007). Current knowledge of the large RhoGAP family of proteins. *Biology of the Cell*, *99*(2), 67–86. http://dx.doi.org/10.1042/BC20060086.

Thumkeo, D., Shinohara, R., Watanabe, K., Takebayashi, H., Toyoda, Y., Tohyama, K., et al. (2011). Deficiency of mDia, an actin nucleator, disrupts integrity of neuroepithelium and causes periventricular dysplasia. *PLoS One*, *6*(9), e25465. http://dx.doi.org/10.1371/journal.pone.0025465.

Thumkeo, D., Watanabe, S., & Narumiya, S. (2013). Physiological roles of Rho and Rho effectors in mammals. *European Journal of Cell Biology*, *92*(10–11), 303–315. http://dx.doi.org/10.1016/j.ejcb.2013.09.002.

Totsukawa, G., Yamakita, Y., Yamashiro, S., Hartshorne, D. J., Sasaki, Y., & Matsumura, F. (2000). Distinct roles of ROCK (Rho-kinase) and MLCK in spatial regulation of MLC phosphorylation for assembly of stress fibers and focal adhesions in 3T3 fibroblasts. *The Journal of Cell Biology*, *150*(4), 797–806.

Vargo-Gogola, T., Heckman, B. M., Gunther, E. J., Chodosh, L. A., & Rosen, J. M. (2006). P190-B Rho GTPase-activating protein overexpression disrupts ductal morphogenesis and induces hyperplastic lesions in the developing mammary gland. *Molecular Endocrinology*, *20*(6), 1391–1405. http://dx.doi.org/10.1210/me.2005-0426.

Vasioukhin, V., Bauer, C., Yin, M., & Fuchs, E. (2000). Directed actin polymerization is the driving force for epithelial cell-cell adhesion. *Cell*, *100*(2), 209–219. http://dx.doi.org/10.1016/S0092-8674(00)81559-7.

Verma, S., Han, S. P., Michael, M., Gomez, G. A., Yang, Z., Teasdale, R. D., et al. (2012). A WAVE2-Arp2/3 actin nucleator apparatus supports junctional tension at the epithelial zonula adherens. *Molecular Biology of the Cell*, *23*(23), 4601–4610. http://dx.doi.org/10.1091/Mbc.E12-08-0574.

Vicente-Manzanares, M., Ma, X., Adelstein, R. S., & Horwitz, A. R. (2009). Non-muscle myosin II takes centre stage in cell adhesion and migration. *Nature Reviews Molecular Cell Biology*, *10*(11), 778–790. http://dx.doi.org/10.1038/nrm2786, nrm2786 [pii].

Watabe-Uchida, M., Uchida, N., Imamura, Y., Nagafuchi, A., Fujimoto, K., Uemura, T., et al. (1998). alpha-Catenin-vinculin interaction functions to organize the apical junctional complex in epithelial cells. *The Journal of Cell Biology*, *142*(3), 847–857.

Weed, S. A., & Parsons, J. T. (2001). Cortactin: Coupling membrane dynamics to cortical actin assembly. *Oncogene*, *20*(44), 6418–6434.

Wei, L., Roberts, W., Wang, L., Yamada, M., Zhang, S. X., Zhao, Z. Y., et al. (2001). Rho kinases play an obligatory role in vertebrate embryonic organogenesis. *Development*, *128*(15), 2953–2962.

Wennerberg, K., Forget, M. A., Ellerbroek, S. M., Arthur, W. T., Burridge, K., Settleman, J., et al. (2003). Rnd proteins function as RhoA antagonists by activating p190 RhoGAP. *Current Biology*, *13*(13), 1106–1115. http://dx.doi.org/10.1016/S0960-9822(03)00418-4.

Werner, M., & Glotzer, M. (2008). Control of cortical contractility during cytokinesis. *Biochemical Society Transactions*, *36*(Pt 3), 371–377. http://dx.doi.org/10.1042/BST0360371, BST0360371 [pii].

Wildenberg, G. A., Dohn, M. R., Carnahan, R. H., Davis, M. A., Lobdell, N. A., Settleman, J., et al. (2006). p120-catenin and p190RhoGAP regulate cell-cell adhesion by coordinating antagonism between Rac and Rho. *Cell*, *127*(5), 1027–1039. http://dx.doi.org/10.1016/j.cell.2006.09.046.

Wolfe, B. A., & Glotzer, M. (2009). Single cells (put a ring on it). *Genes & Development*, *23*(8), 896–901. http://dx.doi.org/10.1101/gad.1801209, 23/8/896 [pii].

Wolfe, B. A., Takaki, T., Petronczki, M., & Glotzer, M. (2009). Polo-like kinase 1 directs assembly of the HsCyk-4 RhoGAP/ECT2 RhoGEF complex to initiate cleavage furrow formation. *PLoS Biology*, 7(5), e1000110. http://dx.doi.org/10.1371/journal.pbio.1000110.

Wu, S. K., Gomez, G. A., Michael, M., Verma, S., Cox, H. L., Lefevre, J. G., et al. (2014). Cortical F-actin stabilization generates apical-lateral patterns of junctional contractility that integrate cells into epithelia. *Nature Cell Biology*, *16*(2), 167–178. http://dx.doi.org/10.1038/ncb2900.

Yamada, S., Pokutta, S., Drees, F., Weis, W. I., & Nelson, W. J. (2005). Deconstructing the cadherin-catenin-actin complex. *Cell*, *123*(5), 889–901. http://dx.doi.org/10.1016/j.cell.2005.09.020.

Yao, M., Qiu, W., Liu, R., Efremov, A. K., Cong, P., Seddiki, R., et al. (2014). Force-dependent conformational switch of alpha-catenin controls vinculin binding. *Nature Communications*, *5*, 4525. http://dx.doi.org/10.1038/ncomms5525.

Ydenberg, C. A., Smith, B. A., Breitsprecher, D., Gelles, J., & Goode, B. L. (2011). Cease-fire at the leading edge: New perspectives on actin filament branching, debranching, and cross-linking. *Cytoskeleton (Hoboken)*, *68*(11), 596–602. http://dx.doi.org/10.1002/cm.20543.

Yonemura, S., Wada, Y., Watanabe, T., Nagafuchi, A., & Shibata, M. (2010). alpha-Catenin as a tension transducer that induces adherens junction development. *Nature Cell Biology*, *12*(6), 533–542. http://dx.doi.org/10.1038/Ncb2055.

Yuce, O., Piekny, A., & Glotzer, M. (2005). An ECT2-centralspindlin complex regulates the localization and function of RhoA. *Journal of Cell Biology*, *170*(4), 571–582.

Zhang, J., Betson, M., Erasmus, J., Zeikos, K., Bailly, M., Cramer, L. P., et al. (2005). Actin at cell-cell junctions is composed of two dynamic and functional populations. *Journal of Cell Science*, *118*(Pt 23), 5549–5562.

Zhang, B., & Zheng, Y. (1998). Regulation of RhoA GTP hydrolysis by the GTPase-activating proteins p190, p50RhoGAP, Bcr, and 3BP-1. *Biochemistry*, *37*(15), 5249–5257. http://dx.doi.org/10.1021/bi9718447.